UNIVERSIDAD DE SANTIAGO DE COMPOSTELA

FACULTAD DE FARMACIA

DEPARTAMENTO DE FARMACIA Y TECNOLOGÍA FARMACÉUTICA

Tesis Doctoral

NANOCÁPSULAS DIRIGIDAS AL SISTEMA LINFÁTICO: UNA APROXIMACIÓN AL TRATAMIENTO DEL CÁNCER METASTÁSICO

Raquel Abellán Pose

Santiago de Compostela, 2015

USC
UNIVERSIDADE
DE SANTIAGO
DE COMPOSTELA

Dra. María José Alonso Fernández, Catedrática del Departamento de Tecnología Farmacéutica de la Universidad de Santiago de Compostela

Dra. Noémi Stefania Csaba, Investigadora Parga Pondal del Departamento de Tecnología Farmacéutica de la Universidad de Santiago de Compostela

Dr. Rafael López López, Jefe del Servicio de Oncología del Hospital Clínico Universitario de Santiago de Compostela

HACEN CONSTAR:

Que la presente memoria experimental titulada: "**Nanocápsulas dirigidas al sistema linfático: Una aproximación al tratamiento del cáncer metastásico**", elaborada por **Raquel Abellán Pose**, ha sido realizada bajo su dirección en el Departamento de Farmacia y Tecnología Farmacéutica y, hallándose concluida, autorizan su presentación a fin de que pueda ser juzgada por el tribunal correspondiente.

Y para que conste, expiden y firman el presente certificado en Santiago de Compostela, el 25 de Septiembre de 2015.

Fdo. María José Alonso Fdo. Noemi S. Csaba Fdo. Rafael López

USC
UNIVERSIDADE
DE SANTIAGO
DE COMPOSTELA

A mi familia

USC
UNIVERSIDADE
DE SANTIAGO
DE COMPOSTELA

La ciencia está hecha de datos, como una casa de piedras. Pero un montón de datos no es ciencia más de lo que un montón de piedras es una casa.

Henri Poincaré, La ciencia y la hipótesis

USC
UNIVERSIDADE
DE SANTIAGO
DE COMPOSTELA

AGRADECIMIENTOS

En estas líneas quiero expresar mi más sincero agradecimiento a todas las personas que me han prestado su ayuda intelectual, material o emocional, durante todo el camino recorrido para finalizar esta tesis doctoral y en especial:

A mis directores de tesis, Mª José Alonso, Noémi Csaba y Rafael López, por haberme dado la oportunidad de realizar esta tesis doctoral y por dirigir este trabajo.

Al proyecto LYMPHOTARG y a la Escuela de Doctorado Internacional de Ciencias Biomédicas y Tecnologías de la Salud de la Universidad de Santiago de Compostela por la financiación de esta tesis.

A los colaboradores del proyecto: Anxo Vidal, Marcos García, Dolores Torres, Miguel Abal y María de La Fuente y también a Erea Borrajo y Marta Alonso, con las que he trabajado mano a mano tantos años.

A las profesoras May Évora y Araceli Delgado del Dpto. de Ingeniería Química y Tecnología Farmacéutica de la Universidad de La Laguna, por acogerme en su grupo para hacer los ensayos de biodistribución con radiactividad y por la inmensa ayuda prestada antes, durante y después de las estancias. También a María Rosa, María y Domingo su colaboración con las ratas, y a Sariña por sus sabios consejos antes del viaje.

Al profesor Manuel Santander por la ayuda para realizar e interpretar los ensayos de estabilidad coloidal y su enorme disponibilidad.

Al INSERM U646 de la Universidad d'Angers, y en especial a Jean Pierre Benoît, Guillaume Bastiat, Elodie, Stephanie y Severine por lo bien que me trataron durante mi estancia allí, justo al comenzar la tesis. También a François (mon petit bleu), Clément y Khaled por adoptarme en la pandilla y hacer que los partidos del mundial del 2010 en el exilio fueran igual de divertidos.

A los demás profesores del Departamento de Farmacia y Tecnología Farmacéutica, por la ayuda brindada en diferentes momentos durante los casi nueve años que llevo en este departamento. También a Rafa, Puri y Belén.

Al servicio de microscopía de la Universidad de Santiago de Compostela.

A todos y cada uno de mis compañeros de laboratorio, a los que están ahora y a todos los que ya se han ido. En este punto, se mezclan los agradecimientos profesionales y personales. Y quiero mencionar en especial a Carmen, JV, Sara, Ana González y Cadete, Inma, Belén, Jorge y Tania por los consejos, los abrazos, las risas, las clases de zumba y los "vamos que tú puedes". Yo no tenía tanta fe, gracias por prestarme la vuestra y hacer esta tesis más llevadera.

También a mis farmacéuticas por el mundo, a Cris y Diana y los primos "que no amigos" (que útil ha sido saber jugar al mus...).

Y quiero dar las gracias en mayúsculas a mi familia. En especial a mis padres, Berta y Diego, mis cuatro pilares. Por el amor y apoyo incondicional, por crecer conmigo, completar mi vida y hacerme feliz. Diego, prometo compensarte por estos años. También me gustaría darle las gracias a mis abuelos Matilde, Benigno y Antonio y a mi tía Bea, porque su recuerdo constante me animó a embarcarme en esta odisea y me dio fuerzas en muchas ocasiones. Espero que mi nano-granito de arena sirva para ganar pronto la lucha contra el cáncer.

Raquel Abellán Pose

23 de septiembre de 2015

ÍNDICE DE CONTENIDOS

USC
UNIVERSIDADE
DE SANTIAGO
DE COMPOSTELA

RESUMEN/ABSTRACT

USC
UNIVERSIDADE
DE SANTIAGO
DE COMPOSTELA

RESUMEN

El objetivo principal de esta tesis ha sido el desarrollo y evaluación de nanocápsulas de poliaminoácidos diseñadas para favorecer el transporte selectivo de fármacos al sistema linfático. Estas nanocápsulas constituidas por un núcleo oleoso y una cubierta polimérica de ácido poliglutámico (PGA), ácido poliglutámico PEGilado (PGA-PEG) o poliasparagina (PASN), poseen atractivas características fisicoquímicas para promover su acceso al sistema linfático, como un tamaño de partícula reducido cercano a 100 nm, potencial zeta negativo y una superficie hidrofílica. Estas formulaciones presentan una adecuada estabilidad y capacidad para encapsular y liberar de forma controlada fármacos hidrofóbicos como el docetaxel. Los estudios de biodistribución realizados mediante imagen de fluorescencia y radioactividad han demostrado que las nanocápsulas basadas en ácido poliglutámico logran una notable distribución a los ganglios linfáticos tras su administración subcutánea o intravenosa. Se ha estudiado el potencial de las nanocápsulas de PGA-PEG como plataforma de liberación de docetaxel para el tratamiento del cáncer metastásico de pulmón. Además, las nanocápsulas de PGA-PEG mostraron una reducida toxicidad in vivo en comparación con la formulación comercial Taxotere® y mejoraron de forma significativa la eficacia antitumoral en un modelo de cáncer de pulmón metastatizante, tanto en el tumor primario como en las metástasis linfáticas. De hecho, a diferencia del Taxotere®, las nanocápsulas de PGA-PEG lograron producir la regresión de la carga tumoral en los ganglios mediastinos, aumentando considerablemente su supervivencia.

Todos estos resultados ponen de manifiesto la capacidad de estas nanocápsulas para liberar fármacos al sistema linfático y su potencial para tratar diversas patologías como el cáncer metastásico.

USC
UNIVERSIDADE
DE SANTIAGO
DE COMPOSTELA

ABSTRACT

The main goal of this thesis has been the development and evaluation of polyaminoacid-based nanocapsules intended to promote the lymphatic delivery of drugs. These nanocapsules, consisting of an oily core and a polymeric coating of polyglutamic acid (PGA), PEGylated polyglutamic acid (PGA-PEG) or polyasparagine (PASN), exhibit attractive physicochemical characteristics to promote their access to the lymphatic system, such as small particle size close to 100 nm, negative zeta potential and hydrophilic surface. These formulations have suitable stability and ability to encapsulate and release hydrophobic drugs such as docetaxel in a controlled manner. Biodistribution studies performed by fluorescence imaging and radioactivity have shown a marked distribution of polyglutamic acid-based nanocapsules to the lymph nodes after both subcutaneous and intravenous administration. The potential of PGA-PEG nanocapsules as a delivery platform for the treatment of metastatic lung cancer has been studied in *vitro* and *in vivo*. Moreover, PGA-PEG nanocapsules displayed reduced in vivo toxicity as compared to the commercial formulation Taxotere® and significantly improved antitumor efficacy in an orthotopic metastasizing lung cancer model both in the primary tumor and in the lymphatic metastasis. In fact, PGA-PEG nanocapsules were able to produce the regression of the tumor load of the mediastinal lymph nodes, which could not be achieved with the same dose of Taxotere®, improving substantially the survival rates.

All these results highlight the ability of these nanocapsules to deliver drugs to the lymphatic system and their potential to treat different pathologies such as metastatic cancer.

USC
UNIVERSIDADE
DE SANTIAGO
DE COMPOSTELA

LISTADO DE ABREVIATURAS

AP	Aqueous phase	Fase acuosa
AUC	Area under the curve	Área bajo la curva
BKC	Benzalkonium chloride	Cloruro de benzalconio
CCC	Critical coagulation concentration	Concentración crítica de coagulación
Cl	Cleareance	Aclaramiento
CSC	Critical stabilization concentration	Concentración crítica de estabilización
CTAB	Hexadecyltrimethylammonium bromide	Bromuro de hexadeciltrimetilamonio
DCX	Docetaxel	Docetaxel
DTPA-PE	Diethylene triamine pentaacetic acid-conjugated phosphoethanolamine	Fosfoetanolamina conjugada con ácido dietilentriaminopentaacético
ECM	Extracellular matrix	Matriz extracelular
EE	Encapsulation efficiency	Eficacia de encapsulación
HPLC	High perfomance liquid chromatography	Cromatografía líquida de alta eficacia
ID	Intradermal injection	Inyección intradérmica
IFP	Interstitial fluid pressure	Presión del líquido intersticial
IM	Intramuscular injection	Inyección intramuscular
IP	Intraperitoneal injection	Inyección intraperitoneal
IV	Intravenous injection	Inyección intravenosa
IVIS	*In vivo* imaging system	Sistema de imágenes *in vivo*
LDA	Laser doppler anemometry	Anemometría láser doppler
LECs	Lymphatic endothelial cells	Células endoteliales linfáticas
MPS	Mononuclear phagocytic system	Sistema fagocítico mononuclear
MRT	Mean residence time	Tiempo medio de residencia
MTD	Maximun tolerated dose	Dosis máxima tolerada

NC	Nanocapsule	Nanocápsula
NE	Nanoemulsion	Nanoemulsión
NP	Nanoparticle	Nanopartícula
OP	Organic phase	Fase orgánica
PASN	Polyasparagine	Poliasparagina
PCS	Photon correlation spectroscopy	Espectroscopía de correlación fotónica
PEG	Polyethylene glycol	Polietilenglicol
PGA	Poly glutamic acid	Ácido poliglutámico
PI	Polydispersity index	Índice de polidispersión
PLGA	Poly(lactic-co-glycolic acid)	Ácido poliláctico glicólico
SC	Subcutaneous injection	Inyección subcutánea
SD	Standard deviation	Desviación estándar
SEM	Standard error of the mean	Error estándar de la media
TEM	transmission electron microscopy	Microscopía electrónica de transmisión
TXT	Taxotere®	Taxotere®
$t_{1/2}$	Half life time	Tiempo de vida media
Vz	Volume distribution terminal phase	Volumen de distribución durante la fase terminal
Vss	Volume distribution (steady state)	Volumen de distribución (estado de equilibrio)
W	Fuchs stability factor	Factor de estabilidad de Fuchs

INTRODUCCIÓN

USC
UNIVERSIDADE
DE SANTIAGO
DE COMPOSTELA

INTRODUCCIÓN

El objetivo de esta introducción es aportar una visión somera sobre la contribución de la nanotecnología al desarrollo de nuevas terapias, en particular basadas en taxanos, en oncología. Esta visión, junto con el conocimiento relacionado con el potencial de la nanotecnología para lograr la vehiculización de fármacos al sistema linfático, aspecto recogido en el capítulo 1, representan el marco conceptual en el que se centran los objetivos de la presente tesis doctoral.

El cáncer

La palabra cáncer es un término genérico que designa un amplio grupo de enfermedades que pueden afectar a cualquier parte del organismo. Se caracteriza por la rápida multiplicación de células anormales que se extienden más allá de sus límites habituales y pueden invadir tejidos adyacentes o propagarse a otros órganos a través del sistema circulatorio y/o linfático. Este proceso, conocido como metástasis, es el responsable principal de la elevada mortalidad asociada al cáncer.

El cáncer es la principal causa de muerte a escala mundial. La Agencia Internacional para la Investigación del Cáncer (IARC), dependiente de la Organización Mundial de la Salud, le atribuye 8.2 millones de defunciones ocurridas en todo el mundo en 2012 y prevé 15.2 millones de nuevos casos y 8.8 millones de muertes para este año 2015 [1]. En muchos países occidentales, el cáncer con mayor tasa de mortalidad es el cáncer de pulmón. De hecho, sólo este tipo de cáncer representa un 26% de las defunciones por cáncer en mujeres y del 28% en hombres en Estados Unidos [2]. Esta alta mortalidad se debe a que en el momento del diagnóstico el tumor ya ha diseminado a los ganglios linfáticos en el 80% de los pacientes [3].

El tratamiento del cáncer se basa fundamentalmente en la quimioterapia, radioterapia y cirugía. A pesar de que en los últimos años se han logrado grandes avances en estas modalidades terapéuticas, los efectos secundarios asociados al tratamiento oncológico pueden ser graves y mermar de forma significativa la calidad de vida del paciente. En particular, la quimioterapia presenta varias limitaciones importantes como son (i) la distribución inespecífica de los fármacos en el organismo, responsable de gran parte de

los efectos secundarios; (ii) la resistencia desarrollada por células tumorales a ciertos fármacos y (iii) la incapacidad para alcanzar concentraciones suficientemente elevadas en el tumor y/o ganglios linfáticos que puedan evitar las recidivas del tumor y metástasis.

Los taxanos en el tratamiento del cáncer

Los taxanos son un conjunto de fármacos antineoplásicos producidos por plantas del género Taxus que impiden la división de las células y, por tanto, inhiben el crecimiento celular. Concretamente, estos fármacos estimulan el ensamblaje de los microtúbulos y estabilizan su formación inhibiendo su depolimerización. Como consecuencia, se produce la parada del ciclo celular en la fase G2/M, apoptosis y finalmente muerte celular.

El primer fármaco taxano, descubierto en los años 60, fue el paclitaxel. Este fármaco presenta una solubilidad en agua muy baja, por lo que para administrarlo como inyectable (Taxol®, Bristol-Myers Squibb, EEUU) fue formulado bajo la forma de una solución en Cremophor® EL (aceite de castor polioxietilado) y alcohol [4]. Años más tarde, se comercializó un fármaco análogo semisintético, con el nombre de docetaxel. Este fármaco presenta una mayor afinidad por los microtúbulos y, consecuentemente, una mayor eficacia antitumoral [5,6]. Este taxano de segunda generación presenta también una reducida solubilidad en agua, por lo que la formulación actualmente comercializada (Taxotere®, Sanofi, Francia) contiene polisorbato 80 y etanol para lograr su solubilización [6].

En la actualidad los taxanos son ampliamente prescritos para el tratamiento de diversos tipos de cáncer como el cáncer de pulmón, mama, próstata, cabeza y cuello, adenocarcinoma gástrico y sarcoma de Kaposi, entre otros. A pesar de su efectividad, el uso continuado en clínica de Taxol® y Taxotere® está limitado por sus graves efectos secundarios, debidos en parte a la elevada concentración de tensioactivos, pero sobre todo a su distribución inespecífica en el organismo [7,8]. Para superar estas limitaciones y mejorar la eficacia antitumoral de estas formulaciones, se han investigado diversos nanosistemas que evitan el uso de estos disolventes y permiten dirigir el tratamiento con mayor selectividad hacia el tumor o lugar de acción [9]. Estos nanovehículos, además

de modular la farmacocinética y el perfil de distribución de los fármacos asociados, pueden proteger el fármaco frente a la degradación y favorecer la penetración y distribución intracelular [10].

Nanosistemas comercializados con quimioterapéuticos

En las últimas dos décadas se han aprobado y comercializado varios nanosistemas para la administración de fármacos antitumorales (**Tabla 1**). Entre ellos, los nanosistemas desarrollados para la administración de paclitaxel han conseguido evitar por completo el uso del Cremophor y ofrecen una alternativa terapéutica al Taxol®.

Tabla 1. Nanomedicamentos aprobados para el tratamiento de diversos tipos de cáncer.

Nombre comercial	Nanosistema / fármaco	Indicación (tipo de cáncer)	Aprobación	Compañía
Abraxane®	Nanopartículas / paclitaxel	Mama metastásico y pulmón	2005, FDA	Abraxis Bioscience
DaunoXome	Liposomas / daunorubicina	Sarcoma de Kaposi	1996, FDA	Galen Ltd
Doxil	Liposomas PEGylados / doxorubicina	Ovario	1995, FDA	Ortho Biotech
Genexol-PM	Micelas poliméricas / paclitaxel	Mama, pulmón, ovario	2001, Corea	Samyang Pharmaceuticals
Lipusu	Liposomas/ paclitaxel	Ovario, pulmón	2003, CFDA	Luye Pharma Group Ltd
Nanoxel	Micelas poliméricas / paclitaxel	Mama metastásico, ovario, pulmón	2006, DCGI	Dabur Pharma
Myocet	Liposomas / doxorubicina	Mama metastásico	2000, EMA	Sopherion Therapeutics/ Cephalon
Onco-TCS (Marqibo)	Liposomas / Vincristina	Linfoma No-Hodgkin	FDA, 2012	Talon Therapeutics

Abreviaturas: CDFA: China Food and Drug Administration; DCGI: Drug Controller General of India; EMA: European Medicines Agency; FDA: US Food and Drug Administration.

El Abraxane® es una suspensión de nanopartículas de albúmina y paclitaxel de tamaño comprendido entre los 130-150 nm. Esta formulación presenta varias ventajas frente al Taxol®, incluyendo i) reducción del tiempo de infusión (30 min frente a las 3 h de la formulación comercial), ii) menor incidencia o ausencia de reacciones de hipersensibilidad que permiten prescindir de la premedicación y iii) mejora de la eficacia antitumoral por la capacidad de administrar una dosis un 50% más alta sin comprometer la seguridad [11]. El Abraxane® está indicado para el tratamiento de cáncer de mama metastásico tras el fracaso de la quimioterapia combinada o recaída dentro de los 6 meses de quimioterapia adyuvante, cáncer de páncreas metastásico (combinado con gemcitabina) y cáncer de pulmón no microcítico (combinado con carboplatino) [12].

El Lipusu® es una formulación constituida por liposomas de aproximadamente 400 nm para la administración de paclitaxel. Esta formulación presenta una eficacia similar y un mejor perfil toxicológico que el Taxol®. Fue aprobado en el año 2003 en China, donde está comercializado para el tratamiento de cáncer de ovario y pulmón no microcítico [13]. Actualmente, se está evaluando su eficacia sobre las metástasis linfáticas del cáncer de pulmón en combinación con cisplatino [14].

Genexol-PM es una formulación de micelas poliméricas (20-50 nm) constituidas por un copolímero de ácido poliláctico-PEG para la administración de paclitaxel [15]. Recibió la aprobación de la FDA en 2002 y está comercializado desde el año 2007 en Corea y otros países como primera línea de terapia para el tratamiento del cáncer de mama metastásico o recurrente y cáncer de pulmón no microcítico localmente avanzado o metástasico [12]. También está indicado como terapia de primera línea para el tratamiento del cáncer de ovario en combinación con otros fármacos. En la actualidad se están realizando ensayos clínicos para evaluar esta formulación en terapia combinada con otros fármacos [12].

Otra formulación comercializada en la India y otros países desde 2007 para la administración de paclitaxel es el Nanoxel-PM En este caso se trata de micelas de un copolímero de polivinilpirrolidona y poliisopropilacrilamida y presentan un tamaño de 80-100 nm [16]. Está aprobado para el tratamiento del cáncer de mama metastásico, cáncer de ovario, cáncer de pulmón no microcítico y sarcoma de Kaposi [12].

En los últimos años se han diseñado numerosos nanosistemas para la administración de taxanos, tales como nanopartículas poliméricas y lipídicas, conjugados fármaco-polímero, micelas, liposomas y dendrímeros [17]. Tres de los nanosistemas desarrollados para la administración de paclitaxel se encuentran en una fase avanzada de su evaluación clínica (**Tabla 2**).

Tabla 2. Nanosistemas con paclitaxel en fase de evaluación clínica.

Producto	Formulación	Indicación (tipo de cáncer)	Compañía	Estado, identificador
NK-105	Micelas poliméricas	Mama	NanoCarrier	Fase III NCT01644890[18]
Opaxio	Conjugados	Pulmón Ovario, peritoneo y trompas de Falopio	Cell Therapeutics	Fase III NCT00054184[19] NCT00054197[20] NCT00108745[21]
Taxoprexin	Conjugados	Melanoma, Pulmón	Luitpold Pharmaceuticals	Fase III NCT00087776[22,23] NCT00243867[24]

El NK105 es una formulación consistente en micelas de ácido poliaspártico-PEG que presentan un tamaño medio de 85 nm (rango de tamaños 20-430 nm)[25]. Este sistema micelar ha demostrado una mejora en la farmacocinética y toxicidad frente al Taxol® y se encuentra actualmente en evaluación clínica fase III para el tratamiento del cáncer de mama metastásico o recurrente [18].

Dos conjugados fármaco-polímero también han conseguido llegar a ensayos clínicos. El primero de ellos ha sido el paclitaxel poliglumex (también denominado CT-2103, Xyotax® y más recientemente Opaxio®), un conjugado de ácido poliglutámico y paclitaxel que ha permitido reducir el tiempo de infusión, reducir la toxicidad y aumentar la eficacia del Taxol® [26]. Está siendo evaluado en fase III para el tratamiento del cáncer de ovario, peritoneo y trompas de Falopio [21] y del cáncer de pulmón no microcítico en monoterapia [19,20,27] o combinado con carboplatino [28]. La otra formulación basada en conjugados es el Taxoprexin®, constituido por un

conjugado de paclitaxel y un ácido graso, concretamente el ácido docosahexaenoico. Esta formulación ha sido diseñada para aumentar la entrega selectiva en el tumor basándose en la idea de que los tumores presentan una gran avidez de ácidos grasos necesarios para el crecimiento tumoral. Para mejorar su limitada solubilidad acuosa contiene Cremophor, pero en niveles un 80% inferiores a los del Taxol®, por lo que presenta un mejor perfil toxicológico. Esta formulación ha completado la fase III para el tratamiento el melanoma metastásico [23] y para el cáncer de pulmón en combinación con carboplatino [24]. En concreto, los ensayos realizados en pacientes con melanoma revelaron una eficacia similar a la dacarbazina y una mayor incidencia de mielosupresión [23].

Nanosistemas para la administración de docetaxel

En la actualidad no existe ningún nanomedicamento comercializado para la administración de docetaxel que ofrezca una alternativa al Taxotere® aunque algunos nanomedicamentos han alcanzado la fase de evaluación clínica, por lo que es posible que alguno de ellos sea comercializado en un futuro próximo (**Tabla 3**).

El ANX-514 es una nanoemulsión liofilizada de docetaxel inyectable por vía intravenosa libre de polisorbato 80 y etanol, desarrollada por Adventrx pharmaceuticals (San Diego, EEUU) para reducir la gravedad y/o incidencia de reacciones de hipersensibilidad asociadas al tratamiento con Taxotere®. Esta formulación demostró su bioequivalencia con el Taxotere a nivel preclínico, pero no ha conseguido este reconocimiento en los ensayos realizados recientemente en humanos [12,29,30].

También se han evaluado dos formulaciones basadas en liposomas. El LE-DT desarrollado por NeoPharm (Lake Forrest, EEUU) ha completado los ensayos clínicos fase I y II para evaluar su eficacia y seguridad en el cáncer de páncreas localmente avanzado o metastásico y cáncer de próstata metastásico [31–33]. Por su parte, los ensayos clínicos fase I de la formulación ATI-1123 desarrollada por Azaya Therapeutics (San Antonio, EEUU) han evaluado su seguridad para el tratamiento de tumores sólidos avanzados [7,34].

Tabla 3. Nanosistemas con docetaxel en fase de evaluación clínica.

Producto	Formulación	Indicación (tipo de cáncer)	Compañía	Estado, identificador
ANX-514	NE	Avanzados	Adventrx pharmaceuticals Inc	Fase I NCT00664170[30]
ATI-1123	Liposomas	Tumores sólidos avanzados	Azaya Therapeutics	Fase I NCT01041235 [34]
BIND-014	NPs	CPNM y próstata metastásico resistente a la castración	Bind Therapeutics Inc	Fase II NCT01792479 [35] NCT01812746 [36] NCT02283320 [37]
Cripec	NPs	Tumores sólidos	Cristal Therapeutics	Fase I NCT02442531 [38]
Dendrimer-DTX	Dendrímeros	Mama	Sylvania Platinum Ltd	Aprobado para Fase I/II [39]
DTX-PNP	NPs poliméricas	Tumores sólidos avanzados	Samyang Pharmaceuticals	Fase I (Corea)[40]
LE-DT	Liposomas	Páncreas avanzado o metastásico, próstata metastásico	Insys Therapeutics Inc	Fase II NCT01186731 [32] NCT01188408 [33]
NKTR-105	Conjugado docetaxel-PEG	Tumores sólidos	Nektar Thera-peutics	Fase I [41]
CRLX301	NPs	Tumores sólidos	Cerulean Pharma Inc	Fase I [42]

Abreviaturas: CPNM: carcinoma pulmonar no microcítico, NE: nanoemulsión; NPs: nanopartículas.

Uno de los nanosistemas más prometedores hasta la fecha es el BIND-014, una formulación de nanopartículas constituidas por ácido poli(ácido láctico)-poli(etilenglicol) propiedad de BIND Therapeutics (Cambridge, EEUU). Estas nanopartículas presentan un tamaño de partícula en torno a 100 nm y contienen un ligando denominado ACUPA (S, S-2-[3- [-1-carboxipentil 5-amino] ureido] ácido pentanodióico) para vectorizarlas de forma activa hacia el antígeno prostático específico

de membrana (PSMA) expresado en las células de cáncer de próstata y en la neovasculatura de otros tumores sólidos [43]. Esta formulación ha sido seleccionada a partir de una biblioteca combinatoria de más de 100 composiciones de nanopartículas con diferente peso molecular de los polímeros, tamaño de partícula, propiedades superficiales, densidad de ligando, carga de fármaco y propiedades de liberación. BIND-014 se encuentra actualmente en ensayos clínicos fase II para cáncer de pulmón no microcítico y cáncer de próstata metastásico resistente a la castración. Ha demostrado que su prolongado tiempo de circulación en sangre (vida media en torno a 20 horas), capacidad para vehiculizar activamente las nanopartículas y lograr la liberación controlada de docetaxel, aumenta considerablemente la cantidad de docetaxel entregada al tumor y consigue inhibir el crecimiento tumoral durante un largo periodo de tiempo con menor toxicidad que el Taxotere® [44].

Otra formulación basada en nanopartículas que ha alcanzado la fase de evaluación clínica es el DTX-PNP. Estas nanopartículas poliméricas desarrolladas por Samyang Pharmaceuticals (Seúl, Corea) están constituidas por una mezcla de sales de metales monovalentes de poli(ácido láctico) y copolímeros dibloque anfifílicos. Han sido evaluadas en ensayos fase I para el tratamiento de varios tumores sólidos en Corea [40].

También objeto de ensayos clínicos es la formulación denominada NKTR-105, un conjugado docetaxel-PEG desarrollado por Nektar Therapeutics (San Francisco, EEUU) para pacientes con tumores sólidos como el cáncer de próstata hormono-refractario (fase I) [41] y una formulación basada en dendrímeros (dendrimer-DTX) desarrollada por Sylvania Platinum Ltd (Hamilton, Bermudas), cuyos ensayos clínicos fase I/II han sido recientemente aprobados [39].

Este mismo año dos nuevas formulaciones basadas en nanopartículas conjugadas con docetaxel, CRLX301 [42] y Cripec® [38,45], han alcanzado la evaluación clínica fase I para el tratamiento de tumores sólidos. Ambas formulaciones ha demostrado en la evaluación preclínica una eficacia antitumoral y seguridad superiores al Taxotere®.

Algunos nanosistemas basados en lípidos ofrecen resultados prometedores por su capacidad para la liberación de fármacos de naturaleza hidrofóbica como los taxanos. Por ejemplo, las nanocápsulas recubiertas de poliaminoácidos y polisacáridos desarrolladas por nuestro grupo para la liberación de docetaxel han demostrado una alta

capacidad de internalización en células tumorales y una elevada eficacia antitumoral con baja toxicidad en diversos modelos *in vitro* e *in vivo* [46–51], motivo por el cual constituyen una importante línea de investigación.

En conjunto de entre todos los sistemas desarrollados para la liberación de taxanos destacan el Abraxane® (nanopartículas de albúmina), el NK-105 (NanoCarrier, micelas poliméricas), BIND-014 (BIND Therapeutics, nanopartículas de PLA-PEG ACUPA) y aquellos que contienen los taxanos unidos covalentemente como Opaxio® (conjugado ácido poliglutámico-paclitaxel), Taxoprexin® (conjugado ácido docosahexaenoico-paclitaxel), CRLX301 (Cerulean Pharma, nanopartículas de ciclodextrina) y Cripec® (nanopartículas poliméricas). A pesar de los notables avances logrados con estas terapias, la opinión generalizada es que el éxito globalmente alcanzado con estos nanosistemas es aún moderado. Esto se explica en parte por la limitada acumulación del fármaco citotóxico en el tejido tumoral y también en el sistema linfático, lo que se traduce en un balance eficacia/toxicidad lejos de ser óptimo. Cabe destacar además que la información disponible sobre los ensayos clínicos realizados y, en general, sobre la farmacocinética y eficacia de las formulaciones investigadas, es limitada. De hecho, en muchos casos no se valora la eficacia de los nanosistemas sobre las metástasis, lo que podría explicar la falta de resultados positivos a largo plazo y el fracaso de algunos de los nanosistemas investigados.

REFERENCIAS

[1] Ferlay J, Soerjomataram I, Ervik M, Dikshit R, Eser S, Mathers C, et al. GLOBOCAN 2012 v1.0, Cancer Incidence and Mortality Worldwide [Internet]. IARC CancerBase No. 11 [Internet]. Lyon, Fr. Int. Agency Res. Cancer2013 [cited 2014 Oct 3];Available from: http://globocan.iarc.fr

[2] Siegel RL, Miller KD, Jemal A. Cancer Statistics, 2015. CA. Cancer J. Clin. 2015;65:5–29.

[3] Schroeder A, Heller DA, Winslow MM, Dahlman JE, Pratt GW, Langer R, et al. Treating metastatic cancer with nanotechnology. Nat. Rev. Cancer 2012;12:39–50.

[4] Yared JA, Tkaczuk KHR. Update on taxane development: new analogs and new formulations. Drug Des. Devel. Ther. 2012;6:371–84.

[5] Ringel I, Horwitz S. Studies With RP 56976 (Taxotere): A Semisynthetic Analogue of Taxol. J. Natl. Cancer Inst. 1991;83:288–91.

[6] Feng L, Mumper RJ. A critical review of lipid-based nanoparticles for taxane delivery. Cancer Lett. 2013;334:157–75.

[7] Zhang L, Zhang N. How nanotechnology can enhance docetaxel therapy. Int. J. Nanomedicine 2013;8:2927–41.

[8] Weiszhár Z, Czúcz J, Révész C, Rosivall L, Szebeni J, Rozsnyay Z. Complement activation by polyethoxylated pharmaceutical surfactants: Cremophor-EL, Tween-80 and Tween-20. Eur. J. Pharm. Sci. 2012;45:492–8.

[9] Hervella P, Lozano V, Garcia-Fuentes M, Alonso MJ. Nanomedicine : New Challenges and Opportunities in Cancer Therapy. J. Biomed. Nanotechnol. 2008;4:1–17.

[10] Peer D, Karp JM, Hong S, Farokhzad OC, Margalit R, Langer R. Nanocarriers as an emerging platform for cancer therapy. Nat. Nanotechnol. 2007;2:751–60.

[11] Ibrahim NK, Desai N, Legha S, Soon-Shiong P, Theriault RL, Rivera E, et al. Phase I and Pharmacokinetic Study of ABI-007, a Cremophor-free, Protein-stabilized, Nanoparticle Formulation of Paclitaxel. Clin. Cancer Res. 2002;8:1038–44.

[12] Reddy LH, Bazile D. Drug delivery design for intravenous route with integrated physicochemistry, pharmacokinetics and pharmacodynamics: Illustration with the case of taxane therapeutics. Adv. Drug Deliv. Rev. 2014;71:34–57.

[13] Ye L, He J, Hu Z, Dong Q, Wang H, Fu F, et al. Antitumor effect and toxicity of Lipusu in rat ovarian cancer xenografts. Food Chem. Toxicol. 2013;52:200–6.

[14] Hu L, Liang G, Yuliang W, Bingjing Z, Xiangdong Z, Rufu X. Assessing the effectiveness and safety of liposomal paclitaxel in combination with cisplatin as first-line chemotherapy for patients with advanced NSCLC with regional lymph-node metastasis: study protocol for a randomized controlled trial (PLC-GC trial). Trials 2013;14:45.

[15] Kim SC, Kim DW, Shim YH, Bang JS, Oh HS, Kim SW, et al. In vivo evaluation of polymeric micellar paclitaxel formulation: Toxicity and efficacy. J. Control. Release 2001;72:191–202.

[16] Maitra A, Sahoo SK, Ghosh PK, Burman AC, Mukherjee R, Khattar D, et al. Formulations of paclitaxel, its derivatives or its analogs entrapped into nanoparticles of polymeric micelles, process for preparing same and the use thereof. 2001;

[17] Zhang L, Zhang N. How nanotechnology can enhance docetaxel therapy. Int. J. Nanomedicine 2013;8:2927–41.

[18] A Phase III Study of NK105 in Patients With Breast Cancer [Internet]. [cited 2015 Jul 29];ClinicalTrials.gov. Available from: https://clinicaltrials.gov/ct2/show/NCT01644890?term=nk105&rank=1

[19] Polyglutamate Paclitaxel Compared With Docetaxel in Treating Patients With Progressive Non-Small Cell Lung Cancer [Internet]. [cited 2015 Jul 29];clinicaltrials.gov. Available from: https://clinicaltrials.gov/ct2/show/NCT00054184?term=paclitaxel+poliglumex++and+phase+III&rank=2

[20] Polyglutamate Paclitaxel Compared With Gemcitabine or Vinorelbine in Treating Patients With Advanced or Recurrent Non-Small Cell Lung Cancer [Internet]. [cited 2015 Jul 29];clinical trials.gov. Available from: https://clinicaltrials.gov/ct2/show/NCT00054197?term=paclitaxel+poliglumex++and+phase+III&rank=4

[21] Paclitaxel or Polyglutamate Paclitaxel or Observation in Treating Patients With Stage III or Stage IV Ovarian Epithelial or Peritoneal Cancer or Fallopian Tube Cancer [Internet]. [cited 2015 Jul 29];clinicaltrials.gov. Available from: https://clinicaltrials.gov/ct2/show/NCT00108745?term=paclitaxel+poliglumex++and+phase+III&rank=1

[22] Study of Taxoprexin Injection vs. Dacarbazine in Patients With Metastatic Malignant Melanoma [Internet]. [cited 2015 Jul 29];clinicaltrials.gov. Available from: https://clinicaltrials.gov/ct2/show/NCT00087776?term=taxoprexin&rank=6

[23] Bedikian AY, DeConti RC, Conry R, Agarwala S, Papadopoulos N, Kim KB, et al. Phase 3 study of docosahexaenoic acid-paclitaxel versus dacarbazine in patients with metastatic malignant melanoma. Ann. Oncol. 2011;22:787–93.

[24] Taxoprexin Plus Carboplatin Treatment for Advanced Lung Cancer [Internet]. [cited 2015 Jul 29];clinicaltrials.gov. Available from: https://clinicaltrials.gov/ct2/show/NCT00243867?term=taxoprexin&rank=1

[25] Hamaguchi T, Matsumura Y, Suzuki M, Shimizu K, Goda R, Nakamura I, et al. NK105, a paclitaxel-incorporating micellar nanoparticle formulation, can extend in vivo antitumour activity and reduce the neurotoxicity of paclitaxel. Br. J. Cancer 2005;92:1240–6.

[26] Singer JW. Paclitaxel poliglumex (XYOTAX, CT-2103): A macromolecular taxane. J. Control. Release 2005;109:120–6.

[27] Paz-Ares L, Ross H, O'Brien M, Riviere A, Gatzemeier U, Von Pawel J, et al. Phase III trial comparing paclitaxel poliglumex vs docetaxel in the second-line treatment of non-small-cell lung cancer. Br. J. Cancer 2008;98:1608–13.

[28] Polyglutamate Paclitaxel Plus Carboplatin Compared With Paclitaxel Plus Carboplatin in Treating Patients With Advanced or Recurrent Non-Small Cell Lung Cancer [Internet]. [cited 2015 Jul 29];clinicaltrials.gov. Available from: https://clinicaltrials.gov/ct2/show/NCT00054210?term=paclitaxel+poliglumex++and+phase+III&rank=3

[29] Cantwell M, Robbins J, Chen A. A novel emulsion formulation of docetaxel eliminates hypersensitivity reactions without impacting pharmacokinetics or antitumor activity. In: Research AA for C, editor. Molecular cancer therapeutics. Los Angeles, CA: 2007. page C118.

[30] A Bioequivalence Study of Docetaxel for Injectable Emulsion (ANX-514) in Patients With Advanced Cancer [Internet]. [cited 2015 May 1];Clinicaltrials.gov. Available from: https://clinicaltrials.gov/ct2/results?term=ANX-514&Search=Search

[31] Deeken JF, Slack R, Weiss GJ, Ramanathan RK, Pishvaian MJ, Hwang J, et al. A phase I study of liposomal-encapsulated docetaxel (LE-DT) in patients with advanced solid tumor malignancies. Cancer Chemother. Pharmacol. 2013;71:627–33.

[32] Efficacy and Safety Study of LE-DT to Treat Locally Advanced or Metastatic Pancreatic Cancer [Internet]. [cited 2015 May 1];Clinicaltrials.gov. Available from: https://clinicaltrials.gov/ct2/results?term=NCT01186731&Search=Search

[33] Efficacy and Safety Study of LE-DT to Treat Metastatic Castrate Resistant Prostate Cancer [Internet]. [cited 2015 May 1];Clinicaltrials.gov. Available from: https://clinicaltrials.gov/ct2/show/study/NCT01188408?term=LE-DT&rank=3

[34] Safety Study of a Liposomal Docetaxel Formulation in Patients With Solid Tumors Who Have Failed Previous Therapies [Internet]. [cited 2015 May 1];Clinicaltrials.gov. Available from: https://clinicaltrials.gov/ct2/results?term=NCT01041235&Search=Search

[35] A Phase 2 study to determine the safety and efficacy of BIND-014 (docetaxel nanoparticles injectable suspension) as second line therapy to patients with non-small cell lung cancer [Internet]. [cited 2015 May 1];ClinicalTrials.gov. Available from: http://clinicaltrials.gov/show/NCT01792479

[36] A Phase 2 study to determine the safety and efficacy of BIND-014 (docetaxel nanoparticles injectable suspension), administered to patients with metastatic castration-resistant prostate cancer [Internet]. [cited 2015 May 1];ClinicalTrials.gov. Available from: http://clinicaltrials.gov/show/NCT01812746

[37] A Study of BIND-014 (Docetaxel Nanoparticles for Injectable Suspension) as Second-line Therapy for Patients With KRAS Positive or Squamous Cell Non-Small Cell Lung Cancer [Internet]. [cited 2015 May 1];Clinicaltrials.gov. Available from: https://clinicaltrials.gov/ct2/show/NCT02283320?term=BIND-014&rank=4

[38] A Study of CriPec® Docetaxel Given to Patients With Solid Tumours (NAPOLY) [Internet]. Clin. trilas.gov [cited 2015 Sep 18];Available from: https://clinicaltrials.gov/ct2/show/NCT02442531?term=Cripec&rank=1

[39] Tan Q, Liu X, Fu X, Li Q, Dou J, Zhai G. Current development in nanoformulations of docetaxel. Expert Opin. Drug Deliv. 2012;9:975–90.

[40] Svenson S. Clinical translation of nanomedicines. Curr. Opin. Solid State Mater. Sci. 2012;16:287–94.

[41] Vicent MJ, Ringsdorf H, Duncan R. Polymer therapeutics : Clinical applications and challenges for development. Adv. Drug Deliv. Rev. 2009;61:1117–20.

[42] Phase 1/2a Dose-Escalation Study of CRLX301 in Patients With Advanced Solid Tumors [Internet]. Clin. trilas.gov [cited 2015 Sep 4];Available from: https://clinicaltrials.gov/ct2/show/NCT02380677?term=CRLX301&rank=1

[43] Hrkach J, Von Hoff D, Mukkaram Ali M, Andrianova E, Auer J, Campbell T, et al. Preclinical development and clinical translation of a PSMA-targeted docetaxel nanoparticle with a differentiated pharmacological profile. Sci. Transl. Med. 2012;4:128ra39.

[44] Sanna V, Pala N, Sechi M. Targeted therapy using nanotechnology: Focus on cancer. Int. J. Nanomedicine 2014;9:467–83.

[45] Hu Q, Rijcken CJ, Bansal R, Hennink WE, Storm G, Prakash J. Complete regression of breast tumour with a single dose of docetaxel-entrapped core-cross-linked polymeric micelles. Biomaterials 2015;53:370–8.

[46] Lozano M V, Torrecilla D, Torres D, Vidal A, Domínguez F, Alonso MJ. Highly efficient system to deliver taxanes into tumor cells: docetaxel-loaded chitosan oligomer colloidal carriers. Biomacromolecules 2008;9:2186–93.

[47] Torrecilla D, Lozano M V., Lallana E, Neissa JI, Novoa-Carballal R, Vidal A, et al. Anti-tumor efficacy of chitosan-g-poly(ethylene glycol) nanocapsules containing docetaxel: Anti-TMEFF-2 functionalized nanocapsules vs. non-functionalized nanocapsules. Eur. J. Pharm. Biopharm. 2013;83:330–7.

[48] Lozano M V, Esteban H, Brea J, Loza MI, Torres D, Alonso MJ. Intracellular delivery of docetaxel using freeze-dried polysaccharide nanocapsules. J. Microencapsul. 2013;30:181–8.

[49] Oyarzun-Ampuero FA, Rivera-Rodríguez GR, Alonso MJ, Torres D. Hyaluronan nanocapsules as a new vehicle for intracellular drug delivery. Eur. J. Pharm. Sci. 2013;49:483–90.

[50] Rivera-Rodriguez GR, Lollo G, Montier T, Benoit JP, Passirani C, Alonso MJ, et al. In vivo evaluation of poly-l-asparagine nanocapsules as carriers for anti-cancer drug delivery. Int. J. Pharm. 2013;458:83–9.

[51] Lollo G, Rivera-Rodriguez GR, Bejaud J, Passirani C, Benoit JP, García-Fuentes M, et al. Polyglutamic acid-PEG nanocapsules as long circulated carriers for the delivery of docetaxel. Eur. J. Pharm. Biopharm. 2014;87:47–54.

Capítulo 1

Lymphatic Targeting of Nanosystems for Anticancer Drug Therapy

USC
UNIVERSIDADE
DE SANTIAGO
DE COMPOSTELA

ABSTRACT

The lymphatic system represents a major route of dissemination in metastatic cancer. Given the lack of selectivity of conventional chemotherapy to prevent lymphatic metastasis, in the last years there has been a growing interest in the development of nanocarriers showing lymphotropic characteristics. The goal of this lympho-targeting strategy is to facilitate the delivery of anticancer drugs to the lymph node-resident cancer cells, thereby enhancing the effectiveness of the anti-cancer therapies. This article focuses on the nanosystems described so far for the active or passive targeting of oncological drugs to the lymphatic circulation. To understand the design and performance of these nanosystems, we will discuss first the physiology of the lymphatic system and how physiopathological changes associated to tumor growth influence the biodistribution of nanocarriers. Second, we provide evidence on how the tailoring of the physicochemical characteristics of nanosystems, *i.e.* particle size, surface charge and hydrophilicity, allows the modulation of their access to the lymphatic circulation. Finally, we provide an overview of the relationship between the biodistribution and anti-metastatic activity of the nanocarriers loaded with oncological drugs, and illustrate the most promising active targeting approaches investigated so far.

Keywords: Lymphatic targeting, lymph nodes, anticancer drug delivery, metastases, nanocarriers, particle size, surface properties.

USC
UNIVERSIDADE
DE SANTIAGO
DE COMPOSTELA

1 Introduction: Overview of the Lymphatic System

1.1 Physiological and Biomechanical Considerations

The lymphatic system is a highly specialized part of the vascular system, whose functions are i) the maintenance of normal tissue fluid balance, ii) the uptake of lipids and liposoluble vitamins ingested with the diet and iii) the trafficking of immune cells. It consists of a branched network of conduits such as capillaries and collecting vessels that transport fluid, proteins and cellular elements from the interstitial tissue towards the circulatory system. In addition to this capillary network, the lymphatic system also comprises lymphatic organs such as lymph nodes, the spleen, thymus, Peyer's patches and tonsils [1]. The lymphatic capillaries are blind-ending vessels, consisting of non-fenestrated lymphatic endothelial cells (LECs) with a discontinuous, non-prominent basement membrane. These cells are generally non-contractile, lack tight and adherens junctions and are attached to the extracellular matrix (ECM) by elastic anchoring filaments. When the extravasated fluid accumulates in the interstitial space, the increased pressure promotes the opening of the cell-cell junctions, making the lymphatic capillaries highly permeable. Once the fluid enters, the pressure difference across the vessel wall diminishes and prevents retrograde flow [2–4]. This functional structure is very different from that of the blood vessels where a continuous endothelium provided with tight junctions which make them much less permeable [5].

In general, the composition of lymph is essentially the same as the one of the interstitial fluid, with the exception of the intestinal lymph, which contains a much higher concentration of lipids [3]. Once formed, lymph is unidirectionally pumped from the capillaries to the collecting vessels due to the pressure dependent contractility of the smooth muscle cells lining the lymphatics [6,7]. During its return to the blood circulation, lymph passes through one or more lymph nodes, where it is filtered by the reticular fibers and the activity of node-resident macrophages and lymphocytes [7,8]. Once filtered, the lymph is driven to the lymphatic trunks and ducts, reaching ultimately the venous circulation at the junction of the left internal jugular and the left subclavian veins [5].

1.2 The Lymphatic System: a Pathway for Metastatic Spreading

Primary tumors may disseminate through both the blood and the lymphatic vascular routes. Unlike the extensive amount of knowledge accumulated on the blood-related metastatic process, the role of the lymphatic system on the dissemination of metastatic cells has only attracted the attention of scientists in the last decades [3]. The recent identification of a number of lymphatic markers expressed in the LECs, such as the vascular endothelium growth factor-3 (VEGF-3) [9], the Lymphatic Vessel Endothelial Hyaluronan Receptor-1 (LYVE-1) [10], the membrane glycoprotein podoplanin and the transcription factors Prox-1 [11] and SOX-18 [12,13], and the development of suitable animal models to study lymphangiogenesis, have contributed to the understanding of the way cancer cells exploit the lymphatic system as a route of dissemination [14,15]. Nowadays, it is accepted that the spread of cancer cells through the lymphatic vessels is particularly efficient due to the large size of the lymphatic vessels and to the slow flow of the fluid. Moreover, cancer cells can accumulate in the lymph nodes and access the bloodstream from there. The fact that lymph has almost the same composition as the interstitial fluid also promotes cell viability in the lymphatic system. On the contrary, cancer cells in the bloodstream are exposed to high shear stresses and mechanical deformation, which may hinder the metastatic process [16].

In pathological conditions such as cancer, tumor cells, endothelial cells and inflammatory cells produce lymphangiogenic growth factors and other molecules such as chemokines and cytokines, which may activate tumor-induced lymphangiogenesis or stimulate the attraction and invasion of cancer cells into the lymphatics [17–20]. The first, and most studied, growth factors involved in the tumor-stimulated lymphangiogenesis are the vascular endothelial growth factors VEGF-C and VEGF-D, which activate the vascular endothelial growth factor receptor 3 (VEGFR3) expressed on the lymphatic endothelium [18,19]. They promote lymphangiogenesis and the sprouting of new lymphatic vessels within the tumor, its periphery [18,21] or even in the sentinel lymph node. This latter process may occur even before the arrival of the cancer cells, forming a pre-metastatic niche that facilitates subsequent tumor growth and distant metastasis [22]. Thus, a direct correlation between the levels of these growth factors with the lymphangiogenesis and metastasis has been evidenced [23–26]. Factors overexpressed by tumor cells or LECs may also stimulate the attraction and invasion of

cancer cells into the lymphatics, for instance, by mimicking the physiologic mechanism of cytokine-mediated migration of lymphocytes [17,26].

Over the last years a debate has been raised about the functionality of the tumor-associated lymphatic vessels, which, in general, varies depending on the type, stage and tumor localization [27]. It is generally accepted that the solid tumor environment usually exhibits a disturbed fluid balance [28–30] with an increased interstitial fluid pressure (IFP). This is due to the hyperpermeability of the immature tumor vessels and the mechanical stress associated to the ECM production [30]. The resulting strong pressure gradient promotes the flow of the interstitial fluid from the tumor towards the peritumoral lymphatic vessels [31,32]. These alterations may also contribute to the entrance of tumor cells into the lymphatics. Once inside the lymphatic system, cancer cells can settle and stay in the draining lymph nodes before spreading to other lymph nodes or distant sites [33]. As a consequence, these so-called sentinel lymph nodes may be important targets for diagnostic and therapeutic purposes.

2 Critical Factors in Nanocarrier-Mediated Lymphatic Targeting

Traditionally, anticancer therapy research has been focused on the delivery of drugs to the tumor microenvironment. The outcome of such conventional intravenous chemotherapy in metastatic cancer has been limited by the incapacity of drugs to reach the target cells, both in the tumor site and in the lymphatic system [34,35]. Nanocarrier-based drug delivery to the lymph nodes is not only considered relevant in the treatment of lymphatic cancers, such as lymphoma or leukemia, but also in the treatment of cancers with lymphatic metastases, such as breast, lung, head and neck squamous cell cancers, and intraperitoneal tumors, among others [36–38]. Nanocarriers can promote both the uptake and the retention of the associated drugs in the lymph nodes, thus improving the treatment of lymph node-resident cancers. The extent and rate at which nanosystems reach and accumulate in the lymphatic system are influenced by physiological factors associated with the route of administration and with the lymphatic/tumor physiology, and also by the physicochemical properties of the nanocarriers. These parameters should be carefully considered for the rational design of

lymphotropic nanocarriers and will, therefore, be discussed in detail in the following sections.

2.1 Route of Administration

The choice of the administration route is critical for achieving efficient lymphatic delivery of anticancer drugs (**Figure 1**). Extravascular routes, such as the subcutaneous (SC), intratumoral or intraperitoneal (IP) ones, have been widely investigated for the lymphatic targeting of nanosystems, as shown in Table 1. Upon **subcutaneous or intratumoral injection,** the nano-sized drug delivery systems must migrate through the interstitial space in order to access the lymphatic system. The interstitial space consists of a mix of fibrous collagen and negatively charged proteoglycans, which act as physical and electrostatic barrier to nanoparticle transport [5]. Despite this barrier, it has been shown that specific nanocarriers, are able to drain from the injection site to the local lymphatics [39–41] and transport the associated drugs to the lymph nodes, thereby enhancing the antitumor efficacy in lymph node-resident metastatic cancer cells [37,42–44]. As indicated in a previous report, the anatomical site of injection influenced the delivery of the drug associated to the nanocarriers [39]. Namely, this report disclosed that, in healthy rats, the lymphatic uptake of liposomes was much higher after injection to the footpad than to the flank. This behavior was attributed to the local rise in the interstitial pressure in the footpad due to the different structural organization of the subcutaneous tissue (*e.g.* presence or absence of adipose tissue) at these two anatomical sites [39]. On the other hand, it has been reported that the concentrations of the nanosystems in the injected liquid may also influence their lymphatic targeting capacity. A high concentration may promote the aggregation of the nanostructures and make the drainage from the injection site to the initial lymphatic vessels more difficult [45,46]. This accumulation of drug in the subcutaneous tissue represents a critical hurdle, which restricts the potential of this route of administration.

In the case of the **intraperitoneal** administration, the lymphatic drainage from the abdominal cavity occurs through the subdiaphragmic stomata, which connect to the lymphatic vessels located in deep diaphragmic tissues [47,48]. The intraperitoneal administration has been used to facilitate the concentrations of antitumor drug within this cavity and also in its draining lymph nodes [47,49]. This route is particularly

interesting for the treatment of cancers, such as pancreatic, ovarian, liver, gastric and colon carcinomas, which are known to disseminate the peritoneum and the surrounding lymphatic system [50]. For instance, *Lu et al*. have shown that the intraperitoneal injection of paclitaxel loaded nanoparticles led to a 20-fold higher concentration in the pelvic lymph nodes, achieving higher antitumor efficacy in an orthotopic ovarian cancer model than free paclitaxel [49].

In order to get access to the lymphatic system following intravenous administration, drugs should first extravasate from the systemic circulation, go through the interstitial space and be collected by the lymphatics [51] (Figure 1). Overall, the lymphatic targeting of nanosystems by intravenous (IV) route has not been extensively studied [35]. This might be due to the well-known clearance of the nanocarriers by the Mononuclear Phagocyte System (MPS) [36] and the nature of the endothelial tissue which, in normal conditions, restricts the possibility of extravasation to small molecules and nanocarriers of a few nm [52]. Nevertheless, tumor growth involves the formation of new blood vessels with severe abnormalities that enable the extravasation of larger nanocarriers [53,54].

Despite the promoted extravasation of nanocarriers from the tumor-associated blood vessels to the interstitial space, it has been traditionally assumed that deficiencies in the lymphatic system at the tumor site could hinder their lymphatic drainage, increasing their residence into the tumor. This has been the basis for the Enhanced Penetration Retention (EPR) effect [53–57]. However, currently it is known that this is not always the case. In fact, in some situations the peritumoral lymphatic vessels remain functional and the high interstitial pressure within the tumor drives the interstitial flow through the tumor stroma towards them, thereby enabling the lymphatic drainage of nanocarriers [27]. As an example, the work by Qin *et al*. [35] has shown that polymeric micelles of PEG-phosphatidylethanolamine intravenously administered to mice can extravasate from the blood vessels into the interstitial tissue, be collected by the lymphatics and accumulate in the lymph nodes. As a consequence, these micelles encapsulating vinorelbine were found to efficiently reduce the metastasis and increase survival rate as compared to the free drug. This extravasation has also been found in the case of other nanocarriers such as polylactide (PLA)-PEG based micelles [58], PEG-L-glutamic acid block copolymer micelles [59] and polylysine dendrimers [60]. In all these cases, a

small enough particle size, some flexibility in the structure and long circulating properties were needed for a successful extravasation from the bloodstream (detailed in section 2.2 and 2.3). Overall, intravenous administration should be considered a suitable route of choice for the treatment of distant lymphatic metastasis [51] and, in particular for the delivery of drugs that may cause local damage due to their cytotoxicity [35].

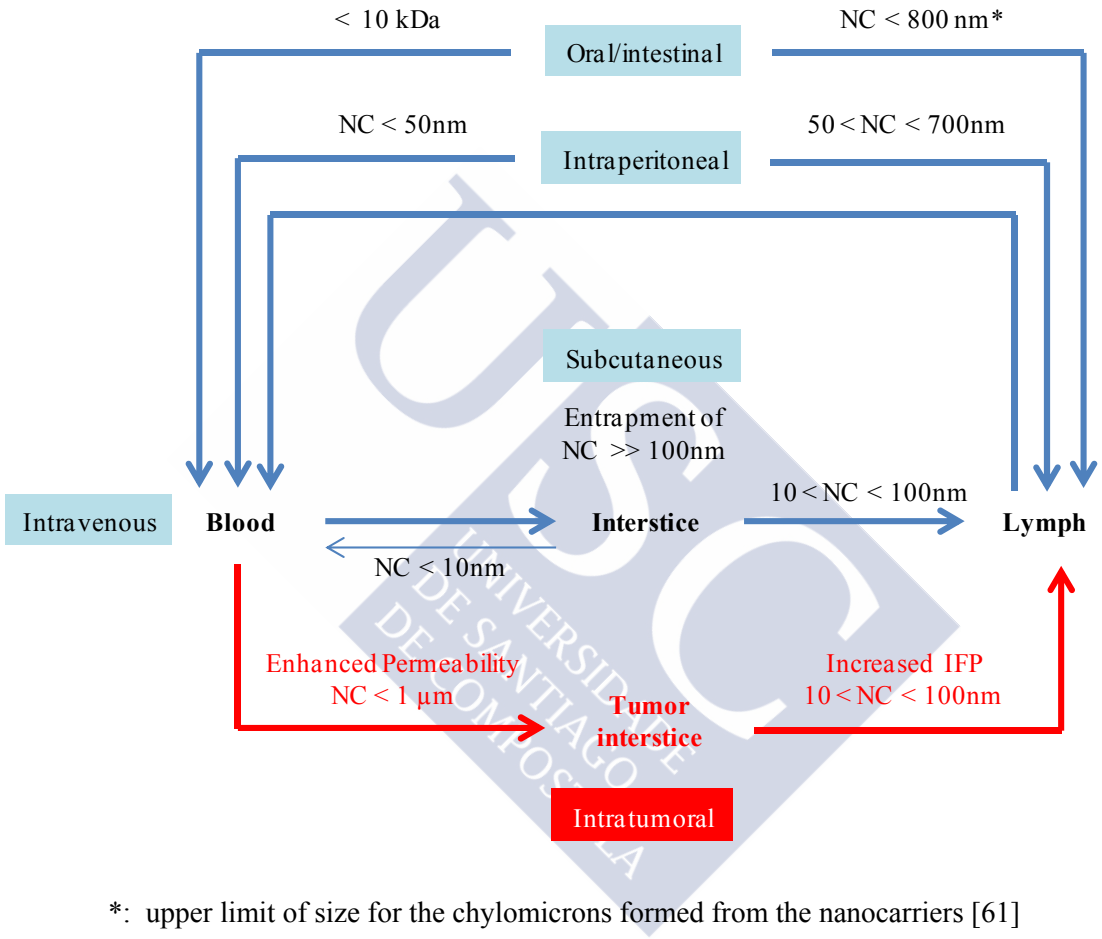

*: upper limit of size for the chylomicrons formed from the nanocarriers [61]

Figure 1. Pathways to access the lymphatic system depending on the administration route and the particle size of the administered nanocarriers (NC).

The delivery of anticancer drugs to the lymphatic system has also been attempted using the **oral** route, in particular for the treatment of gastrointestinal or mesenteric cancers. It is known that the lymphatic transport of lipophilic compounds is facilitated by the production of chylomicrons in the enterocytes, which dissolve and assimilate the lipids and lipophilic drugs [61–63]. In order to further promote this transport nanocarriers for

oral anticancer drug delivery have been mainly based on lipids. In addition to the treatment of lymph-resident cancers, the intestinal lymphatic transport of lipid nanocarriers is being investigated to enhance the lymphatic absorption of antitumor drugs with a high first-pass metabolism [43,64] and for the administration of drugs for which the intravenous route may be not recommended (*e.g.* edelfosine owing to its dose-dependent hemolytic effects) [65].

Although much less explored, the **pulmonary** route of administration has also been proposed as a way to reach the lymphatic system [36,66]. Pulmonary administration may be advantageous to treat lung tumors and their metastasis in adjacent draining lymph nodes [66,67], while avoiding high concentration of the drug at non-target tissues [36,68].

Despite the importance of the route of the administration, only a limited number of studies have been conducted to compare systematically lymphatic uptake and biodistribution of nanocarriers with the same composition and different routes of administration in a cancer model. For example, some authors have recently showed that the access of lipid nanocapsules to the lymph nodes, was more effective upon SC as compared to IV injection [41]. Similarly Reddy *et al*. have found that the lymphatic uptake of etoposide-loaded tripalmitin nanoparticles (390 nm) in lymphoma bearing mice was more successful after subcutaneous than after intraperitoneal injection, which in turn was also better than the intravenous injection [42]. In another work, Chen and coworkers investigated the antitumor effect of doxorubicin-loaded liposomes (size ~120 nm) administered by SC, IV or a combination of both routes in a metastatic breast cancer model [69]. While the IV route showed a significant inhibitory effect on breast tumors and distant metastases, those in axillary and mediastinal lymph nodes were more efficiently inhibited after SC injection. Furthermore, doxorubicin-loaded liposomes administered concurrently through both, IV and SC routes, were more effective for the treatment of breast tumors with metastases in local-regional lymph nodes, lungs and liver, thus suggesting that this combined administration fashion may be advantageous for the treatment of metastatic cancer.

2.2 Particle Size and Shape of Nanocarriers

Irrespective of the route of administration, the uptake of nanocarriers by the lymphatics is highly dependent on their size (Figure 1) [70,71]. It has been reported that upon subcutaneous administration, very small liposomes (few nm) were exchanged through blood capillaries, whereas larger liposomes (10-100 nm) could migrate from the injection point and reach lymphatic vessels through interstitial aqueous channels (100 nm) [72]. In contrast, larger liposomes (several hundreds of nm) were supposed to get trapped in the interstitial space, forming a reservoir, from which the associated drug may be released [73] and/or be transported to the lymphatics upon their uptake by the antigen presenting cells (APCs) [74,75]. The same kind of conclusion was reached when comparing the behavior of PLGA-PEG-based nanoparticles with a size comprised between 50 and 200 nm [71]. In addition to these reports on the lymphatic delivery of anticancer drugs, the different fate of small and large particles has been actively investigated in the vaccine delivery and immunotherapy fields [76–78].

The above-indicated 100 nm size limitation for the diffusion of the nanocarriers from the SC tissue to the lymphatics, also applies to intravenously administered nanocarriers. In this case this size limit is essential for the transport of the nanocarriers from the blood capillaries into the interstitial space and subsequent access to the lymphatics [51,57,79]. In contrast, in the case of intraperitoneal administration, the only important barrier the nanocarriers need to overcome before reaching the lymphatic system is the lymphatic capillary walls. This explains the observed fact that nanosystems with a size in the 50-700 nm range have been directly cleared through the lymphatic system [47,80]. In addition to the access to the lymphatics, the size of the nanocarriers has been reported to influence their retention into the lymph nodes. Namely, large nanocarriers are more efficiently retained than the smaller ones [47]. As a consequence, the overall influence of the size of the nanocarriers with regard to their efficacy for the treatment of lymphatic-spreading cancers depends on the balance of their access and retention dynamics within the lymphatics.

Besides particle size, particle shape can also influence the biodistribution of nanocarriers [81,82]. Several studies have indicated that the flexibility and deformability of nanocarriers can influence the blood circulation time, extravasation and

migration, thus affecting their ability to reach the lymph nodes [35,82–84]. However, the effects of particle shape and flexibility for specific lymphatic targeting have not been further elucidated in detail yet.

2.3 Surface Charge, Hydrophilic-Lipophilic Character of the Nanocarriers. Surface Modifications

The surface composition and charge of the nanocarriers are critical factors on their lymphatic targeting properties (Figure 2). A number of examples has been reported disclosing that anionic nanosystems can move more easily than the positively charged ones across the interstitial space. This is due to the electrostatic repulsion between the anionic nanosystems and negatively charged compounds of the extracellular matrix [85]. Namely, negatively charged liposomes were found to have a greater access to the lymph nodes than positive or neutral ones, following either subcutaneous [86,87], or intraperitoneal administration [80]. Similarly, the negative charge density of PLGA-based nanoparticles was also reported to influence positively both its lymphatic uptake and its retention [71]. On the contrary, positively charged nanocarriers have been reported to form a reservoir in the subcutaneous tissue from which they can be slowly drained into the lymphatics and/or taken-up by antigen presenting cells [88,89].

The hydrophilic-lipophilic character of the nanocarriers has been identified as one of the major determinants of the nanocarrier's access to the lymphatics. Generally, proteins and in particular opsonins, have a tendency to adsorb onto lipophilic surfaces and present them to the MPS. These phagocytic cells may eventually transport the engulfed particles to the lymph nodes [46,90]. On the contrary, nanocarriers with hydrophilic surfaces are prone to diffuse through the interstitial space and reach the lymphatics [71,91,92]. This lymphatic drainage may result more effective than the MPS mediated transport of the lipophilic carriers. However, once in the lymph nodes hydrophilic nanocarriers are expected to have a greater tendency than the hydrophobic ones, to escape into the blood circulation and this may be a drawback for their effectiveness. This hypothesis is supported by several studies reporting the *in vivo* biodistribution of liposomes or nanoparticles coated with polyethylene glycol (PEG) [72,91] or polyethylene oxide derivatives, such as poloxamers [93–95] and poloxamines [96]. The results of these studies indicated that liposomes with a more dense and longer PEG

coating had greater access to the lymphatics [91,97] but a lower retention in the lymph nodes [97]. Similarly, the lymphatic delivery of PLGA-PEG nanoparticles was found to be more pronounced when compared to that of hydrophobic polystyrene nanoparticles [71]. Taking this into account, it could be presumed that a nanocarrier with a hydrophobic core and a hydrophilic and detachable surface would fulfill the characteristics for an efficient drainage and subsequent retention in the lymph nodes.

In addition to the hydrophilic/lipophilic character, the chemical composition of the nanocarriers surface is a key determinant of their biodistribution and access to the lymphatics. Among the biomaterials used to facilitate the access of nanocarriers to the lymphatic system, hyaluronic acid is particularly well-known. It was chosen because it is a constituent of the extracellular matrix that is naturally cleared from the interstitial space by the lymphatic system. In addition, hyaluronic acid is able to interact with CD44 receptors that are overexpressed in many cancer cells and also with the LYVE-1 receptors expressed in the lymphatic endothelial cells [98]. For example, Tiantian *et al.* studied the pharmacokinetics and distribution of docetaxel associated to hyaluronic acid-modified liposomes following subcutaneous administration to mice and observed an increased lymphatic drainage and accumulation in the lymph nodes [99]. Similar results were reported for hyaluronic acid modified transfersomes with regard to their capacity to deliver doxorubicin to lymphatics through the transdermal route [83].

In addition to the possibility of using functional hydrophilic polymers, the surface of the nanocarriers can be decorated with specific ligands towards receptors expressed on the tumor lymphatic vessels or the metastatic lymph nodes. These actively targeted nanocarriers are described with more detail in section 3.8.

Carrier (10-100 nm)	Main route of access to lymphatic system
Anionic	**Diffusion through the interstitial space**
Cationic	**Migration mediated by APCs**
Neutral	**Diffusion/ Migration mediated by APCs**
Hydrophobic	**Migration mediated by APCs**
Hydrophilic	**Diffusion through the interstitial space**

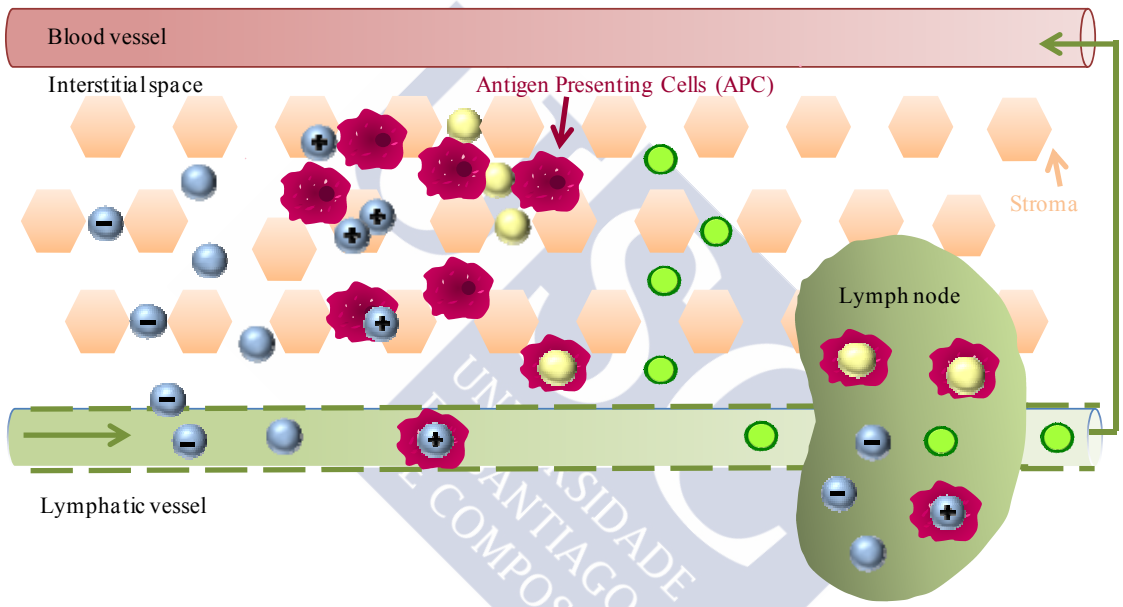

Figure 2. Illustration of the access of nanosystems with different surface properties to the lymphatic system (lymphatic vessels and lymph nodes). Anionic nanocarriers can diffuse through the interstitial space more easily than the positively charged ones, due to the electrostatic repulsion with the negatively charged compounds of the extracellular matrix. Nanocarriers with a hydrophilic surface are prone to migrate more easily than the hydrophobic ones towards the lymphatic vessels, although this approach may limit their retention in the lymph nodes. Both, positively charged and hydrophobic nanocarriers, may reach the lymph nodes mainly by the uptake of APC.

3 Nanocarriers for the Lymphatic Delivery of Antitumor Drugs

In the area of anticancer drug delivery, there are already a number of review articles describing the strategies attempted so far to reach the primary tumor [100,101]. There are also several review articles in the area of vaccine delivery and immunotherapies dealing with the targeting of the lymph nodes and other secondary lymph organs [102,103]. This review differs from the ones just mentioned, in that it aims to analyze the behavior of nanocarriers loaded with anticancer drugs designed to have a preferential accumulation in the lymphatic system and to be used for the treatment of metastatic cancer.

3.1 Liposomes

Liposomes have been the nanocarriers most studied for passive lymphatic targeting, often administered by intraperitoneal, subcutaneous or intramuscular route. They are spherical nanovesicles constituted by one, or more, lipid bilayers with an aqueous phase inside. As indicated, their lymphatic drainage from the interstitial injection site has been improved by coating them with a hydrophilic layer, most commonly with PEG [73]. One of the first works showing the potential of liposomes as carriers for the lymphatic targeting of anticancer drugs, *i.e.* doxorubicin, was reported by Parker and co-workers in 1981 [104]. Subsequently, this lympho-targeting behavior was used to explain the efficacy of doxorubicin-loaded liposomes to prevent the metastatic lymph node recurrence in different tumor animal models and, more importantly, in patients with gastric carcinoma [105]. More recently, a new liposomal formulation of paclitaxel commercialized in China (Lipusu®) for the treatment of ovarian cancer has been claimed to exhibit an accumulation in lymph nodes following intravenous administration [106,107]. Although the key for this lymphotropic behavior was not disclosed, apparently these promising data were the basis for the clinical development of a liposomal formulation containing paclitaxel combined with cisplatin, for the indication of advanced NSCLC with regional lymph-node metastasis [106,108].

The capacity of liposomes to reach the lymphatics has also been explored following pulmonary administration. For example, it has been shown that paclitaxel-loaded

liposomes could significantly reduce lymphatic metastasis in a renal [109] or breast cancer [110] mice models. Similar results were also obtained using a 9-nitro camptothecin and a vitamin E analogue (a-tocopheroyloxy acetic acid) liposomal formulation in a metastatic murine mammary tumor model [111]. Curiously, these liposomes were not PEGylated and their lymphatic uptake might be related to the route of administration.

Overall, liposomes have shown to be promising nanocarriers for the passive delivery of antitumor drugs to the lymphatics by different routes of administration. Current research is focused on the conjugation of PEGylated liposomes with different molecules to promote the active delivery to the targeted lymph nodes [112].

3.2 Nanoparticles

Nanoparticles are solid matrix systems that contain the drug dispersed within the particle or conjugated to the polymeric backbone. Among the wide range of materials used for the development of nanoparticles, synthetic polymers such as poly (lactides) (PLA) [49] and polyalkylcyanoacrylates (PACA) [50] and different lipid compounds including triglycerides, partial glycerides, fatty acids, cholesterol and waxes [43] have been the most studied for the lymphatic delivery of anticancer drugs.

In one specific study, (PLA) nanoparticles of 200 nm were reported to significantly increase the delivery of paclitaxel to both, the tumor and pelvic lymph nodes, following intraperitoneal administration. This translated into a higher reduction of tumor growth and ascites volume in an ovarian cancer model, as compared to the free drug [49]. On the other hand, it is worth mentioning that actively targeted docetaxel-loaded PLGA-PEG nanoparticles are currently in Phase II clinical trials for the treatment of NSLC and prostate cancer. In theory, these nanoparticles, due to their small size and PEGylation might be more appropriate for the lymphatic targeting. Although no claim of lymphatic targeting has been made so far, the successful results reported in the study mentioned above suggest that metastatic cancers might be related to a certain accumulation of these small (100 nm) nanoparticles in the lymph nodes [113–116].

Other polymeric system based on expansile nanoparticles has been recently developed for the administration of paclitaxel [117]. These crosslinked nanoparticles can be

prepared from diverse hydroxylated monomers (*e.g.* methyl-phenyl-dioxanylmethanol derivatives) through a miniemulsion-photopolymerization technique using pH sensitive protective groups. The advantage of these pH-responsive expansile nanoparticles lies in their ability to specifically release paclitaxel at the mildly acidic pH (<5) found within the cellular endosome of cancer cells and in the microenvironment of some solid tumors [118]. The migration of the intratumorally injected nanoparticles to the axillary lymph nodes resulted in a high intranodal paclitaxel concentration and therefore, in a significantly lower incidence of lymph node metastasis in an orthotopic breast cancer model [117]. Furthermore, the intradermal administration of these expansile nanoparticles in a swine model has also shown an efficient delivery of paclitaxel in the regional lymph nodes [119].

Nanoparticles based on PACA have also been explored for the lymphatic targeting of drugs. Maincent *et al.* have shown a significant accumulation in the lymph nodes of polyhexylcyanoacrylate nanoparticles following intraperitoneal administration to rats [50]. This and several other studies have been the basis for the clinical development of doxorubicin-polyisocyanoacrylate nanoparticles for cancer therapy [120], currently under investigation in phase II/III clinical trials [121]. More recently, Tan *et al.* have developed poly(butylcyanoacrylate) nanoparticles with a mean diameter of 115 nm, and a surface modified with Pluronic® F127 to improve the lymphatic targeting of vincristine [95]. These authors showed that, following intravenous administration, these nanoparticles were able to facilitate the accumulation of vincristine in the lymphatics, thereby increasing the efficacy of this drug in the treatment of Burkitt's lymphoma.

Although in a less advanced stage, solid lipid nanoparticles have also shown potential for the lymphatic targeting of anticancer drugs. For example, Lu *et al.* showed that the administration of mitoxantrone encapsulated in solid lipid nanoparticles led to an enhanced drug concentration in the regional lymph nodes and an improved therapeutic effect against breast cancer with lymph node metastases in an orthotopic mouse model [122].

Solid lipid nanoparticles have also shown to be promising for lymphatic targeting via the oral route [123]. This is due to the evidence that some of the lipids commonly used for their preparation (triglycerides, partial glycerides, fatty acids, cholesterol or waxes)

can promote lymphatic absorption through the intestine, as previously described in section 2.1 [43,65]. Based on this, some authors have developed edelfosine-loaded solid lipid nanoparticles (made of Compritol® 888 ATO or Precirol® ATO 5) intended for oral administration. The results observed in mantel cell lymphoma-bearing mice indicated that the lipid nanoparticles led to a significant accumulation of edelfosine in the lymph nodes, a result that translated into a slower tumor growth and a complete inhibition of the metastatic dissemination when compared to the effect of free edelfosine [65].

Other authors have attempted to increase the lymphatic absorption of paclitaxel by the oral route, using hydroxypropyl-β-cyclodextrin surface-modified solid lipid nanoparticles [124]. These nanoparticles led to a 12.5-fold lymphatic uptake in rats as compared to the paclitaxel solution and 1.2-fold compared to the non-modified solid lipid nanoparticles. More recently, Cho *et al.* developed tristearin-based lipidic nanoparticles for the lymphatic delivery of docetaxel [125]. The intraduodenal administration of these nanoparticles resulted in an enhanced intestinal absorption through lymphatic uptake via chylomicron formation, and a higher relative oral bioavailability of docetaxel as compared to Taxotere®. Despite these positive bioavailability data, the efficacy of these taxane-loaded nanoparticles for tackling metastatic cancer has not been reported yet. This could be due to the potential toxicity of the taxanes at the level of the intestinal mucosa.

In addition to oral administration, the lymphatic delivery of paclitaxel-loaded solid lipid nanoparticles has also been evaluated following pulmonary administration in the form of aerosols [67]. These solid lipid nanoparticles were more effective than the intravenous Taxol® suppressing the pulmonary metastases [67] due to the lymphatic clearance of these aerosolized particles from the lungs [66].

Although beyond the scope of this review, it is worth mentioning the lymphotropic superparamagnetic nanoparticle contrast nanoparticles developed for diagnostic purposes. These formulations, marketed as Combidex®/Sinerem®, allow the visualization of lymph node metastasis with improved accuracy through magnetic resonance imaging [126].

Altogether, these studies indicate that nanoparticles are versatile and efficient nanocarriers for the lymphatic delivery of drugs due to their small particle size ranging from 60 to 200 nm and their negative surface charge. Moreover, the lipid composition of solid lipid nanoparticles makes these nanocarriers particularly interesting for the oral administration of anticancer drugs. Despite all this, the amount of work performed in this field to date is still limited, and, thus, there is room to further optimize these nanoparticles and improve their lymphotropic behavior.

3.3 Nanocapsules

Nanocapsules are vesicular nanosystems in which the drug is confined in a cavity consisting of an inner liquid (often oily) core, surrounded by a polymeric shell. These nanocarriers could be advantageous as lymphotropic carriers since the polymeric coating enables the modulation of their surface properties and, thus, of improving their physiological stability and biodistribution [127]. Despite their potential, nanocapsules have been barely exploited for the lymphatic delivery of antitumor drugs. As an example, lipid nanocapsules with a size between 25 and 100 nm, developed by Benoit and his group showed the capacity to reach the lymph nodes following subcutaneous and, to lesser extent, intravenous administration [41,79]. When loaded with gemcitabine, these nanocapsules were found to enhance the efficacy of this drug in metastasizing orthotopic lung tumor model, resulting in a significant delay of animal death [128].

Our group has also contributed to this field with the development of polyaminoacid and polysaccharide-based nanocapsules. These nanocapsules have been loaded with drugs such as plitidepsine or docetaxel and administered to different tumor-bearing mice models. Overall, the results indicated that the nanoencapsulation of the drugs led to a significant improvement of their PK/PD profile in addition to a decrease in their toxicity [129–134]. Polysaccharide-based immunostimulating nanocapsules developed for vaccination have also demonstrated prolonged lymph node retention [88]. Based on this experience, we are currently exploring the potential of optimized polyaminoacid and polysaccharide-based nanocapsules for the lymphatic delivery of antitumor drugs [135].

A very different approach was the one reported by Huang et al, who used nanocapsules functionalized with T cells homing receptors to deliver the anticancer drug SN-38 to the lymphoid organs. This cell-mediated delivery increased SN-38 in lymph nodes at levels 90-fold greater than free drug intravenously administered at 10-fold higher doses [136].

Nanocapsules have also been explored for their use as oral anticancer drug carriers. For example, PLGA nanocapsules [137] entrapped within gastro-resistant microparticles were absorbed via lymphatic system, extending the blood circulation time of docetaxel in a metastatic lung cancer model. This formulation showed an improved anticancer activity, as compared to the control Taxotere® administered intravenously, this effect being attributed to a prolonged accumulation of the loaded nanocapsules in the lung tumor.

3.4 Polymeric Micelles

Polymeric micelles are nanostructures formed by the self-assembly of amphiphilic macromolecules, typically organized as a hydrophobic core surrounded by a hydrophilic shell. This hydrophilic character together with their small size, ranging from 20 to 100 nm, are known to be responsible for their prolonged blood circulation and enhanced accumulation in the tumor and the lymphatics [59]. As previously mentioned (section 2.1) such a behavior has been disclosed for vinorelbine-loaded PEG-phosphatidylethanolamine micelles [35]. Similarly, Rafi *et al.* showed that intravenously injected PEG-L-glutamic acid block copolymer micelles of 30 nm containing oxaliplatin can extravasate and penetrate into the tumor and lymph node metastasis, eliciting a remarkable antitumor activity, in an orthotopic mouse scirrhous gastric tumor model [59]. Similar results have been recently obtained for these polymeric micelles in a melanoma model [138]. More recently, Li *et al*. developed poly(D,L-lactide)-b-polyethylene glycolmethoxy-based polymeric micelles for the delivery of docetaxel in a highly-metastatic mouse mammary tumor model [58]. They observed that although the efficacy in terms of suppression of the primary tumor growth was similar to that of the free docetaxel, its capacity to reduce metastatic burden was notably improved.

In conclusion, there is evidence for the potential of small hydrophilic micelles to facilitate the accumulation of drugs in the lymphatics following intravenous

administration. However, the poor *in vivo* stability and premature release of the associated drug are a possible limitation of some micellar systems [139,140].

3.5 Dendrimers

Dendrimers are macromolecular polymers constructed by the stepwise addition of layers around a central polyfunctional core. These branched structures exhibit a very small size (< 10 nm), although their surface conjugation with other molecules, such as polymers or proteins, can lead to the formation of larger structures up to 20 nm. The access to the lymphatic system following subcutaneous administration or after the extravasation from the systemic circulation can be favored by selecting dendrimers of suitable size and molecular weight [60,141]. An interesting study was performed by Ryan and coworkers, who compared the lymphatic exposure of doxorubicin administered in PEGylated poly-lysine dendrimers (size 12 nm), PEGylated liposomes (100 nm) and various micellar formulations of Pluronics® (5 nm), following subcutaneous and intravenous administration to healthy rats [140]. Micelles showed similar doxorubicin levels to the same dose of free drug solution due to their poor *in vivo* stability. Conversely, liposomes and, to a much greater extent dendrimers, significantly increased the accumulation of doxorubicin in the thoracic lymph. These results were consistent with other works which have shown the increased lymph node biodistribution of methotrexate or doxorubicin conjugated dendrimers [44,142]. However, recent works have reported a poor correlation between the high levels of dendrimers accumulated in the lymph nodes and their antitumor activity in metastatic tumors [44,142]. This limited efficacy has been attributed to the physical retention of dendrimers in the lymph node parenchyma, which limits their ability to reach and be internalized by tumor cells residing in distant lymph nodes, also hindering efficient drug release from the dendrimer [44,142].

3.6 Other Nanosystems

Carbon nanotubes are defined as long cylindrical carbon structures consisting of hexagonal graphite molecules attached at the edges. Although they are mostly being investigated for dual-modal imaging guided photothermal therapy, their potential for drug delivery has been also explored [143,144]. Drugs can be incorporated into the

numerous inner spaces and/or into the tube walls. Moreover, other functional molecules can be attached to the edge of the tubes [145]. A lymphatic targeted drug delivery system using magnetic multi-walled carbon nanotubes (40–60 nm) has been developed and applied to the delivery of gemcitabine under the guidance of a magnetic field [37,146]. The efficacy of this formulation was assessed upon its SC injection into a pancreatic cancer mice model and the results showed efficient lymphatic delivery and internalization by cancer cells [37]. Other researchers have assessed the potential of water-dispersed single-wall carbon nanotubes for local delivery of doxorubicin in human NSCLC bearing mice [147]. After intratumoral injection, they observed high antitumor activity associated to a substantial retention of the nanohorns in the tumor tissue, and a partial migration to the axillary lymph nodes, thus indicating the potential of this nanosystem for local chemotherapy against solid tumors with lymph node metastasis.

3.7 Drug-polymer Conjugates

Natural and biodegradable polymers, such as dextran [148] and hyaluronic acid [34] have been conjugated with antitumor dugs to investigate their potential use as carriers for lymphatic drug delivery. Hyaluronan is an ideal candidate for the preparation of such conjugates due to its natural ability to be drained by the lymphatic system from the interstitial space and interact with the CD44 receptors overexpressed in lymphatic vessels and tumor cells [98]. For example, conjugates of hyaluronan with cisplatin or doxorubicin were shown to enhance the delivery to these drugs to the draining lymph nodes in different tumor models, following either intratumoral or pulmonary administration. These approaches have improved the therapeutic efficacy and toxicity with respect to the standard intravenous cisplatin or doxorubicin treatments [149–154]. On the other hand, the synthesis of dextran-mitomycin C conjugates resulted in a high and sustained accumulation of mitomycin-C in the regional lymph nodes following intramuscular administration, leading to a more effective inhibition of lymph node metastases in a rat leukemia model as compared to the free drug solution [148]. This enhanced access to the lymphatic system is mainly due to the high molecular weight of the conjugate, which prevents its drainage through the blood capillaries.

Table 1. Representative list of nanocarriers tested in vivo for the passive lymphatic targeting of anticancer drugs.

Drug/Carrier	Administration route	Tumor animal/human model	Key result	Refs.
Paclitaxel / **Liposomes**	IV, IP	Orthotopic ovarian, rats	Higher accumulation in the pelvic lymph nodes	[107]
	Pulmonary	Orthotopic renal, mice	Inhibition of pulmonary metastasis	[109]
	Pulmonary	Orthotopic mammary, mice	Reduction of metastatic cells in the lymph nodes	[110]
Methotrexate / **Liposomes**	IV	Normal rats	Accumulation in the lymph nodes	[155]
	IM	Normal rats	Accumulation in the regional lymph nodes	[156]
Doxorubicin / **Liposomes**	IP	Normal rats	Accumulation in the draining lymph nodes	[104]
	IV, IP	Normal rats	Accumulation in the renal and mediastinal lymph nodes	[157]
	Bladder SM	Normal dogs	Accumulation in the regional lymph nodes	[158]
	Gastric SM	Patients with gastric carcinoma	High specific delivery to the draining lymph nodes	[105]
	SC	Orthotopic breast carcinoma, rabbits	Reduction of metastatic cells in the lymph nodes	[159]
	SC and/or IV	Orthotopic breast carcinoma, rabbits	IV more efficient on distant metastasis, SC for those in draining lymph nodes. Higher efficacy against the lymph nodes metastasis for combined therapy	[69]
	IV , IP	B-cell lymphoma, mice	Accumulation in mesenteric lymph nodes	[160]
9-Nitro camptothecin / **Liposomes**	Pulmonary	Orthotopic mammary, mice	Reduction of metastases in axillary and brachial lymph nodes	[111]
Honokiol / **Liposomes**	IP	Heterotopic lung, mice	Inhibition of lymphangiogenesis and metastasis due to the effect of honokiol. Liposomes improves its solubility	[161]
Melphalan / **Liposomes**	SC	Heterotopic mammary, rats	Small liposomes leads to high delivery to regional lymph nodes	[162,163]
Carboplatin / **Liposomes**	NI	Xenograft gastric, mice	Inhibition of the lymph nodes metastasis	[164]
Paclitaxel / **Nanoparticles**	IP	Xenograft ovarian, rats	Accumulation in the pelvic lymph nodes	[49]
	Intratumoral	Orthotopic breast, mice	Accumulation in the axillary lymph nodes and reduction of lymph node metastasis	[117]
	ID	Normal swine	Accumulation in the regional lymph nodes	[119]
Vincristine / **Nanoparticles**	IV	Burkitt's lymphoma, mice	Accumulation in the lymph nodes and reduction of the lymphoma	[95]
Doxorubicin / **Nanoparticles**	IV	Orthotopic pancreatic, mice model	Reduction of the lymphatic metastasis	[165]
Edelfosine / **SLNs**	Oral	MCL, mice	High lymphatic absorption, inhibition of the lymph nodes metastasis	[65]
Mitoxantrone / **SLNs**	SC	Orthotopic breast, mice	Accumulation in the axillary lymph nodes and reduction of the lymph nodes metastases	[122]
Paclitaxel / **SLNs**	Oral	Normal rats	Accumulation in the lymph nodes	[124]

Docetaxel / **SLNs**	Pulmonary	Orthotopic mammary, mice model	Suppression of the pulmonary metastases due to the lymphatic delivery	[67]
	Intraduodenal	Normal rats	Accumulation in the mesenteric lymph nodes	[125]
Docetaxel / **Nanocapsules**	IV	Orthotopic lung, mice	High efficacy against the mediastinal lymph nodes metastasis	(Abellán-Pose et al.*)
Docetaxel / **Nanocapsules**	Oral	Orthotopic lung, mice	High lymphatic absorption increases bioavailability and antitumor efficacy	[137]
Tamoxifen / **NLC**	Oral	Heterotopic mammary mice	High lymphatic absorption increases oral bioavailability and antitumor efficacy	[166,167]
Pro-drug gemcitabine / **Nanocapsules**	SC, IV	Orthotopic lung, mice	Higher lymphatic delivery to mediastinal lymph nodes and delay death by SC	[128]
Methotrexate / **Emulsomes**	Oral	Normal rats	High lymphatic absorption and higher bioavailability	[168]
Teniposide / **Self-assembled nanocarriers**	Oral	Xenograft breast, mice	High lymphatic absorption increases oral bioavailability	[169]
Oxaliplatin / **Micelles**	IV	Orthotopic scirrhous gastric & melanoma, mice	High accumulation and antitumor efficacy on the metastatic lymph nodes	[59,138]
Doxorubicin / **Micelles**	IV	Normal mice	Accumulation in lymph nodes	[35]
Vinorelbine / **Micelles**	IV	Orthotopic mammary, mice	Accumulation in lymph nodes and reduction of lymph node metastasis	[35]
Docetaxel / **Micelles**	IV	Orthotopic mammary, mice	Accumulation in lymph nodes improves anti-metastatic efficacy	[58]
Doxorubicin / **Dendrimers**	SC, IV	Normal rats	Higher lymphatic delivery than other nanocarriers, especially by SC route	[140]
	Pulmonary, IV	Syngeneic breast, rats	Higher anti-metastatic efficacy by pulmonary route	[142]
Methotrexate / **Dendrimers**	SC, IV	Syngeneic breast, rats	Higher distribution to the lymph nodes by SC route. Similar reduction of lymph node metastasis by both routes	[44]
Gemcitabine / **mMWNTs**	SC	Heterotopic pancreatic, mice	Inhibition of popliteal node metastasis	[37]
Doxorubicin / **SWNHs**	Intratumoral	Heterotopic lung, mice	Partial migration to the axillary lymph nodes	[147]
Mitomycin C / **Nanoconjugates**	IM	Leukemia, rats	Delivery to the regional lymph nodes and reduction of lymph node metastasis	[148]
Cisplatin / **Nanoconjugates**	SC	Orthotopic breast, mice	Accumulation in the axillary lymph nodes	[149,151, 170]
	Intratumoral	Soft tissue sarcoma, dogs	Accumulation in the draining lymph nodes	[152]
	Pulmonary, IV	Normal rats	Accumulation in the draining lymph nodes after both routes	[153]
Doxorubicin / **Nanoconjugates**	Intratumoral	Heterotopic colon, mice	Accumulation in the draining lymph nodes	[154]
	Peritumoral	Orthotopic breast, mice	Accumulation in the breast lymphatics	[150]

Abbreviations: ID: intradermal; IM: intramuscular; IP: intraperitoneal; IV: intravenous; MCL: mantel cell lymphoma; mMWNTs: magnetic multiwalled carbon nanotubes; NI: not indicated; NLC: nanostructured lipid carrier; PK: pharmacokinetic; SC: subcutaneous; SLNs: solid lipid nanoparticles; SM: submucosal; SWNHs: single-wall carbon nanohorns. *: manuscript in preparation.

3.8 Actively Targeted Nanosystems

In addition to passive targeting, efficient delivery of nanocarriers to the tumor-affected lymphatic vessels or lymph nodes can be achieved by attaching targeting ligands to the surface of nanocarriers. This strategy may enhance the cellular specificity of the nanosystems and stimulate their receptor-mediated internalization into cancer cells. Table 2 summarizes nanocarriers investigated specifically for the active targeting of anticancer drugs to the lymphatic system. A promising ligand for active lymphatic targeting in cancer therapy is Lyp-1. This nine amino acid cyclic peptide (CGNKRTRGC) is a specific tumor and lymphatic endothelial cell marker, that, unlike other vascular-homing peptides, is selective for tumor lymphatic vessels [171]. LyP-1 binds to the protein p32 (gC1qR), a surface receptor expressed on the cells of the tumor lymphatics, tumor-associated macrophages and tumor cells from hypoxic regions of the tumors [172]. Moreover, it has been observed that Lyp-1 may induce cell death when recognized and internalized (*e.g.* by MDA-MB-435 human carcinoma cells), hence presenting a certain antitumor effect itself [173]. The quantitative *in vivo* imaging of Lyp-1 conjugated PEG-PLGA nanoparticles in a xenograft pancreatic cancer model with lymphatic metastasis [174] showed their significant accumulation in the tumor and also in the lymph nodes (8-fold) with the targeting motif. LyP-1-functionalized PEGylated liposomes were loaded with doxorubicin and administered subcutaneously in metastatic lung [175] and breast carcinoma [176] mice models. The results showed an improved uptake of the encapsulated drug in the metastatic lymph nodes, and tumor-associated macrophages [175]. As a result of this high specificity, targeted liposomes suppressed lymphatic metastasis by simultaneously inhibiting cell spreading and destroying tumor lymphatics in lymph nodes [176]. Similar efficacy was observed for Lyp-1 modified micelles loaded with artemisinin in a MDA-MB-435S breast tumor model, showing significant inhibitory effects of tumor growth and metastasis [177]. Gursoy *et al*. have shown *in vitro* that the presence of Lyp-1 in self-microemulsifying drug delivery systems also decrease significantly the viability of the breast cancer cell line MDA-MB-231 [178]. In another study, nanogels have been decorated with LyP-1, enhancing the binding efficacy of these nanocarriers with cancer cells [179]. The administration of gemcitabine in this targeted nanoformulation in a gemcitabine-

resistant xenograft lymphoma model showed 2-fold more efficient tumor growth inhibition than the non-targeted nanogel.

Another possible ligand for active targeting is folic acid. The folate receptor is significantly overexpressed on some cancers, both in the tumors and in the metastatic lymph nodes. Along this line, several nanocarriers such as a conjugate folate-PEG-CKK_2-DTPA [180], magnetic carbon nanotubes [146] or PEGylated liposomes [181] have been designed to include folate with the purpose of improving drug delivery to the lymph nodes and hence prevent lymphatic metastasis. However, the efficacy of this ligand for the specific targeting of the lymphatics has not yet been demonstrated *in vivo*.

As previously described (section 1.2), tumor cells secrete several vascular growth factors essential for their progression and metastasis. Vascular endothelial growth factor (VEGF-C) activates the vascular endothelial growth factor receptor-3 (VEGFR3) expressed on the LECs, increasing the intratumoral lymphangiogenesis and promoting metastasis to the regional lymph nodes. Along this line, He *et al.* have developed calcium carbonate nanoparticles containing small interfering RNA (siRNA) against VEGF-C [182]. These nanoparticles showed high transfection efficiency in the gastric cancer cell line SGC-7901, decreasing significantly the concentration of VEGF mRNA and VEGF-C as compared to nanoparticles containing nonspecific siRNA. Moreover, the intratumoral administration of the siRNA-targeted nanoparticles led to a significant reduction of the tumor lymphangiogenesis, tumor growth and lymph node metastasis in this gastric cancer model.

In a recent study, Ye *et al.* have considered the potential of low molecular weight heparin (LMWHEP) to target nanoliposomes to the lymph node metastasis [183]. LMWHEP can bind and inhibit heparanase (HPA), an enzyme involved in the remodeling of the ECM that is preferentially secreted by metastatic tumor cells, especially in the lymph nodes and therefore might improve the metastatic lymph node targeting. Using this hydrophilic polysaccharide it was possible to obtain nanoliposomes with suitable surface properties to promote their lymphatic drainage. Based on these properties, these authors prepared LMWHEP-coated nanoliposomes for the administration of docetaxel. Their *in vitro* results indicate that this strategy improved the LMWHEP-coated nanoliposomes cellular uptake in a HPA overexpressing cancer

cell line (Human cervical cancer cells, Hela). Moreover, subcutaneously injected LMWHEP-nanoliposomes evidenced higher uptake and retention in metastatic lymph nodes than non-targeted liposomes.

Table 2. Representative ligands and nanocarriers specifically studied for the active lymphatic targeting of anticancer drugs.

Ligand	Receptor/ Enzyme	Target site	Nanosystem	Refs.
Lyp-1	p32	tumor lymphatic vessels, tumor-associated macrophages and cancer cells from hypoxic regions of tumors	Albumin-embedded paclitaxel nanoparticles	[187]
			PLGA-PEG nanoparticles	[174]
			Doxorubicin-loaded PEGylated liposomes	[175,176]
			Artemisinin-loaded PEG-PCL micelles	[177]
			SMEDDS	[178]
			Gemcitabine-loaded Nanogels	[179]
Folic acid	Folate	tumors and the metastatic lymph nodes	Conjugate folate-PEG-CKK_2-DTPA	[180]
			Magnetic carbon nanotubes	[146]
			PEGylated liposomes	[181]
siRNA	VEGFR-3	LECs	Calcium carbonate nanoparticles	[182]
LMWHEP	HPA	tumors and metastatic lymph nodes	Nanoliposome	[183]

Abbreviations: HPA: heparanase; LECs: lymphatic endothelial cells; LMWHEP: low molecular weight heparin; SMEDDS: Self-microemulsifying drug delivery systems; PLGA: poly(lactic-co-glycolic acid); PEG-PCL: poly(ethylene glycol)-block-poly(3-caprolactone); VEGFR-3: vascular endothelial growth factor receptor-3

Regarding lymphatic targeting as a diagnostic tool, a dextran-based polymeric system called Lymphoseek® has been recently approved by FDA and EMA as a targeted lymphatic mapping agent for solid tumors. Lymphoseek® has a small molecular size (7

nm) and carries multiple units of mannose [184,185]. Mannose has a high affinity for CD-206 receptors highly overexpressed on the surface of macrophages and dendritic cells. By tightly binding to these mannose receptors, Lymphoseek® accumulates in lymphatic tissue within minutes and localizes tumor-draining lymph nodes [186]. Although this strategy has been investigated with diagnostic purposes, similar approaches could also be explored for drug delivery in the future.

4 Conclusions and Perspectives

Over the last years, there has been an increased interest in targeting anticancer drugs to the lymphatic system as a strategy for the treatment of metastatic cancer. The recent understanding of the role that the lymphatic system plays in the spread of metastatic cells has been followed by the incipient development of nanocarriers intended to target antitumor drugs to this specific compartment within the body [188,189]. It is currently known that the route of administration and physiopathological changes associated to the tumor progression are key factors for the design of nanocarriers with a lymphotropic behavior. Moreover, it is broadly accepted that the particle size and surface composition of nanosystems are clear determinants of this behavior. However, the requirements and impact of an optimal lympho-targeting vs. tumor-targeting balance have not been fully elucidated yet. In other words, currently it is not clear whether the anti-metastatic effect observed for some drug-loaded nanocarriers is due to their direct effect on the lymph nodes-resident cancer cells or if it is secondary to a size reduction of the primary tumor, decreasing cell spreading. Further studies are needed in order to understand the consequences of the different targeting possibilities and, thus, to provide criteria for the design of optimized lymphonanocarriers. Therefore, our overall conclusion is that the development of nanocarriers with a lymphotropic behavior is still at a very early stage and that rigorous pharmacokinetic studies including the lymphatic drug accumulation at the preclinical and clinical level would be necessary in order to obtain further advances in this field.

Conflict of Interest

Authors declare no potential conflict of interest regarding the content of this work.

Acknowledgements

The authors acknowledge financial support given by the European Commission FP7 EraNet-EuroNanoMed Program-Instituto Carlos III (Lymphotarg, Ref. PS09/02670) and Xunta de Galicia (Isidro Parga Pondal Fellowhsip and Competitive Reference Groups-FEDER Funds Ref 2013/043). Raquel Abellan-Pose also acknowledges her fellowship from the Biomedical Sciences and Health Technologies Doctoral School-Universidad Santiago de Compostela.

REFERENCES

[1] Rinderknecht M, Detmar M. Tumor lymphangiogenesis and melanoma metastasis. J. Cell. Physiol. 2008;216:347–54.

[2] Leak L V. The structure of lymphatic capillaries in lymph formation. Fed. Proccedings 1976;35:1863–71.

[3] Swartz MA. The physiology of the lymphatic system. Adv. Drug Deliv. Rev. 2001;50:3–20.

[4] Schulte-Merker S, Sabine A, Petrova T V. Lymphatic vascular morphogenesis in development, physiology, and disease. J. Cell Biol. 2011;193:607–18.

[5] Porter CJ, Charman SA. Lymphatic transport of proteins after subcutaneous administration. J. Pharm. Sci. 2000;89:297–310.

[6] Wiig H, Keskin D, Kalluri R. Interaction between the extracellular matrix and lymphatics: consequences for lymphangiogenesis and lymphatic function. Matrix Biol. 2010;29:645–56.

[7] Swartz MA, Hubbell JA, Reddy ST. Lymphatic drainage function and its immunological implications: from dendritic cell homing to vaccine design. Semin. Immunol. 2008;20:147–56.

[8] O'Driscoll CM. Anatomy and physiology of the lymphatics. In: Charman W, Stella V, editors. Lymphatic Transport of Drugs. London: CRC Press; 1992. page 1–35.

[9] Kaipainen A, Korhonen J, Mustonen T, Van Hinsbergh V, Fang G, Dumont D, et al. Expression of the fms-like tyrosine kinase 4 gene becomes restricted to lymphatic endothelium during development. Proc. Natl. Acad. Sci. U. S. A. 1995;92:3566–70.

[10] Banerji S, Ni J, Wang SX, Clasper S, Su J, Tammi R, et al. LYVE-1, a new homologue of the CD44 glycoprotein, is a lymph-specific receptor for hyaluronan. J. Cell Biol. 1999;144:789–801.

[11] Wigle JT, Oliver G. Prox1 function is required for the development of the murine lymphatic system. Cell 1999;98:769–78.

[12] François M, Caprini A, Hosking B, Orsenigo F, Wilhelm D, Browne C, et al. Sox18 induces development of the lymphatic vasculature in mice. Nature 2008;456:643–7.

[13] Duong T, Proulx ST, Luciani P, Leroux JC, Detmar M, Koopman P, et al. Genetic ablation of SOX18 function suppresses tumor lymphangiogenesis and metastasis of melanoma in mice. Cancer Res. 2012;72:3105–14.

[14] Wiig H, Swartz MA. Interstitial fluid and lymph formation and transport: physiological regulation and roles in inflammation and cancer. Physiol. Rev. 2012;92:1005–60.

[15] Witte MH, Jones K, Wilting J, Dictor M, Selg M, McHale N, et al. Structure function relationships in the lymphatic system and implications for cancer biology. Cancer Metastasis Rev. 2006;25:159–84.

[16] Swartz MA, Skobe M. Lymphatic Function , Lymphangiogenesis , and Cancer Metastasis. Microsc. Res. Tech. 2001;55:92–9.

[17] McAllaster JD, Cohen MS. Role of the lymphatics in cancer metastasis and chemotherapy applications. Adv. Drug Deliv. Rev. 2011;63:867–75.

[18] Joukov V, Pajusola K, Kaipainen A, Chilov D, Lahtinen I, Kukk E, et al. A novel vascular endothelial growth factor, VEGF-C, is a ligand for the Flt4 (VEGFR-3) and KDR (VEGFR-2) receptor tyrosine kinases. EMBO J. 1996;15:1751.

[19] Achen M, Jeltsch M, Kukk E, Makinen T, Vitali A, Wilks A, et al. Vascular endothelial growth factor D (VEGF-D) is a ligand for the tyrosine kinases VEGF receptor 2 (Flk1) and VEGF receptor 3 (Flt4). Proc. Natl. Acad. Sci. U. S. A. 1998;95:548–53.

[20] Alitalo K. The lymphatic vasculature in disease. Nat. Med. 2011;17:1371–80.

[21] Proulx ST, Detmar M. Molecular mechanisms and imaging of lymphatic metastasis. Exp. Cell Res. 2013;319:1611–7.

[22] Qian C-N, Berghuis B, Tsarfaty G, Bruch M, Kort EJ, Ditlev J, et al. Preparing the “soil”: the primary tumor induces vasculature reorganization in the sentinel lymph node before the arrival of metastatic cancer cells. Cancer Res. 2006;66:10365–76.

[23] Skobe M, Hawighorst T, Jackson DG, Prevo R, Janes L, Velasco P, et al. Induction of tumor lymphangiogenesis by VEGF-C promotes breast cancer metastasis. Nat. Med. 2001;7:192–8.

[24] Stacker SA, Caesar C, Thornton GE, Williams RA, Prevo R, Jackson DG, et al. VEGF-D promotes the metastatic spread of tumor cells via the lymphatics. Nat. Med. 2001;7:186–91.

[25] Mandriota SJ, Jussila L, Jeltsch M, Compagni A, Baetens D, Prevo R, et al. Vascular endothelial growth factor-C-mediated lymphangiogenesis promotes tumour metastasis. EMBO J. 2001;20:672–82.

[26] Pepper MS, Skobe M. Lymphatic endothelium: morphological, molecular and functional properties. J. Cell Biol. 2003;163:209–13.

[27] Proulx ST, Luciani P, Dieterich LC, Karaman S, Leroux J-C, Detmar M. Expansion of the lymphatic vasculature in cancer and inflammation: New opportunities for in vivo imaging and drug delivery. J. Control. Release 2013;172:550–7.

[28] Butler TP, Grantham FH, Gullino PM. Bulk Transfer of Fluid in the Interstitial Compartment of Mammary Tumors. Cancer Res. 1975;75:3084–8.

[29] Netti PA, Baxter LT, Boucher Y, Skalak R, Jam RK. Time-dependent Behavior of Interstitial Fluid Pressure in Solid Tumors: Implications for Drug Delivery. Cancer Res. 1995;55:5451–8.

[30] Fukumura D, Jain RK. Tumor microenvironment abnormalities: causes, consequences, and strategies to normalize. J. Cell. Biochem. 2007;101:937–49.

[31] Dafni H, Israely T, Bhujwalla ZM, Albumin T. Overexpression of Vascular Endothelial Growth Factor 165 Drives Peritumor Interstitial Convection and Induces Lymphatic Drain: Magnetic Resonance Imaging, Confocal Microscopy, and Histological Tracking of Triple-labeled Albumin. Cancer Res. 2002;62:6731–9.

[32] Swartz MA, Lund AW. Lymphatic and interstitial flow in the tumour microenvironment: linking mechanobiology with immunity. Nat. Rev. Cancer 2012;12:210–9.

[33] Cabanas R. An approach for the treatment of penile carcinoma. Cancer 1977;39:456–66.

[34] Xie Y, Bagby TR, Cohen M, Forrest ML. Drug delivery to the lymphatic system: importance in future cancer diagnosis and therapies. Expert Opin. Drug Deliv. 2009;6:785–92.

[35] Qin L, Zhang F, Lu X, Wei X, Wang J, Fang X, et al. Polymeric micelles for enhanced lymphatic drug delivery to treat metastatic tumors. J. Control. Release 2013;171:133–42.

[36] Cai S, Yang Q, Bagby TR, Forrest ML. Lymphatic drug delivery using engineered liposomes and solid lipid nanoparticles. Adv. Drug Deliv. Rev. 2011;63:901–8.

[37] Yang F, Jin C, Yang D, Jiang Y, Li J, Di Y, et al. Magnetic functionalised carbon nanotubes as drug vehicles for cancer lymph node metastasis treatment. Eur. J. Cancer 2011;47:1873–82.

[38] Schroeder A, Heller D a, Winslow MM, Dahlman JE, Pratt GW, Langer R, et al. Treating metastatic cancer with nanotechnology. Nat. Rev. Cancer 2012;12:39–50.

[39] Oussoren C, Zuidema J, Croramelin D, Storm G. Lymphatic uptake and biodistribution of liposomes after subcutaneous injection I . Influence of the anatomical site of injection. J. Liposome Res. 1997;7:85–99.

[40] Brigger I, Dubernet C, Couvreur P. Nanoparticles in cancer therapy and diagnosis. Adv. Drug Deliv. Rev. 2002;54:631–51.

[41] Pitorre M, Bastiat G, dit Chatel EM, Benoit J-P. Passive and specific targeting of lymph nodes: the influence of the administration route. Eur. J. Nanomedicine 2015;7:121–8.

[42] Harivardhan Reddy L, Sharma RK, Chuttani K, Mishra AK, Murthy RSR. Influence of administration route on tumor uptake and biodistribution of etoposide loaded solid lipid nanoparticles in Dalton's lymphoma tumor bearing mice. J. Control. Release 2005;105:185–98.

[43] Ali Khan A, Mudassir J, Mohtar N, Darwis Y. Advanced drug delivery to the lymphatic system: lipid-based nanoformulations. Int. J. Nanomedicine 2013;8:2733–44.

[44] Kaminskas LM, McLeod VM, Ascher DB, Ryan GM, Jones S, Haynes JM, et al. Methotrexate-Conjugated PEGylated Dendrimers Show Differential Patterns of Deposition and Activity in Tumor-Burdened Lymph Nodes after Intravenous and Subcutaneous Administration in Rats. Mol. Pharm. 2015;12:432–43.

[45] Bettendorf U. Electronmicroscopic studies on the peritoneal resorption of intraperitoneally injected latex particles via the diaphragmatic lymphatics. Lymphology 1979;12:66–70.

[46] Hawley AE, Davis SS, Illum L. Targeting of colloids to lymph nodes: influence of lymphatic physiology and colloidal characteristics. Adv. Drug Deliv. Rev. 1995;17:129–48.

[47] Lu Z, Wang J, Wientjes M, Au JL-S. Intraperitoneal therapy for peritoneal cancer. Futur. Oncol 2010;6:1625–41.

[48] Hirano K, Hunter C. Lymphatic Transport of Liposome-Encapsulated Agents: Effects of Liposome Size Following lntraperitoneal Administration. Pharm. Sci. 1985;74.

[49] Lu H, Li B, Kang Y, Jiang W, Huang Q, Chen Q, et al. Paclitaxel nanoparticle inhibits growth of ovarian cancer xenografts and enhances lymphatic targeting. Cancer Chemother. Pharmacol. 2007;59:175–81.

[50] Maincent P, Thouvenot P, Amicabile C, Hoffman M, Kreuter J, Couvreur P, et al. Lymphatic targeting of polymeric nanoparticles after intraperitoneal administration in rats. Pharm. Res. 1992;9:1534–9.

[51] Ryan GM, Kaminskas LM, Porter CJH. Nano-chemotherapeutics: Maximising lymphatic drug exposure to improve the treatment of lymph-metastatic cancers. J. Control. Release 2014;193:241–56.

[52] Baban D, Seymour L. Control of tumour vascular permeability. Adv. Drug Deliv. Rev. 1998;34:109–19.

[53] Matsumura Y, Maeda H. A New Concept for Macromolecular Therapeutics in Cancer Chemotherapy: Mechanism of Tumoritropic Accumulation of Proteins and the Antitumor Agent Smancs. Cancer Res. 1986;46:6387–92.

[54] Yuan F, Dellian M, Fukumura D, Leunig M, Berk DA, Torchilin VP, et al. Vascular Permeability in a Human Tumor Xenograft: Molecular Size Dependence and Cutoff Size. Cancer Metastasis Rev. 1995;55:3752–6.

[55] Hervella P, Lozano V, Garcia-fuentes M, Alonso MJ. Nanomedicine : New Challenges and Opportunities in Cancer Therapy. J. Biomed. Nanotechnol. 2008;4:1–17.

[56] Danhier F, Feron O, Préat V. To exploit the tumor microenvironment: Passive and active tumor targeting of nanocarriers for anti-cancer drug delivery. J. Control. Release 2010;148:135–46.

[57] Svenson S. What nanomedicine in the clinic right now really forms nanoparticles? Wiley Interdiscip. Rev. Nanomed. Nanobiotechnol. 2014;6:125–35.

[58] Li Y, Jin M, Shao S, Huang W, Yang F, Chen W, et al. Small-sized polymeric micelles incorporating docetaxel suppress distant metastases in the clinically-relevant 4T1 mouse breast cancer model. BMC Cancer 2014;14:329.

[59] Rafi M, Cabral H, Kano MR, Mi P, Iwata C, Yashiro M, et al. Polymeric micelles incorporating (1,2-diaminocyclohexane)platinum (II) suppress the growth of orthotopic scirrhous gastric tumors and their lymph node metastasis. J. Control. Release 2012;159:189–96.

[60] Kaminskas LM, Kota J, McLeod VM, Kelly BD, Karellas P, Porter CJ. PEGylation of polylysine dendrimers improves absorption and lymphatic targeting following SC administration in rats. J. Control. Release 2009;140:108–16.

[61] O'Driscoll CM. Lipid-based formulations for intestinal lymphatic delivery. Eur. J. Pharm. Sci. 2002;15:405–15.

[62] Chaudhary S, Garg T, Murthy RSR, Rath G, Goyal AK. Recent approaches of lipid-based delivery system for lymphatic targeting via oral route. J. Drug Target. 2014;22:1–12.

[63] Porter CJ, Charman WN. Intestinal lymphatic drug transport: an update. Adv. Drug Deliv. Rev. 2001;50:61–80.

[64] Trevaskis NL, Charman WN, Porter CJH. Lipid-based delivery systems and intestinal lymphatic drug transport: a mechanistic update. Adv. Drug Deliv. Rev. 2008;60:702–16.

[65] Estella-Hermoso de Mendoza A, Campanero MA, Lana H, Villa-Pulgarin JA, de la Iglesia-Vicente J, Mollinedo F, et al. Complete inhibition of extranodal dissemination of lymphoma by edelfosine-loaded lipid nanoparticles. Nanomedicine (Lond). 2012;7:679–90.

[66] Videira MA, Botelho MF, Santos AC, Gouveia LF, de Lima JJP, Almeida AJ. Lymphatic uptake of pulmonary delivered radiolabelled solid lipid nanoparticles. J. Drug Target. 2002;10:607–13.

[67] Videira M, Almeida AJ, Fabra A. Preclinical evaluation of a pulmonary delivered paclitaxel-loaded lipid nanocarrier antitumor effect. Nanomedicine 2012;8:1208–15.

[68] Videira MA, Santos AC, Botelho MF. Biodistribution of Lipid Nanoparticles: A Comparative Study of Pulmonary versus Intravenous Administration in Rats. Curr. Radiopharm. 2012;5:158–65.

[69] Chen JH, Ling R, Yao Q, Li Y, Chen T, Wang Z, et al. Effect of small-sized liposomal Adriamycin administered by various routes on a metastatic breast cancer model. Endocr. Relat. Cancer 2005;12:93–100.

[70] Oussoren C, Zuidema J, Crommelin DJA, Storm G. Lymphatic uptake and biodistribution of liposomes after subcutaneous injection. II. Influence of liposomal size, lipid composition and lipid dose. Biochim. Biophys. Acta 1997;261–72.

[71] Rao DA, Forrest ML, Alani AWG, Kwon GS, Robinson JR. Biodegradable PLGA Based Nanoparticles for Sustained Regional Lymphatic Drug Delivery. J. Pharm. Sci. 2010;99:2018–31.

[72] Illum L, Church AE, Butterworth MD, Arien A, Whetstone J, Davis SS. Development of systems for targeting the regional lymph nodes for diagnostic imaging: in vivo behaviour of colloidal PEG-coated magnetite nanospheres in the rat following interstitial administration. Pharm. Res. 2001;18:640–5.

[73] Oussoren C, Storm G. Liposomes to target the lymphatics by subcutaneous administration. Adv. Drug Deliv. Rev. 2001;50:143–56.

[74] Reddy ST, Rehor A, Schmoekel HG, Hubbell JA, Swartz MA. In vivo targeting of dendritic cells in lymph nodes with poly(propylene sulfide) nanoparticles. J. Control. Release 2006;112:26–34.

[75] Oussoren C, Velinova M, Scherphof G, van der Want JJ, van Rooijen N, Storm G. Lymphatic uptake and biodistribution of liposomes after subcutaneous injection . IV. Fate of liposomes in regional lymph nodes. Biochim. Biophys. Acta 1998;1370:259–72.

[76] Hernandez-Gil J, Cobaleda-Siles J, Zabaleta A, Salassa L, Calvo J, Mareque-Rivas J. An Iron Oxide Nanocarrier Loaded with a Pt(IV) Prodrug and Immunostimulatory dsRNA for Combining Complementary Cancer Killing Effects. Adv. Healthc. Mater. 2015;4:2015.

[77] Paulis LE, Mandal S, Kreutz M, Figdor CG. Dendritic cell-based nanovaccines for cancer immunotherapy. Curr. Opin. Immunol. 2013;25:389–95.

[78] Mohanan D, Slütter B, Henriksen-Lacey M, Jiskoot W, Bouwstra JA, Perrie Y, et al. Administration routes affect the quality of immune responses: A cross-sectional evaluation of particulate antigen-delivery systems. J. Control. Release 2010;147:342–9.

[79] Hirsjärvi S, Dufort S, Gravier J, Texier I, Yan Q, Bibette J, et al. Influence of size, surface coating and fine chemical composition on the in vitro reactivity and in vivo biodistribution of lipid nanocapsules versus lipid nanoemulsions in cancer models. Nanomedicine Nanotechnology, Biol. Med. 2013;9:375–87.

[80] Hirano K, Hunter C, Strubbe A, MacGregor R. Lymphatic transport of liposome encapsulated drugs following intraperitoneal administration-Effect lipid composition. Pharm. Res. 1985;6:271–8.

[81] Decuzzi P, Pasqualini R, Arap W, Ferrari M. Intravascular delivery of particulate systems: Does geometry really matter? Pharm. Res. 2009;26:235–43.

[82] Longmire MR, Ogawa M, Choyke PL, Kobayashi H. Biologically optimized nanosized molecules and particles: More than just size. Bioconjug. Chem. 2011;22:993–1000.

[83] Kong M, Hou L, Wang J, Feng C, Liu Y, Cheng X, et al. Enhanced transdermal lymphatic drug delivery of hyaluronic acid modified transfersomes for tumor metastasis therapy. Chem. Commun. 2015;51:1453–6.

[84] Huynh NT, Roger E, Lautram N, Benoît J-P, Passirani C. The rise and rise of stealth nanocarriers for cancer therapy: passive versus active targeting. Nanomedicine (Lond). 2010;5:1415–33.

[85] Reddy ST, Berk DA, Jain RK, Swartz MA. A sensitive in vivo model for quantifying interstitial convective transport of injected macromolecules and nanoparticles. J. Appl. Physiol. 2006;101:1162–9.

[86] Kaur CD, Nahar M, Jain NK. Lymphatic targeting of zidovudine using surface-engineered liposomes. J. Drug Target. 2008;16:798–805.

[87] Patel H, Boodle M, Vaughan-Jones R. Assessment of the potential uses of liposomes for lymphoscintigraphy and lymphatic drug delivery: Failure of 99m-Technetium marker to represent intact liposomes in lymph nodes. Biochim. Biophys. Acta 1984;801:76–86.

[88] Vicente S, Goins BA, Sanchez A, Alonso MJ, Phillips WT. Biodistribution and lymph node retention of polysaccharide-based immunostimulating nanocapsules. Vaccine 2014;32:1685–92.

[89] Zhao L, Seth A, Wibowo N, Zhao CX, Mitter N, Yu C, et al. Nanoparticle vaccines. Vaccine 2014;32:327–37.

[90] Hawley AE, Illum L, Davis SS. Lymph node localisation of biodegradable nanospheres surface modified with poloxamer and poloxamine block co-polymers. FEBS Lett. 1997;400:319–23.

[91] Moghimi SM. The effect of methoxy-PEG chain length and molecular architecture on lymph node targeting of immuno-PEG liposomes. Biomaterials 2006;27:136–44.

[92] Oussoren C, Storm G. Targeting to lymph nodes by subcutaneous administration of liposomes. Int. J. Pharm. 1998;162:39–44.

[93] Moghimi S. Modulation of lymphatic distribution of subcutaneously injected poloxamer 407-coated nanospheres: the effect of the ethylene oxide chain configuration. FEBS Lett. 2003;540:241–4.

[94] Kourtis IC, Hirosue S, de Titta A, Kontos S, Stegmann T, Hubbell JA, et al. Peripherally administered nanoparticles target monocytic myeloid cells, secondary lymphoid organs and tumors in mice. PLoS One 2013;8:e61646.

[95] Tan R, Niu M, Zhao J, Liu Y, Feng N. Preparation of vincristine sulfate-loaded poly (butylcyanoacrylate) nanoparticles modified with pluronic F127 and evaluation of their lymphatic tissue targeting. J. Drug Target. 2014;22:509–17.

[96] Moghimi SM, Hawley AE, Christy NM, Gray T, Illum L, Davis SS. Surface engineered nanospheres with enhanced drainage into lymphatics and uptake by macrophages of the regional lymph nodes. FEBS Lett. 1994;344:25–30.

[97] Oussoren C, Storm G. Lymphatic uptake and biodistribution of liposomes after subcutaneous injection: III. Influence of surface modification with poly(ethyleneglycol). Pharm. Res. 1997;14:1479–84.

[98] Teijeiro C, Mcglone A, Csaba N, Garcia-Fuentes M, Alonso MJ. Polysaccharide-Based Nanocarriers for Drug Delivery. In: Torchilin V, editor. Handbook of

Nanobiomedical Research: Fundamentals, Applications and Recent Development. World Scientific; 2014. page 235–78.

[99] Tiantian Y, Wenji Z, Mingshuang S, Rui Y, Shuangshuang S, Yuling M, et al. Study on intralymphatic-targeted hyaluronic acid-modified nanoliposome: Influence of formulation factors on the lymphatic targeting. Int. J. Pharm. 2014;471:245–57.

[100] Pérez-Herrero E, Fernández-Medarde A. Advanced targeted therapies in cancer: Drug nanocarriers, the future of chemotherapy. Eur. J. Pharm. Biopharm. 2015;93:52–79.

[101] Durymanov M, Rosenkranz A, Sobolev A. Current Approaches for Improving Intratumoral Accumulation and Distribution of Nanomedicines. Theranostics 2015;5:1007–20.

[102] Shao K, Singha S, Clemente-Casares X, Tsai S, Yang Y, Santamaria P. Nanoparticle-Based Immunotherapy for Cancer. ACS Nano 2015;9:16–30.

[103] Silva JM, Videira M, Gaspar R, Préat V, Florindo HF. Immune system targeting by biodegradable nanoparticles for cancer vaccines. J. Control. Release 2013;168:179–99.

[104] Parker RJ, Hartman KD, Sieber SM. Lymphatic Absorption and Tissue Disposition of Liposome-entrapped [14C] Adriamycin following Intraperitoneal Administration to Rats. Cancer Res. 1981;41:1311–7.

[105] Akamo Y, Mizuno I, Yotsuyanagi T, Ichino T, Tanimoto N, Yamamoto T, et al. Chemotherapy targeting regional lymph-nodes by gastric submucosal injection of liposomal adriamycin in patients with gastric-carcinoma. Japanish J. Cancer Res. 1994;85:652–8.

[106] Hu L, Liang G, Yuliang W, Bingjing Z, Xiangdong Z, Rufu X. Assessing the effectiveness and safety of liposomal paclitaxel in combination with cisplatin as first-line chemotherapy for patients with advanced NSCLC with regional lymph-node metastasis: study protocol for a randomized controlled trial (PLC-GC trial). Trials 2013;14:45.

[107] Ye L, He J, Hu Z, Dong Q, Wang H, Fu F, et al. Antitumor effect and toxicity of Lipusu in rat ovarian cancer xenografts. Food Chem. Toxicol. 2013;52:200–6.

[108] Third Military Medical University of Chongqing. An Open-label,Randomized Controlled Clinical Study :Paclitaxel Liposomes in Combination With Cisplatin Verus Gemcitabine Combined With Cisplatin in Treatment of III and IV stage NSCLC with regional lymph node metastasis [Internet]. Chinese Clin. Trial [cited 2015 Apr 1];Available from: http://www.chictr.org/en/proj/show.aspx?proj=2795

[109] Koshkina N V, Waldrep JC, Roberts LE, Golunski E, Melton S, Knight V. Paclitaxel Liposome Aerosol Treatment Induces Inhibition of Pulmonary Metastases in Murine Renal Carcinoma Model. Clin. cancer Res. 2001;7:3258–62.

[110] Latimer P, Menchaca M, Snyder RM, Yu W, Gilbert BE, Sanders BG, et al. Aerosol Delivery of Liposomal Formulated Paclitaxel and Vitamin E Analog Reduces Murine Mammary Tumor Burden and Metastases. Exp. Biol. Med. 2009;234:1244–52.

[111] Lawson KA, Anderson K, Snyder RM, Simmons-Menchaca M, Atkinson J, Sun L-Z, et al. Novel vitamin E analogue and 9-nitro-camptothecin administered as liposome aerosols decrease syngeneic mouse mammary tumor burden and inhibit metastasis. Cancer Chemother. Pharmacol. 2004;54:421–31.

[112] Cuong N-V, Hsieh M-F. Molecular targeting of liposomal nano-particles to lymphatic system. Curr. Cancer Drug Targets 2011;11:147–55.

[113] Hrkach J, Von Hoff D, Mukkaram Ali M, Andrianova E, Auer J, Campbell T, et al. Preclinical development and clinical translation of a PSMA-targeted docetaxel nanoparticle with a differentiated pharmacological profile. Sci. Transl. Med. 2012;4:128ra39.

[114] A Phase 2 study to determine the safety and efficacy of BIND-014 (docetaxel nanoparticles injectable suspension), administered to patients with metastatic castration-resistant prostate cancer [Internet]. [cited 2015 May 1];ClinicalTrials.gov. Available from: http://clinicaltrials.gov/show/NCT01812746

[115] A Phase 2 study to determine the safety and efficacy of BIND-014 (docetaxel nanoparticles injectable suspension) as second line therapy to patients with non-small cell lung cancer [Internet]. [cited 2015 May 1];ClinicalTrials.gov. Available from: http://clinicaltrials.gov/show/NCT01792479

[116] A Study of BIND-014 (Docetaxel Nanoparticles for Injectable Suspension) as Second-line Therapy for Patients With KRAS Positive or Squamous Cell Non-Small Cell Lung Cancer [Internet]. [cited 2015 May 1];Clinicaltrials.gov. Available from: https://clinicaltrials.gov/ct2/show/NCT02283320?term=BIND-014&rank=4

[117] Liu R, Gilmore DM, Zubris KA V, Xu X, Catalano PJ, Padera RF, et al. Prevention of nodal metastases in breast cancer following the lymphatic migration of paclitaxel-loaded expansile nanoparticles. Biomaterials 2013;34:1810–9.

[118] Griset AP, Walpole J, Liu R, Gaffey A, Colson YL, Grinstaff MW. Expansile nanoparticles: synthesis, characterization, and in vivo efficacy of an acid-responsive polymeric drug delivery system. J. Am. Chem. Soc. 2009;131:2469–71.

[119] Khullar O V, Griset AP, Gibbs-Strauss SL, Chirieac LR, Zubris KA V, Frangioni J V, et al. Nanoparticle migration and delivery of paclitaxel to regional lymph nodes in a large animal model. J. Am. Coll. Surg. 2012;214:328–37.

[120] Kattan J, Droz JP, Couvreur P, Marino JP, Boutan-Laroze A, Rougier P, et al. Phase I clinical trial and pharmacokinetic evaluation of doxorubicin carried by polyisohexylcyanoacrylate nanoparticles. Invest. New Drugs 1992;10:191–9.

[121] Alonso MJ, Couvreur P. Historical view of the design and development of nanocarriers for overcoming biological barriers. In: Alonso MJ, Csaba N, editors. Nanostructured Biomaterials for Overcoming Biological Barriers. Cambridge, UK: 2012. page 3–36.

[122] Lu B, Xiong S-B, Yang H, Yin X-D, Chao R-B. Solid lipid nanoparticles of mitoxantrone for local injection against breast cancer and its lymph node metastases. Eur. J. Pharm. Sci. 2006;28:86–95.

[123] Lasa-Saracibar B, Estella-Hermoso de Mendoza A, Guada M, Dios-Vieitez C, Blanco-Prieto MJ. Lipid nanoparticles for cancer therapy: state of the art and future prospects. Expert Opin. Drug Deliv. 2012;9:1245–61.

[124] Baek J-S, So J-W, Shin S-C, Cho C-W. Solid lipid nanoparticles of paclitaxel strengthened by hydroxypropyl-β-cyclodextrin as an oral delivery system. Int. J. Mol. Med. 2012;30:953–9.

[125] Cho H-J, Park JW, Yoon I-S, Kim D-D. Surface-modified solid lipid nanoparticles for oral delivery of docetaxel: enhanced intestinal absorption and lymphatic uptake. Int. J. Nanomedicine 2014;9:495–504.

[126] NCT00147238. A Validation Study of MR Lymphangiography Using SPIO, a New Lymphotropic Superparamagnetic Nanoparticle Contrast [Internet]. [cited 2015 Jun 6];Available from: https://clinicaltrials.gov/ct2/show/NCT00147238?term=lymph&cond=drug&rank=35

[127] Hervella P, Lollo G, Oyarzún-Ampuero F, Rivera G, Torres D, Alonso M. Nanocapsules as carriers for the transport and targeted delivery of bioactive molecules. In: Da Silva AL, Trindade T, editors. Nanocomposite Particles for Bio-Applications - Materials and Bio-Interfaces. Pan Stanford Publishing Pte Ltd; 2011. page 45–68.

[128] Wauthoz N, Bastiat G, Moysan E, Cieslak A, Kondo K, Zandecki M, et al. Safe lipid nanocapsule-based gel technology to target lymph nodes and combat mediastinal metastases from an orthotopic non-small-cell lung cancer model in SCID-CB17 mice. Nanomedicine Nanotechnology, Biol. Med. 2015;1.

[129] Gonzalo T, Lollo G, Garcia-Fuentes M, Torres D, Correa J, Riguera R, et al. A new potential nano-oncological therapy based on polyamino acid nanocapsules. J. Control. Release 2013;169:10–6.

[130] Lollo G, Hervella P, Calvo P, Avilés P, Guillén MJ, Garcia-Fuentes M, et al. Enhanced in vivo therapeutic efficacy of plitidepsin-loaded nanocapsules decorated with a new poly-aminoacid-PEG derivative. Int. J. Pharm. 2015;483:212–9.

[131] Lollo G, Rivera-Rodriguez GR, Bejaud J, Passirani C, Benoit J-P, García-Fuentes M, et al. Polyglutamic acid-PEG nanocapsules as long circulated carriers for the delivery of docetaxel. Eur. J. Pharm. Biopharm. 2014;87:47–54.

[132] Rivera-Rodriguez GR, Lollo G, Montier T, Benoit JP, Passirani C, Alonso MJ, et al. In vivo evaluation of poly-l-asparagine nanocapsules as carriers for anti-cancer drug delivery. Int. J. Pharm. 2013;458:83–9.

[133] Oyarzun-Ampuero FA, Brea J, Loza MI, Alonso MJ, Torres D. A potential nanomedicine consisting of heparin-loaded polysaccharide nanocarriers for the treatment of asthma. Macromol. Biosci. 2012;12:176–83.

[134] Torrecilla D, Lozano M V., Lallana E, Neissa JI, Novoa-Carballal R, Vidal A, et al. Anti-tumor efficacy of chitosan-g-poly(ethylene glycol) nanocapsules containing docetaxel: Anti-TMEFF-2 functionalized nanocapsules vs. non-functionalized nanocapsules. Eur. J. Pharm. Biopharm. 2013;83:330–7.

[135] Abellan-Pose R, Borrajo E, Rodriguez-Evora M, Delgado A, Evora C, Vicente S, et al. New Strategy to Tackle Lymphatic Metastasizing Tumors Based on Polyaminoacid Nanocapsules. In: Journal of Nanomaterials & Molecular Nanotechnology. 2014. page 22.

[136] Huang B, Abraham WD, Zheng Y, López SCB, Luo SS, Irvine DJ. Active targeting of chemotherapy to disseminated tumors using nanoparticle-carrying T cells. Sci. Transl. Med. 2015;7:291ra94.

[137] Attili-Qadri S, Karra N, Nemirovski A, Schwob O, Talmon Y, Nassar T, et al. Oral delivery system prolongs blood circulation of docetaxel nanocapsules via lymphatic absorption. Proc. Natl. Acad. Sci. U. S. A. 2013;110:17498–503.

[138] Cabral H, Makino J, Matsumoto Y, Mi P, Wu H, Nomoto T, et al. Systemic Targeting of Lymph Node Metastasis through the Blood Vascular System by Using Size-Controlled Nanocarriers. ACS Nano 2015;9:4957–67.

[139] Kim S, Shi Y, Kim JY, Park K, Cheng J-X. Overcoming the barriers in micellar drug delivery: loading efficiency, in vivo stability, and micelle-cell interaction. Expert Opin. Drug Deliv. 2010;7:49–62.

[140] Ryan GM, Kaminskas LM, Bulitta JB, McIntosh MP, Owen DJ, Porter CJH. PEGylated polylysine dendrimers increase lymphatic exposure to doxorubicin when compared to PEGylated liposomal and solution formulations of doxorubicin. J. Control. Release 2013;172:128–36.

[141] Kaminskas LM, Porter CJH. Targeting the lymphatics using dendritic polymers (dendrimers). Adv. Drug Deliv. Rev. 2011;63:890–900.

[142] Kaminskas LM, McLeod VM, Ryan GM, Kelly BD, Haynes JM, Williamson M, et al. Pulmonary administration of a doxorubicin-conjugated dendrimer enhances drug exposure to lung metastases and improves cancer therapy. J. Control. Release 2014;183:18–26.

[143] Liang C, Diao S, Wang C, Gong H, Liu T, Hong G, et al. Tumor metastasis inhibition by imaging-guided photothermal therapy with single-walled carbon nanotubes. Adv. Mater. 2014;5646–52.

[144] Vardharajula S, Ali SZ, Tiwari PM, Eroğlu E, Vig K, Dennis VA, et al. Functionalized carbon nanotubes: Biomedical applications. Int. J. Nanomedicine 2012;7:5361–74.

[145] Ajima K, Murakami T, Mizoguchi Y, Tsuchida K, Ichihashi T, Iijima S, et al. Enhancement of In Vivo Anticancer Inside Single-Wall Carbon Nanohorns. ACS Nano 2008;2:2057–64.

[146] Yang F, Fu DL, Long J, Ni QX. Magnetic lymphatic targeting drug delivery system using carbon nanotubes. Med. Hypotheses 2008;70:765–7.

[147] Murakami T, Sawada H, Tamura G, Yudasaka M, Iijima S, Tsuchida K. Water-dispersed single-wall carbon nanohorns as drug carriers for local cancer chemotherapy. Nanomedicine (Lond). 2008;3:453–63.

[148] Takakura Y, Matsumoto S, Hashida M, Sezaki H. Enhanced Lymphatic Delivery of Mitomycin C Conjugated with Dextran. Cancer Res. 1984;44:2505–10.

[149] Cai S, Xie Y, Bagby TR, Cohen MS, Forrest ML. Intralymphatic chemotherapy using a hyaluronan-cisplatin conjugate. J. Surg. Res. 2008;147:247–52.

[150] Cai S, Thati S, Bagby TR, Diab HM, Davies NM, Cohen MS, et al. Localized doxorubicin chemotherapy with a biopolymeric nanocarrier improves survival and reduces toxicity in xenografts of human breast cancer. J. Control. Release 2010;146:212–8.

[151] Cohen MS, Cai S, Xie Y, Forrest ML. A novel intralymphatic nanocarrier delivery system for cisplatin therapy in breast cancer with improved tumor efficacy and lower systemic toxicity in vivo. Am. J. Surg. 2009;198:781–6.

[152] Venable RO, Worley DR, Gustafson DL, Hansen RJ, Ehrhart III EJ, Cai S, et al. Effects of intratumoral administration of a hyaluronan-cisplatin nanoconjugate to five dogs with soft tissue sarcomas. Am. J. Vet. Res. 2012;73:1969–76.

[153] Xie Y, Aillon KL, Cai S, Christian JM, Davies NM, Berkland CJ, et al. Pulmonary delivery of cisplatin-hyaluronan conjugates via endotracheal instillation for the treatment of lung cancer. Int. J. Pharm. 2010;392:156–63.

[154] Jhan H-J, Liu J-J, Chen Y-C, Liu D-Z, Sheu M-T, Ho H-O. Novel injectable thermosensitive hydrogels for delivering hyaluronic acid–doxorubicin nanocomplexes to locally treat tumors. Nanomedicine (Lond). 2015;10:1263–74.

[155] Kim C, Lee M, Han J, Lee B. Pharmacokinetics and tissue distribution of methotrexate after intravenous injection of differently charged liposome-entrapped methotrexate to rats. Int. J. Pharm. 1994;108:21–9.

[156] Kim CK, Han JH. Lymphatic delivery and pharmacokinetics of methotrexate after intramuscular injection of differently charged liposome-entrapped methotrexate to rats. J. Microencapsul. 1995;12:437–46.

[157] Parker R, Priester E, Sieber SM. Effect of route administration and liposome entrapment on the metabolism and disposition of adriamycin in the rat. Drug Metab. Dispos. 1982;10:499–504.

[158] Kiyokawa H, Igawa Y, Muraishi O, Katsuyama Y, Iizuka K, Nishizawa O. Distribution of doxorubicin in the bladder wall and regional lymph nodes after bladder submucosal injection of liposomal doxorubicin in the dog. J. Urol. 1999;161:665–7.

[159] Ling R, Li Y, Yao Q, Chen T, Zhu D, Jun Y, et al. Lymphatic chemotherapy induces apoptosis in lymph node metastases in a rabbit breast carcinoma model. J. Drug Target. 2005;13:137–42.

[160] Lopes de Menezes DE, Pilarski LM, Belch AR, Allen TM. Selective targeting of immunoliposomal doxorubicin against human multiple myeloma in vitro and ex vivo. Biochim. Biophys. Acta 2000;1466:205–20.

[161] Wen J, Fu AF, Chen LJ, Xie XJ, Yang GL, Chen XG, et al. Liposomal honokiol inhibits VEGF-D-induced lymphangiogenesis and metastasis in xenograft tumor model. Int. J. Cancer 2009;124:2709–18.

[162] Khato J, Priester ER, Sieber SM. Enhanced lymph node uptake of melphalan following liposomal entrapment and effects on lymph nodemetastasis in rats. Cancer Treat. Rep. 1982;66:517–27.

[163] Khato J, del Campo AA, Sieber SM. Carrier activity of sonicated small liposomes containing melphalan to regional lymph nodes of rats. Pharmacology 1983;26:230–40.

[164] Zhang J, Huang C, Huang H. Antitumor and antimetastasis effects of carboplatin liposomes with polyethylene glycol-2000 on SGC-7901 gastric cell-bearing nude mice. Oncol. Lett. 2014;2209–14.

[165] Murphy E a, Majeti BK, Barnes L a, Makale M, Weis SM, Lutu-Fuga K, et al. Nanoparticle-mediated drug delivery to tumor vasculature suppresses metastasis. Proc. Natl. Acad. Sci. U. S. A. 2008;105:9343–8.

[166] Shete H, Chatterjee S, De A, Patravale V. Long chain lipid based tamoxifen NLC. Part II: pharmacokinetic, biodistribution and in vitro anticancer efficacy studies. Int. J. Pharm. 2013;454:584–92.

[167] Shete HK, Selkar N, Vanage GR, Patravale VB. Tamoxifen nanostructured lipid carriers: enhanced in vivo antitumor efficacy with reduced adverse drug effects. Int. J. Pharm. 2014;468:1–14.

[168] Paliwal R, Paliwal SR, Mishra N, Mehta A, Vyas SP. Engineered chylomicron mimicking carrier emulsome for lymph targeted oral delivery of methotrexate. Int. J. Pharm. 2009;380:181–8.

[169] Zhang Z, Ma L, Jiang S, Liu Z, Huang J, Chen L, et al. A self-assembled nanocarrier loading teniposide improves the oral delivery and drug concentration in tumor. J. Control. Release 2013;166:30–7.

[170] Cai S, Xie Y, Davies NM, Cohen MS, Forrest ML. Pharmacokinetics and Disposition of a Localized Lymphatic Polymeric Hyaluronan Conjugate of Cisplatin in Rodents. J. Pharm. Sci. 2010;99:2664–71.

[171] Laakkonen P, Porkka K, Hoffman JA, Ruoslahti E. A tumor-homing peptide with a targeting specificity related to lymphatic vessels. Nat. Med. 2002;8:751–5.

[172] Fogal V, Zhang L, Krajewski S, Ruoslahti E. Mitochondrial/cell-surface protein p32/gC1qR as a molecular target in tumor cells and tumor stroma. Cancer Res. 2008;68:7210–8.

[173] Laakkonen P, Akerman ME, Biliran H, Yang M, Ferrer F, Karpanen T, et al. Antitumor activity of a homing peptide that targets tumor lymphatics and tumor cells. Proc. Natl. Acad. Sci. U. S. A. 2004;101:9381–6.

[174] Luo G, Yu X, Jin C, Yang F, Fu D, Long J, et al. LyP-1-conjugated nanoparticles for targeting drug delivery to lymphatic metastatic tumors. Int. J. Pharm. 2010;385:150–6.

[175] Yan Z, Wang F, Wen Z, Zhan C, Feng L, Liu Y, et al. LyP-1-conjugated PEGylated liposomes: a carrier system for targeted therapy of lymphatic metastatic tumor. J. Control. Release 2012;157:118–25.

[176] Yan Z, Zhan C, Wen Z, Feng L, Wang F, Liu Y, et al. LyP-1-conjugated doxorubicin-loaded liposomes suppress lymphatic metastasis by inhibiting lymph node metastases and destroying tumor lymphatics. Nanotechnology 2011;22:415103.

[177] Wang Z, Yu Y, Ma J, Zhang H, Zhang H, Wang X, et al. LyP-1 Modification To Enhance Delivery of Artemisinin or Fluorescent Probe Loaded Polymeric Micelles to Highly Metastatic Tumor and Its Lymphatics. Mol. Pharm. 2012;9:2646–57.

[178] Gürsoy RN, Çevik Ö. Design, characterization and in vitro evaluation of SMEDDS containing an anticancer peptide, linear LyP-1. Pharm. Dev. Technol. 2014;19:486–90.

[179] Galmarini CM, Warren G, Senanayake MT, Vinogradov S V. Efficient overcoming of drug resistance to anticancer nucleoside analogs by nanodelivery of active phosphorylated drugs. Int. J. Pharm. 2010;395:281–9.

[180] Gu B, Xie C, Zhu J, He W, Lu W. Folate-PEG-CKK(2)-DTPA, A Potential Carrier for Lymph-Metastasized Tumor Targeting. Pharm. Res. 2010;27:933–42.

[181] Cho H, Lee CK, Lee Y. Preparation and Evaluation of PEGylated and Folate-PEGylated Liposomes Containing Paclitaxel for Lymphatic Delivery. J. Nanomater. 2015;2015:1–10.

[182] He X, Liu T, Chen Y, Cheng D, Li X, Xiao Y, et al. Calcium carbonate nanoparticle delivering vascular endothelial growth factor-C siRNA effectively inhibits lymphangiogenesis and growth of gastric cancer in vivo. Cancer Gene Ther. 2008;15:193–202.

[183] Ye T, Jiang X, Li J, Yang R, Mao Y, Li K, et al. Low molecular weight heparin mediating targeting of lymph node metastasis based on nanoliposome and enzyme–substrate interaction. Carbohydr. Polym. 2015;122:26–38.

[184] Biopharmaceuticals N, Inc. Lymphoseek (prescribing information). 2014;

[185] Wallace AM, Han LK, Povoski SP, Deck K, Schneebaum S, Hall NC, et al. Comparative evaluation of [99mTc]Tilmanocept for sentinel lymph node mapping in breast cancer patients: results of two phase 3 trials. Ann. Surg. Oncol. 2013;20:2590–9.

[186] Surasi DS, O'Malley J, Bhambhvani P. 99mTc-Tilmanocept: A Novel Molecular Agent for Lymphatic Mapping and Sentinel Lymph Node Localization. J. Nucl. Med. Technol. 2015;43:87–91.

[187] Karmali PP, Kotamraju VR, Kastantin M, Black M, Missirlis D, Tirrell M, et al. Targeting of albumin-embedded paclitaxel nanoparticles to tumors. Nanomedicine 2009;5:73–82.

[188] Liu H, Moynihan KD, Zheng Y, Szeto GL, Li A V, Huang B, et al. Structure-based programming of lymph-node targeting in molecular vaccines_Supple. Nature 2014;507:519–22.

[189] Jewell CM, Bustamante Lopez SC, Irvine DJ. In situ engineering of the lymph node microenvironment via intranodal injection of adjuvant-releasing polymer particles. Proc. Natl. Acad. Sci. 2011;108:15745–50.

ANTECEDENTES, HIPÓTESIS Y OBJETIVOS

USC
UNIVERSIDADE
DE SANTIAGO
DE COMPOSTELA

ANTECEDENTES

1. Las nanocápsulas constituidas por un núcleo oleoso y una cubierta polimérica permiten encapsular, proteger y liberar eficazmente fármacos hidrofóbicos, así como mejorar su internalización celular, por lo que resultan vehículos prometedores para diversas aplicaciones biomédicas [1,2].

2. Nuestro grupo ha desarrollado nanocápsulas con cubiertas de ácido poliglutámico (PGA), ácido poliglutámico PEGilado (PGA-PEG) o poliasparagina (PASN), de tamaño comprendido entre 170 y 220 nm, para la administración intravenosa de fármacos antitumorales [3,4]. Estos nanosistemas han mostrado un prolongado tiempo de permanencia en plasma y una eficacia antitumoral comparable con la formulación comercial, con menor toxicidad y mejor tasa de supervivencia [5,6].

3. El sistema linfático actúa como sede de numerosas enfermedades de carácter vírico, bacteriano, autoinmune y cáncer. Para la mayoría de tumores sólidos el sistema linfático supone además una importante vía de diseminación [7]. El éxito de la quimioterapia convencional sobre las células cancerosas que diseminan por esta vía es muy limitado, ya que las propiedades anatómicas del sistema linfático dificultan la llegada de concentraciones adecuadas de fármacos al mismo [8].

4. El uso de nanosistemas de liberación de fármacos es una prometedora estrategia para vehiculizar fármacos antitumorales al sistema linfático y tratar las metástasis [9,10]. Estos nanosistemas deben ser diseñados teniendo en cuenta la fisiología del sistema linfático, fisiopatología del tumor y los requerimientos asociados a la vía de administración. En este sentido, las características fisicoquímicas de los nanosistemas tienen una crucial importancia, ya que condicionan la velocidad y extensión con la que pueden acceder al sistema linfático [10,11].

USC
UNIVERSIDADE
DE SANTIAGO
DE COMPOSTELA

HIPÓTESIS

1. La optimización de varios parámetros implicados en la técnica del desplazamiento del disolvente puede permitir elaborar nanocápsulas de tamaño reducido y composición sencilla, capaces de encapsular y liberar de forma eficaz fármacos hidrofóbicos.

2. Las nanocápsulas de pequeño tamaño (en torno a 100 nm) constituidas por un núcleo oleoso y una cubierta polimérica de carácter hidrofílico pueden resultar adecuadas para dirigir fármacos u otras moléculas hacia el sistema linfático. Esta distribución a la linfa puede ser lograda mediante diferentes vías de administración, como la vía intravenosa y la vía subcutánea.

3. Las nanocápsulas pueden ser vehículos eficaces para dirigir fármacos antitumorales a los ganglios linfáticos afectados por metástasis y promover su internalización en las células tumorales. Esta estrategia puede mejorar la eficacia antitumoral del fármaco, tanto sobre el tumor primario como sobre las células metastásicas allí presentes, y, al mismo tiempo, disminuir la toxicidad del tratamiento.

USC
UNIVERSIDADE
DE SANTIAGO
DE COMPOSTELA

OBJETIVOS

Teniendo en cuenta los antecedentes expuestos y las hipótesis planteadas, el objetivo principal de esta tesis doctoral ha sido el desarrollo y evaluación de nanocápsulas, con una cubierta de poliaminoácidos y características adecuadas para favorecer la vehiculización de fármacos antitumorales al sistema linfático, como nueva estrategia para mejorar el tratamiento del cáncer metastásico.

Para lograr este objetivo se han planteado las siguientes etapas:

1 Desarrollo de nanocápsulas de PGA, PGA-PEG y PASN de pequeño tamaño.

Esta etapa se ha dirigido a la optimización de la técnica de desplazamiento del disolvente con el fin de obtener nanoemulsiones y nanocápsulas de PGA, PGA-PEG o PASN que presenten un tamaño cercano a los 100 nm. Se han realizado estudios para evaluar su capacidad para encapsular y liberar de forma eficaz el fármaco antitumoral docetaxel, así como amplios estudios de estabilidad coloidal de las formulaciones.

Los resultados de este apartado se recogen en el capítulo 2: Polyaminoacid Nanocapsules for Lymphatic Drug Delivery: Influence of the Particle Size.

2 Evaluación de la biodistribución de las nanocápsulas de PGA y PGA-PEG

El objetivo de esta etapa ha sido el estudio de la distribución y capacidad de vectorización linfática de las nanocápsulas de PGA y PGA-PEG. También se ha pretendido valorar el efecto del PEG sobre la cubierta de las nanocápsulas de PGA y la influencia de la vía de administración sobre su biodistribución.

Los resultados de este apartado se recogen en el capítulo 3: Biodistribution of Radiolabeled Polyglutamic acid and PEGylated-Polyglutamic Acid Nanocapsules.

3 Evaluación de la capacidad de las nanocápsulas de PGA-PEG para vehiculizar fármacos al sistema linfático y tratar el cáncer metastásico.

El objetivo de esta etapa es la evaluación del potencial de las nanocápsulas de PGA-PEG para acceder al sistema linfático y actuar sobre las células tumorales allí presentes

para evitar la metástasis en un modelo de cáncer de pulmón que metastatiza al ganglio mediastino. También se ha pretendido estudiar la toxicidad asociada a este tratamiento.

Los resultados de este apartado se recogen en el anexo I (evaluación *in vitro*) y capítulo 4 (evaluación *in vivo*).

Anexo 1: Internalization of PGA-PEG Nanocapsules in A549 Human Lung Adenocarcinoma Cells.

Capítulo 4: Docetaxel-loaded PEGylated-Polyglutamic Acid Nanocapsules for the Treatment of Metastatic Cancer.

REFERENCES

[1] Lozano M V, Torrecilla D, Torres D, Vidal A, Domínguez F, Alonso MJ. Highly efficient system to deliver taxanes into tumor cells: docetaxel-loaded chitosan oligomer colloidal carriers. Biomacromolecules 2008;9:2186–93.

[2] Oyarzun-Ampuero FA, Rivera-Rodríguez GR, Alonso MJ, Torres D. Hyaluronan nanocapsules as a new vehicle for intracellular drug delivery. Eur. J. Pharm. Sci. 2013;49:483–90.

[3] Gonzalo T, Lollo G, Garcia-Fuentes M, Torres D, Correa J, Riguera R, et al. A new potential nano-oncological therapy based on polyamino acid nanocapsules. J. Control. Release 2013;169:10–6.

[4] Rivera-Rodríguez GR, Alonso MJ, Torres D. Poly-L-asparagine nanocapsules as anticancer drug delivery vehicles. Eur. J. Pharm. Biopharm. 2013;85:481–7.

[5] Lollo G, Rivera-Rodriguez GR, Bejaud J, Passirani C, Benoit JP, García-Fuentes M, et al. Polyglutamic acid-PEG nanocapsules as long circulated carriers for the delivery of docetaxel. Eur. J. Pharm. Biopharm. 2014;87:47–54.

[6] Rivera-Rodriguez GR, Lollo G, Montier T, Benoit JP, Passirani C, Alonso MJ, et al. In vivo evaluation of poly-l-asparagine nanocapsules as carriers for anti-cancer drug delivery. Int. J. Pharm. 2013;458:83–9.

[7] Stacker SA, Achen MG, Jussila L, Baldwin ME, Alitalo K. Lymphangiogenesis and cancer metastasis. Nat. Rev. Cancer 2002;2:573–83.

[8] Xie Y, Bagby TR, Cohen M, Forrest ML. Drug delivery to the lymphatic system: importance in future cancer diagnosis and therapies. Expert Opin. Drug Deliv. 2009;6:785–92.

[9] Cai S, Yang Q, Bagby TR, Forrest ML. Lymphatic drug delivery using engineered liposomes and solid lipid nanoparticles. Adv. Drug Deliv. Rev. 2011;63:901–8.

[10] Ryan GM, Kaminskas LM, Porter CJH. Nano-chemotherapeutics: Maximising lymphatic drug exposure to improve the treatment of lymph-metastatic cancers. J. Control. Release 2014;193:241–56.

[11] Oussoren C, Storm G. Liposomes to target the lymphatics by subcutaneous administration. Adv. Drug Deliv. Rev. 2001;50:143–56.

USC
UNIVERSIDADE
DE SANTIAGO
DE COMPOSTELA

Capítulo 2

Polyaminoacid Nanocapsules for Lymphatic Drug Delivery: Influence of the Particle Size

USC
UNIVERSIDADE
DE SANTIAGO
DE COMPOSTELA

Polyaminoacid Nanocapsules for Lymphatic Drug Delivery: Influence of the Particle Size

Este trabajo ha sido realizado en colaboración con Carmen Teijeiro[1], Manuel Santander[2], Erea Borrajo[3], Anxo Vidal[3] y Marcos García[1].

[1] Nanobiofar Group, IDIS, CIMUS. (USC). Santiago de Compostela, Spain.

[2] Cellular Neurobiology and Molecular Chemistry of the Central Nervous System Group, University of Castilla La Mancha, Spain

[3] Cell Cycle and Oncology group CiClOn, IDIS, CIMUS. (USC). Santiago de Compostela, Spain.

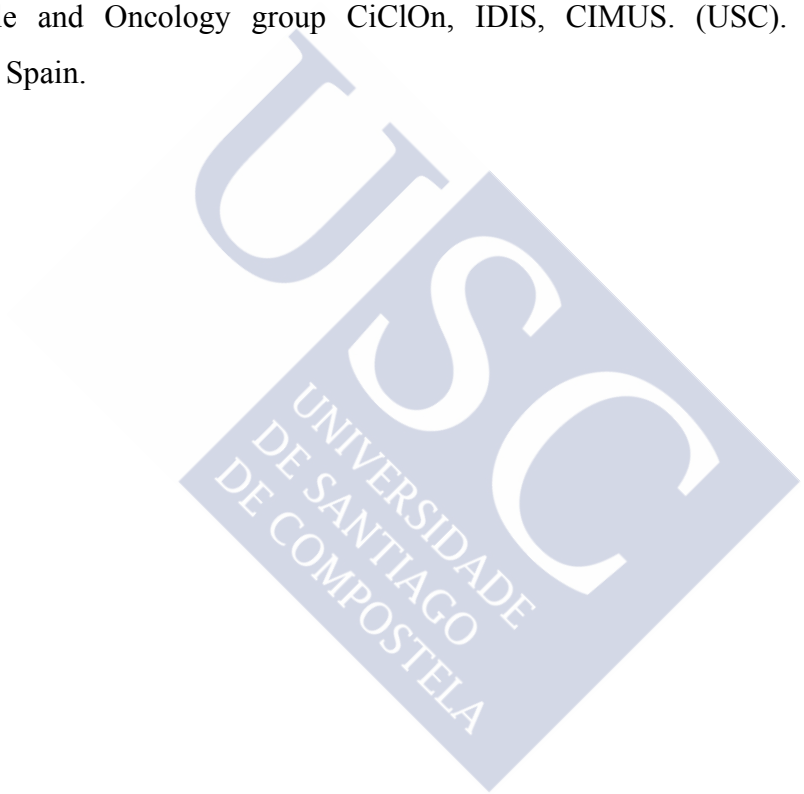

USC
UNIVERSIDADE
DE SANTIAGO
DE COMPOSTELA

ABSTRACT

We have previously shown that polyaminoacid nanocapsules with a size larger than 200 nm have a potential as vehicles for the intravenous administration of the anti-cancer drug docetaxel. Based on the hypothesis that a reduction in their size might facilitate their access to the lymphatic system, the objective of this work has been to develop polyaminoacid nanocapsules with a particle size close to 100 nm, and to study their properties as lymphotropic drug carriers. For this, we chose the solvent displacement technique, and analyzed the influence a number of formulation parameters on the characteristics of polyglutamic acid (PGA), PEGylated polyglutamic acid (PGA-PEG) and polyasparagine (PASN) nanocapsules. From this analysis, we could identify the conditions that led to the formation of nanocapsules exhibiting a size in the range of 70 – 120 nm and a capacity to encapsulate the antitumor drug docetaxel and released it in a sustained manner under physiological conditions. In addition, a detailed study of the colloidal stability led to the conclusion that the polyaminoacid shell of the nanocapsules has a critical role on their stability in biologically relevant media. Finally, we have studied the influence of the particle size (100 nm vs 200 nm) on the biodistribution of PGA-PEG nanocapsules following subcutaneous injection, with particular emphasis on their distribution to the lymphatics. Our results showed that the 100 nm nanocapsules had a faster accumulation in the lymph nodes than the larger ones (200 nm). Therefore, overall, these nanocapsules represent a new platform for the lymphatic drug delivery.

Keywords: lymphatic targeting; polyaminoacid nanocapsules; particle size.

USC
UNIVERSIDADE
DE SANTIAGO
DE COMPOSTELA

1 INTRODUCTION

Currently, there is significant evidence of the potential of polymeric nanocarriers for the targeted delivery of anticancer drugs to the tumor tissue. Indeed, some of them, i.e. docetaxel-loaded poly(lactic acid-glycolic acid)-polyethyleneglicol (PLGA-PEG) nanoparticles [1], and polyglutamic acid (PGA)-paclitaxel and PGA-camptothecin conjugates [2] are currently in Phase II and Phase III clinical trials. In addition, several polymeric micelles based on PGA-PEG (NK012, NC-6004, NC-4016), are also under clinical evaluation for the delivery of SN38, cisplatin and oxaliplatin, respectively, exhibiting enhanced antitumor efficacy and reduced side effects [3,4]. As an alternative, our group has contributed to this field of research with the design of polymeric nanocapsules, consisting in a lipid core surrounded by a polymer shell [5–7]. This nanocarrier exhibit competitive advantages as compared to other delivery nanovehicles. Namely, their oily core that enables the encapsulation of high loads of hydrophobic drugs and their polymer shell helps preserving their stability and controlling the release of the encapsulated drugs. Among the polymers used to form the nanocapsule's shell, polyaminoacids result particularly attractive, not only due of their low toxicity, but also because they can have reactive functional groups at their side chains such as carboxyl, amide, amino, hydroxyl and thiol groups, that enable various chemical modifications [2,3]. Among the polyaminoacids, polyglutamic acid (PGA) and polyasparagine (PASN) are particularly interesting, as they have been widely used for the formation of drug-polymer conjugates. On the other hand, the potential of polyasparagine (PASN) as a biomaterial for anticancer drug delivery has been justified by the avidity of tumor cells towards this polyaminoacid that is essential for their growth [8]. Overall, the analysis of the *in vivo* behavior of these nanocapsules has led us to the conclusion that they are able to modulate the biodistribution and facilitate the intracellular delivery of anticancer drugs [9–11]. Moreover, following intravenous administration PGA, PGA-PEG [9] and PASN nanocapsules [12] with a size in the range of 170 and 220 nm, we have observed comparable effects in terms of primary tumor growth inhibition, together with higher survival rates and lower toxicity than those achieved of the commercial formulation of docetaxel [10,13].

Despite the advances on the use of nanocarriers for the delivery of drugs to the tumor tissue, researchers in the field are becoming conscious of the necessity to target the drug to the lymphatic system. In fact, nowadays it is accepted that an important limitation of the conventional intravenous chemotherapy relies on the incapacity of cytotoxic drugs to reach metastatic cells, frequently accumulated in the lymphatic system [14]. Taking this into account, we started the "LYMPHOTARG" European Consortium with the final goal of identifying the key properties for specific nanocarriers to reach the lymphatics. Within this context, the objective of the work presented here has been to design polymer nanocapsules specifically tailored for the delivery of drugs to the lymphatic system. In this sense, several studies have shown that subcutaneously administered nanosystems with a size up to 100 nm, and a hydrophilic and negatively charged surface maybe easily drained by the lymphatic system [15–17]. These requirements may be also applied to nanocarriers administered by the intravenous route, which must extravasate from the tumor-associated blood vessels and traverse the tumor interstice before entering the functional peritumoral lymphatic vessels [18,19]. The information reported so far in this regard indicates that nanocarriers with a size close to 100 nanometers are the most appropriate based on their ability to reach the lymphatic capillaries from the interstice and remain entrapped in the lymphatic system [15,20].

The production of nanocapsules with a size close to 100 nm is a substantial technological challenge since conventional preparation techniques generally yield nanocapsules larger than 200 nm [21]. Smaller nanocapsules have been produced by employing high surfactant concentrations and high temperatures through a phase inversion method [22]. As an alternative, in the present work we opted to adapt a mild and easily scalable solvent diffusion method by the systematic screening of the formulation parameters, in order to identify the optimal conditions for the preparation of nanocapsules with simple and flexible composition, combined with a reduced particle size suitable for the lymphatic targeting of drugs. Furthermore, we have studied the biodistribution of PGA-PEG nanocapsules with different sizes in order to validate our strategy and confirm the influence of the particle size on lymphatic uptake.

2 MATERIALS AND METHODS

2.1 Chemicals

Miglyol®812, a neutral oil formed by esters of caprylic and capric fatty acids and glycerol, was donated by Sasol Germany GmbH (Germany). The surfactant Epikuron® 145V, a deoiled phosphatidylcholine enriched fraction of soybean lecithin, was donated by Cargill (Spain). Hexadecyltrimethylammonium bromide (CTAB), poly-L-glutamic acid (PGA; Mw 15-50 kDa), poly-L-asparagine (PASN; Mw 5-15 kDa), benzalkonium chloride, poloxamer 188 (Pluronic® F68) and docetaxel (DCX) were obtained from Sigma-Aldrich (Spain). Methoxy-poly(ethylene glycol)-block-poly(L-glutamic acid sodium salt) (PGA-PEG; Mw 35 kDa) is a diblock copolymer composed of poly-L-glutamic acid (chains length 15 kDa) and 57% of PEG (w/w, chains length 20 kDa) was supplied by Alamanda Polymers (USA). The near infrared dye 1,1′-dioctadecyl-3,3,3′,3′-tetramethylindodicarbocyanine perchlorate (DiD) (Em 644 nm; Ex 664 nm) was purchased from Molecular Probes-Invitrogen (USA).

2.2 Preparation of nanoemulsions and polyaminoacid nanocapsules

Anionic nanoemulsions were prepared by the solvent displacement technique, following the procedure previously described by our group [9]. Briefly, 30 mg of Epikuron® 145V were dissolved in 0.25 ml of ethanol. After mixing, 125 µl of Miglyol® 812 and 9.5 ml of acetone were also incorporated. This organic phase was immediately added to 20 ml of ultrapure water, at room temperature and under magnetic stirring, which led to the instantaneous formation of the nanoemulsion. Solvents were evaporated under vacuum at 37ºC (Buchi Labortechnik AG, Flawil, Switzerland) up to a final volume of 10 ml.

The influence of the parameters indicated in the **Table 1** on the particle size was investigated. In each set of experiments one single parameter was changed at a time while the other formulation variables were kept equal to those described for the reference nanoemulsion.

Table 1. Formulation parameters studied regarding their influence on the particle size distribution of the nanoemulsion.

Temperature of AP	4, 25, 40°C
AP:OP volume ratio	2:1, 3:1, 4.5:1
Oil concentration in the OP *	11.8, 5.9, 2.9, 1.5, 0.7 mg/ml
Addition rate of the OP	Direct addition of the whole volume (10 ml) vs aliquots of 250 µl/15 seconds

AP: aqueous phase. OP: organic phase. *: maintaining constant the mass ratio oil:lecithin 4:1.

After selecting the optimal formulation conditions for obtaining the nanoemulsions of suitable droplet size (AP at 4ºC, AP:OP 2:1, C=3.7 mg/ml, addition in aliquots), the cationic surfactant hexadecyltrimethylammonium bromide (CTAB) was incorporated in the organic phase as an ethanolic solution. To determine the minimum required amount, different concentrations of CTAB from 1 to 5.7% w/w were tested.

Nanocapsules were prepared according to the optimized procedure (containing 3.9% w/w of CTAB), by replacing the aqueous phase by the polyaminoacid aqueous solution. Based on the previous work, two different concentrations of polyaminoacid were assessed to ensure a proper coating (6.1 and 11.5 % w/w) [12].

2.3 Encapsulation of docetaxel and/or DiD

Both the antitumor drug docetaxel and the fluorescent marker DiD were incorporated from fresh ethanol stock solutions into the organic phase. Concretely, 25 µl of a docetaxel solution (C=1 mg/ml) and/or 200 µl of a DiD solution (C= 2.5 mg/ml) were added in the organic phase. The concentration of polyaminoacid in the aqueous phase was 0.25 mg/ml. Finally, once prepared through the procedure previously described, the nanocapsules were isolated by ultracentrifugation in Herolab® tubes (Herolab GmbH, Germany) at 84035xg for 1 hour at 15°C (Optima™ L-90K Ultracentrifuge, Beckmann Coulter; Fullerton, CA).

The encapsulation efficiency (E.E.) of docetaxel was determined both directly and indirectly by the quantification of the drug in the non-isolated nanocapsules, the isolated

nanocapsules and the infranatant collected upon ultracentrifugation. For this, aliquots of these fractions were dissolved with acetonitrile and centrifuged during 20 min at 4000xg. The samples were analyzed through high-performance liquid chromatography (HPLC) system, adapted from the method described by Lee et al. [23]. The HPLC system consisted of an Agilent 1100 Series Instrument equipped with a UV detector set at 227 nm and a reverse phase Zorbax Eclipse XDB-C8 column (4.6 x 150 mm id., pore size 5 µm Agilent USA). The mobile phase was a mixture of 0.1% v/v ortophosphoric acid and acetonitrile (55:45 v/v) and the flow rate was 1 ml/minute. The standard calibration curves of docetaxel were linear in the range of 0.2-0.6 µg/ml (r^2 = 0.999).

DiD encapsulation efficiency was also determined directly in the isolated nanocapsules and indirectly by difference between the total amount and the free dye in the infratant after the ultracentrifugation (84035xg 15°C, 1h). For the DiD quantification, aliquots of these fractions were diluted with acetonitrile and analyzed by UV spectrophotometry at λ=646 nm.

Encapsulation efficiencies indirectly determined were calculated as follows:

$$E.E.\% = \frac{(A-B)}{A} \times 100$$

Where A is the total docetaxel/DiD concentration and B the free docetaxel/DiD concentration measured after nanocapsule isolation by ultracentrifugation.

2.4 Preparation and characterization of PGA-PEG nanocapsules 200 nm

For the comparative biodistribution study, larger DiD-loaded PGA-PEG nanocapsules of particle size ≈ 200 nm were prepared following the method previously published by our group [9,10]. Briefly, the organic phase was constituted by 30 mg of Epikuron® 145V, 0.5 ml of a DiD stock solution (2.5 mg/ml), 0.125 mg of Miglyol® 812 and 7 mg of the cationic surfactant benzalkonium chloride in 9.5 ml of acetone. This organic phase was poured over an aqueous phase containing 10 mg of PGA-PEG and 50 mg of poloxamer 188. Afterwards, the organic solvents were eliminated and the nanocapsules

isolated by ultracentrifugation (84035xg for 1 hour at 15°C), as previously described. DiD quantification was also performed as reported in section 2.3.

2.5 Physicochemical characterization

Size and polydispersity index of all developed nanosystems were analyzed by photon correlation spectroscopy (PCS) after appropriate dilution with ultrapure water. Each analysis was performed at 25°C with an angle detection of 90°. The zeta potential (ζ) was determined by laser Doppler anemometry (LDA) after dilution with KCl 1mM. The PCS and LDA analysis were performed in triplicate using a Zetasizer Nano ZS® (Malvern Instruments, Malvern, UK).

Particle size distribution and morphology were evaluated by transmission electron microscopy (TEM) using a JEOL JEM-2010 microscope (Tokyo, Japan). Samples were stained with a phosphotungstic acid solution (2% w/w) and placed on a copper grid with Formvar films prior to analysis.

2.6 Stability of nanocapsules

Colloidal stability of the nanocapsules was studied from three different key points of view in the design of new nanomedicines:

i) Storage stability, a key parameter for the handling of the formulation, was determined in an aqueous medium at 4ºC by measuring particle size, polydispersity index and zeta potential over 2 months as described in 2.4.

ii) Colloidal stability as a function of the medium salinity at pH 7 using NaCl as aggregating electrolyte (one of the most relevant electrolytes present in serum). This study allowed us to understand the role of the surface components on the behavior of the nanocapsules after administration. Concretely, 1 ml of 2 mM phosphate buffer with a NaCl concentration varying from 2 up to 500 mM, was added over 30 µl of nanocapsules, rapidly mixed and the hydrodynamic mean size was measured every 30 seconds during three minutes. The diameter of the particles was plotted against time to construct the aggregation kinetics. The initial slopes of these curves indicate the aggregation rate (k) for the different samples and enable calculate the Fuchs stability factor (W) defined by:

$$W = \frac{k_f}{k_s}$$

where k_f is the rate constant in the fastest aggregation kinetic detected and k_s is the rate constant of the slower kinetics. The plotting of W as a function of the medium salinity in a double-logarithmic scale allows to estimate the Critical Coagulation Concentration (CCC) – the point where W reduces to 1 – that represents the electrolyte concentration where the repulsive potential barrier that keeps stable nanoparticles in suspension reduces to cero and the formulation becomes totally unstable [24].

iii) Colloidal behavior of the nanocapsules after administration depends not only on the interaction with the medium electrolytes, but also with the proteins and macromolecules present on the serum milieu. Bearing this in mind, the stability of nanocapsules has been also studied in the presence of human plasma proteins. Isolated blank nanocapsules were incubated with human plasma at dilution 1:10 at 37ºC with horizontal shaking. Samples were withdrawn at different times (0, 0.5, 1, 2, 4, 8 and 24 hours) and their particle size and polydispersity index were measured as described in 2.4.

2.7 *In vitro* release studies

Docetaxel release from polyaminoacid nanocapsules was performed by incubating the nanocapsules in phosphate buffer of low ionic strength pH 7 under sink conditions. The vials were placed in an incubator at 37 °C with horizontal shaking. At different time intervals, samples were withdrawn and ultracentrifuged (84035 x g for 1 hour at 15°C) in order to isolate the nanocapsules. The released docetaxel was calculated by determining the free drug in the aqueous release medium by HPLC, using the direct and indirect methods described in 2.3.

2.8 *In vivo* distribution studies

Animals

Female severe combined immunodeficiency (SCID) mice weighing about 20-25 g and at the age of 8-12 weeks were used in the *in vivo* studies (Harlan Laboratories, Inc). The animals were acclimatized for at least 1 week before experimentation; they were housed in ventilated polypropylene cages at an average temperature of 22 ˚C, with exposure to 12 hours of light and 12 hours of darkness each day. All mice received a standard laboratory diet of food and water *ad libitum*. The experiments were carried out according to the Rules of the Santiago de Compostela University Bioethics Committee and in compliance with the Principles of Laboratory Animal Care according to Spanish national law (RD 53/2013).

Biodistribution studies

Female SCID mice were injected subcutaneously in the interscapular region with a suspension of 100 µl of DiD-labeled nanocapsules measuring 100 or 200 nm. For the comparison of both formulations, the amount of administered nanocapsules was previously equalized according to their intensity of fluorescence. Biodistribution was assessed by an In Vivo Imaging System (IVIS, Living Image® System, Caliper Life Sciences, Hopkinton, MA). For non-invasive tests, mice were anesthetized with 4% isoflurane inhalation. Once laid in the acquisition chamber, the anesthesia was maintained with a 2% air-isofluran mixture during the *in vivo* acquisition. To compare the nanocapsules distribution on a semi-quantitative basis, mice were sacrificed at 24 or 48 hours after the administration, and the excised tissues, which included liver, lungs, spleen, kidneys, as well as axillary, cervical, inguinal, mediastinal and mesenteric lymph nodes, were compared with organs from non-injected animal as negative controls. Semi-quantitative data of the biodistribution were obtained from the fluorescence images by drawing regions of interest and using identical illumination settings. Organ fluorescence was quantified through mean radiance values.

Statistical analysis

A Mann-Whitney Test was used to determine differences in biodistribution studies. The mean ± SD was determined for each treatment group. The differences were considered significant for *p < 0.05, and very significant for *p < 0.01. All of the statistical analysis was carried out with GraphPad Prism Version 5.0 software.

3 RESULTS AND DISCUSSION

Previous studies from our group have shown the potential of polyaminoacid nanocapsules with a size of 200 nm as vehicles for the delivery of anticancer drugs. Given the importance of the particle size to promote the lymphatic access of nanocarriers, herein we report the experimental conditions that enable us to obtain 100 nm nanocapsules with different polymer shells, PGA, PGA-PEG and PASN, as well as their characterization and their capacity to reach the lymphatic circulation following subcutaneous administration. Prior to the formation of the said nanocapsules, we perform a thoughtful analysis of the oil-in water emulsification process, as described below.

3.1 Preparation of nanoemulsions and polyaminoacid nanocapsules

It is well known that the physicochemical properties of drug carriers play a critical role in their ability to reach the tumor and the lymphatics following either intravenous or subcutaneous administration [20]. Among these properties, size is particularly important since it influences both access to and retention into the lymphatic system. It has been reported by some authors that small lipid nanosystems having particle sizes of tens of nanometers up to 100 nm [25], anionic surface charge [26], and hydrophilic surface [27] are suitable nanocarriers for the passive targeting of nanocarriers to the lymphatic system following subcutaneous administration.

Polyaminoacid nanocapsules previously reported by our group were produced by the solvent displacement technique. These nanocapsules exhibited a particle size in the range of 150 nm-500 nm [28]. Previous studies from our research group have evidenced that by selecting the oil concentration, amount of polymer and volume of the organic

phase is possible to obtain polyester nanocapsules in a particle size range 213-280 nm [29]. As indicated, the main aim of this work has been to identify the experimental factors that are crucial for the control of the particle size distribution for the preparation of polyaminoacid nanocapsules. For identifying the parameters that would allow us to obtain nanocapsules of small particle size, we selected as starting point an anionic nanoemulsion that is constituted solely by oil and lecithin. The influence of temperature, the oil concentration, the aqueous phase:organic phase volume ratio, and the mixing rate of these two phases were evaluated. The results showed that the temperature does not exert any influence on the size of the resulting nanoemulsions (Table 1 Supporting information) whereas the increase of the AP:OP volume ratio produces slightly smaller nanoemulsions (**Table 2A**). The greatest effect on the size was achieved by reducing the oil and surfactant concentration as reflected in **Table 2B** [29]. The reduction of the lipidic components leads to a homogeneous and monodisperse population of nanoemulsions with smaller droplet size, reaching values under 100 nm. This size reduction effect is in line with previous studies reporting the preparation of polyester [29,30] nanocapsules, although the size of these nanocapsules was above 200 nm. On the other hand, the slow addition of the organic phase over the aqueous one (10 ml in 40 fractions, rate 250 µl/15 seconds), instead of the direct addition, also led to a considerable reduction of droplet size. This effect may be explained by the supersaturation phenomenon produced when the total volume of both phases are mixed together. This process, which constitutes the driving force of the particle formation, determines the nucleation rate and thus influence the resulting particle size [31,32]. The slow mixing of both phases, achieved with the addition in aliquots, could increase the nucleation rate, which would lead to the formation of a more numerous population of smaller particles. These results are line with other works that have thoroughly studied the influence of the mixing rate for the preparation of nanoemulsions [32] and nanoparticles [31]. Therefore, both strategies, the reduction of the lipid components and the slow mixing of aqueous and oily phases, were simultaneously applied in order to obtain small droplet sizes without a drastic reduction of the lipidic components that could compromise production yield and/or drug loading.

Table 2A. Effect of the aqueous phase:organic phase (AP:OP) volume ratio on the mean size and polydispersity index of the nanoemulsion. (mean ± SD, n=3).

AP:OP volume ratio	2:1	3:1	4.5:1
Size (nm)	178 ± 1	159 ± 7	155 ± 0
P.I.	0.1	0.1	0.1

Table 2B. Effect of the oil concentration and the addition method of the organic phase on the mean droplet size and polydispersity index of the nanoemulsion. (mean ± SD, n=3).

Addition method	Direct addition of the whole volume (10 ml)					40 fractions of 250 µl/15 seconds	
Oil concentration (mg/ml)	11.8	5.9	2.9	1.5	0.7	11.8	2.9
Size (nm)	178 ± 1	163 ± 6	134 ± 9	109 ± 5	87 ± 14	149 ± 11	99 ± 4
P.I.	0.1	0.1	0.1	0.1	0.1	0.2	0.2

In order to facilitate the deposition of the polyaminoacid onto the oily cores, we introduced a cationic surfactant, CTAB in concentrations varying 1 and 5.7% (w/w). **Figure 1** shows how the addition of CTAB reversed the zeta potential from -60 mV to positive values. For the 1% CTAB concentration, a great enlargement of the droplet size was observed together with high polydispersity, a result that was attributed to the aggregation produced by the neutralization of charges. The 3.9% CTAB concentration led to the formation of positively charged oily droplets with the smallest particle size and, thus, this concentration was selected for the preparation of nanocapsules.

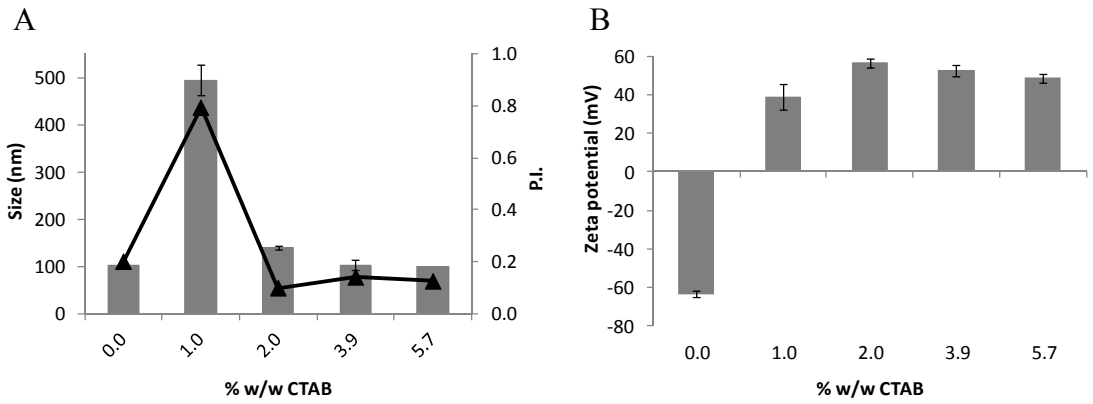

Figure 1. Physicochemical characterization of cationic nanoemulsions prepared with hexadecyltrimethylammonium bromide (CTAB). A) Size (represented by columns) and polydispersity index (P.I., shown as lines) and B) zeta potential.

For the preparation of polyaminoacid-based nanocapsules, the corresponding polymer was added in the aqueous phase during the preparation.

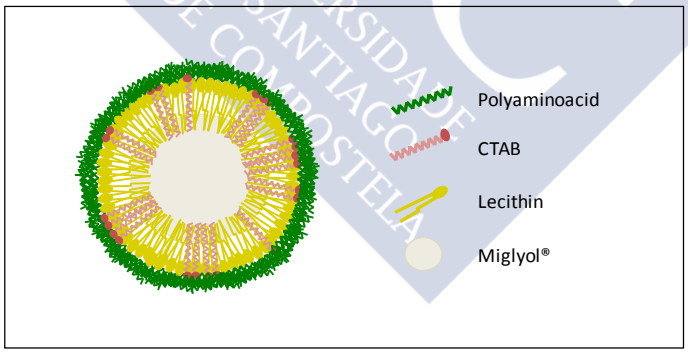

Figura 2. Representation of the structure of polyaminoacid nanocapsules.

To determine the optimal polymer quantity required for the formation of a polymeric shell around the nanoemulsion, two different concentrations of polyaminoacid (6.1 and 11.5 % w/w) were studied. Table 3 shows the physicochemical characteristics of these nanocarriers. TEM images confirmed the values of mean particle size and homogeneity of the particle size distribution for all polyaminoacid-based nanocapsules as measured

by PCS, and revealed the spherical and regular morphology of these nanosystems (**Figure 3**). As expected, for the PGA and PGA-PEG nanocapsules, the addition of polyaminoacid reverses the positive zeta potential to negative values, indicating the polymer deposition over the cationic oily droplets. The highest polymer concentrations produced nanocapsules with a more negative zeta potential value, suggesting a more efficient polymeric coating. As previously observed, PASN nanocapsules also exhibited a negative zeta potential [12,13], which could indicate a certain presence of free aspartic acid in the polymer. PGA-PEG and PASN nanocapsules prepared with the highest polymer concentration also exhibited a slightly lower particle size, as we previously observed with similar nanocapsules [12]. According to this work, a further increase in the polymer concentrations would barely affect the zeta potential value or particle size due to the saturation in the polymer deposition. Therefore, nanocapsules were prepared onwards with 11.5 % (w/w) of polyaminoacid, exhibiting a particle size in the range 100-115 nm and a zeta potential value comprised between -25 and -54 mV.

Tabla 1. Physicochemical characteristics of the cationic nanoemulsion (NE) and the nanocapsules (NCs) prepared with different types and concentrations of polyaminoacids. (mean ± SD; n=3).

Formulation	Polyaminoacid (% w/w)	Size (nm)	P.I.	ζ Potential (mV)
Cationic NE	0	103 ± 10	0.1	+52 ± 3
PGA NCs	6.1	97 ± 1	0.1	-34 ± 0
	11.5	100 ± 2	0.1	-54 ± 1
PGA-PEG NCs	6.1	136 ± 3	0.2	-21 ± 5
	11.5	115 ± 9	0.1	-29 ± 2
PASN NCs	6.1	125 ± 10	0.1	-20 ± 4
	11.5	111 ± 2	0.1	-25 ± 9

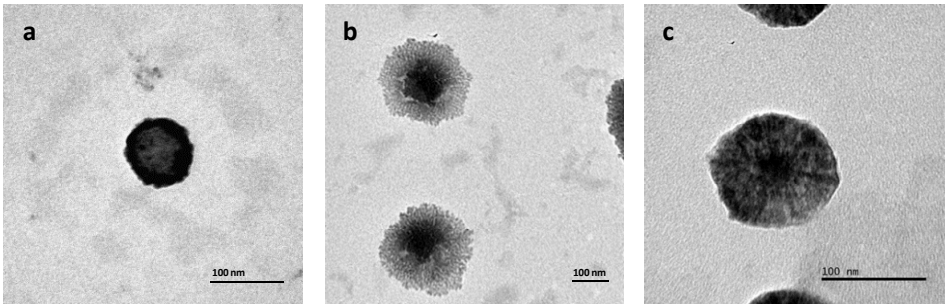

Figura 3. TEM images of polyaminoacid nanocapsules: (a) PGA, (b) PGA-PEG, (c) PASN coating. Scale bar = 100 nm.

3.2 Docetaxel and DiD encapsulation into the nanocapsules

Normally, a reduction in the globule size of the emulsions leads to a decrease in the drug encapsulation due to the increase in the specific surface area available for the diffusion of the encapsulated drug from the oily core to the external aqueous phase. As shown in Table 4, in this study the encapsulation efficiencies achieved for PGA and PGA-PEG nanocapsules were 67% and 60%, respectively, values that are comparable to those obtained for larger nanocapsules with similar compositions [33]. However, in the case of the PASN nanocapsules the docetaxel encapsulation efficiency went from 76% to 56% [12]. These differences could be related to the different stabilizing properties of the polymer shells under the conditions investigated. On the other hand, the results in **Table 4** indicate that the incorporation of docetaxel barely modified the physicochemical characteristics of these nanocapsules, although a slight reduction on the mean particle size of the docetaxel loaded PGA-PEG and PASN have been observed.

Table 4. Physicochemical characteristics and corresponding encapsulation efficiency of the blank, docetaxel and/or DiD loaded PGA, PGA-PEG and PASN nanocapsules.

Nanocapsules	Loading	Size (nm)	P.I.	ζ Potential (mV)	Docetaxel E.E (%)	DiD E.E (%)
PGA	-	99 ± 3	0.1	-51 ± 6	-	-
	Docetaxel	95 ± 8	0.1	-53 ± 7	67 ± 2	-
	DiD	106 ± 4	0.1	-58 ± 4	-	66 ± 6
PGA-PEG	-	116 ± 5	0.1	-29 ± 5	-	-
	Docetaxel	99 ± 4	0.2	-35 ± 4	60 ± 2	-
	DiD	107 ± 9	0.1	-36 ± 4	-	56 ± 3
	Docetaxel + DiD	109 ± 13	0.2	-39 ± 1	48 ± 8	52 ± 15
PASN	-	111 ± 2	0.1	-25 ± 9	-	-
	Docetaxel	81 ± 3	0.2	-27 ± 2	56 ± 2	-
	DiD	87 ± 4	0.1	-31 ± 4	-	63 ± 1

P.I.: polydispersity index. E.E.: encapsulation efficiency. Values are given as mean ± SD; n=3.

Polyaminoacid nanocapsules were also loaded with the fluorescent dye DiD. This near infrared fluorophore is weakly fluorescent in water but highly fluorescent and quite photostable when incorporated into nanocapsules thanks to its lipophilic nature. In addition, it has high tissue penetration and low interference with the autofluorescence of animal tissues. The encapsulation efficiencies of DiD were comprised between 56 and 66%, similarly to the previously obtained values for docetaxel. Therefore, these optimized nanocapsules can be considered as flexible carriers, able to associate different types of molecules. DiD encapsulation efficiencies were slightly lower than the ones obtained for the larger nanocapsules, which were in the range 67-79% [10,12]. On the other hand, the encapsulation of this fluorophore did not involve significant changes in the physicochemical characteristics of nanocapsules, except for a slight decrease in the size of PASN nanocapsules that may be due to the compaction of the inner oily core, as mentioned above within the context of docetaxel encapsulation. Finally, PGA-PEG

nanocapsules have also been loaded simultaneously with docetaxel and DiD, without affecting their physicochemical properties and only with a slight decrease in docetaxel loading. This ability to administer antitumor drugs and imaging markers the same time could be exploited for the future development of a multifunctional platform with therapeutic and diagnostic purposes.

3.3 Stability of the nanocapsules

The stability of nanosystems during long-term storage is important for the adequate handling of the formulations. The stability profiles of the aqueous suspension of nanocapsules stored at 4ºC (**Figure 4**), indicate that the particle size and polydispersity index of the nanocapsules remain unmodified over at least 2 months. The zeta potential measurements also confirmed that the surface electrical charge of nanocapsules was maintained (data not shown). These results agree with those previously observed for blank and drug-loaded polyaminoacid nanocapsules [9,12]. According to the DLVO theory, the high negative Z-potential of the nanocapsules illustrates the presence of repulsive electrostatic forces that are responsible for their colloidal stability. However, the stability of colloidal carriers, in particular those provided with a PEG coating, may also be attributed to a steric stabilization, as previously reported [34].

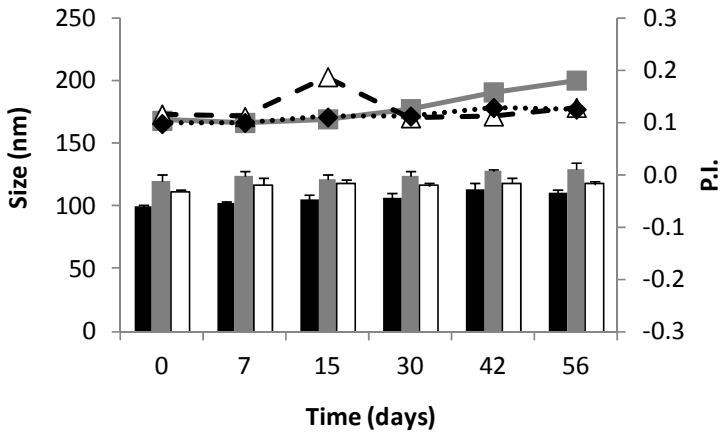

Figure 4. Stability of polyaminoacid nanocapsules in aqueous medium during storage at 4ºC: A) Size (represented by columns) and polydispersity index (P.I., shown as lines) of PGA (black), PGA-PEG (dark grey) and PASN (white) nanocapsules.

In order to achieve a better insight on the role of the polymeric coating on the colloidal stability of the nanocapsules we monitored the behavior of the nanocapsules exposed to phosphate buffer pH 7 at increasing NaCl concentrations. This study was expected to help understanding the behavior of the nanosystems after *in vivo* administration. **Figures 5 A-C** show the evolution of the mean particle size of the nanocapsules over time at the different salt concentrations. As indicated in the Materials and Methods section, the slopes of the aggregation kinetics were linear from time 0 up to 180 seconds, enabling the calculation of the Fuchs stability factor (W). This experimental parameter provides information on the coagulation probability. Namely, when $W \rightarrow 1$ the system is completely unstable, while when $W \rightarrow \infty$ indicates total stability. The plotting of the Fuchs stability factor as a function of NaCl concentration (**Figure 5D**) led to the estimation of the Critical Coagulation Concentration (CCC), which indicates the minimum salt concentration at which the potential barrier that avoids the aggregation of particles is completely cancelled.

As expected, despite having the same oily core, the colloidal stability of these systems was determined by the composition of the polymeric shell. Namely, PASN nanocapsules exhibited a CCC value lower than 2 mM, PGA nanocapsules presented a CCC value of 90 mM, and the PEGylation of the polymer (PGA-PEG) led to a CCC value of 150 mM (see **Figure 5D**). These results helped us to understand the arrangement of the polymers onto the oily drops. The incorporation of PASN to the nanocapsules resulted in a clear reduction of their superficial charge (-29 mV), which agrees with the low stability exhibited by this formulation as a function of the medium salinity (CCC < 2 mM). In contrast, PGA nanocapsules, exhibiting a high Z-potential (-51 mV), were more stable and they needed a higher saline concentration than the PASN nanocapsules to become unstable (CCC ≈ 90 mM). Finally, the incorporation of PEG moieties to the PGA polymer reduced the superficial charge of the nanocapsules, however their stability in high salinity conditions was very high (increase in CCC value from 90 mM up to 150 mM). This enhanced stability of the PEGylated nanocapsules was attributed to the steric protection of the PEG shell [35]. Interestingly, overall these data indicate that the three types of nanocapsules undergo a destabilization followed by a re-stabilization process when exposed to NaCl concentrations higher than the CCC ($W \rightarrow \infty$). This re-stabilization mechanism at high electrolyte concentrations is attributed

to repulsive hydration forces, which depends on the aggregating electrolyte and also on the hydrophilic character of the nanocapsules surface [35,36]. This colloidal behavior introduces a new stability parameter, the Critical Stabilization Concentration (CSC), which is defined as the minimum salt concentration at which re-stabilization by hydration forces starts and $W \rightarrow \infty$.

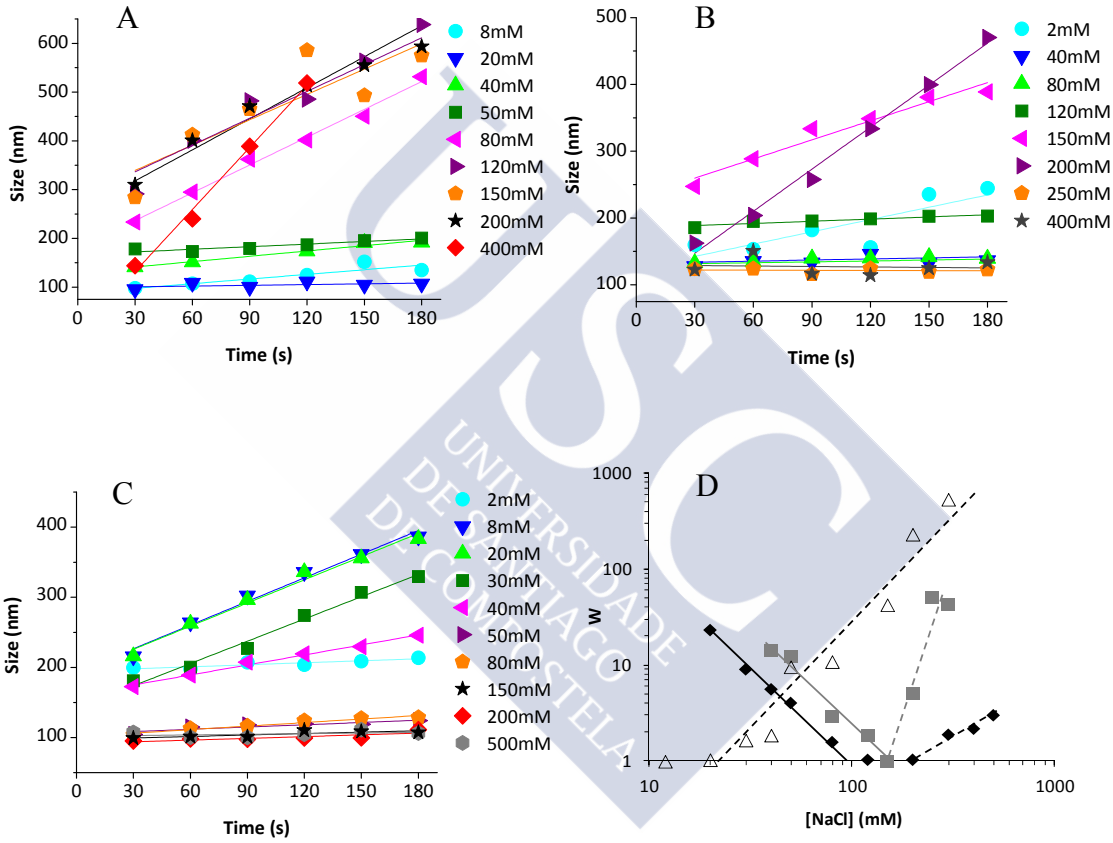

Figure 5. Particle size evolution of (A) PGA, (B) PGA-PEG and (C) PASN nanocapsules in saline phosphate buffer with different NaCl concentrations. (D) Fuchs stability factor of PGA (black rhombus), PGA-PEG (grey squares) and PASN (white triangles) nanocapsules as a function of the salinity of the medium. The continuous line point to the CCC values, while dashed lines depart from the CSC.

As observed in Figure 5D, PGA nanocapsules presented a CSC value of 200 mM, PGA-PEG 155 mM and PASN close to 20 mM. The reduction on the CSC value of PGA-PEG in comparison with PGA nanocapsules (from 200 mM to 155 mM) is in agreement with to the higher surface hydrophilicity of the PEGylated formulation [35]. On the other hand, the explanation for the low CSC value observed for PASN nanocapsules, which could be an indication of the hydrophilic character of the polymer shell, requires further investigation.

These colloidal stability studies provide valuable information about the surface of nanocapsules, suggesting the effective incorporation of the polyaminoacids previously observed through the inversion of the zeta potential values. However, it should be taken into account that cell culture media and physiological fluids are very complex, so additional experiments must be conducted to predict more precisely the stability of the systems in these media. Both blood and interstitial fluids are constituted by different electrolytes and proteins which can generate repulsive hydration forces strong enough to maintain the colloidal stability of the nanocarriers [37,38]. It is known that the formation of a protein corona around colloidal particles can stabilize them at high salt concentrations, and the nature – hydrophilicity/hydrophobicity and conformation – of the adsorbed protein molecules determines the efficiency of this phenomenon [38]. Also the presence of divalent ions, such as Ca^{2+} or Mg^{2+}, which are much more hydrated than Na^{+}, promote the restabilization of nanosystems at lower CSC values by increasing the hydration forces. The magnitude of these repulsive structural forces, in addition to the surface hydrophilicity, strongly depends on the concentration and hydration degree of the ions surrounding the surface [34,39].

In order to complete the analysis of the colloidal stability of the nanocapsules, we study the stability of nanocapsules in human plasma at 37ºC. Given the fact that the plasma contains colloidal structures that interfere with the particle size measurements, the evolution of both, the plasma and nanocapsule size distributions were compared. The monitoring of the particle size represented in **Figure 6** shows that PEGylated and non-PEGylated polyaminoacid-based nanocapsules exhibit a similar behavior in plasma. After the initial contact, both PGA and PGA-PEG nanocapsules instantly doubled their particle size. PASN nanocapsules also increased its size during the first 1 hour of incubation (113 ± 3 nm vs 315 ± 93 nm). This enlargement in the particle size may be

due to the interaction of the nanocapsules with proteins and other components of the complex plasma milieu.

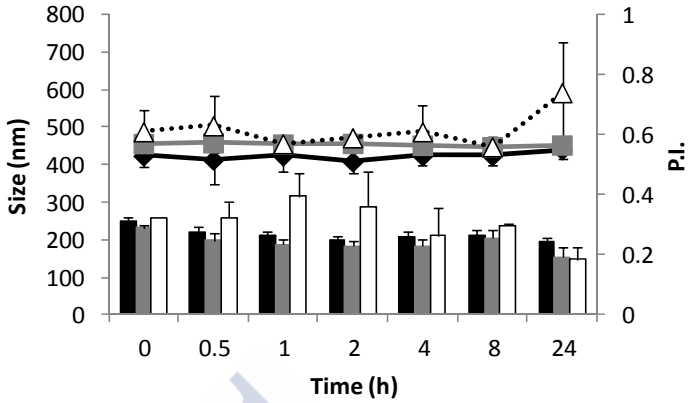

Figure 6. Stability of PGA (black), PGA-PEG (dark grey) and PASN (white) nanocapsules in human plasma at 37 °C. Size is represented by columns and polydispersity index (P.I.) by lines.

It has been reported that the interaction of nanoparticles with plasma proteins can result in their aggregation or to the formation of a protein corona, which may contribute to the stabilization of the nanoparticles under physiological conditions [36,40]. This corona is known to have an effect on the pharmacokinetic behaviour of the nanoparticles and, consequently in their *in vivo* performance and toxicity [41].

3.4 *In vitro* release studies of docetaxel loaded nanocapsules

The release studies of docetaxel were carried out by incubation of highly diluted nanocapsules (sink conditions) in simulated medium at 37°C during 48 hours. All formulations showed a similar biphasic drug release profile (**Figure 7**), characterized by a rapid initial release (33-40% of the loaded docetaxel) followed by a second phase in which no significant amounts of drug was released. The characteristic initial burst release has been attributed to the partition of the lipophilic drug between the oily core and the external aqueous release medium, whereas the lack of release in the second phase confirms the high affinity of the docetaxel for the oily core [5,42]. The amount of docetaxel that remained encapsulated in the nanocapsules during the release study could also be quantified, thus showing its integrity. This biphasic release profile has been

typically observed in other nanocapsule compositions. Regarding the extent of release, previous studies with polyaminoacid nanocapsules showed significantly higher burst release than those observed herein (60% vs ≈35%) [9,12]. This indicates that the nanocapsules reported here have a consistent polymer shell that prevents the premature release of the drug from the nanocapsules. This could be also related to the differences in the preparation method and in particular, to the different addition of the organic phase during nanocapsule formation. Indeed, some works have reported that the mixing rate of both phases may affect the encapsulation efficiency and release of drugs [43,44]. Thus, the preparation of nanocapsules through this optimized preparation method may not only control the particle size and enhance the drug loading into the oily core, but could also limit the burst effect during the release, developing drug delivery systems more advantageous for the treatment of metastatic cancer.

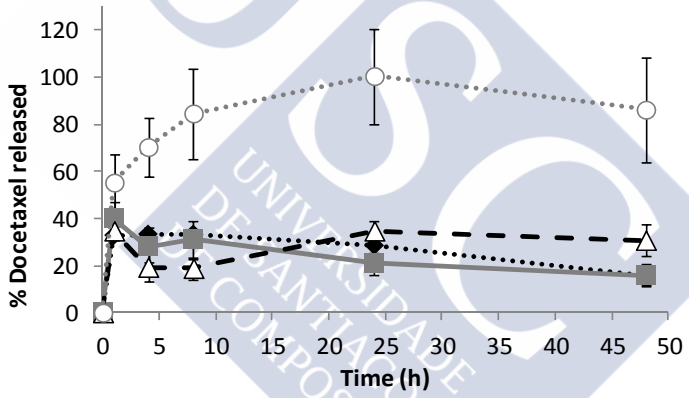

Figure 7. Docetaxel release profiles from PGA (···◆···), PGA-PEG (—■—), PASN (—△—) nanocapsules and anionic nanoemulsion (···○···) in phosphate buffer (pH 7) at 37ºC.

3.5 Biodistribution of PGA-PEG nanocapsules

Based on previous reports disclosing the importance of the nanocarrier's size and hydrophilicity on their lymphatic uptake [20], we decided to study if the size of PGA-PEG nanocapsules –those with the most hydrophilic surface and favorable stability and controlled release properties- influences their biodistribution. Thus, we compared the biodistribution of the DiD-labeled PGA-PEG nanocapsules developed in this study

(mean size ~100 nm) with that of PGA-PEG nanocapsules, previously developed by our group (mean size ~200 nm). Irrespective of their different size, both types of nanocapsules exhibited the same Z-potential values (Table 2 Supporting information).

For the biodistribution studies, PGA-PEG nanocapsules with the same fluorescence intensity were administered by subcutaneous route and the fluorescence was analyzed over time by fluorescence imaging in a semiquantitative fashion. At 24 hours post-administration, clear differences in the biodistribution patterns were observed. The fluorescence observed in liver, lung, heart and kidneys was significantly higher in animals injected with 100 nm nanocapsules compared to those injected with 200 nm nanocapsules. Similarly, the fluorescence detected in the mesenteric, axillary, mediastinal and cervical nodes was the highest for mice treated with 100 nm nanocapsules (**Figure 8A**). These differences in fluorescence intensity levels in irrigated organs and lymph nodes of animals, become smaller over the time, reaching at 48 hours post-injection similar values, regardless of the size of the nanocapsules (**Figure 8B**). Thus, these results indicate that 100 nm PGA-PEG nanocapsules were more rapidly drained to the lymph nodes, as compared to 200 nm PGAPEG nanocapsules. To reach the lymphatic system, nanocarriers must first pass through the interstice, which is a physically and electrostatically hindered gel structure consisting of fibrous collagen network, and diffuse through aqueous pores of the gel, which are of approximately 100 nm in diameter [45]. In this scenario, the 100 nm-nanocapsules may have a facilitated migration through the interstitial aqueous channels and, as consequence, a higher lymphatic uptake than the large nanocapsules. On the other hand, based on the high fluorescence observed in highly irrigated organs, it could also be presumed that, these small nanocapsules could pass through the lymph nodes and reach the blood circulation. By contrast, 200 nm nanocapsules due to their large size might have been retained in the interstitial space and had a slower drainage to the lymphatics. These interpretation agrees with the one previously reported to explain the behavior of liposomes and PLGA-PEG based nanoparticles following subcutaneous administration. In these studies, the lymph node uptake was found to occur more rapidly for 50 nm nanoparticles and 70 nm liposomes, as compared to 100 nm and 200 nm nanoparticles and 170 nm-liposomes, respectively [15,17].

Overall, a key conclusion, from the biodistribution study indicates that the 100 nm PGA-PEG nanocapsules reported here have a marked distribution to the lymph nodes. This lymphotropic behavior could be exploited for the treatment of a number of diseases and, in particular, metastatic cancer. In this context, the peritumoral administration of these nanocapsules could enhance the selective delivery of anticancer drugs as docetaxel to the metastatic draining lymph nodes.

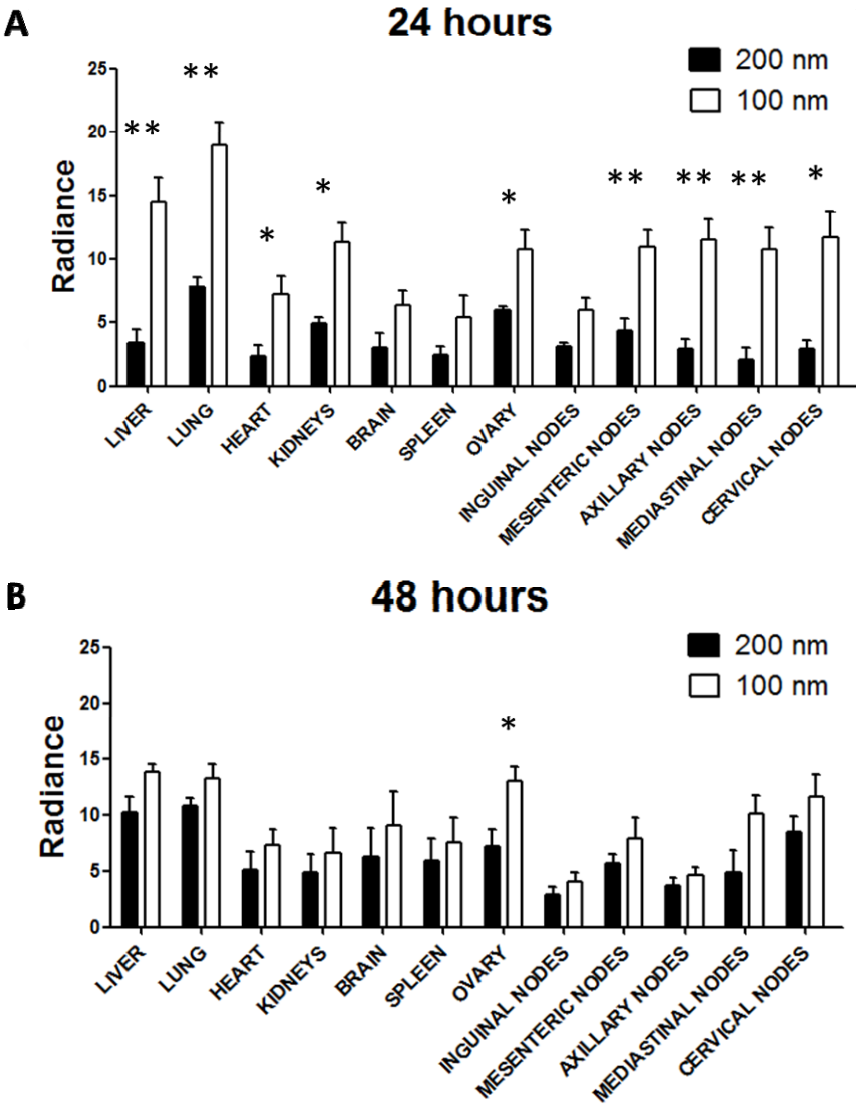

Figure 8. Biodistribution of DiD-labeled PGA-PEG nanocapsules of 200 and 100 nm after subcutaneous injection. Radiance (Photons/sec/cm^2/sr x 10^7) was measured in excised organs at (A) 24 and (B) 48 hours after injection. Data represents mean ± SEM; n=4. Mann Whitney test ((*) $p < 0.05$, (**) $p < 0.01$).

4 Conclusions

Herein we report for the first time the synthesis and characterization of a variety of polyaminoacid nanocapsules (PGA, PGA-PEG and PASN) of 100 nm using the solvent displacement technique. These nanocapsules were shown to be stable in plasma and provide and controlled release of the associated drug docetaxel. Biodistribution studies performed with the most hydrophilic prototype, PGA-PEG nanocapsules, showed their marked distribution to the lymph nodes after subcutaneous administration. Overall, these results suggest that these polyaminoacid-based nanocapsules could be an interesting platform to enhance the lymphatic delivery of drugs, and in particular, anticancer drugs.

Supporting information

Table 1. Effect of the temperature of the aqueous phase on mean droplet size and polydispersity index of the nanoemulsion. (mean ± SD, n=3).

	Temperature (°C)		
	4	25	40
Size (nm)	190 ± 2	178 ± 1	187 ± 1
P.I.	0.2	0.1	0.1

Data represents mean ± SD; n=3.

Table 2. Physicochemical characteristics of blank and DiD-loaded PGA-PEG nanocapsules of 100 nm and 200 nm.

Nanocapsules	Size (nm)	P.I.	ζ Potential (mV)
Blank-100	116 ± 5	0.1	-29 ± 5
DiD-100	107 ± 9	0.1	-36 ± 4
Blank-200	200 ± 8	0.1	-25 ± 4
DiD-200	203 ± 11	0.1	-30 ± 2

P.I.: polydispersity index. Data represents mean ± SD; n=3.

Acknowledgments

The authors acknowledge financial support given by the European Commission FP7 EraNet-EuroNanoMed Program-Instituto Carlos III (Lymphotarg, Ref. PS09/02670) and Xunta de Galicia (Isidro Parga Pondal Fellowhsip and Competitive Reference Groups-FEDER Funds Ref 2013/043). Raquel Abellan-Pose also acknowledges her fellowship from the Biomedical Sciences and Health Technologies Doctoral School-Universidad Santiago de Compostela.

REFERENCES

[1] Hrkach J, Von Hoff D, Mukkaram Ali M, Andrianova E, Auer J, Campbell T, et al. Preclinical development and clinical translation of a PSMA-targeted docetaxel nanoparticle with a differentiated pharmacological profile. Sci. Transl. Med. 2012;4:128ra39.

[2] González-Aramundiz JV, Lozano MV, Sousa-Herves A, Fernandez-Megia E, Csaba N. Polypeptides and polyaminoacids in drug delivery. Expert Opin. Drug Deliv. 2012;9:183–201.

[3] Duro-Castano A, Conejos-Sánchez I, Vicent M. Peptide-Based Polymer Therapeutics. Polymers (Basel). 2014;6:515–51.

[4] Matsumura Y, Kataoka K. Preclinical and clinical studies of anticancer agent-incorporating polymer micelles. Cancer Sci. 2009;100:572–9.

[5] Lozano M V, Torrecilla D, Torres D, Vidal A, Domínguez F, Alonso MJ. Highly efficient system to deliver taxanes into tumor cells: docetaxel-loaded chitosan oligomer colloidal carriers. Biomacromolecules 2008;9:2186–93.

[6] Oyarzun-Ampuero FA, Rivera-Rodríguez GR, Alonso MJ, Torres D. Hyaluronan nanocapsules as a new vehicle for intracellular drug delivery. Eur. J. Pharm. Sci. 2013;49:483–90.

[7] Hervella P, Alonso-Sande M, Ledo F, Lucero ML, Alonso MJ, Garcia-Fuentes M. PEGylated Lipid Nanocapsules with Improved Drug Encapsulation and Controlled Release Properties. Curr. Top. Med. Chem. 2014;14:1115–23.

[8] Verma N, Kumar K, Kaur G, Anand S. L-asparaginase: a promising chemotherapeutic agent. Crit. Rev. Biotechnol. 2007;27:45–62.

[9] Gonzalo T, Lollo G, Garcia-Fuentes M, Torres D, Correa J, Riguera R, et al. A new potential nano-oncological therapy based on polyamino acid nanocapsules. J. Control. Release 2013;169:10–6.

[10] Lollo G, Rivera-Rodriguez GR, Bejaud J, Passirani C, Benoit JP, García-Fuentes M, et al. Polyglutamic acid-PEG nanocapsules as long circulated carriers for the delivery of docetaxel. Eur. J. Pharm. Biopharm. 2014;87:47–54.

[11] Lollo G, Hervella P, Calvo P, Avilés P, Guillén MJ, Garcia-Fuentes M, et al. Enhanced in vivo therapeutic efficacy of plitidepsin-loaded nanocapsules decorated with a new poly-aminoacid-PEG derivative. Int. J. Pharm. 2015;483:212–9.

[12] Rivera-Rodríguez GR, Alonso MJ, Torres D. Poly-L-asparagine nanocapsules as anticancer drug delivery vehicles. Eur. J. Pharm. Biopharm. 2013;85:481–7.

[13] Rivera-Rodriguez GR, Lollo G, Montier T, Benoit JP, Passirani C, Alonso MJ, et al. In vivo evaluation of poly-l-asparagine nanocapsules as carriers for anti-cancer drug delivery. Int. J. Pharm. 2013;458:83–9.

[14] Xie Y, Bagby TR, Cohen M, Forrest ML. Drug delivery to the lymphatic system: importance in future cancer diagnosis and therapies. Expert Opin. Drug Deliv. 2009;6:785–92.

[15] Oussoren C, Zuidema J, Crommelin DJA, Storm G. Lymphatic uptake and biodistribution of liposomes after subcutaneous injection. II. Influence of liposomal size, lipid composition and lipid dose. Biochim. Biophys. Acta 1997;261–72.

[16] Oussoren C, Storm G. Lymphatic uptake and biodistribution of liposomes after subcutaneous injection: III. Influence of surface modification with poly(ethyleneglycol). Pharm. Res. 1997;14:1479–84.

[17] Rao DA, Forrest ML, Alani AWG, Kwon GS, Robinson JR. Biodegradable PLGA Based Nanoparticles for Sustained Regional Lymphatic Drug Delivery. J. Pharm. Sci. 2010;99:2018–31.

[18] Proulx ST, Luciani P, Dieterich LC, Karaman S, Leroux J-C, Detmar M. Expansion of the lymphatic vasculature in cancer and inflammation: New opportunities for in vivo imaging and drug delivery. J. Control. Release 2013;172:550–7.

[19] Qin L, Zhang F, Lu X, Wei X, Wang J, Fang X, et al. Polymeric micelles for enhanced lymphatic drug delivery to treat metastatic tumors. J. Control. Release 2013;171:133–42.

[20] Abellan-Pose R, Csaba N, Alonso MJ. Lymphatic Targeting of Nanosystems for Anticancer Drug Therapy. Curr. Pharm. Des. Submitted.

[21] Mora-Huertas CE, Fessi H, Elaissari A. Polymer-based nanocapsules for drug delivery. Int. J. Pharm. 2010;385:113–42.

[22] Heurtault B, Saulnier P, Pech B, Venier-Julienne M-C, Proust J-E, Phan-Tan-Luu R, et al. The influence of lipid nanocapsule composition on their size distribution. Eur. J. Pharm. Sci. 2003;18:55–61.

[23] Lee SH, Yoo SD, Lee KH. Rapid and sensitive determination of paclitaxel in mouse plasma by high-performance liquid chromatography. J. Chromatogr. Biomed. Sci. Appl. 1999;724:357–63.

[24] Santander-Ortega MJ, Lozano-López M V, Bastos-González D, Peula-García JM, Ortega-Vinuesa JL. Novel core-shell lipid-chitosan and lipid-poloxamer nanocapsules: stability by hydration forces. Colloid Polym. Sci. 2009;288:159–72.

[25] Oussoren C, Storm G. Liposomes to target the lymphatics by subcutaneous administration. Adv. Drug Deliv. Rev. 2001;50:143–56.

[26] Kaur CD, Nahar M, Jain NK. Lymphatic targeting of zidovudine using surface-engineered liposomes. J. Drug Target. 2008;16:798–805.

[27] Moghimi SM. The effect of methoxy-PEG chain length and molecular architecture on lymph node targeting of immuno-PEG liposomes. Biomaterials 2006;27:136–44.

[28] Hervella P, Lollo G, Oyarzún-Ampuero F, Rivera G, Torres D, Alonso M. Nanocapsules as carriers for the transport and targeted delivery of bioactive molecules. In: Da Silva AL, Trindade T, editors. Nanocomposite Particles for Bio-Applications - Materials and Bio-Interfaces. Pan Stanford Publishing Pte Ltd; 2011. page 45–68.

[29] Calvo P, Sanchez A, Martinez J, Lopez M, Calonge M, JC P, et al. Polyester Nanocapsules as New Topical Ocular Delivery Systems for Cyclosporin A. Pharm. Res. 1996;13:311–5.

[30] Calvo P, Remunan-Lopez C, Vila-Jato J, Alonso M. Development of positively charged colloidal drug carriers:chitosan-coated polyester nanocapsules and submicron-emulsions. Colloid Polym. Sci. 1997;275:46–53.

[31] Lince F, Marchisio DL, Barresi AA. Strategies to control the particle size distribution of poly-epsilon-caprolactone nanoparticles for pharmaceutical applications. J. Colloid Interface Sci. 2008;322:505–15.

[32] Mitri K, Vauthier C, Huang N, Menas A, Ringard-Lefebvre C, Anselmi C, et al. Scale-up of Nanoemulsion Produced by Emulsification and Solvent Diffusion. J. Pharm. Sci. 2012;101:4240–7.

[33] Alonso MJ, Torres D, Rivera-Rodríguez GR, Oyarzun-Ampuero FA, Lollo G, Gonzalo T, et al. Patent WO2012095543 A1 -Nanocapsules with a polymer shell. 2012;

[34] Israelachvili JN. Intermolecular & Surface Forces. Second. London: 1995.

[35] Santander-Ortega MJ, Jódar-Reyes AB, Csaba N, Bastos-González D, Ortega-Vinuesa JL. Colloidal stability of Pluronic F68-coated PLGA nanoparticles: A variety of stabilisation mechanisms. J. Colloid Interface Sci. 2006;302:522–9.

[36] Santander-Ortega MJ, de la Fuente M, Lozano M V, Bekheet ME, Progatzky F, Elouzi A, et al. Hydration forces as a tool for the optimization of core–shell nanoparticle vectors for cancer gene therapy. Soft Matter 2012;8:12080.

[37] Sánchez-Moreno P, Ortega-Vinuesa JL, Boulaiz H, Marchal JA, Peula-García JM. Synthesis and characterization of lipid immuno-nanocapsules for directed

drug delivery: selective antitumor activity against HER2 positive breast-cancer cells. Biomacromolecules 2013;14:4248–59.

[38] Molina-Bolívar JA, Ortega-Vinuesa JL. How Proteins Stabilize Colloidal Particles by Means of Hydration Forces. Langmuir 1999;2644–53.

[39] Santander-Ortega MJ, Peula-García JM, Goycoolea FM, Ortega-Vinuesa JL. Chitosan nanocapsules: Effect of chitosan molecular weight and acetylation degree on electrokinetic behaviour and colloidal stability. Colloids Surf. B. Biointerfaces 2011;82:571–80.

[40] Santander-Ortega MJ, de la Fuente M, Lozano M V, Tsui ML, Bolton K, Uchegbu IF, et al. Optimisation of synthetic vector systems for cancer gene therapy - the role of the excess of cationic dendrimer under physiological conditions. Curr. Top. Med. Chem. 2014;14:1172–81.

[41] Aggarwal P, Hall JB, McLeland CB, Dobrovolskaia MA, McNeil SE. Nanoparticle interaction with plasma proteins as it relates to particle biodistribution, biocompatibility and therapeutic efficacy. Adv. Drug Deliv. Rev. 2009;61:428–37.

[42] Calvo P, Vila-Jato JL, Alonso MJ. Comparative in Vitro Evaluation of Several Colloidal Systems, Nanoparticles, Nanocapsules, and Nanoemulsions, as Ocular Drug Carriers. J. Pharm. Sci. 1996;85:530–6.

[43] Lince F, Bolognesi S, Stella B, Marchisio DL, Dosio F. Preparation of polymer nanoparticles loaded with doxorubicin for controlled drug delivery. Chem. Eng. Res. Des. 2011;89:2410–9.

[44] Anton N, Bally F, Serra C a., Ali A, Arntz Y, Mely Y, et al. A new microfluidic setup for precise control of the polymer nanoprecipitation process and lipophilic drug encapsulation. Soft Matter 2012;8:10628.

[45] Porter CJ, Charman SA. Lymphatic transport of proteins after subcutaneous administration. J. Pharm. Sci. 2000;89:297–310.

Capítulo 3

Biodistribution of Radiolabeled Polyglutamic Acid and PEGylated-Polyglutamic Acid Nanocapsules

USC
UNIVERSIDADE
DE SANTIAGO
DE COMPOSTELA

Biodistribution of Radiolabeled Polyglutamic Acid and PEGylated-Polyglutamic Acid Nanocapsules

Este trabajo ha sido realizado en colaboración con Araceli Delgado[1] y Carmen Évora[1].

[1] Departamento de Ingeniería Química y Tecnología Farmacéutica de la Universidad de La Laguna (Tenerife, España)

USC
UNIVERSIDADE
DE SANTIAGO
DE COMPOSTELA

ABSTRACT

We have recently reported preliminary data on the potential of polyglutamic acid (PGA)-based nanocapsules as anticancer drug delivery vehicles. In this work, we have quantitatively analyzed the *in vivo* biodistribution of ^{111}In-PGA and ^{111}In-PGA-PEG nanocapsules with the final goal of elucidating their potential "lympho-targeting" properties, following intravenous or subcutaneous administration. The results indicated that, following intravenous administration, both types of nanocapsules exhibit a fast and significant accumulation in all the examined lymph nodes as well as in the liver. In contrast, following subcutaneous administration, and irrespective of the presence of PEG on their surface, the nanocapsules were found to form a reservoir at the injection site, from which they were slowly drained into the popliteal and the iliac lymph nodes. Altogether, our results confirm the ability of PGA and PGA-PEG nanocapsules to reach the lymphatic system, in particular following subcutaneous administration.

USC
UNIVERSIDADE
DE SANTIAGO
DE COMPOSTELA

1 INTRODUCTION

Nanotechnology offers promising perspectives for the diagnostic and treatment of many diseases related to the lymphatic system, such as cancer, viral and bacterial infections or autoimmune diseases [1]. In the last years, several nanometric carriers have been developed with the objective of helping diagnostic agents and drugs to reach the lymphatic system [2]. The knowledge accumulated until now has led to the identification of a number of factors, which could potentially influence the access of the nanocarriers to the lymphatic system. These factors include the particle size [3,4] and surface properties of the nanocarriers [5,6] as well as the administration route [7,8]. For example, several studies have shown that, following subcutaneous administration, nanocarriers of small particle size (close to 100 nm) can be efficiently drained from the interstice of the injection site into the lymphatics and be retained in the lymph nodes [9,10]. On the other hand, it has also been shown that following intravenous administration, nanocarriers of very small particle size have the ability to extravasate from the blood vessels into the interstitial tissue and subsequently be collected by the lymphatics [7,11,12]. Besides particle size, surface modification of the nanocarriers has been another strategy to enhance their access to the lymphatic system. One of the most commonly used approaches consists of providing the nanocarriers with polyethylene glycol (PEG) coating in order to prolong their circulation time for long enough to enable their access to the lymphatic system [13]. This hydrophilic surface has also been found to improve the migration of the nanocarriers through the tumor interstice towards the lymphatics, as well as through the subcutaneous tissue, following intravenous or subcutaneous administration respectively [14]. Unfortunately, this hydrophilic coating may also result in a reduced retention into the lymph nodes [6,10]. As a consequence, the overall effect of a PEG corona around the nanocarrier in terms of access and retention in the lymphatic system maybe highly dependent on the composition of the nanocarrier and its potential alteration during the in vivo distribution process.

Recently, our group reported for the first time the potential of 200 nm polyaminoacid nanocapsules for modifying the biodistribution and, ultimately, reducing the toxicity of anticancer drugs (14-16). Based on this information and trying to improve their lymphotropic properties, we have developed (PGA) or PEGylated polyglutamic acid

(PGA-PEG) nanocapsules with a size of 100 nm (Abellan-Pose, manuscript in preparation). In addition to their small particle size (100 nm approximately) and a negative zeta potential, these nanocapsules exhibited a satisfactory stability in human plasma during at least 24 hours and the capacity to control the release of docetaxel. In addition, using fluorescence imaging, we could verify that their reduced particle size led to an improvement of their lymphatic uptake when administered either subcutaneously or intravenously. Furthermore, we have evaluated the performance of docetaxel-loaded PGA-PEG nanocapsules in an orthotopic metastasizing lung tumor murine model and showed their extraordinary capacity to significantly inhibit metastasis in the mediastinal lymph nodes, thereby extending notably the lifespan of animals.

As a way to progress in the assessment of the lymphotropic behavior of PGA and PGA-PEG nanocapsules, our objective in this work was to radiolabel them and to quantitatively investigate their biodistribution following either intravenous or subcutaneous administration. Overall, the final goal was investigate the potential of these nanocapsules for the lymphatic delivery of drugs, and notable anticancer drugs.

2 MATERIALS AND METHODS

2.1 Materials

Miglyol® 812, a neutral oil formed by esters of caprylic and capric fatty acids and glicerol, was donated by Sasol Germany GmbH (Germany). The surfactant Epikuron 145V, a deoiled phosphatidylcholine enriched fraction of soybean lecithin, was donated by Cargill (Spain). Hexadecyltrimethylammonium bromide (CTAB), poly-L-glutamic acid (PGA) (Mw 15-50 kDa) and D-(+)-Trehalose dihydrate were purchased from Sigma-Aldrich (Spain). Polyglutamic acid-polyethylene glycol (PGA-PEG Mw 35 kDa) was supplied by Alamanda Polymers (USA). 1,2-dimyristoyl-sn-glycero-3-phosphoethanolamine-N-diethylenetriaminepentaacetic acid (14:0 DTPA-PE) was purchased from Avanti Polar Lipids, Inc. (USA). Indium-^{111} chloride ($^{111}InCl_3$) was obtained from PerkinElmer (USA) and Mallinckrodt Pharmaceuticals (USA).

2.2 Preparation and radiolabeling of polyaminoacid nanocapsules

Nanocapsules (NCs) were prepared by the solvent displacement technique as previously described (ref primer Raquel). Nanocapsules labeled with ^{111}In were prepared as followed. DTPA-conjugated phosphoethanolamine (DTPA-PE) was dissolved in a mixture of ethanol:chloroform (65/35 v/v) at 10 mg/ml. 150 µl of DTPA-PE was incubated with 0.16-1 mCi (6-37 MBq) of $^{111}InCl_3$ (1.5-10 µl) for 30 minutes. Then, 270 µl of Epikuron (25 mg/ml in ethanol), 100 µl of the cationic surfactant CTAB (15 mg/ml in ethanol), 31.3 µl Miglyol®812 and 9.5 ml of acetone were added. This organic phase was then added dropwise to the aqueous polymer solution (PGA or PGA-PEG at 0.25 mg/ml) under constant magnetic stirring, resulting in the spontaneous formation of nanocapsules. Organic solvents were removed under reduced pressure using a rotary evaporator and the final suspension volume was corrected to 1.8 ml.

2.3 Physicochemical characterization of nanocapsules

Particle size and polydispersity index were measured by photon correlation spectroscopy (PCS) using a Zetasizer Nano ZS (Malvern Instruments, Malvern, UK). Nanocapsules were diluted in filtered water and analyzed at 25ºC with a detection angle of 90º. The zeta potential (ζ) was determined by laser Doppler anemometry (LDA) after dilution with KCl 1mM using the same equipment. Characterization of ^{111}In-nanocapsules was carried out after more than 10 half-lifes (2.83 days) to avoid contamination.

2.4 Radiolabeling efficiency of nanocapsules

Labeling efficiency of polyaminoacid nanocapsules was calculated by two different methods:

a) Ultrafiltration/centrifugation:

The ^{111}In-nanocapsules suspension (300 µL) was centrifuged in Amicon® Ultra-0.5 ml 10K centrifugal filter devices (Merck Millipore, Germany) at 14000 x g for 30 minutes at 20ºC. Free ^{111}In was collected in the ultrafiltrate and the ^{111}In-

nanocapsules were retained in the upper compartment of the device. The activity of each fraction was measured using a gamma counter (Cobra II, Packard). The labeling efficiency was determined by the following Eq.:

$$\%\ Labeling\ efficiency = \frac{Activity\ of\ filter\ with\ NCs}{Total\ activity} \times 100$$

b) Size-exclusion chromatography (SEC):

The labeling efficiency was also determined using an equilibrated PD-10 Sephadex G-25 Column (GE Healthcare Bio-Sciences AB, Sweden). The column was loaded with 1.8 ml of ^{111}In-nanocapsules suspension and centrifuged at x 1000 g for 2 minutes at 20ºC. The ^{111}In-nanocapsules were collected in the eluate whereas the free ^{111}In was retained within the column. The activities in the column and in the eluate were measured using a dose calibrator (Capintec, CRC-15R).

$$\%\ Labeling\ efficiency = \frac{Activity\ of\ eluate\ with\ NCs}{Total\ activity} \times 100$$

This second method was always used to check the radiolabeled nanocapsules quality before any use.

2.5 Assessment of the radiolabeling stability

^{111}In-Nanocapsules were incubated with rat blood plasma at 37ºC under horizontal agitation. Nanocapsules (≈18 mg/ml) were added to the blood plasma in a proportion 1:1 and 1:100 (v/v) to simulate the dilution produced under the conditions of subcutaneous and intravenous administration, respectively. Samples were withdrawn at previously established time points and free ^{111}In was separated by ultrafiltration/centrifugation and measured as described in 2.4.

2.6 Animals

All experiments were carried out with healthy female Sprague Dawley rats (130-290 g) in conformity with the E.C. (2010/63/EU) on care and use of animals in experimental procedures. Animal experiments were approved by the local Research Ethics

Committee (CEIBA) of La Laguna University. Rats were housed in metabolic cages under controlled conditions and provided with food and water *ad libitum*.

2.7 Biodistribution and pharmacokinetic study by intravenous administration

200 µl (1-6 µCi, 37-222 KBq) of ^{111}In-PGA-PEG-nanocapsules, ^{111}In-PGA-nanocapsules or $^{111}InCl_3$ in solution were administered in the tail vein of rats. ^{111}In-nanocapsules suspension and $^{111}InCl_3$ solution were previously isotonized with trehalose at 10% (w/v) and saline solution, respectively. The concentration of injected nanocapsules was kept constant for all experiments (≈ 17 mg/ml). At 0.25, 1.75, 4, 24 and 48 hours post-injection animals (4 rats per group) were sacrificed. Blood samples were collected by cardiac puncture and, if any, urine and feces were collected from the cage. Spleen, brain, heart, liver, ovaries, lungs, kidneys and the axillary, cervical, iliac, inguinal, mediastinal, mesenteric and popliteal lymph nodes were harvested. All samples were weighed and the radioactivity measured in the gamma counter (Cobra II, Packard). Standards to correct the decay of activity were prepared by taking an aliquot from the injected formulation. Blood activity was calculated on the assumption that female Sprague-Dawley rats have 70 ml of blood circulating per kg.

Furthermore, a pharmacokinetic analysis was also performed based on the blood activity data. Parameters were calculated through a non-compartmental pharmacokinetic method using the PK Solver menu-driven add-in program for Microsoft Excel.

2.8 Local residence and biodistribution study of subcutaneously injected nanocapsules

Retention of the nanocapsules was followed up by a non-invasive method as previously described and validated by Delgado *et al.* [15]. Briefly, 50 µl (~1 µCi, 37 KBq) of ^{111}In-PGA-PEG-nanocapsules, ^{111}In-PGA-nanocapsules, or $^{111}InCl_3$ were administered in the right rear footpad of four anesthetized rats, followed by a gentle massage during four minutes. Rats were anesthetized with isoflurane/oxygen and their body temperature was maintained using a heating plate at 37ºC during the entire procedure. During 7 days, periodic assessment of the remaining radioactivity at the administration site was carried

out using an external probe-type gamma counter (Captus®, Nuclear Iberica). To measure the remaining radioactivity in the injection site, the detector was focused with a collimator on the footpad. At each time point, four consecutive readings were performed and the ^{111}In emission peaks (245 and 173 keV) were integrated for the cumulative events registered over 1 min. Mean values were considered as the remaining radioactivity at each time point. Measurement at time point 0 was assumed as the total administered dose (100%). After recovering from anesthesia, animals were allowed to move freely in their cage.

Biodistribution assays by subcutaneous route were performed similarly to the intravenous ones. 50 µl of ^{111}In-NC suspension or $^{111}InCl_3$ solution (0.5-2 µCi, 18.5-74 KBq) were injected in each footpad as was described above. The amount of injected nanocapsules was also kept constant for all experiments. Animals were euthanized at 24 and 48 hours after the administration. Samples extraction and radioactivity quantification was carried out as described in section 2.7.

2.9 Statistical analysis

Statistical analysis was performed using Statgraphics Centurion XVI.1.15. For comparison between interventions, Kruskal-Wallis analysis was employed in order to establish significant differences between groups. Differences were considered significant at a level of $p<0.05$.

3 RESULTS AND DISCUSSION

Recently we reported the development of nanocapsules, consisting on a lipophilic core surrounded by a PGA or PGA-PEG coating, which were supposed to exhibit lymphotropic properties. In particular, these nanocapsules are flexible nanocarriers that exhibit a small particle size close to 100 nm, a negative zeta potential and a hydrophilic polymer surface that helps preserving their stability in plasma and enable the controlled release of the associated drug. The main aim of this work has been to compare the *in vivo* distribution of PGA-nanocapsules and PGA-PEG-nanocapsules labeled with ^{111}In and their ability to specifically reach the lymph nodes after intravenous and subcutaneous administration.

3.1 Preparation and radiolabeling of polyaminoacid nanocapsules

PGA-based nanocapsules were obtained according to a modified solvent displacement technique [16], which was conveniently optimized in order to obtain nanocapsules with characteristics that would be potentially appropriate for lymphotargeting purposes [10]. For the radiolabeling of these nanocapsules with ^{111}In, phosphoethanolamine (PE) conjugated with the chelating agent diethylenetriamine pentacetic acid (DTPA) was incorporated in the oily core of the nanocapsules. The high affinity of ^{111}In for the DTPA-PE molecule enabled its incorporation together with lecithin, used as a surfactant for the stabilization of the oily core. The results presented in **Table 1** indicate that the presence of DTPA-PE and the subsequent labeling with ^{111}In did not modify substantially the size or the polydispersity index of the nanocapsules. The zeta potential was slightly modified towards more negative values, likely due to the presence of phosphoethanolamine; however, the differences were not statistically significant.

The labeling efficiency was determined by both, ultrafiltration/centrifugation and size exclusion chromatography, with congruent results. Both nanocapsule compositions showed a labeling efficiency, which was close to 50% (**Table 1**), a result that suggested that not all the DTPA-PE included in the formulation was effectively incorporated in the nanocapsules. Nevertheless, the purification of nanocapsules through size exclusion chromatography allowed to remove the non-associated ^{111}In (free ^{111}In and ^{111}In-DTPA-PE) and to obtain purified ^{111}In-nanocapsules.

Formulation	Size (nm)	P.I.	Zeta potential (mV)	L.E. (%)
PGA-NCs	100 ± 2	0.1	-54 ± 1	--
^{111}In-PGA-NCs	112 ± 14	0.1	-84 ± 19	42 ± 8
PGA-PEG-NCs	116 ± 5	0.1	-29 ± 5	--
^{111}In-PGA-PEG-NCs	103 ± 5	0.1	-58 ± 15	53 ± 4

Table 1. Physicochemical characterization and labeling efficiency of polyaminoacid nanocapsules. NCs: nanocapsules; P.I.: polidispersity index; L.E.: Labeling efficiency. Mean ± S.D.; n=3.

3.2 Assessment of the radiolabeling stability

The quality and stability of the radiolabeling was assessed by measuring the release of the radiotracer in rat plasma using different dilution factors, namely 1:1 and 1: 100. Although the release profile was related to the dilution factor (15% released after 96 hours and 28% after 48 hours for the low and high dilution factors), the amount released was moderate and compatible with their use for the *in vivo* biodistribution studies **(Figure 1)**.

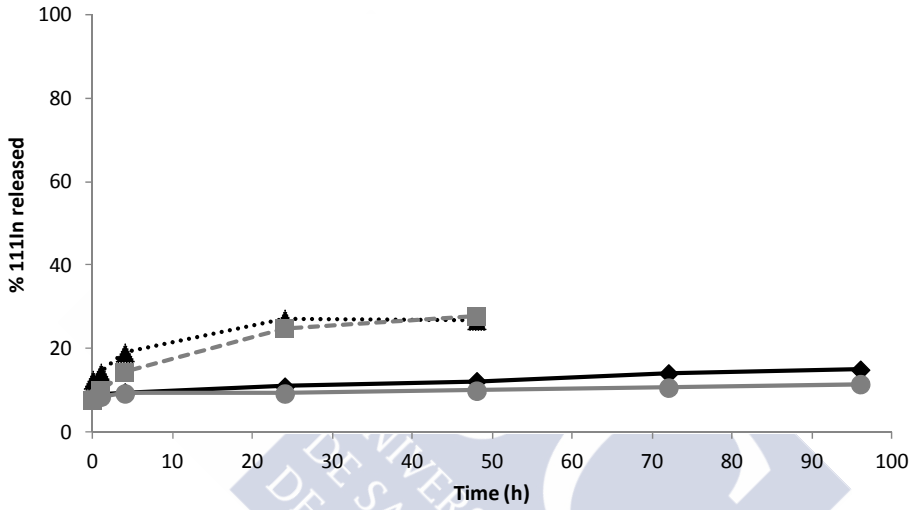

Figure 1. Radiolabeling stability. 111In release profile from 111In-PGA-PEG nanocapsules (black) and 111In-PGA nanocapsules (grey) after incubation in rat blood plasma at proportion 1:1 (continuous lines) and 1:100 (discontinuous lines) (v/v).

3.3 Pharmacokinetics and biodistribution of polyaminoacid nanocapsules after intravenous administration

As shown in **Figure 2**, after intravenous administration, the nanocapsules exhibited biphasic pharmacokinetic profile, with an initial fast plasma elimination phase (first 4 hours) associated to the biodistribution of the nanocapsules, followed by a slow elimination phase. The highest radioactivity levels determined in blood were 4.5, 3.5% and 3.2% ID/g for PGA-PEG-nanocapsules, PGA-nanocapsules and $^{111}InCl_3$, respectively (0.25 hours post-administration). After 24 hours, the radioactivity

corresponding to the nanocapsules was still detectable, although at low levels (approximately 0.1%ID/g), which was in accordance with the results reported for other lipid nanocarriers such as lipid nanocapsules [17] and nanostructured lipid carriers [18].

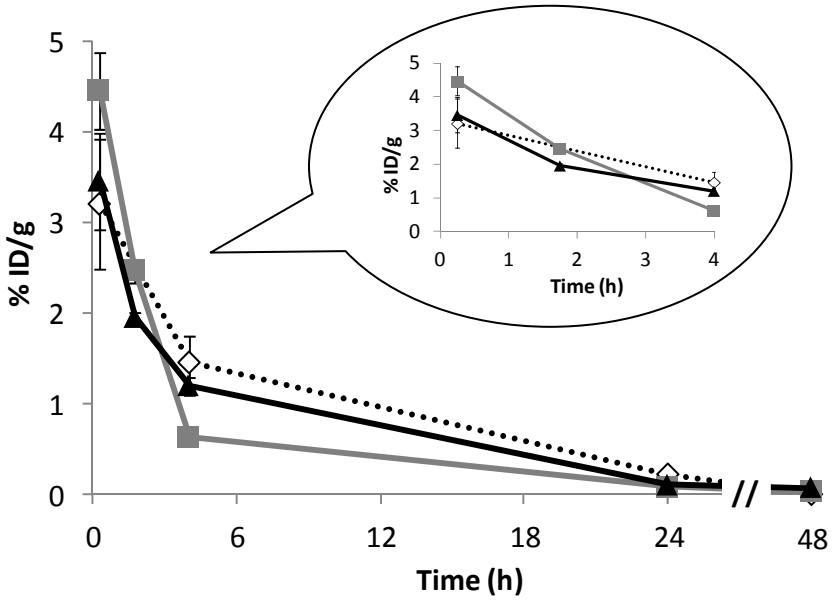

Figure 2. Evolution of the activity detected in the blood after intravenous administration of 111InCl3 (··◇··), 111In-PGA-PEG-nanocapsules (—■—) and 111In-PGA-nanocapsules (—▲—). Values are expressed as percentage of the injected dose per gram of blood (%ID/g) (mean ± SEM; n=4).

The estimated pharmacokinetic parameters by a non-compartmental analysis (**Table 2**) evidenced that the elimination parameters ($t_{1/2}$, Cl and MRT) were higher for the nanocapsules and the control, $^{111}InCl_3$, and these differences become more drastic in the distribution phase. Indeed, he volumes of distribution (V_z and V_{ss}) of the nanocapsules were 2 or 3-fold that of the control $^{111}InCl_3$, indicating a more extensive distribution of the nanocapsules. In this regard, we should keep in mind that ^{111}In is known to have a high affinity towards serum proteins, such as transferrin [19], a fact that contributes to its relatively long half-life.

Table 2. Pharmacokinetic parameters estimated through a non-compartmental analysis for the nanocapsules and control after intravenous administration to rats. NCs: nanocapsules, λz: terminal rate constant, AUC: area under the curve, MRT: mean residence time, Vz: volume of distribution during the terminal phase, Vss: volume of distribution at steady-state.

Formulation	λ_z (1/h)	$t_{½}$ (h)	AUC $_{0-\infty}$ (%ID/g*h)	MRT (h)	V_z (g)	Cl (g/h)	V_{ss} (g)
$^{111}InCl_3$	0.12	6.0	34.9	6.5	24.7	2.9	18.7
^{111}In-PGA-PEG-NCs	0.06	10.9	19	7.4	82.6	5.3	38.6
^{111}In-PGA-NCs	0.08	8.9	24.9	9	51.5	4	36.3

Biodistribution of PGA and PGA-PEG nanocapsules after intravenous administration

The percentages of the radioactivity injected dose per gram of tissue (%ID/g) detected in major organs and lymph nodes are represented in **Figure 3 and 5,** respectively. After injection of the nanocapsules, the highest activity levels were found in the liver, and to lesser extent, in the spleen **(Figure 3)**. The maximum radioactivity levels in the liver were achieved at 1.75 and 4 h post-administration and were 5.4, 6.3% and 1.6 %ID/g tissue for PGA-PEG-nanocapsules, PGA-nanocapsules and $^{111}InCl_3$, respectively. This represents around the 45% of the total injected dose for both nanocapsules and 12 %ID for the control (**Figure 4A**). As occurred in the liver, significantly higher activity levels were found in the spleen during the first 4 hours in the groups treated with nanocapsules than in the control group ($^{111}InCl_3$). Although this organ is known to be highly involved in the clearance of particles, the activity levels observed in this study were below 3.5%ID/g tissue, which represents less than 2% of the total injected dose. This accumulation could be attributed to two processes: i) the escape of nanosystems from the circulation through the open fenestrae of the hepatic and splenic sinusoidal capillaries [20]; ii) the uptake by the macrophages of the Mononuclear Phagocyte System (MPS) located in these organs, which is largely responsible for the clearance of particles from the bloodstream [17,21]. The observed accumulation of the nanocapsules in the liver and spleen, following intravenous administration, is in line with that

observed for other types of nanocapsules [17,22] and it is much lower that the reported for PEGylated liposomes [23,24]. These results may underline the superiority of the nanocapsules vs. liposomes in terms of reduced hepatic clearance.

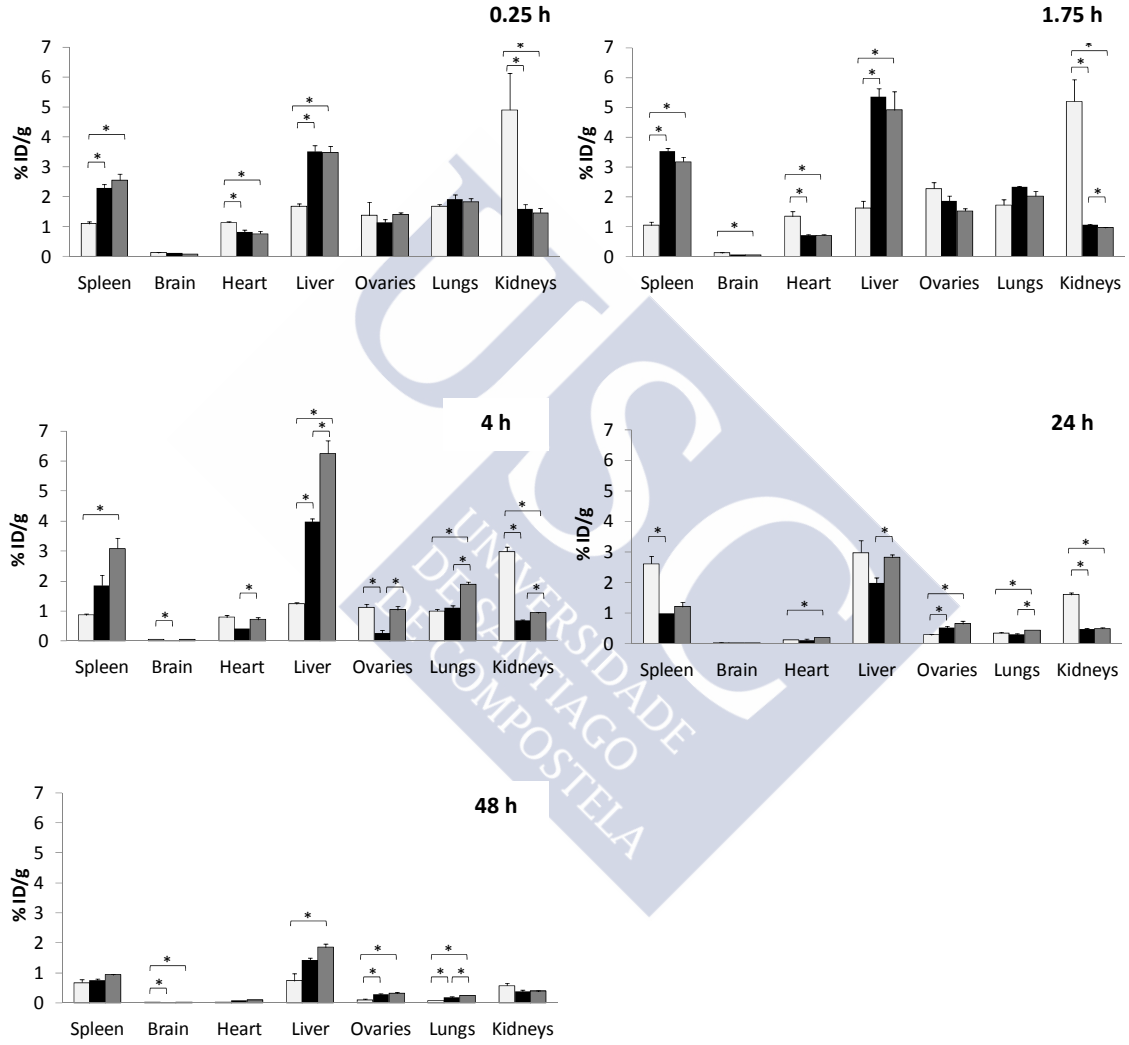

Figure 3. Organ distribution at different times after the intravenous administration of $^{111}InCl_3$ (□), ^{111}In-PGA-PEG nanocapsules (■) and ^{111}In-PGA nanocapsules (▩). Values are expressed as percentage of the injected dose per gram of organ (mean ± SEM; n=4). * Statistically significant differences ($p<0.05$).

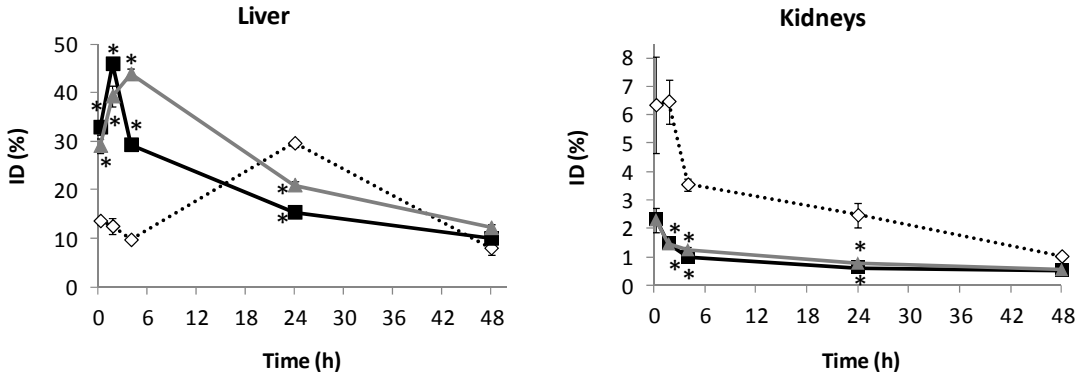

Figure 4. Evolution of activity in the liver and kidneys during 48 hours after intravenous administration of $^{111}InCl_3$ (··◇··), ^{111}In-PGA-PEG nanocapsules (—■—) and ^{111}In-PGA nanocapsules (—▲—). Values are expressed as percentage of the injected dose (mean ± SEM; n=4). *Statistically significant differences between nanocapsules and $^{111}InCl_3$ ($p<0.05$).

On the other hand, the results in **Figure 4B** indicate that the radioactivity levels in the kidneys were significantly higher for the $^{111}InCl_3$-injected rats than the groups of nanocapsules at all time points. This was expected as it is known that both, the free ^{111}In and ^{111}In-DTPA are known to be substantially excreted by the kidneys [25,26]. These results agree with the activity recovered in the urine at 48 hours, 26% ID for PGA-PEG-nanocapsules and 18% ID for PGA-nanocapsules versus the 89% ID quantified in the control group. More surprising was the fact that a significant amount of radioactivity was detected in the harvested feces of rats injected with nanocapsules at 24 hours (around 41% and 33% ID for PGA-PEG-nanocapsules and PGA-nanocapsules, respectively) and 48 hours (around 65% ID for both formulations) whereas a limited activity was determined in the feces of the control group (close to 1% at 24 hours and 25% at 48 hours). On the other hand, part of the activity was also recovered in the urine at 48 hours, 26% ID for PGA-PEG-nanocapsules and 18% ID for PGA-nanocapsules versus the 89% ID quantified in the control group. Altogether, these data indicate that the main elimination route of ^{111}In-nanocapsules was through the liver and the biliary excretion, whereas that of free $^{111}InCl_3$ through the kidneys and liver. This conclusion was in line with the previous observations of Vicente *et al.* for the biodistribution of ^{111}In-labeled polyglucosamine nanocapsules [27].

Finally, it is important to mention that radioactivity levels in the brain was negligible for both nanocarriers at all times studied (less than 0.06% ID/g), evidencing the inability of these nanocapsules to cross the blood-brain barrier and hence, indicates the interest of these carriers to minimize adverse effects associated to the intravenous administration of potentially neurotoxic drugs.

In conclusion, overall, the blood kinetics and biodistribution pattern of both types of nanocapsules upon intravenous administration is similar, with some minor differences being observed with regard to their accumulation in liver and lung. In fact, at 4 and 24 hours post administration the accumulation of the PEGylated nanocapsules in these organs was lower than that observed for PGA nanocapsules (**Figure 3**). This could be attributed to a reduced recognition of the PEGylated nanocapsules by the resident macrophages [28].

Regarding the lymphatic uptake, as reflected in **Figure 5**, the radioactivity levels detected in the lymph nodes at 0.25 and 1.75 hours post-administration of ^{111}In-nanocapsules were lower than those observed for the control. However, the radioactivity levels went rapidly down for the control animals, whereas they gradually increased in iliac, mesenteric and popliteal nodes for the group injected with ^{111}In-PGA-PEG-nanocapsules. At 24 hours post-administration, the accumulation levels of the nanocapsules-associated radioactivity in the inguinal, mediastinal and mesenteric lymph nodes were significant higher than that of the control. In the case of PGA-PEG-nanocapsules, the radioactivity levels were additionally higher in the axillary and cervical lymph nodes. In general, at 48 hours the radioactivity levels were reduced and statistically significant differences between the nanocapsules and control were only observed in the mediastinal and mesenteric lymph nodes. Overall, the conclusion is that nanocapsules and notably, PEGylated nanocapsules, helped the accumulation of the radioactive marker in the lymphatic system over the time and that this accumulation was particularly noticeable in the time frame of 4-24 h in the inguinal, mediastinal and mesenteric lymph nodes.

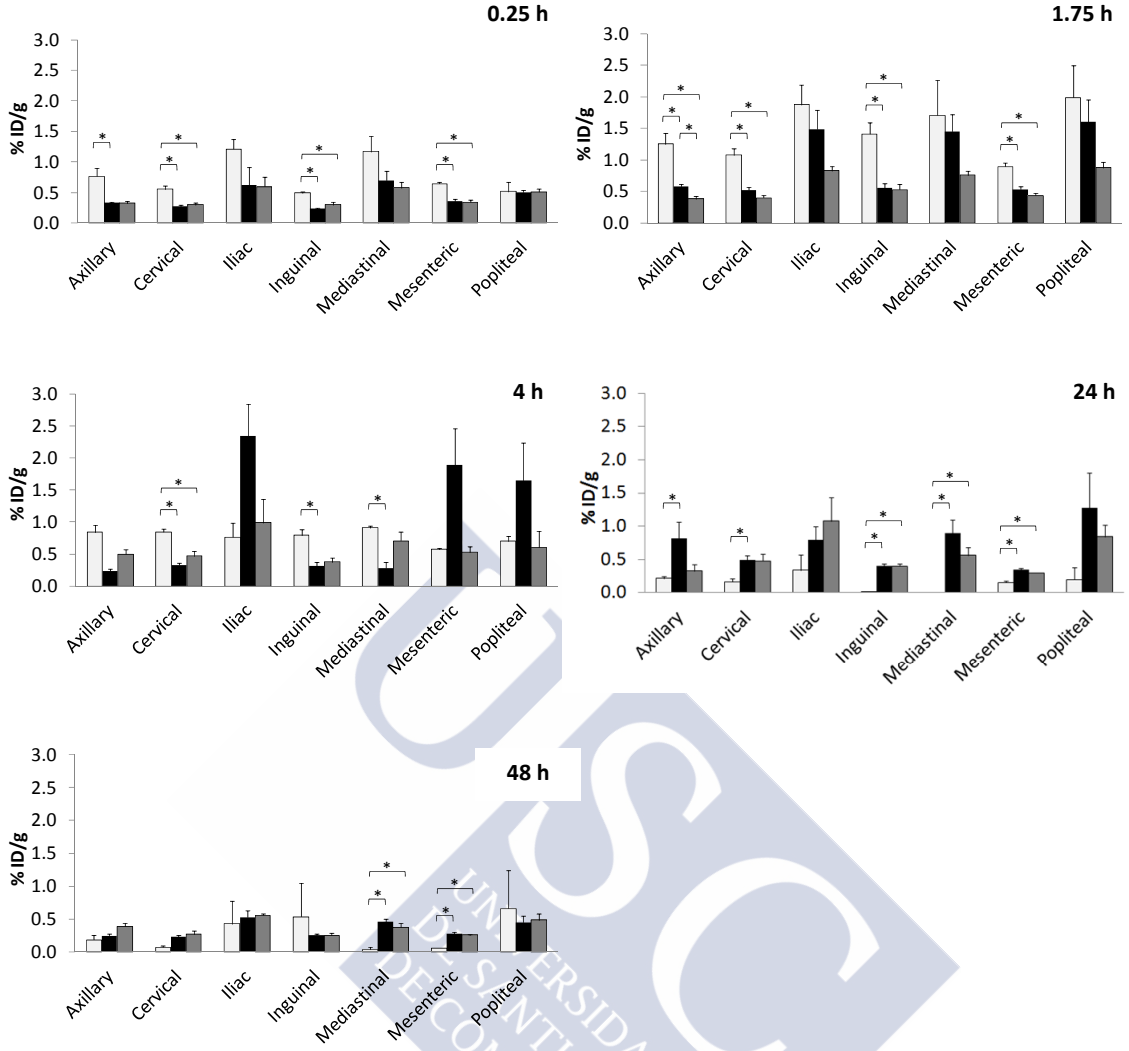

Figure 5. Lymph node distribution at different times after the intravenous administration of $^{111}InCl_3$ (□), ^{111}In-PGA-PEG nanocapsules (■) and ^{111}In-PGA nanocapsules (▩). Values are expressed as percentage of the injected dose per gram of organ (mean ± SEM; n=4). * Statistically significant differences ($p<0.05$).

3.4 Biodistribution of polyaminoacid nanocapsules after subcutaneous administration

Evaluation of the residence time of the nanocapsules at the injection site

The drainage of ^{111}In-nanocapsules or the $^{111}InCl_3$ solution from the administration site was monitored for up to seven days by measuring the radioactivity levels remaining at

the injected footpad. As observed in **Figure 6**, the control $^{111}InCl_3$ was rapidly drained during the first 24 h post-injection. The same pattern was reported by Harrington *et al.* for subcutaneously injected ^{111}In-DTPA in the flank of mice [29]. After this period, the activity levels remained constant around 27 %ID up until the end of the study (7 days). This prolonged permanence of $^{111}InCl_3$ may be explained by a decrease in the solubility of ionic ^{111}In, which forms insoluble hydrated indium oxide at the physiological pH [30]. In contrast, the %ID levels in the footpad injected with ^{111}In-nanocapsules at the end of the study were significantly lower for both prototypes (5.9% for PGA-nanocapsules and 12.5% for PGA-PEG-nanocapsules) than for those receiving the control. This result indicates that a high proportion of nanocapsules are efficiently drained from the footpad in a sustained manner over a week. In fact, PGA-PEG and PGA nanocapsules showed a slow and gradual drainage profile, which suggests that nanocapsules are drained through the lymphatic system thanks to their adequate physicochemical characteristics. These results are in line with the lymphatic drainage previously observed by Vicente *et al*. for ^{111}In-labeled polyglucosamine nanocapsules administered in the footpad of rabbits although their drainage was slightly slower with larger remaining fractions at the injection site, probably due to their larger particle size (230 ± 12 nm) and positively charged surface (+20 ± 4 mV) [27].

Based on previous literature reports, we hypothesized that the PEGylation would reduce the interactions of nanocarriers with the interstitial surroundings and, thereby enhance their migration from the interstice towards the lymphatics [10,31]. Nevertheless, the statistical comparison of the radioactivity drainage profiles presented in **Figure 6** indicate that both, PEGylated and non-PEGylated PGA nanocapsules, have the same behavior. Therefore, the conclusion of this study is that the PEGylation of PGA does not contribute to the migration of the nanocapsules from the injection site. These observations, together with those determined for the intravenous route indicate that the PGA as polymeric coating material can provide by itself interesting properties for the lymphatic targeting of nanocarriers of drugs and diagnostic agents.

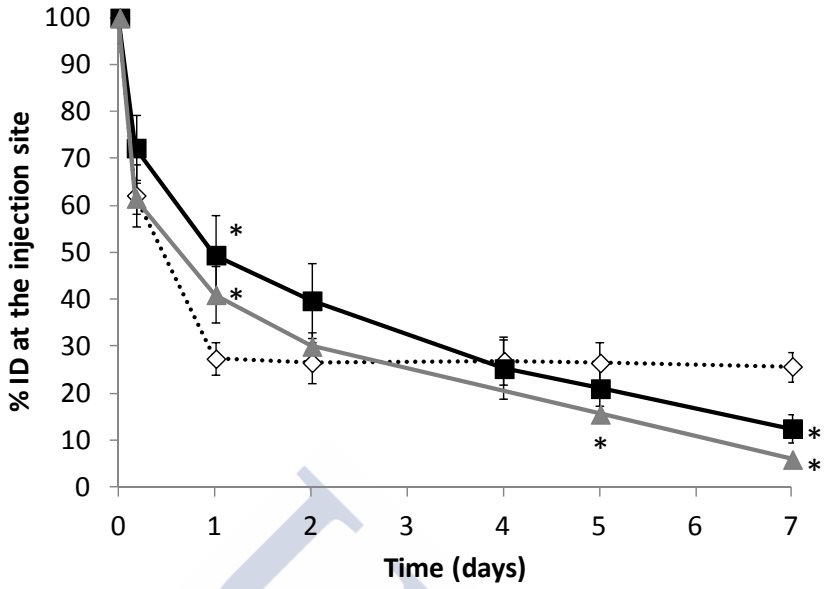

Figure 6. Radioactivity levels remaining in the injection site over time after subcutaneous administration of 111InCl3 (··◇··), 111In-PGA-PEG nanocapsules (—■—) and 111In-PGA nanocapsules (—▲—), expressed as percentage of injected dose (%ID) at the footpad (mean ± S.D.; n=4)* Statistically significant differences between nanocapsules and 111InCl3 ($p<0.05$).

Biodistribution of the nanocapsules after subcutaneous administration

The results of the biodistribution of ^{111}In either in a free form or associated to the nanocapsules, after subcutaneous administration are reported in **Figure 7 and 8.** The data presented in **Figure 7** evidenced the high accumulation of both nanocapsules prototypes in the popliteal (PGA-PEG-nanocapsules 186.5 ± 64.7% and PGA-nanocapsules 165.6 ± 68.3% ID/g) and the iliac lymph nodes (PGA-PEG-nanocapsules 123.5 ± 53.4% and PGA- nanocapsules 85.8 ± 31.9% ID/g). In agreement with previous data (28), the control $^{111}InCl_3$, hardly reached the lymphatics and was mainly absorbed from the interstice by the blood capillaries as a consequence of its small molecular weight, exhibiting a distribution pattern consistent with the observed after the intravenous administration.

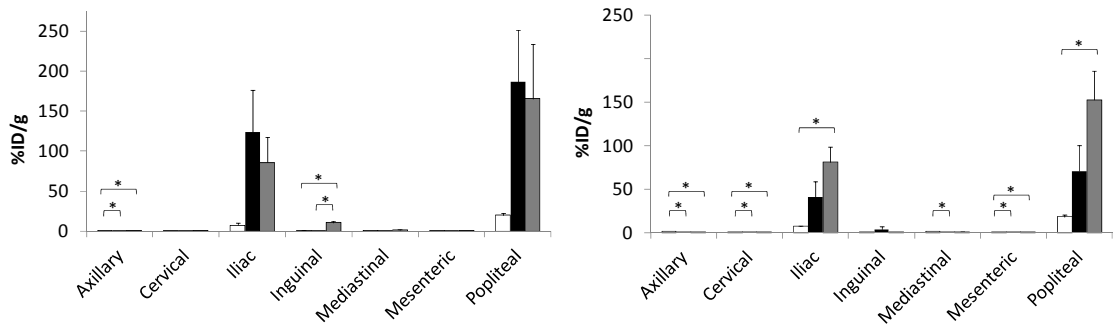

Figure 7. Lymph node distribution at 24 and 48 hours following the subcutaneous administration of 111InCl3 (□), 111In-PGA-PEG-nanocapsules (■) and 111In-PGA-nanocapsules (▩). Values are expressed as percentage of the injected dose per gram of tissue (mean ± SEM.; n=4). * Statistically significant differences ($p<0.05$).

Overall, the activity found in the draining lymph nodes (popliteal, inguinal and iliac lymph nodes) represents a 4.5% ID and 5.2% ID at 24 hours, and 3% ID and 2.3% ID at 48 hours, for PGA-PEG and PGA nanocapsules, respectively (vs 0.5% ID and 0.2% ID of the control at 24 and 48 hours), indicating the preferential accumulation of these nanostructures in the lymphatic system, in line with the results previously obtained for the polyglucosamine nanocapsules [27]. The explanation of the lymphatic accumulation of the nanocapsules could be as follows. The nanocapsules injected into the hind footpad were firstly drained to the popliteal lymph node and then, via the efferent popliteal trunk, they migrate to the iliac lymph node [32,33]. High activity levels in these draining lymph nodes were maintained for the duration of the experiment. This could be due to the retention of nanocapsules as a consequence of the mechanical filtration, the action of MPS cells, and/or their continuous lymphatic uptake from the interstice [2]. In addition, nanocapsules were also detected in the inguinal lymph nodes (10.7 ± 1.96% ID/g for PGA-nanocapsules at 24 h and 3.6 ± 3.18% ID/g for PGA-PEG-nanocapsules at 48 h), likely as a result of the drainage from the peripheral area around the injection point [33].

On the other hand, low levels of nanocapsules-associated radioactivity could be detected in the blood samples and highly irrigated organs (**Figure 8)**. This observation suggests that the nanocarriers were not entirely retained within the lymphatic system and a small

fraction could reach the bloodstream via the subclavian veins. At 24 and 48 hours, activity levels found for nanocapsules in the liver and spleen were comparable to the control but significantly lower in the kidneys. These data, together with the activity levels measured in feces and urine (data not shown), confirm that nanocapsules and $^{111}InCl_3$ are mainly excreted through the biliary and urinary routes, respectively. Besides, as observed by intravenous administration, radioactivity in the brain was practically negligible for nanocapsules because of the restriction of the blood-brain barrier.

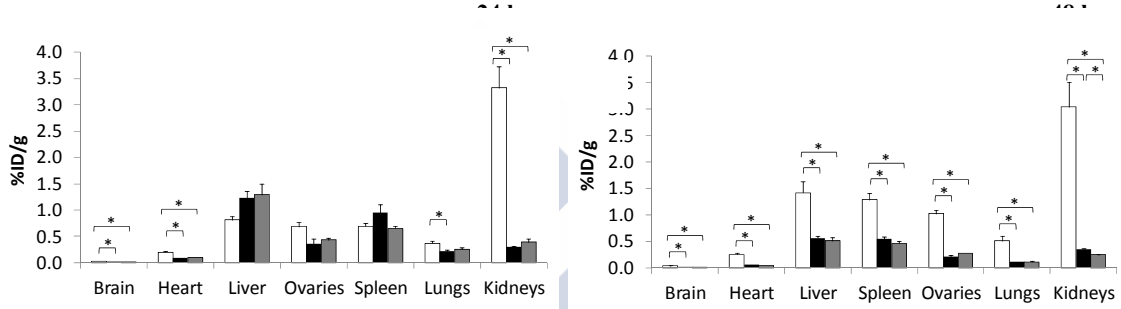

Figure 8. Organ distribution at 24 and 48 hours following the subcutaneous administration of 111InCl3 (□), 111In-PGA-PEG-nanocapsules (■) and 111In-PGA-nanocapsules (■). Values are expressed as percentage of the injected dose per gram of tissue (mean ± SEM.; n=4). * Statistically significant differences ($p<0.05$).

Overall our results indicate that, in the absence of pathological conditions affecting biodistribution, the subcutaneous administration of polyaminoacid nanocapsules leads to highly efficient accumulation of nanocapsules in the draining lymph nodes. Therefore, subcutaneous route can be more advantageous than the intravenous one for a selective lymphatic delivery of diagnostic agents or drugs [7,34]. However, since certain diseases such as cancer may affect the lymphatic delivery of nanocarriers, the optimal administration route should be selected case-by-case, based on the specific physiopathological conditions and the nature of the diagnostic or therapeutic agent to be delivered.

4 CONCLUSIONS

Herein we report the biodistribution of PGA and PGA-PEG nanocapsules, designed with the aim of promoting their access and retention into the lymph node. Our results indicated that both formulations have the capacity to reach the lymph nodes when administered by intravenous or subcutaneous route. However, the access of the nanocapsules to the lymphatics was significantly enhanced when administered by the subcutaneous route. In addition, the accumulation in liver and spleen was significantly more pronounced following intravenous administration. In conclusion, the lymphotargeting properties of the polyaminoacid nanocapsules could be particularly exploited following their administration by the subcutaneous route of administration.

REFERENCES

[1] Singh I, Swami R, Khan W, Sistla R. Lymphatic system: a prospective area for advanced targeting of particulate drug carriers. Expert Opin. Drug Deliv. 2014;11:211–29.

[2] Abellan-Pose R, Csaba N, Alonso MJ. Lymphatic Targeting of Nanosystems for Anticancer Drug Therapy. Curr. Pharm. Des. Submitted.

[3] Bergqvist L, Strand SE, Persson BR. Particle sizing and biokinetics of interstitial lymphoscintigraphic agents. Semin. Nucl. Med. 1983;13:9–19.

[4] Cabral H, Makino J, Matsumoto Y, Mi P, Wu H, Nomoto T, et al. Systemic Targeting of Lymph Node Metastasis through the Blood Vascular System by Using Size-Controlled Nanocarriers. ACS Nano 2015;9:4957–67.

[5] Patel H, Boodle M, Vaughan-Jones R. Assessment of the potential uses of liposomes for lymphoscintigraphy and lymphatic drug delivery: Failure of 99m-Technetium marker to represent intact liposomes in lymph nodes. Biochim. Biophys. Acta 1984;801:76–86.

[6] Moghimi SM, Hawley AE, Christy NM, Gray T, Illum L, Davis SS. Surface engineered nanospheres with enhanced drainage into lymphatics and uptake by macrophages of the regional lymph nodes. FEBS Lett. 1994;344:25–30.

[7] Pitorre M, Bastiat G, dit Chatel EM, Benoit J-P. Passive and specific targeting of lymph nodes: the influence of the administration route. Eur. J. Nanomedicine 2015;7:121–8.

[8] Kaminskas LM, McLeod VM, Ascher DB, Ryan GM, Jones S, Haynes JM, et al. Methotrexate-Conjugated PEGylated Dendrimers Show Differential Patterns of Deposition and Activity in Tumor-Burdened Lymph Nodes after Intravenous and Subcutaneous Administration in Rats. Mol. Pharm. 2015;12:432–43.

[9] Oussoren C, Zuidema J, Crommelin DJA, Storm G. Lymphatic uptake and biodistribution of liposomes after subcutaneous injection. II. Influence of liposomal size, lipid composition and lipid dose. Biochim. Biophys. Acta 1997;261–72.

[10] Oussoren C, Storm G. Liposomes to target the lymphatics by subcutaneous administration. Adv. Drug Deliv. Rev. 2001;50:143–56.

[11] Qin L, Zhang F, Lu X, Wei X, Wang J, Fang X, et al. Polymeric micelles for enhanced lymphatic drug delivery to treat metastatic tumors. J. Control. Release 2013;171:133–42.

[12] Hirsjärvi S, Dufort S, Gravier J, Texier I, Yan Q, Bibette J, et al. Influence of size, surface coating and fine chemical composition on the in vitro reactivity and

in vivo biodistribution of lipid nanocapsules versus lipid nanoemulsions in cancer models. Nanomedicine Nanotechnology, Biol. Med. 2013;9:375–87.

[13] Tobío M, Gref R, Sánchez A, Langer R, Alonso M. Stealth PLA-PEG Nanoparticles as Protein Carriers for Nasal Administration. Pharm. Res. 1998;

[14] Moghimi SM. The effect of methoxy-PEG chain length and molecular architecture on lymph node targeting of immuno-PEG liposomes. Biomaterials 2006;27:136–44.

[15] Delgado JJ, Evora C, Sánchez E, Baro M, Delgado A. Validation of a method for non-invasive in vivo measurement of growth factor release from a local delivery system in bone. J. Control. Release 2006;114:223–9.

[16] Gonzalo T, Lollo G, Garcia-Fuentes M, Torres D, Correa J, Riguera R, et al. A new potential nano-oncological therapy based on polyamino acid nanocapsules. J. Control. Release 2013;169:10–6.

[17] Ballot S, Noiret N, Hindré F, Denizot B, Garin E, Rajerison H, et al. 99mTc/188Re-labelled lipid nanocapsules as promising radiotracers for imaging and therapy: formulation and biodistribution. Eur. J. Nucl. Med. Mol. Imaging 2006;33:602–7.

[18] Beloqui A, Solinís MA, Delgado A, Evora C, del Pozo-Rodríguez A, Rodríguez-Gascón A. Biodistribution of Nanostructured Lipid Carriers (NLCs) after intravenous administration to rats: influence of technological factors. Eur. J. Pharm. Biopharm. 2013;84:309–14.

[19] Konikowski T, Haynie TP, Glenn HJ. Kinetics of 111In-Bleomycin and 111In-Chlorides in Mice. J. Nucl. Med. 1975;16:738–43.

[20] Moghimi SM, Hunter AC, Murray JC. Long-Circulating and Target-Specific Nanoparticles : Theory to Practice. Pharmacol. Rev. 2001;53:283–318.

[21] Hoarau D, Delmas P, David S, Roux E, Leroux J. Novel Long-Circulating Lipid Nanocapsules. Pharm. Res. 2004;21:1783–9.

[22] Khalid MN, Simard P, Hoarau D, Dragomir A, Leroux J-C. Long circulating poly(ethylene glycol)-decorated lipid nanocapsules deliver docetaxel to solid tumors. Pharm. Res. 2006;23:752–8.

[23] ElBayoumi TA, Torchilin VP. Enhanced accumulation of long-circulating liposomes modified with the nucleosome-specific monoclonal antibody 2C5 in various tumours in mice: gamma-imaging studies. Eur. J. Nucl. Med. Mol. Imaging 2006;33:1196–205.

[24] ElBayoumi TA, Torchilin VP. Tumor-targeted nanomedicines: enhanced antitumor efficacy in vivo of doxorubicin-loaded, long-circulating liposomes

modified with cancer-specific monoclonal antibody. Clin. Cancer Res. 2009;15:1973–80.

[25] GE Healthcare (Medi-Physics Inc). INDIUM DTPA In 111. 2006.

[26] Harrington KJ, Rowlinson-Busza G, Syrigos KN, Uster PS, Abra RM, Stewart JS. Biodistribution and pharmacokinetics of 111In-DTPA-labelled pegylated liposomes in a human tumour xenograft model: implications for novel targeting strategies. Br. J. Cancer 2000;83:232–8.

[27] Vicente S, Goins BA, Sanchez A, Alonso MJ, Phillips WT. Biodistribution and lymph node retention of polysaccharide-based immunostimulating nanocapsules. Vaccine 2014;32:1685–92.

[28] Storm G, Belliot S, Daemenb T, Lasic DD. Surface modification of nanoparticles to oppose uptake by the mononuclear phagocyte system. Adv. Drug Deliv. Rev. 1995;17:31–48.

[29] Harrington KJ, Rowlinson-busza G, Syrigos KN, Uster PS, Vile RG, Stewart JSW. Pegylated Liposomes Have Potential as Vehicles for Intratumoral and Subcutaneous Drug Delivery. Clin. cancer Res. 2000;6:2528–37.

[30] Castronovo FP J, Wagner HR J. Comparative toxicity and pharmacodynamics of ionic indium chloride and hydrated indium oxide. J. Nucl. Med. 1973;14:677–82.

[31] Rao DA, Forrest ML, Alani AWG, Kwon GS, Robinson JR. Biodegradable PLGA Based Nanoparticles for Sustained Regional Lymphatic Drug Delivery. J. Pharm. Sci. 2010;99:2018–31.

[32] Tilney NL. Patterns of lymphatic drainage in the adult laboratory rat. J. Anat. 1971;109:369–83.

[33] Bagby TR, Cai S, Duan S, Thati S, Aires DJ, Forrest L. Impact of molecular weight on lymphatic drainage of a biopolymer-based imaging agent. Pharmaceutics 2012;4:276–95.

[34] Harivardhan Reddy L, Sharma RK, Chuttani K, Mishra AK, Murthy RSR. Influence of administration route on tumor uptake and biodistribution of etoposide loaded solid lipid nanoparticles in Dalton's lymphoma tumor bearing mice. J. Control. Release 2005;105:185–98.

.

Capítulo 4

Docetaxel-loaded PEGylated-Polyglutamic Acid Nanocapsules for the Treatment of Metastatic Cancer

USC
UNIVERSIDADE
DE SANTIAGO
DE COMPOSTELA

Docetaxel-loaded PEGylated-Polyglutamic Acid Nanocapsules for the Treatment of Metastatic Cancer

Este trabajo ha sido realizado en colaboración con Erea Borrajo[1], Anxo Vidal[1] y Marcos García[2].

[1] Cell Cycle and Oncology group CiClOn, IDIS, CIMUS. (USC). Santiago de Compostela, Spain.

[2] Nanobiofar Group, IDIS, CIMUS. (USC). Santiago de Compostela, Spain.

USC
UNIVERSIDADE
DE SANTIAGO
DE COMPOSTELA

ABSTRACT

The design of nanomedicines with high lymphotropic properties is of great interest in oncology given the frequent accumulation of metastatic cells in the lymph nodes. Recently, we reported the potential of polyaminoacid nanocapsules, to enhance the antitumor activity and reduce the toxicity of anti-cancer drugs. The objective of this work was to evaluate the lymphotargeting capacity of a new generation of 100 nm polyglutamic acid-polyethylene glycol (PGA-PEG) nanocapsules and to assess their value for the treatment of cancer with lymphatic metastatic spreading. For this purpose, we studied the biodistribution of fluorescently labeled PGA-PEG nanocapsules (100 nm), following, either intravenous or subcutaneous, administration. The results confirmed the accumulation of nanocapsules in the lymphatic system, especially upon subcutaneous administration. In a second stage, we evaluated the efficacy and toxicity of the nanocapsules loaded with docetaxel in an orthotopic lung cancer model that metastasizes to the lymph nodes. As expected from the rational design, DCX-loaded PGA-PEG nanocapsules exhibited a greatly enhanced antitumoral efficacy and a reduced toxicity when compared with the commercial formulation Taxotere®. Furthermore, DCX-loaded PGA-PEG nanocapsules resulted in an efficient treatment for the practical elimination of the metastatic load in the mediastinal lymph nodes, whereas the commercial formulation had a minor effect. These findings demonstrate that PGA-PEG nanocapsules, which are prepared thanks to the use of a simple and scalable nanotechnology, could be a new platform for the treatment of metastasic cancer.

USC
UNIVERSIDADE
DE SANTIAGO
DE COMPOSTELA

1 INTRODUCTION

According to predictions of World Health Organization, 15.2 million of new cancer cases and 8.8 million of deaths are expected in 2015 worldwide [1]. Lung cancer is the most common cancer and the leading cause of cancer deaths. Despite the advances in early detection techniques and significant improvement of surgical procedures, the survival rate for lung cancer is still low even at early stages of the disease [2]. From the clinical point of view, one of the major problems of lung cancer is that, at the moment of diagnosis, tumor has already disseminated to the lymph nodes, aggravating patient prognosis [3]. Because of the well-known role of the lymphatic system in tumor cell spreading [4], the selective delivery of anticancer drugs, not only to the tumor but also to the draining lymph nodes, has been conceived as a therapeutic strategy to control metastatic spreading and reduce systemic toxicity (Abellan-Pose R., submitted). In this regard, a number of reports have already shown the capacity of different nanocarriers, including micelles [5–8], nanoparticles [9–12] and nanocapsules [13] to improve the delivery of anticancer drugs to the draining lymph nodes. The results of these studies have underlined the enhanced therapeutic efficacy of the anticancer drug associated to the nanocarriers, as compared to the corresponding solutions of the free drug. In addition, the knowledge generated in this field has led to the conclusion that the particle size, the surface charge and the surface hydrophilicity may influence the lymphotropic behavior of the nanocarriers [14,15]. Namely, several studies have shown that nanocarriers of small particle size close to 100 nm [16], negative zeta potential [17] and a hydrophilic surface [16,18] can easily migrate through the interstice, reach the lymphatic vessels and accumulate into the lymph nodes following subcutaneous administration (SC). On the other hand, it has also been shown that, following intravenous administration (IV), nanocarriers of very small particle size (usually from 15 to 40 nm, larger in the presence of tumor) may have the possibility to extravasate from the bloodstream to the interstice and be drained by the lymphatic system [6,7,19,20].

Within this frame of knowledge, our group has developed nanocapsules, constituted by an oily core and a hydrophilic polymer shell, with the capacity to encapsulate drugs such as plitidepsine [21,22] or docetaxel (DCX) [23] and with a potential affinity for the

lymphatic system. Up until now, we have been able to show that following IV administration to mice, these nanocapsules led to a increased efficacy of the associated drugs, together with a reduction of their systemic toxicity, as compared to the corresponding reference formulations. This enhanced efficacy/toxicity balance was attributed to the capacity of the nanocapsules to modify the biodistribution of the encapsulated drugs.

With the intention to improve the lymphatic targeting capacity of PGA-PEG nanocapsules, we recently managed to reduce their particle size down to ~100 nm. In a preliminary *in vitro* screening in an A549 tumor cell/lymphocyte 3D co-culture that simulates a metastatic lymph node, we observed that these small nanocapsules had a preferable uptake by the cancer cells. Moreover, we have observed that following SC administration, these small 100 nm-nanocapsules are mobilized faster to the lymph nodes than the larger ones (200 nm). Based on this background experience, in the present work, our goal was to further investigate the biodistribution of these nanocapsules following administration by SC and IV routes and to validate their potential as a new oncological therapy by analyzing their antitumoral efficacy and toxicity in a metastasizing orthotopic lung cancer model.

2 MATERIALS AND METHODS

2.1 Chemicals

Miglyol®812 was donated by Sasol Germany GmbH (Germany). The surfactant Epikuron® 145V was donated by Cargill (Spain). Hexadecyltrimethylammonium bromide (CTAB) and docetaxel (DCX) were obtained from Sigma-Aldrich (Spain). Polyglutamic acid-polyethylene glycol (PGA-PEG; Mw 35 kDa), a diblock copolymer of poly-L-glutamic acid (Mw=15 kDa) and PEG (Mw=20 kDa), was supplied by Alamanda Polymers, Inc. (USA). The near infrared dye 1,1′-dioctadecyl-3,3,3′,3′-tetramethylindodicarbocyanine perchlorate (DiD) was purchased from Molecular Probes-Invitrogen (USA). Taxotere® was kindly provided by the Medical Oncology Department of the University Clinical Hospital of Santiago de Compostela.

2.2 Preparation and characterization of nanocapsules

Polyglutamic acid-polyethylene glycol (PGA-PEG) nanocapsules were prepared by a solvent-displacement technique as previously published (Abellán-Pose *et al.*, manuscript in preparation). Briefly, nanocapsules were prepared as follows: first, 7.5 mg of Epikuron® 145V were dissolved in 0.4 ml of ethanol. Next, 31.25 µl of Miglyol® 812 and 0.1 ml of a CTAB ethanol solution (15 mg/ml) were added and mixed by vortex. After adding 9.5 ml of acetone, this organic phase was dropped in aliquots of 250 µl every 15 seconds into 20 ml of an aqueous solution of PGA-PEG (0.25 mg/ml), under magnetic stirring. This induced the spontaneous formation of the nanocapsules. The organic solvents were removed and the formulation was concentrated to 10 ml by evaporation under vacuum (Buchi Labortechnik AG, Flawil, Switzerland). The nanocapsules were isolated by ultracentrifugation in Herolab® tubes (Herolab GmbH, Germany) at 84035 RCF for 1 hour at 15°C (Optima™ L-90K Ultracentrifuge, Beckmann Coulter; Fullerton, CA).

The size and polydispersity index of nanocapsules were analyzed by photon correlation spectroscopy (PCS) after appropriate dilution with ultrapure water. Each analysis was performed in triplicate at 25°C with an angle detection of 90°. The zeta potential was determined by laser Doppler anemometry (LDA) with the same sample. The PCS and LDA analysis were performed using a Zetasizer Nano ZS (Malvern Instruments, Malvern, UK).

2.3 Preparation and characterization of fluorescently-labeled nanocapsules

Nanocapsules were fluorescently labeled by incorporating DiD into the organic phase during the preparation from an ethanol stock solution of 2.5 mg/ml. Nanocapsules were prepared and isolated following the procedure used for blank nanocapsules.

DiD encapsulation efficiency was determined indirectly by the difference between the total amount of fluorescent probe in the formulation and the free dye quantified in the infranatant after nanocapsules isolation. DiD was quantified by UV spectrophotometry at λ=646 nm. For the *in vivo* administration, the DiD encapsulated in the nanocapsules

was also directly quantified by the same method, measuring the absorbance of an aliquot of isolated nanocapsules diluted 1:200 with acetonitrile.

2.4 Animals

Female severe combined immunodeficiency (SCID) mice weighing about 20-25 g and at the age of 8-12 weeks were used in the *in vivo* studies (Harlan Laboratories, Inc). The animals were acclimatized for at least 1 week before experimentation; they were housed in ventilated polypropylene cages at an average temperature of 22 ˚C, with exposure to 12 hours of light and 12 hours of darkness each day. All mice received a standard laboratory diet of food and water *ad libitum*. The experiments were carried out according to the Rules of the Santiago de Compostela University Bioethics Committee and in compliance with the Principles of Laboratory Animal Care according to Spanish national law (RD 53/2013).

2.5 Biodistribution studies

Female SCID mice were injected IV in the tail vein or SC in the interscapular region with a suspension of 100 µl of DiD-labeled nanocapsules (nanocapsules concentration= 13 mg/ml, DiD concentration= 87 µg/ml). Biodistribution of the nanocapsules was assessed by an In Vivo Imaging System (IVIS, Living Image® System, Caliper Life Sciences, Hopkinton, MA).

For non-invasive tests, mice were anesthetized with 4% isoflurane inhalation. Once laid in the acquisition chamber, the anesthesia was maintained with a 2% air-isofluran mixture during the *in vivo* acquisition. To compare the nanocapsules distribution on a semi-quantitative basis, mice were sacrificed at different time points (6, 24 and 48 hours) after the administration, and the excised tissues, which included liver, lungs, spleen, kidneys, as well as axillary, cervical, inguinal, mediastinal and mesenteric lymph nodes, were compared with organs from non-injected animal as negative controls. Semi-quantitative data of the biodistribution were obtained from the fluorescence images by drawing regions of interest and using identical illumination settings. Organ fluorescence was quantified through mean radiance values.

2.6 Preparation of docetaxel-loaded nanocapsules

PGA-PEG nanocapsules loaded with DCX (DCX nanocapsules) were prepared following a method previously described (Abellán-Pose *et al*., manuscript in preparation). Thereby, 75 µl of a DCX stock ethanol solution (20 mg/ml) were added over 7.5 mg of Epikuron® 145V dissolved in 0.325 ml of ethanol. After mixing, 31.25 µl of Miglyol® 812, 0.1 ml of an ethanol solution of CTAB (15 mg/ml) and 9.5 ml of acetone were also incorporated. This organic phase was added dropwise (250 µl every 15 seconds) to 20 ml of a PGA-PEG aqueous solution (0.25 mg/ml) under magnetic stirring, leading to the immediate formation of nanocapsules. Solvents of the resulting suspension were evaporated under vacuum (Buchi Labortechnik AG, Flawil, Switzerland) to a final volume of 4 ml. Lastly, nanocapsules were purified and concentrated by ultracentrifugation in Herolab® tubes (Herolab GmbH, Germany) at 84035 RCF for 1 hour at 15°C (Optima™ L-90K Ultracentrifuge, Beckmann Coulter; Fullerton, CA) and centrifugation in Amicon® Ultra-4 ML 10K centrifugal filter devices (Merck Millipore, Germany) at 7500 RCF, 20°C.

DCX encapsulation efficiency was determined by a direct method, measuring the drug in the concentrated isolated nanocapsules. To quantify the DCX, an aliquot was diluted with acetonitrile 1:1200, centrifuged for 20 minutes at 4000 RCF and analyzed by high performance liquid chromatography (HPLC). DCX was quantified by a slightly modified version of the method described by Lee *et al.* [24]. The HPLC system consisted of an Agilent 1100 Series Instrument equipped with a UV detector set at 227 nm and a reverse phase Zorbax Eclipse XDB-C8 column (4.6 x 150 mm id., pore size 5 µm Agilent USA). The mobile phase was a mixture of 0.1% v/v ortophosphoric acid and acetonitrile (55:45 v/v) and the flow rate was 1 ml/minute. The standard calibration curves of DCX were linear in the range of 0.2-2 µg/ml ($r^2 = 0.999$).

2.7 *In vivo* toxicity studies

The toxicity of DCX nanocapsules was compared with that of the commercial formulation Taxotere® after IV administration of two different doses, 30 and 60 mg/kg, for 5 consecutive days (5 and 10 mg/day, respectively) in SCID non tumor-bearing mice. Animals were weighed daily during the study (15 days) and those showing signs

of extreme weakness were sacrificed. The toxicity was quantified for all groups by comparing the maximum tolerated dose (MTD) defined as the maximum DCX dose resulting in less than 20% body weight loss and no lethality.

2.8 Orthotopic lung cancer model

The antitumor efficacy of DCX nanocapsules was assessed in an orthotopic lung cancer model that metastasizes to the mediastinal lymph nodes, as adapted from Cui *et al*. [25]. Briefly, to generate this model, a suspension of $1x10^6$ luciferase expressing non-small cell lung carcinoma cells (A549Luc cell line) in PBS (50 µl) was injected through the intercostal space into the left lung of SCID mice (8-10 weeks old, 20-25 g). During this procedure mice were anesthetized by 4% isoflurane inhalation. To follow tumor growth, luciferin was injected at different time points into the intraperitoneal cavity at a dose of 150 mg/kg body weight, approximately 5 minutes before imaging. Luciferase bioluminescence was imaged under vaporized isoflurane anesthesia using an IVIS® Spectrum System that allowed monitoring both the primary tumor growth and the cancer cell dissemination in a quantitative fashion. The presence of tumor cells in the lungs was confirmed by histological analysis with a haematoxylin-eosin staining.

At the end of the *in vivo* experiment or at appropriate humane endpoints, mice were sacrificed and proteins were extracted from different organs to quantify luciferase activity. Organs were homogenized in DIP buffer (50 mM pH 7.5, 150 mM NaCl, 1 mM EDTA, 2.5 mM EGTA, 0.1 % Tween-20, 10 mM β-Glycerophosphate, 1 mM sodium orthovanadate, 0.1 M PMSF, 0.1 M NaF and protease inhibitor cocktail) using a tissue homogenizer. After centrifugation at 15000 RCF for 15 minutes, supernatants were quantified by a Bradford colorimetric method and luminescence was measured using a Lumat BL 9507 luminometer (Berthold Technologies). Results were expressed as relative luminescence units (RLU) per µg of extracted protein.

2.9 *In vivo* antitumor efficacy study

The efficacy studies were carried out using DCX nanocapsules and Taxotere® as control. Mice were randomly assigned to experimental and control groups (n=6). The study was performed twice with two different experimental designs. First, we confirmed the capacity of the treatments to block tumor development. Four groups of tumor-

bearing SCID mice were defined: i) control mice without treatment, ii) mice treated with control blank PGA-PEG nanocapsules, iii) mice treated with Taxotere® (20 mg/kg of DCX) and iv) mice treated with DCX nanocapsules (20 mg/kg of DCX). The different formulations were administered IV by two injections of a dose of 10 mg/Kg of DCX each at 5 and 20 days after tumor cell implantation. The concentration of nanocapsules administered was ≈120 mg/ml per injection. Tumor evolution was followed non-invasively by an IVIS® Spectrum System. At the end time point (37 days) the animals were sacrificed and the protein from lungs and mediastinal nodes was extracted for luciferase activity quantification as described above.

In a second experimental design, the efficacy of DCX nanocapsules and Taxotere® was compared in an advanced tumor stage with metastasis. Five groups of tumor-bearing SCID mice were defined (named with the total dose of DCX), with different treatments: i) control mice without treatment, ii) mice injected with Taxotere® (10 mg/kg), iii) mice injected with Taxotere® (20 mg/kg), iv) mice injected with DCX nanocapsules (10 mg/kg) and v) mice injected with DCX nanocapsules (20 mg/kg). The treatments were administered IV by two injections at 20 and 27 days after tumor cell implantation. For the group iv) and v) the concentration of nanocapsules administered were ≈ 90 mg/ml and 120 mg/ml per injection, respectively. Body weight was measured weekly, the animals were monitored daily for clinical signs of stress for the duration of the studies, and tumor evolution was followed by an IVIS® Spectrum System. According to the health conditions of the animals receiving treatment or not, two different end time points were defined, 37 and 47 days after tumor cell injection. At these time points, surviving animals were sacrificed for measuring luciferase activity in protein extracts from lungs and mediastinal nodes.

2.10 Statistical analysis

A Mann-Whitney Test was applied to examine differences in biodistribution and efficacy studies associated with DCX nanocapsules treatments versus Taxotere®. The mean ± SEM was determined for each treatment group. The differences were considered significant for $*p < 0.05$, and very significant for $*p < 0.01$. All of the statistical analysis was carried out with GraphPad Prism Version 5.0 software.

3 RESULTS

3.1 Preparation and characterization of nanocapsules

PGA-PEG nanocapsules were prepared by a modification of the solvent displacement technique recently reported by our group (Abellán-Pose *et al*., manuscript in preparation). The incorporation of DiD or DCX in the PGA-PEG nanocapsules barely modified their physicochemical characteristics (**Table 1**).

Table 1. Physicochemical characteristics of blank, DiD-loaded and DCX-loaded PGA-PEG nanocapsules. PdI: polydispersity index. Data represents mean ± SEM; n=3.

Final loading (%)	Size (nm)	PdI	ζ Potential (mV)
-	116 ± 5	0.1	-29 ± 5
0.04	99 ± 4	0.2	-35 ± 4
1.3	122 ± 2	0.1	-34 ± 5

3.2 Biodistribution by fluorescence imaging

To study the ability of PGA-PEG nanocapsules to reach the lymphatic system their biodistribution was assessed by whole body non-invasive fluorescence imaging in a semiquantitative fashion [26]. These nanocapsules were fluorescently labelled with the near-IR dye DiD. This dye has the advantages of being weakly fluorescent in water but highly fluorescent at lipid/water interfaces. It is also photostable, and has high tissue penetration and low interference with the autofluorescence of animal tissues [27]. The encapsulation of DiD into the nanocapsules did not affect their size and zeta potential significantly. SC administration is often used for the delivery of drugs and diagnostic agents to the lymphatic system as it provides a series of advantages such as slow elimination rate, prolonged release and increased absorption [28]. In our previous biodistribution study (Abellán-Pose *et al*, manuscript in preparation), we observed high

and persistent accumulation of fluorescence at the injection site after SC administration, consistent with previous observations by others for liposomes [28]. Since the final goal of PGA-PEG nanocapsules is to administer DCX, which might produce local damage in the form of a SC depot, we decided to test IV administration as an alternative route. Therefore, herein we compared the biodistribution of PGA-PEG nanocapsules after IV and SC injection, paying particular attention to the fluorescence accumulated in lymph nodes. When PGA-PEG nanocapsules were injected IV we observed a high accumulation in the main MPS organs (liver, heart, lung, kidney and spleen) at all-time points (Figure 1). At 6 and 24 hours after administration, accumulation in these organs was significantly higher in the IV groups than in the SC group. Although at 48 hours, significant differences were only found in liver and spleen. On the other hand, the access of the nanocapsules to the lymphatic system (mesenteric, inguinal and mediastinal nodes) was more significant following IV administration than SC administration (**Figure 1A, 1B**). However the concentration of fluorescent nanocapsules observed at 48 hours post-administration were very similar irrespective of the modality of administration (**Figure 1C**). This biodistribution profile indicates a faster nanocapsule distribution to MPS organs and lymph nodes after IV administration as compared to SC administration. Based on these results, this route was selected for the subsequent *in vivo* studies.

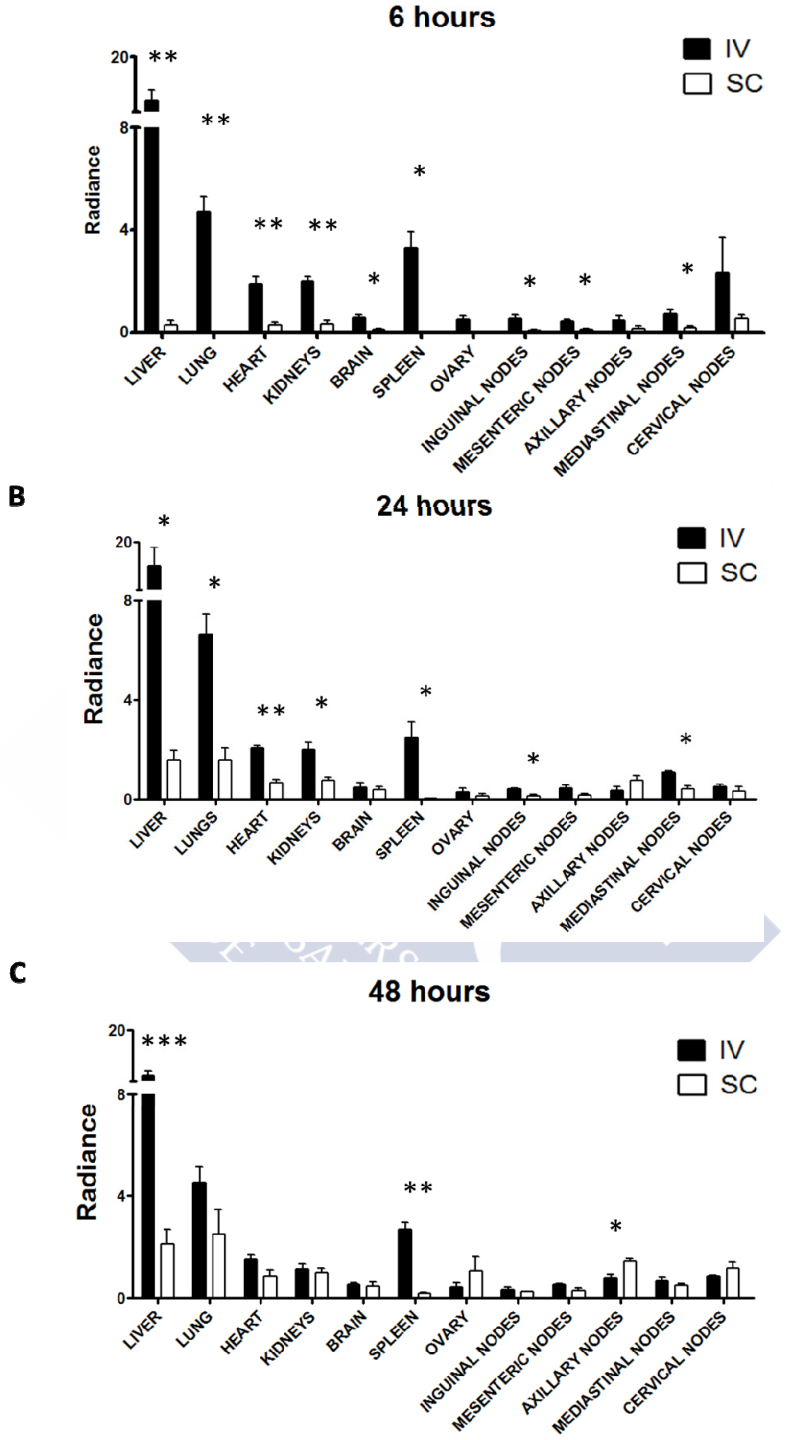

Figure 1. Comparative biodistribution of DiD-loaded PGA-PEG nanocapsules injected IV and SC. Radiance (Photons/sec/cm^2/sr x 10^7) in excised organs at (A) 6, (B) 24 and (C) 48 hours after injection. Data represents mean ± SEM; n=4. Mann Whitney test ((*) $p < 0.05$, (**) $p < 0.01$). Mann Whitney test ((*) $p < 0.05$, (**) $p < 0.01$), (***) $p < 0.001$).

3.3 Toxicological evaluation

We have recently reported the development and optimization of DCX nanocapsules (Abellán-Pose *et al*, manuscript in preparation). According to our previous data, DCX nanocapsules can be loaded with this antitumoral drug with a 0.04% (w/w) final loading with respect to the total amount of compounds. In the present work, for the *in vivo* experiments we also developed the same nanocarriers with a higher loading (1.3% w/w). This increased DCX loading did not lead to major changes in particle size, PdI or zeta potential of the nanocapsules, as compared to the blank nanocarriers (**Table 1**).

The systemic toxicity associated to DCX nanocapsules and the reference commercial formulation Taxotere® was evaluated in non-tumor bearing SCID mice by IV administration. The range of the maximum tolerated dose (MTD) reported in the literature for DCX in its commercial formulation Taxotere® varies within the range from 15 to 40 mg/kg in inmunodeficient mice with heterotopic xenograft. In our experiment, both treatments were administered for 5 consecutive days to achieve total doses of 30 or 60 mg/kg. Body weight for mice treated with 30 mg/kg of Taxotere® or with any dose of DCX nanocapsules barely changed during the whole study that was prolonged up to 10 days after the last administration. Regarding the highest concentrations, at the end of the study, mice treated with 60 mg/kg of DCX nanocapsules lost less than 5% of their body weight and no remarkable effects of toxicity were evidenced during the experiment. On the contrary, mice treated with Taxotere® at the same dose (60 mg/kg) suffered 27.2% loss of body weight (**Figure 2**), showing bad physical conditions with signs of piloerection, tremor and weakness. All these were indications of toxicity, although no mortality was observed. These results indicated that DCX formulated in PGA-PEG nanocapsules present reduced signs of toxicity as compared to the commercial preparation.

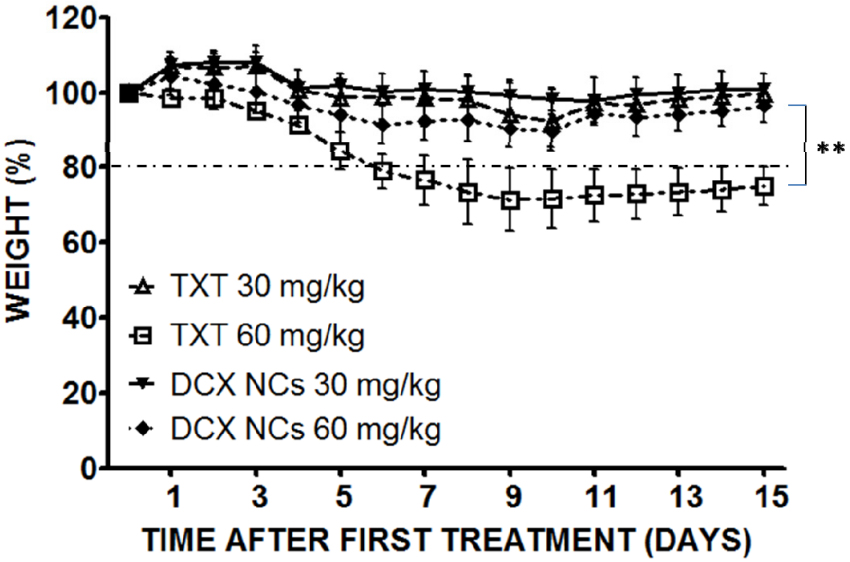

Figure 2. Effect of Taxotere and DCX-loaded PGA-PEG nanocapsules (DCX nanocapsules) on mice body weight over 15 days after the first administration. The formulations tested were: Taxotere and DCX loaded PGA-PEG nanocapsules. The tested doses were 30 and 60 mg/kg for Taxotere (TXT 30 and TXT 60, respectively) and DCX nanocapsules (NCs 30 and NCs 60, respectively). Data represents mean ± SEM.; n=3. Mann Whitney test ((**) $p < 0.01$).

3.4 *In vivo* antitumor efficacy

This study was aimed at evaluating the capacity of DCX nanocapsules to inhibit tumor growth and, more importantly, to prevent cancer cell spreading from the primary tumor. For this purpose, an A549luc orthotopic lung cancer model with characteristic tumor spreading to the mediastinal lymph nodes was used. In this model, metastasis in the lymph nodes could be unequivocally detected 13 days after the injection of tumor cells (Supplemental. material., Figure 1).

To test the antitumoral activity of the DCX nanocapsules, the effect of this formulation and appropriate controls was evaluated both, in the primary tumor and in the lymph nodes, following IV administration. In all experiments, untreated mice were used as negative controls and Taxotere® as positive control. After the orthotopically implantation of A549luc cells, tumor-bearing animals were treated 5 and 20 days later with 20 mg/kg of DCX either as the commercial Taxotere® formulation or as DCX

nanocapsules. The tumor growth was monitored *in vivo* by measuring the bioluminescence of the tumor cells in the lung using the IVIS® Spectrum System. The results showed that, in the case of untreated animals tumor size increased exponentially until the end of the experiment. Similarly, in the case of mice treated with blank nanocapsules tumor growth was comparable to that of the control group. In contrast, both groups of mice receiving DCX (Taxotere® and DCX nanocapsules) showed no tumor growth during the experiment (**Figure 3A-B**).

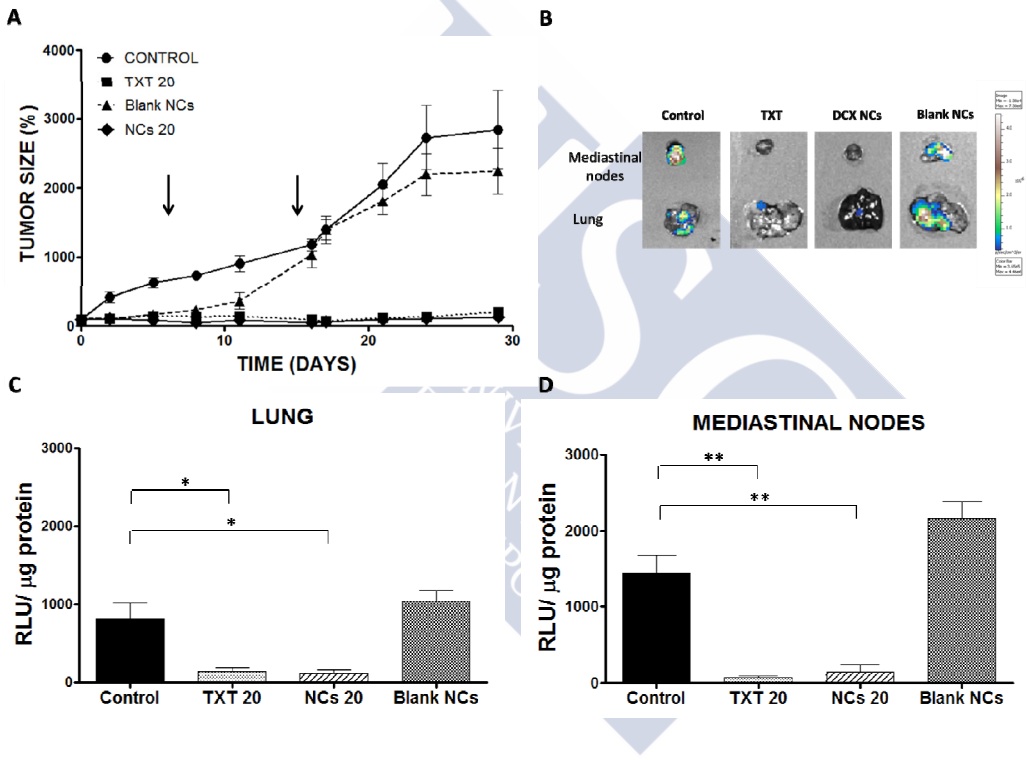

Figure 3. (A) Tumor growth in mice treated with different DCX formulations and controls, measured by in vivo luminescence. Arrows represent DCX administration time points in the study. (B) Images showing tumor cell loading in lung and mediastinal nodes as measured by ex-vivo bioluminescence images with an IVIS® Spectrum. (C) Quantification of luciferase activity (average RLU per µg of protein measured for luciferase activity) measured ex vivo (C) in lung and (D) in mediastinal lymph nodes. Experimental groups were: Taxotere® (TXT 20) and DCX nanocapsules (NCs 20) at 20 mg/kg DCX dose, blank nanocapsules (Blank NCs) and no treatment (Control). Data represents mean ± SEM; n=5. Mann Whitney test ((*) $p < 0.05$, (**) $p < 0.01$) relative to control group.

The comparable antitumoral effect of Taxotere® and DCX nanocapsules was confirmed when animals were sacrificed and luciferase activity determined. Lungs from the untreated or blank nanocapsule-treated groups showed high tumor burden, whereas mice treated with Taxotere® or DCX nanocapsules showed a strong reduction in tumor load (**Figure 3C**).

Interestingly, luciferase activity in mediastinal nodes from the four experimental groups was correlated to that of the primary tumor (**Figure 3D**). All these results suggested that DCX nanocapsules are as effective as Taxotere® in controlling both primary tumor growth and lymphatic metastasis when the treatment is applied at an early stage of tumor development. The reduced number of cancer cells found in the lymph nodes in DCX-treated animals could be either due to a direct effect on the metastasis or to a secondary effect of the size reduction in the primary tumor that would also decrease cell spreading.

To address this issue, the formulations were also tested at a more advanced tumor stage, when lymph node metastasis was already evident. Mice were treated with Taxotere® or DCX nanocapsules 20 and 27 days after the injection of cancer cells. Two doses of DCX were evaluated in this experiment, 10 and 20 mg/kg. Two endpoints were also defined: animals were sacrificed at 37 or 47 days after tumor cell injection according to the different health conditions observed for the different groups. At day 37, untreated animals (control) had to be sacrificed because of their high tumor burden. At this point, Taxotere® and DCX nanocapsules treatments showed a similar effect reducing tumor growth (**Figure 4A**). For these latter treatments, tumor growth was monitored until 47 days. The groups treated with the Taxotere® 10 mg/kg formulation started showing an exponential tumor growth, while for the rest of the experimental groups an inhibitory effect on the tumor growth was noted. The Kaplan-Meier survival plot illustrates the capacity of all DCX formulations to control tumor growth except for Taxotere® 10 mg/kg (**Figure 4B**).

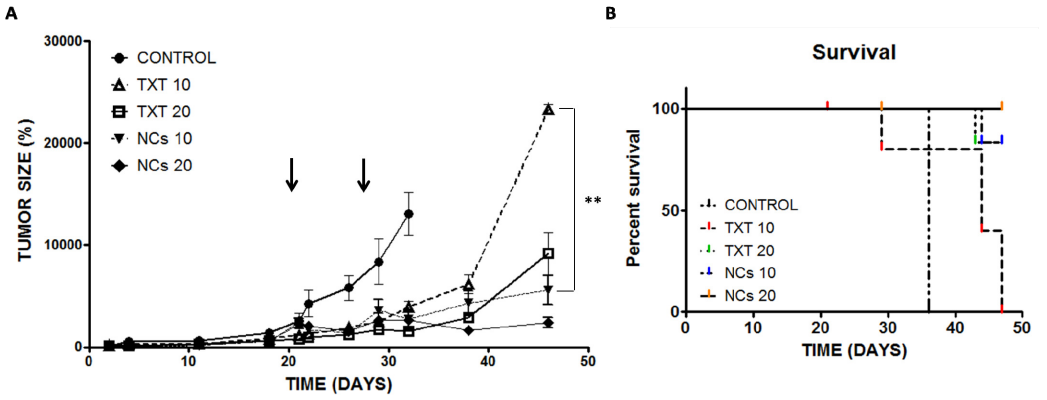

Figure 4. (A) Tumor growth in mice treated with different DCX formulations and doses as measured using a bioluminescence imaging system in vivo IVIS® Spectrum. Arrows represent the administration time points for the experiment. Data represents mean ± SEM; n=6. (B) Kaplan-Meier survival plots. The formulations tested were: Taxotere® and DCX loaded PGA-PEG nanocapsules (DCX nanocapsules). The DCX doses tested were 10 and 20 mg/kg. Survival analysis by Log-rank (Mantel Cox) Test: Taxotere® 10 mg/kg (TXT 10) vs DCX nanocapsules (NCs 10) 10 mg/kg, p= 0.0096, Significative (**); Taxotere® 20 mg/kg (TXT 20) vs NC DCX 20 mg/kg (NCs 20), p= 0.3613, non-significative.

For a more detailed quantitative analysis on the tumor and the lymph nodes, luciferase activity was measured in organs from sacrificed mice to measure cancer cell load. At 37 days, all DCX formulations with 20 mg/kg dose achieved a significant reduction in tumor burden compared to controls (**Figure 5A**). Similar results were found when the mediastinal lymph nodes were analyzed (**Figure 5B**). At 47 days, cancer cell loads in the lungs and in the mediastinal nodes were significantly lower for mice treated with DCX nanocapsules as compared to Taxotere®, and this was observed for the two doses of DCX (**Figure 5 A, B**).

When we compared luciferase activity values in the mediastinal nodes of the treated groups with those before treatment (day 19 after the injection of the tumor cells), we observed that DCX treatments were able to maintain metastatic loads at 37 days. At 47 days, the number of cancer cells found in the nodes was increased in all experimental groups except for DCX nanocapsules at 20 mg/kg. Interestingly, in this group, the metastatic cell load was significantly lower than that found before treatment (Figure

5C). These results show that DCX nanocapsules have a higher and a more prolonged effect on lymphatic metastasis than Taxotere®.

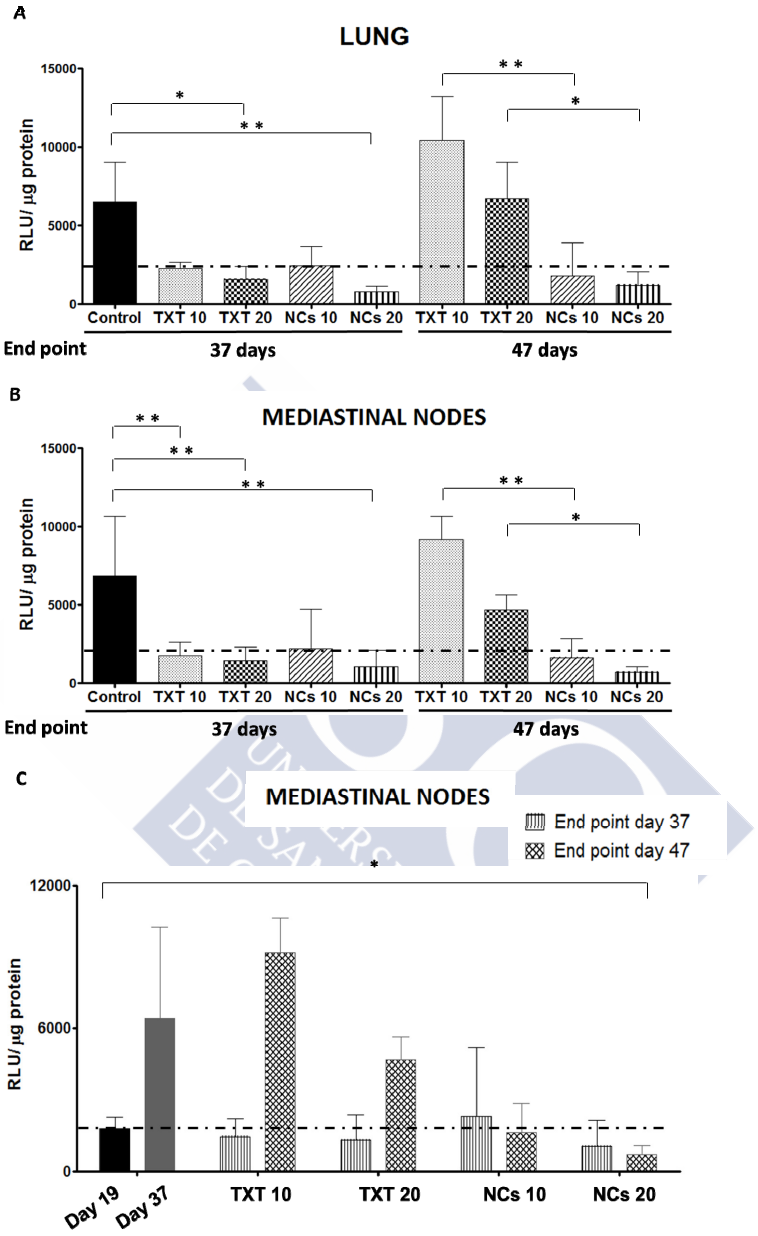

Figure 5. Luciferase activity (average RLU per µg of protein measured for luciferase activity) quantified ex-vivo (A) in the lungs and in (B) mediastinal lymph nodes, 37 and 47 days after the injection of the tumor cells. (C) Comparative graphical representation of the *ex-vivo* luciferase activity quantified in mediastinal lymph nodes before the treatment (T0, day 19) versus the end time at 37 and 47 days after the injection of the tumor cells. Dotted line represents the tumor cell loading before treatments (day 19). Mice were treated with Taxotere® 10 and 20 mg/kg total dose (TXT 10 and TXT 20, respectively) and PGA-PEG nanocapsules at 10 and 20 mg/kg DCX total dose (NCs 10 and NCs 20, respectively). Non treated animals were used as control. Data represents mean ± SEM; n=5. Mann Whitney test ((*) $p < 0.05$, (**) $p < 0.01$)).

4 DISCUSSION

The poor prognosis of most cancer types and, thus, the necessity to fight against the metastatic spread is the driving force in the design of new oncological therapies. The drug delivery field can greatly contribute to this end through the design of drug nanocarriers with lymphotropic properties. In previous reports we have shown the potential of polymer nanocapsules as carriers for the delivery of anticancer drugs [21–23,29–34]. Among them, we have found that those provided with a PGA-PEG shell exhibited a comparable antitumor activity and lower toxicity than the commercial formulation Taxotere® [23]. Subsequently, and based on previous work that underlined the importance of a small size for enhancing the delivery of nanocarriers to the lymph nodes [16,28], we have optimized the PGA-PEG nanocapsules preparation technique in order to reduce their size down to ~100 nm (Abellán-Pose *et al*., manuscript in preparation). As expected, this reduction of size facilitated their migration through the interstitial channels and, thus, their lymphatic drainage following SC administration. However, although this route of administration is traditionally the most explored for the lymphatic targeting of drugs or diagnostic agents, it may present certain limitations for the lymphatic targeting of anticancer drugs such as local toxicity (Abellan-Pose R., submitted). For this reason, in the current work we have comparatively analyzed the lymphatic access of PGA-PEG nanocapsules upon IV and SC administration. The results indicated that following IV administration, fluorescent PGA-PEG nanocapsules accumulate in the MPS organs (liver, lung, spleen) although a significant fluorescent signal was also observed in the lymph nodes. Interestingly, these high fluorescence levels, which are comparable to those reached after SC administration (Figure 1), are in line with those recently reported for lipid nanocapsules [20]. Moreover, as previously observed by other authors, the lymphatic drainage following SC injection in the interescapular region is less effective than in other places (e.g. as the flank or the footpad), where the organization of the subcutaneous tissue promotes the increase of the interstitial fluid pressure and thus the lymphatic drainage [20,35]. Therefore, the administration in this anatomical site may not be the most appropriate from the point of view of lymphatic targeting. The biodistribution studies also evidenced the formation of a long-lasting local depot following SC administration of the nanocapsules, a fact that would discourage the use of this administration route for the administration of DCX-

loaded nanocapsules [36]. Overall, the observed lymphotropic behavior of the nanocapsules upon IV administration led us to assess their performance for the treatment of cancers associated to metastatic spreading in the lymph nodes. In this regard, we have presumed that the enhanced permeability of the tumor-associated blood vessels could further promote the extravasation of nanocarriers to the tumor interstice and their subsequent drainage by the peritumoral lymphatic vessels [15].

With regard to the selection of the cytotoxic drug DCX, and taxanes in general, the inherent toxicity of the marketed formulation has inspired the development of nanotechnology-based targeting strategies (Abellan-Pose R., submitted). Indeed, four formulations have been approved for the administration of paclitaxel (PTX) (Abraxane®, Genexol-PM, Nanoxel-PM and Lipusu) [37] and many others have reached the clinical evaluation due to their efficacy and safety toxicological profile, such as NK-105 [38] and Opaxio [39] or BIND-014 [40] for the administration of PTX and DCX, respectively.

Our results show that the administration of DCX encapsulated in PGA-PEG nanocapsules over five consecutive days with a total accumulated dose of 60 mg/kg does not trigger toxic effects. Indeed, the MTD for DCX nanocapsules was not achieved even when administered at doses that were higher than those commonly used with therapeutics purposes in mice. On the contrary, with the same dosing and schedule, the commercial formulation Taxotere® showed significant toxicity (Figure 2). This improved toxicological profile of the encapsulated drug agrees with the one previously reported by our group for the anticancer drug plitidepsin [21]. In this previous study we could show a 3-fold increase in the single dose MTD of plitidepsin encapsulated in PGA-PEG nanocapsules compared to the standard formulation (i.e. ethanol/Cremophor EL/water vehicle). The reduced toxicity of the DCX nanocapsules as compared to Taxotere® could be attributed to the improved drug distribution within the organism. In addition, the toxicity of the marketed drug has also been attributed to the high concentration of Tween® 80 present in the formulation [41]. These results are also in line with other works reporting the low toxicity of lipid nanocapsules [42] and nanoparticles [43–47] for the administration of taxanes.

Many drugs delivery systems based on nanotechnology with lymphotropic properties have been developed in the last years to fight cancer; however, there are few reports for *in vivo* therapeutic efficacy specifically against lymphatic metastasis. Among them, it is worth mentioning different micelles based on phosphatidylethanolamine, PGA-PEG or poly(lactide)-PEG, and polymeric or lipid-based nanoparticles that have reported an enhanced antitumor efficacy on the metastatic lymph nodes associated to a significant lymphatic delivery achieved by IV or SC administration [5–8,10–12]. However, in some cases it is not clarified if the increased anti-metastatic effect is due to the direct effect on the lymph nodes-resident cancer cells or, secondary, to a size reduction of the primary tumor that decreases the cancer spreading.

To evaluate the anti-metastatic effect we have adapted an orthotopic lung metastasic model, which reproduces tumor environment and cancer dissemination pathways in a more realistic way than the classically used heterotopic subcutaneous implanted cancer models. The results of this *in vivo* efficacy study indicated that DCX nanocapsules administered IV can inhibit both, tumor growth and lymphatic metastasis, as efficiently as Taxotere® when applying the treatments before the spreading of cancer cells to the mediastinal lymph nodes (Figure 3). The small number of cancer cells found in the lymphatic nodes after treatment could be an indirect consequence of the effect achieved over the primary tumor, which loses the capacity to initiate cell spreading, although it could also be due to a combined effect of the DCX formulations both in the primary tumor and the lymph nodes. To test these hypotheses, we performed a second *in vivo* experiment, in which treatments started after the consolidation of lymphatic metastasis in the mediastinal nodes (twenty days after inoculation with A549luc cells in the lung). The results of this experiment led us to the conclusion that DCX nanocapsules (20 mg/kg) were active both, in the primary tumor and in the mediastinal nodes, whereas the commercial formulation was not (Figure 4 and 5). The explanation of a cytotoxic direct effect on the lymphatic nodes is consistent with the results of the biodistribution of the nanocapsules.

The results of the studies presented here indicate that PGA-PEG nanocapsules were able to significantly decrease the tumor cell burden in the lungs (Figure 4 and 5) and the metastatic burden in the lymph nodes at day 47. The increase of the antitumoral activity at late time points, previously reported for other nanocapsules, could indicate that these

nanosystems needed more time to exert an effective antitumor effect, but once initiated, the effect lasted for longer periods of time [31]. Furthermore, our cancer model allowed us to observe that the nanocapsules were the only treatment capable of significantly reducing lymphatic metastases (Figure 5) and substantially improve the survival rate (Figure 4B). The enhanced antitumor efficacy of the nanocapsules could be attributed to higher accumulation in the tumor and draining lymph nodes and to certain controlled release of the drug from the nanoparticle system. Another mechanism that could be implicated in the nanocapsules superiority over Taxotere® could be their preferential internalization in cancer cells. Indeed, our previous *in vitr*o studies performed in a 3D co-culture of A549 and T Jurkat lymphocytes showed that PGA-PEG nanocapsules interact preferentially with the cancer cells. This capacity to act on cancer cells may constitute an important advantage against other lymphotropic nanocarriers which, despite their significant uptake by the lymph nodes, have shown a limited anti-metastatic efficacy due to their inability to interact with cancer cells within the lymph node and release efficiently the antitumor drug [19].

In conclusion, our results show that the association of DCX to small (100 nm) PGA-PEG nanocapsules led to a reduction of systemic toxicity and an improvement of the efficacy in terms of tumor burden and metastatic spread and these positive effects could be related to their ability to reach the lymph nodes and deliver the antitumor drug to the lymph-node resident cancer cells. Therefore, we propose that the use of small PGA-PEG nanocapsules may represent a promising approach for the treatment of metastatic lung cancer.

Supplemental material

Table 1. Physicochemical characteristics of blank and DiD-loaded PGA-PEG nanocapsules of 100 nm and 200 nm. PdI: polydispersity index; E.E.: encapsulation efficiency. Data represents mean ± SD; n=3.

Nanocapsules	Size (nm)	PdI	ζ Potential (mV)	E.E. (%)
Blank-100	116 ± 5	0.1	-29 ± 5	-
DiD-100	107 ± 9	0.1	-36 ± 4	56 ± 3
Blank-200	200 ± 8	0.1	-25 ± 4	-
DiD-200	203 ± 11	0.1	-30 ± 2	90 ± 2

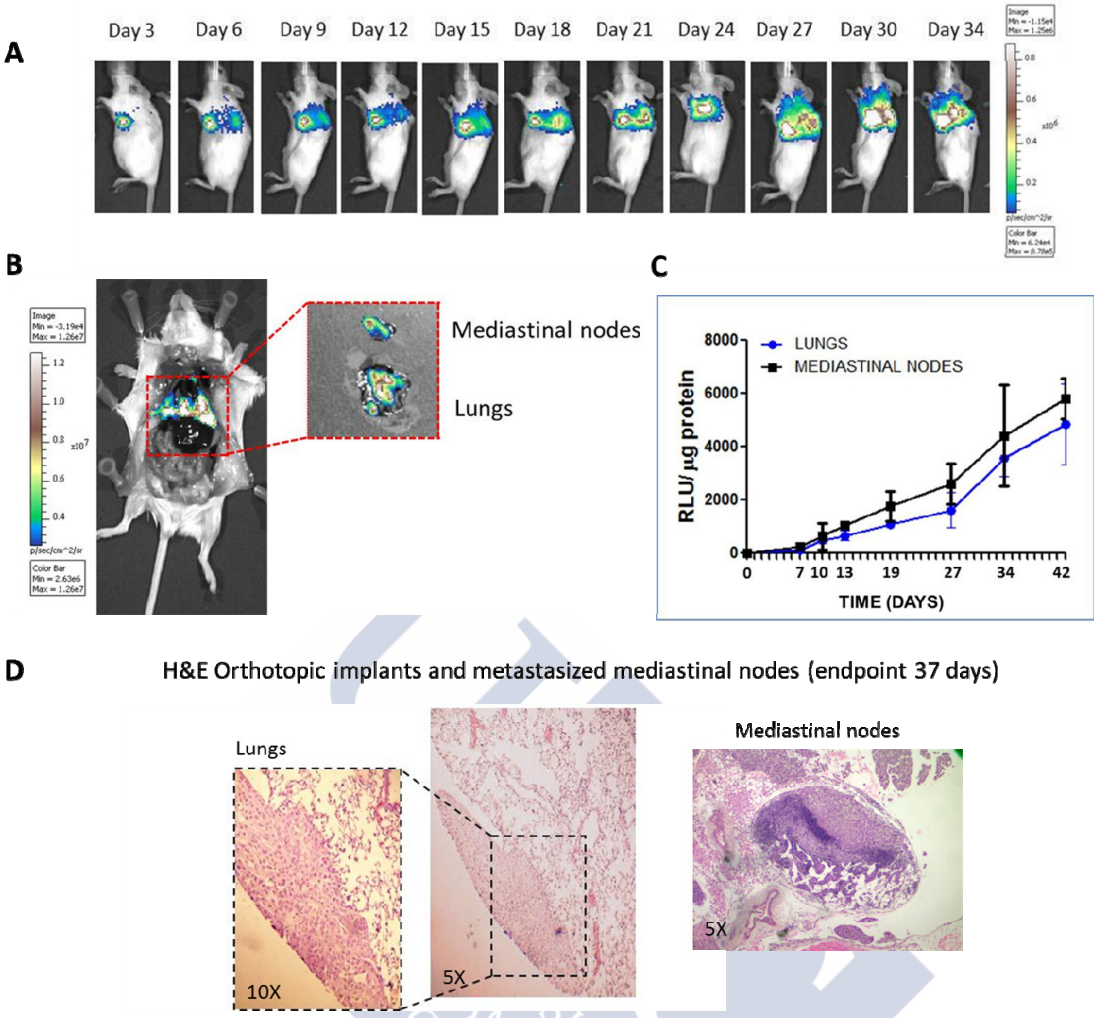

Figure 1. Tumor progression of A549Luc cancer cells growing orthotopically in SCID mice. (A) IVIS® Spectrum images of tumor development in inmunodeficient SCID mice control. (B) IVIS® Spectrum image of lung tumor and metastases in mediastinal lymph at final time of tumor development. (C) Graphical representation of luminescence units per µg of protein of the organs lung and mediastinal lymph nodes at days 7, 10, 13, 19, 27, 34 and 42 after the injection of the tumor cells. Data represents mean ± SD. Error bars represent standard deviation; n=4.(D) Histological sections of lung tumor and metastasized lymph node stained with haematoxylin and eosin at 37 days after the injection of the tumoral cells in lungs.

REFERENCES

[1] Ferlay J, Soerjomataram I, Ervik M, Dikshit R, Eser S, Mathers C, et al. GLOBOCAN 2012 v1.0, Cancer Incidence and Mortality Worldwide [Internet]. IARC CancerBase No. 11 [Internet]. Lyon, Fr. Int. Agency Res. Cancer2013 [cited 2014 Oct 3];Available from: http://globocan.iarc.fr

[2] Siegel RL, Miller KD, Jemal A. Cancer Statistics, 2015. CA. Cancer J. Clin. 2015;65:5–29.

[3] Schroeder A, Heller DA, Winslow MM, Dahlman JE, Pratt GW, Langer R, et al. Treating metastatic cancer with nanotechnology. Nat. Rev. Cancer 2012;12:39–50.

[4] Stacker SA, Achen MG, Jussila L, Baldwin ME, Alitalo K. Lymphangiogenesis and cancer metastasis. Nat. Rev. Cancer 2002;2:573–83.

[5] Rafi M, Cabral H, Kano MR, Mi P, Iwata C, Yashiro M, et al. Polymeric micelles incorporating (1,2-diaminocyclohexane)platinum (II) suppress the growth of orthotopic scirrhous gastric tumors and their lymph node metastasis. J. Control. Release 2012;159:189–96.

[6] Qin L, Zhang F, Lu X, Wei X, Wang J, Fang X, et al. Polymeric micelles for enhanced lymphatic drug delivery to treat metastatic tumors. J. Control. Release 2013;171:133–42.

[7] Cabral H, Makino J, Matsumoto Y, Mi P, Wu H, Nomoto T, et al. Systemic Targeting of Lymph Node Metastasis through the Blood Vascular System by Using Size-Controlled Nanocarriers. ACS Nano 2015;9:4957–67.

[8] Li Y, Jin M, Shao S, Huang W, Yang F, Chen W, et al. Small-sized polymeric micelles incorporating docetaxel suppress distant metastases in the clinically-relevant 4T1 mouse breast cancer model. BMC Cancer 2014;14:329.

[9] Estella-Hermoso de Mendoza A, Campanero MA, Lana H, Villa-Pulgarin JA, de la Iglesia-Vicente J, Mollinedo F, et al. Complete inhibition of extranodal dissemination of lymphoma by edelfosine-loaded lipid nanoparticles. Nanomedicine (Lond). 2012;7:679–90.

[10] Liu R, Gilmore DM, Zubris KA V, Xu X, Catalano PJ, Padera RF, et al. Prevention of nodal metastases in breast cancer following the lymphatic migration of paclitaxel-loaded expansile nanoparticles. Biomaterials 2013;34:1810–9.

[11] Tan R, Niu M, Zhao J, Liu Y, Feng N. Preparation of vincristine sulfate-loaded poly (butylcyanoacrylate) nanoparticles modified with pluronic F127 and evaluation of their lymphatic tissue targeting. J. Drug Target. 2014;22:509–17.

[12] Lu B, Xiong S-B, Yang H, Yin X-D, Chao R-B. Solid lipid nanoparticles of mitoxantrone for local injection against breast cancer and its lymph node metastases. Eur. J. Pharm. Sci. 2006;28:86–95.

[13] Wauthoz N, Bastiat G, Moysan E, Cieslak A, Kondo K, Zandecki M, et al. Safe lipid nanocapsule-based gel technology to target lymph nodes and combat mediastinal metastases from an orthotopic non-small-cell lung cancer model in SCID-CB17 mice. Nanomedicine Nanotechnology, Biol. Med. 2015;1.

[14] Abellan-Pose R, Csaba N, Alonso MJ. Lymphatic Targeting of Nanosystems for Anticancer Drug Therapy. Curr. Pharm. Des. Submitted.

[15] Ryan GM, Kaminskas LM, Porter CJH. Nano-chemotherapeutics: Maximising lymphatic drug exposure to improve the treatment of lymph-metastatic cancers. J. Control. Release 2014;193:241–56.

[16] Rao DA, Forrest ML, Alani AWG, Kwon GS, Robinson JR. Biodegradable PLGA Based Nanoparticles for Sustained Regional Lymphatic Drug Delivery. J. Pharm. Sci. 2010;99:2018–31.

[17] Kaur CD, Nahar M, Jain NK. Lymphatic targeting of zidovudine using surface-engineered liposomes. J. Drug Target. 2008;16:798–805.

[18] Moghimi SM. The effect of methoxy-PEG chain length and molecular architecture on lymph node targeting of immuno-PEG liposomes. Biomaterials 2006;27:136–44.

[19] Kaminskas LM, McLeod VM, Ryan GM, Kelly BD, Haynes JM, Williamson M, et al. Pulmonary administration of a doxorubicin-conjugated dendrimer enhances drug exposure to lung metastases and improves cancer therapy. J. Control. Release 2014;183:18–26.

[20] Pitorre M, Bastiat G, dit Chatel EM, Benoit J-P. Passive and specific targeting of lymph nodes: the influence of the administration route. Eur. J. Nanomedicine 2015;7:121–8.

[21] Gonzalo T, Lollo G, Garcia-Fuentes M, Torres D, Correa J, Riguera R, et al. A new potential nano-oncological therapy based on polyamino acid nanocapsules. J. Control. Release 2013;169:10–6.

[22] Lollo G, Hervella P, Calvo P, Avilés P, Guillén MJ, Garcia-Fuentes M, et al. Enhanced in vivo therapeutic efficacy of plitidepsin-loaded nanocapsules decorated with a new poly-aminoacid-PEG derivative. Int. J. Pharm. 2015;483:212–9.

[23] Lollo G, Rivera-Rodriguez GR, Bejaud J, Passirani C, Benoit JP, García-Fuentes M, et al. Polyglutamic acid-PEG nanocapsules as long circulated carriers for the delivery of docetaxel. Eur. J. Pharm. Biopharm. 2014;87:47–54.

[24] Lee SH, Yoo SD, Lee KH. Rapid and sensitive determination of paclitaxel in mouse plasma by high-performance liquid chromatography. J. Chromatogr. Biomed. Sci. Appl. 1999;724:357–63.

[25] Cui ZY, Ahn JS, Lee JY, Kim WS, Lim YH, Jeon HJ, et al. Mouse Orthotopic Lung Cancer Model Induced by PC14PE6. Cancer Res. Treat. 2006;38:234–9.

[26] Liu Y, Tseng Y-C, Huang L. Biodistribution studies of nanoparticles using fluorescence imaging: a qualitative or quantitative method? Pharm. Res. 2012;29:3273–7.

[27] Mérian J, Gravier J, Navarro F, Texier I. Fluorescent nanoprobes dedicated to in vivo imaging: from preclinical validations to clinical translation. Molecules 2012;17:5564–91.

[28] Oussoren C, Zuidema J, Crommelin DJA, Storm G. Lymphatic uptake and biodistribution of liposomes after subcutaneous injection. II. Influence of liposomal size, lipid composition and lipid dose. Biochim. Biophys. Acta 1997;261–72.

[29] Lozano M V, Torrecilla D, Torres D, Vidal A, Domínguez F, Alonso MJ. Highly efficient system to deliver taxanes into tumor cells: docetaxel-loaded chitosan oligomer colloidal carriers. Biomacromolecules 2008;9:2186–93.

[30] Lozano M V, Esteban H, Brea J, Loza MI, Torres D, Alonso MJ. Intracellular delivery of docetaxel using freeze-dried polysaccharide nanocapsules. J. Microencapsul. 2013;30:181–8.

[31] Torrecilla D, Lozano M V., Lallana E, Neissa JI, Novoa-Carballal R, Vidal A, et al. Anti-tumor efficacy of chitosan-g-poly(ethylene glycol) nanocapsules containing docetaxel: Anti-TMEFF-2 functionalized nanocapsules vs. non-functionalized nanocapsules. Eur. J. Pharm. Biopharm. 2013;83:330–7.

[32] Rivera-Rodríguez GR, Alonso MJ, Torres D. Poly-L-asparagine nanocapsules as anticancer drug delivery vehicles. Eur. J. Pharm. Biopharm. 2013;85:481–7.

[33] Rivera-Rodriguez GR, Lollo G, Montier T, Benoit JP, Passirani C, Alonso MJ, et al. In vivo evaluation of poly-l-asparagine nanocapsules as carriers for anti-cancer drug delivery. Int. J. Pharm. 2013;458:83–9.

[34] Oyarzun-Ampuero FA, Rivera-Rodríguez GR, Alonso MJ, Torres D. Hyaluronan nanocapsules as a new vehicle for intracellular drug delivery. Eur. J. Pharm. Sci. 2013;49:483–90.

[35] Oussoren C, Zuidema J, Croramelin D, Storm G. Lymphatic uptake and biodistribution of liposomes after subcutaneous injection I . Influence of the anatomical site of injection. J. Liposome Res. 1997;7:85–99.

[36] Oussoren C, Storm G. Liposomes to target the lymphatics by subcutaneous administration. Adv. Drug Deliv. Rev. 2001;50:143–56.

[37] Reddy LH, Bazile D. Drug delivery design for intravenous route with integrated physicochemistry, pharmacokinetics and pharmacodynamics: Illustration with the case of taxane therapeutics. Adv. Drug Deliv. Rev. 2014;71:34–57.

[38] Hamaguchi T, Matsumura Y, Suzuki M, Shimizu K, Goda R, Nakamura I, et al. NK105, a paclitaxel-incorporating micellar nanoparticle formulation, can extend in vivo antitumour activity and reduce the neurotoxicity of paclitaxel. Br. J. Cancer 2005;92:1240–6.

[39] Singer JW. Paclitaxel poliglumex (XYOTAX, CT-2103): A macromolecular taxane. J. Control. Release 2005;109:120–6.

[40] Hrkach J, Von Hoff D, Mukkaram Ali M, Andrianova E, Auer J, Campbell T, et al. Preclinical development and clinical translation of a PSMA-targeted docetaxel nanoparticle with a differentiated pharmacological profile. Sci. Transl. Med. 2012;4:128ra39.

[41] Weiszhár Z, Czúcz J, Révész C, Rosivall L, Szebeni J, Rozsnyay Z. Complement activation by polyethoxylated pharmaceutical surfactants: Cremophor-EL, Tween-80 and Tween-20. Eur. J. Pharm. Sci. 2012;45:492–8.

[42] Hureaux J, Lagarce F, Gagnadoux F, Rousselet MC, Moal V, Urban T, et al. Toxicological study and efficacy of blank and paclitaxel-loaded lipid nanocapsules after i.v. administration in mice. Pharm. Res. 2010;27:421–30.

[43] Ernsting MJ, Tang W-L, MacCallum NW, Li S-D. Preclinical pharmacokinetic, biodistribution, and anti-cancer efficacy studies of a docetaxel-carboxymethylcellulose nanoparticle in mouse models. Biomaterials 2012;33:1445–54.

[44] Devalapally H, Shenoy D, Little S, Langer R, Amiji M. Poly(ethylene oxide)-modified poly(beta-amino ester) nanoparticles as a pH-sensitive system for tumor-targeted delivery of hydrophobic drugs: Part 3. Therapeutic efficacy and safety studies in ovarian cancer xenograft model. Cancer Chemother. Pharmacol. 2007;59:477–84.

[45] Peng L, Schorzman AN, Ma P, Madden AJ, Zamboni WC, Benhabbour SR, et al. 2′-(2-Bromohexadecanoyl)-Paclitaxel Conjugate Nanoparticles for the Treatment of Non-Small Cell Lung Cancer in an Orthotopic Xenograft Mouse Model. Int. J. Nanomedicine 2014;9:3601–10.

[46] Zhigaltsev I V, Winters G, Srinivasulu M, Crawford J, Wong M, Amankwa L, et al. Development of a weak-base docetaxel derivative that can be loaded into lipid nanoparticles. J. Control. Release 2010;144:332–40.

[47] Xu Z, Chen L, Gu W, Gao Y, Lin L, Zhang Z, et al. The performance of docetaxel-loaded solid lipid nanoparticles targeted to hepatocellular carcinoma. Biomaterials 2009;30:226–32.

USC
UNIVERSIDADE
DE SANTIAGO
DE COMPOSTELA

DISCUSIÓN GENERAL

USC
UNIVERSIDADE
DE SANTIAGO
DE COMPOSTELA

DISCUSIÓN GENERAL

El sistema linfático está involucrado en diversas enfermedades de carácter bacteriano, vírico y autoinmune y representa una importante vía de diseminación del cáncer. La limitada capacidad de muchos fármacos para actuar sobre el sistema linfático ha generado en los últimos años un creciente interés por el desarrollo de nanosistemas capaces de vehiculizar fármacos o agentes diagnósticos de forma efectiva a este sistema [1–3]. Estos nanovehículos pueden promover la captación linfática de fármacos y favorecer su retención en los ganglios, lo que ofrece la posibilidad de actuar sobre las células metastásicas que frecuentemente residen en ellos. La extensión y velocidad con las que los nanosistemas pueden acumularse en el sistema linfático están fuertemente condicionadas por la fisiología del sistema linfático y la fisiopatología del tumor, la vía de administración seleccionada y las características fisicoquímicas de dichos sistemas [3,4]. En este sentido, varios trabajos han demostrado que nanosistemas administrados por vía subcutánea con un pequeño tamaño (cercano a 100 nm), una superficie hidrofílica y carga superficial negativa presentan las características más adecuadas para promover su entrada por difusión en los capilares linfáticos y, al mismo tiempo, aumentar las posibilidades de que permanezca retenidos en los ganglios linfáticos para evitar que la linfa lo transporte finalmente a la circulación sanguínea [5–7]. Estos requerimientos podrían también aplicarse a los nanosistemas administrados por vía intravenosa, los cuales, en determinadas circunstancias como, por ejemplo, la presencia de un tumor, pueden ver incrementada su extravasación al intersticio tumoral y ser posteriormente drenados por los vasos linfáticos peritumorales funcionales [8,9].

Nuestro grupo de investigación ha demostrado las ventajas que presentan las nanocápsulas como sistemas de liberación de fármacos por su capacidad para incorporar y proteger de la degradación considerables cantidades de fármacos de naturaleza hidrofóbica, modular sus propiedades biofarmacéuticas y facilitar su liberación intracelular [10–13]. En particular, los poliaminoácidos ofrecen numerosas ventajas como polímeros de recubrimiento de las nanocápsulas, ya que son biocompatibles, biodegradables y no tóxicos, lo que ha motivado su uso en diversos sistemas de liberación de fármacos actualmente en fase de evaluación clínica [14,15]. Nuestro grupo ha desarrollado varios prototipos de nanocápsulas con los poliaminoácidos ácido poliglutámico y poliasparagina con un tamaño de partícula en torno a los 200 nm

[16,17]. Estos nanosistemas han demostrado un gran potencial como vehículos para la administración de docetaxel y plitidepsina por vía intravenosa en varios modelos tumorales heterotópicos al lograr eficacias antitumorales comparables con menor toxicidad y mejores tasa de supervivencia que la formulación comercial [18–20].

En este contexto, y teniendo en cuenta los antecedentes e hipótesis recogidos en secciones anteriores, en el presente trabajo se han desarrollado nanocápsulas con una cubierta basada en poliaminoácidos específicamente diseñadas para la entrega de fármacos al sistema linfático. En este sentido, el primer desafío de este proyecto ha sido la formulación de nanosistemas de tamaño reducido.

Análisis de los parámetros experimentales que condicionan el tamaño de partícula en la preparación de nanosistemas mediante la técnica de desplazamiento del disolvente

La producción de nanocápsulas con un tamaño de partícula cercano a 100 nm es un gran reto tecnológico ya que las técnicas habitualmente empleadas permiten producir nanocápsulas con un tamaño superior a 200 nm [21]. La técnica de inversión de fases por temperatura sí permite preparar nanocápsulas más pequeñas, pero requiere el uso de una considerable concentración de surfactantes y altas temperaturas de hasta 90ºC [22], lo que puede comprometer la viabilidad de ciertos principios activos o moléculas delicadas. Como alternativa a este procedimiento, se ha optado por preparar las nanocápsulas mediante la técnica de desplazamiento del disolvente, que permite obtener nanocápsulas con diversas cubiertas poliméricas de forma sencilla y en condiciones suaves y en un rango de tamaños habitualmente comprendido entre 150 nm y 500 nm [23].

Para estudiar las condiciones experimentales que permiten obtener nanocápsulas con un tamaño cercano a 100 nm, se seleccionó como punto de partida la composición de una nanoemulsión aniónica, constituida únicamente por aceite y lecitina, que presenta un tamaño de gotícula de 178 ± 1 nm. La modificación de varias condiciones experimentales como son (i) la temperatura de la fase acuosa, (ii) relación de volúmenes fase acuosa:fase orgánica, (iii) concentración de aceite y lecitina en la fase orgánica y (iv) método de adición de la fase orgánica sobre la fase acuosa, y posterior

caracterización fisicoquímica de la nanoemulsión resultante, permitió estudiar el efecto de esa variable sobre el tamaño de gotícula. Así, se observó que la reducción de componentes lipídicos (aceite y lecitina) y la adición de la fase orgánica de forma gradual en pequeñas alícuotas permitió obtener nanoemulsiones de menor tamaño, logrando valores de hasta 87 ± 14 nm, y bajos índices de polidispersión.

Desarrollo y caracterización fisicoquímica de las nanocápsulas

La preparación de nanocápsulas de PGA, PGA-PEG y PASN a partir de las nanoemulsiones de carácter aniónico requiere de la incorporación de un surfactante catiónico en la interfaz lipídica que permita el recubrimiento con el poliaminoácido. Así, una vez optimizada la concentración lipídica que permitía obtener nanoemulsiones de tamaño reducido, se procedió a identificar la cantidad adecuada de surfactante catiónico, en este caso CTAB, necesaria para producir nanoemulsiones catiónicas pequeñas y estables. Para la elaboración de las nanocápsulas (representadas en la **Figura 1**), se incorporó el correspondiente poliaminoácido en la fase acuosa durante la preparación, lo que permitió obtener nanocápsulas en una sola etapa. La optimización de la cantidad óptima de polímero permitió obtener nanocápsulas con un tamaño comprendido entre 100 y 115 nm y potencial zeta negativo (**Tabla 1**). Los nanosistemas fueron visualizados mediante TEM. Las imágenes obtenidas mostraron una población homogénea de partículas esféricas, confirmando los tamaños de partícula previamente determinados mediante PCS (**Figura 2**). Por tanto, la optimización de los parámetros anteriormente mencionados han permitido producir nanocápsulas de composición sencilla y tamaño más reducido a los descritos hasta la fecha con la técnica del desplazamiento del disolvente.

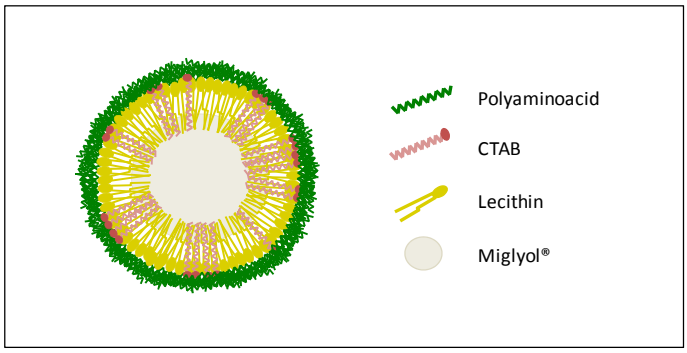

Figura 1. Representación esquemática de la estructura de las nanocápsulas recubiertas de poliaminoácidos.

Tabla 1. Características fisicoquímicas de la nanoemulsión catiónica (NE) y nanocápsulas (NCs) preparadas con diferentes tipos y concentraciones de poliaminoácidos. (Media ± S.D.; n=3).

Formulación	Poliaminoácido (% p/p)	Tamaño (nm)	P.I.	Potencial ζ (mV)
NE catiónica	0	103 ± 10	0.1	+52 ± 3
NCs PGA	6.1	97 ± 1	0.1	-34 ± 0
	11.5	100 ± 2	0.1	-54 ± 1
NCs PGA-PEG	6.1	136 ± 3	0.2	-21 ± 5
	11.5	115 ± 9	0.1	-29 ± 2
NCs PASN	6.1	125 ± 10	0.1	-20 ± 4
	11.5	111 ± 2	0.1	-25 ± 9

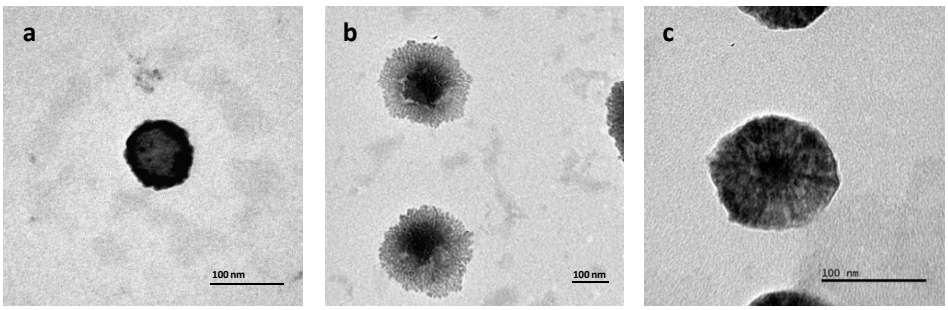

Figura 2. Imágenes TEM de las nanocápsulas de poliaminoácidos: (a) PGA, (b) PGA-PEG, (c) PASN.

Encapsulación de docetaxel y/o DiD en las nanocápsulas

El fármaco antitumoral seleccionado para evaluar la eficacia de estos nanovehículos fue el docetaxel, un fármaco de naturaleza hidrofóbica ampliamente utilizado para el tratamiento del cáncer de pulmón o mama entre otros. Para incorporarlo en las nanocápsulas se adicionó en la fase orgánica durante la preparación. La incorporación de este citostático con una carga final del 0,04% no modificó sustancialmente las características fisicoquímicas de las nanocápsulas (**Tabla 2**), aunque en el caso de las nanocápsulas de PGA-PEG y PASN se observó una ligera reducción del tamaño de partícula. Las eficacias de encapsulación del docetaxel, comprendidas entre el 56 y 67%, pusieron de manifiesto la capacidad de estos nanovehículos para encapsular fármacos hidrofóbicos, obteniéndose valores comparables a los obtenidos para otras formulaciones de nanocápsulas [24].

Tabla 2. Características fisicoquímicas y eficacias de encapsulación de las nanocápsulas de PGA, PGA-PEG y PASN blancas y cargadas con docetaxel y/o DiD. (Media ± S.D.; n=3).

Nanocápsulas	Carga	Tamaño (nm)	P.I.	Potencial ζ (mV)	E.E (%) Docetaxel	E.E (%) DiD
PGA	-	99 ± 3	0.1	-51 ± 6	-	-
	Docetaxel	95 ± 8	0.1	-53 ± 7	67 ± 2	-
	DiD	106 ± 4	0.1	-58 ± 4	-	66 ± 6
PGA-PEG	-	116 ± 5	0.1	-29 ± 5	-	-
	Docetaxel	99 ± 4	0.2	-35 ± 4	60 ± 2	-
	DiD	107 ± 9	0.1	-36 ± 4	-	56 ± 3
	Docetaxel + DiD	109 ± 13	0.2	-39 ± 1	48 ± 8	52 ± 15
PASN	-	111 ± 2	0.1	-25 ± 9	-	-
	Docetaxel	81 ± 3	0.2	-27 ± 2	56 ± 2	-
	DiD	87 ± 4	0.1	-31 ± 4	-	63 ± 1

P.I.: índice de polidispersión; E.E.: eficacia de encapsulación.

La realización de ensayos *in vivo* con las nanocápsulas de PGA-PEG requirió un aumento de la carga del fármaco en esta formulación. La incorporación del docetaxel al 1.3% no alteró ni el tamaño de partícula ni el potencial zeta de las nanocápsulas con respecto a las formulaciones blancas, pero la eficacia de encapsulación del fármaco disminuyó hasta valores cercanos al 40%.

Para los ensayos *in vitro* y estudios de biodistribución mediante fluorescencia también se encapsuló la sonda DiD en las nanocápsulas, incorporándola en la fase orgánica durante el proceso de elaboración. Este fluoróforo que emite en el infrarrojo cercano es débilmente fluorescente en agua, pero muy fluorescente y fotoestable cuando se incorpora en nanocápsulas gracias a su naturaleza anfifílica. Asimismo, el DiD presenta la ventaja de conseguir una alta penetración en los tejidos y una escasa interferencia con la autofluorescencia del animal. La encapsulación apenas modificó las características fisicoquímicas de las nanocápsulas con respecto a las formulaciones blancas, salvo por una ligera disminución en el tamaño de las nanocápsulas de PASN (**Tabla 2**). Las eficacias de encapsulación del DiD, comprendidas entre el 56 y 66%, fueron similares a los valores previamente obtenidos para el docetaxel, demostrando la flexibilidad de estos nanovehículos para asociar diferentes tipos de moléculas.

Además, como se indica en la misma tabla, las nanocápsulas de PGA-PEG fueron simultáneamente cargadas con docetaxel y DiD sin que se vieran afectadas sus características fisicoquímicas y sin reducir significativamente sus eficacias de encapsulación. Esta capacidad para administrar al mismo tiempo fármacos antitumorales y moléculas para imagen podría ser explotada para el desarrollo de una plataforma multifuncional con fines terapéuticos y diagnósticos.

Estudios de liberación *in vitro* de docetaxel

La liberación del docetaxel a partir de las nanocápsulas se estudió en un fluido biológico simulado. Todas las formulaciones mostraron un perfil de liberación bifásico similar, caracterizado por una rápida liberación inicial (33-40% del docetaxel encapsulado) seguido por una segunda fase en la que no se liberan cantidades significativas de fármaco. Esta característica liberación inicial, típicamente observada en otros nanosistemas capsulares, ha sido atribuida a la partición del fármaco lipofílico entre el núcleo oleoso y el medio de liberación acuoso, mientras que la ausencia de

liberación en la segunda fase confirmó la alta afinidad del docetaxel por el núcleo oleoso [10,25]. Aunque los resultados de los ensayos de liberación *in vitro* no pueden ser directamente extrapolados a las condiciones *in vivo* para predecir el comportamiento real, el hecho de que una cantidad significativa de docetaxel pudiera permanecer retenida en las nanocápsulas de forma estable tras la administración sería muy ventajoso para conseguir vehiculizar la mayor cantidad de fármaco hacia el sistema linfático.

Estabilidad de las nanocápsulas

El estudio de estabilidad de las nanocápsulas se realizó en diversas condiciones.

En primer lugar, se comprobó que el tamaño de partícula, índice de polidispersión y potencial zeta de las nanocápsulas no varió al conservarlas a 4ºC, confirmando su estabilidad en estas condiciones de almacenamiento durante al menos dos meses.

Por otro lado, con el objetivo de conocer mejor el papel del recubrimiento polimérico en la estabilidad coloidal de las nanocápsulas y determinar si la presencia de PEG proporcionaba alguna ventaja sobre el recubrimiento con PGA, se decidió evaluar la estabilidad de las nanocápsulas a diferentes condiciones de salinidad. Para ello se monitorizó el tamaño de partícula de las nanocápsulas en un medio constituido por tampón fosfato pH 7 y concentraciones crecientes de NaCl. A partir de las cinéticas de agregación de las nanocápsulas se pudieron estimar los parámetros Concentración de Coagulación Crítica (CCC) y Concentración de Estabilización Crítica (CSC). El valor CCC indica la mínima concentración de sales a la que se cancela totalmente la barrera de energía potencial que evita la agregación de las partículas, mientras que el CSC representa la concentración salina a la que se consigue re-estabilizar las partículas gracias a la aparición de fuerzas repulsivas de hidratación que permiten la recuperación de la barrera energética que dificulta la agregación. Estos parámetros CCC y CSC están relacionados con la carga superficial de las partículas e hidrofilia, respectivamente.

Como cabía esperar, aunque las tres formulaciones tienen el mismo núcleo oleoso, su estabilidad coloidal estuvo determinada por la composición de la cubierta polimérica. Las nanocápsulas que contienen ácido poliglutámico fueron más estables que las de PASN, ya que necesitaron una concentración salina mayor para su inestabilización. Los valores CCC estimados para las nanocápsulas de PGA y PGA-PEG fueron 90 y 150

mM, respectivamente, evidenciando la superioridad de las nanocápsulas de PGA-PEG. El hecho de que estas nanocápsulas tengan un CCC superior a pesar de tener menor carga superficial que las de PGA por el apantallamiento del PEG (como se refleja en los valores de potencial zeta indicados en la **Tabla 3**), indica que el PEG proporciona a estas nanocápsulas una estabilización estérica adicional que incrementa notablemente su estabilidad coloidal. Por otro lado, la comparativa de los valores estimados de CSC para las nanocápsulas de PGA-PEG y PGA (≈155 y 200 mM, respectivamente), refleja la mayor hidrofilia superficial de la formulación PEGilada, que consigue recuperar su estabilidad coloidal a una concentración salina muy próxima a la que se produce la agregación. Así, la conclusión general extraída de este ensayo es que el recubrimiento de las nanocápsulas con PGA-PEG les proporciona una mayor estabilidad coloidal que la conseguida con los otros dos polímeros.

Para asegurar la estabilidad coloidal de las nanocápsulas en el organismo, se estudió la estabilidad en plasma humano, incubando las nanocápsulas a 37ºC en este medio biológico y monitorizando el tamaño de partícula de la población correspondiente a las nanocápsulas. Dada la complejidad de este medio para este tipo de ensayo, también se analizó una muestra de plasma como control. Los resultados mostraron un comportamiento similar de las nanocápsulas de PGA y PGA-PEG, las cuales experimentaron en los primeros instantes un aumento del tamaño que se mantuvo prácticamente constante durante todo el ensayo (**Figura 3**). En el caso de las nanocápsulas de PASN el aumento del tamaño de partícula fue algo más pronunciado.

En general, estos resultados sugieren que las nanocápsulas no agregaron en plasma. El aumento del tamaño de partícula detectado podría ser consecuencia de la interacción de los nanosistemas con las proteínas u otros componentes. En este caso, el recubrimiento proteico alrededor de las nanocápsulas podría contribuir a su estabilización en condiciones fisiológicas [26,27]. En cualquier caso, la corona proteica formada podrá condicionar su farmacocinética y distribución en el organismo, de acuerdo con lo observado para otros nanosistemas [28,29].

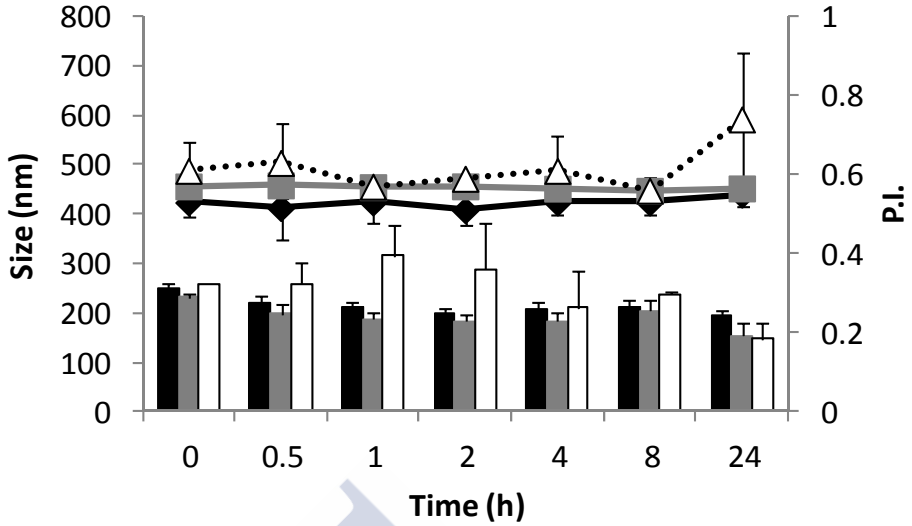

Figura 3. Estabilidad de las nanocápsulas de PGA (negro), PGA-PEG (gris) y PASN (blanco) en plasma humano durante al incubación a 37 °C. Las columnas representan el tamaño y las líneas el índice de polidispersión (P.I.).

Con la información obtenida en estos ensayos de estabilidad, se decidió seleccionar las nanocápsulas de PGA-PEG como el prototipo más idóneo para la vehiculización de fármacos al sistema linfático.

Estudios en cultivos celulares

La capacidad de las nanocápsulas de PGA-PEG para interaccionar con células de cáncer de pulmón A549, se evaluó mediante microscopía confocal y citometría de flujo, tanto en monocultivo como en un co-cultivo con linfocitos T Jurkat (**Anexo 1**). Los resultados revelaron una gran internalización de las nanocápsulas en las células tumorales, así como la liberación intracelular del docetaxel. Asimismo, la evaluación en ese co-cultivo que simula un ganglio linfático afectado de metástasis mostró que las nanocápsulas son captadas preferentemente por la células tumorales antes que por los linfocitos, lo que las convierte en unos nanosistemas muy interesantes para el tratamiento del cáncer (**Figura 4**).

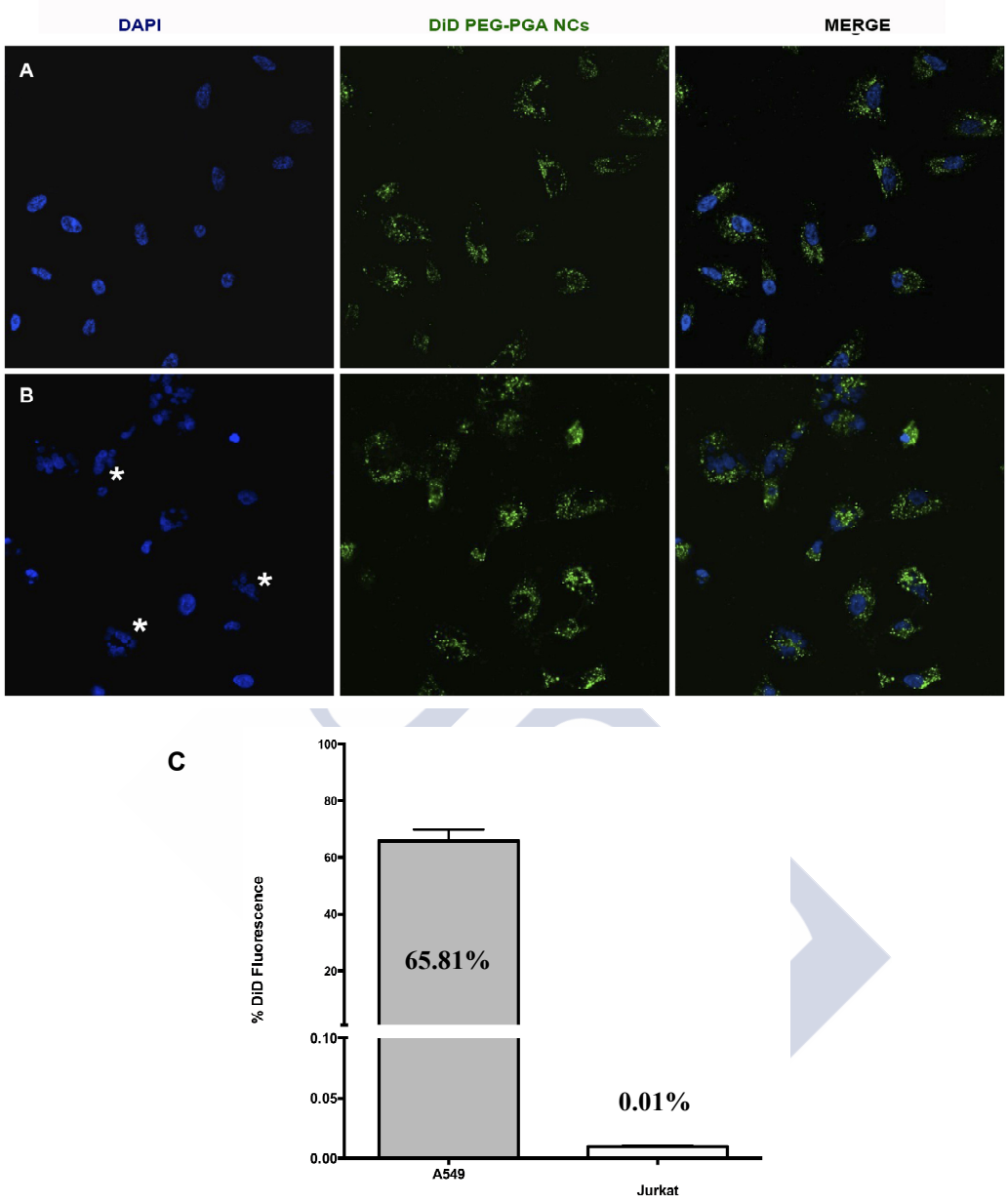

Figura 4. Estudios de captación celular: células (núcleos marcados con DAPI en canal azul) incubadas con (A) Nanocápsulas de PGA-PEG cargadas con DiD (B) Nanocápsulas de PGA-PEG cargadas con DiD y docetaxel (canal verde). La acumulación de nanocápsulas con DiD y docetaxel produjo un efecto citotóxico caracterizado por la fragmentación del núcleo (representado por *). (C) Representación gráfica de la captación de nanocápsulas fluorescentes en co-cultivo con linfocitos T Jurkat determinada por FACS. Media ± DE (n=3).

ESTUDIOS *IN VIVO*

Ensayos de biodistribución por fluorescencia. Efecto del tamaño de partícula en la biodistribución

Teniendo en cuenta la importancia del tamaño de partícula para el acceso efectivo de los nanosistemas al sistema linfático [5,7], se decidió valorar su efecto sobre la biodistribución de las nanocápsulas. Para ello se decidió seleccionar como técnica la imagen por fluorescencia, ya que es una técnica sencilla, rápida, no ionizante y de fácil manejo que, por su carácter semicuantitativo, permite comparar los niveles de fluorescencia detectados para un mismo órgano si se analizan los diversos grupos de forma simultánea [30,31]. Con este objetivo se decidió comparar la biodistribución de las nanocápsulas de PGA-PEG con otras de composición similar, previamente desarrolladas en el grupo, que presentan un tamaño medio cercano a los 200 nm y un valor de potencial zeta parecido. Para ello, se administraron nanocápsulas marcadas con DiD de 100 y 200 nm (con la misma intensidad de fluorescencia) por vía subcutánea en la región interescapular a ratones sanos y se realizó un análisis *ex-vivo* a distintos tiempos post-administración comparando la fluorescencia acumulada en órganos y ganglios linfáticos mediante un sistema de imagen *in vivo* (IVIS®). Se observó que la fluorescencia encontrada en los ganglios mediastino, axilares, cervicales y mesentéricos de los ratones tratados con nanocápsulas de 100 nm a las 24 horas era significativamente superior que en los tratados con las de 200 nm, aunque comparables a las 48 horas (**Figura 5**). Esto indicó que las nanocápsulas de pequeño tamaño se drenaron más rápidamente por el sistema linfático, probablemente porque su tamaño facilita su migración a través del intersticio, favoreciendo así su acceso a los capilares linfáticos. Por otro lado, el hecho de que las nanocápsulas de 100 nm muestren mayor fluorescencia a las 24 horas en órganos irrigados como hígado, pulmón, corazón y riñones sugirió que las nanocápsulas, una vez en el sistema linfático, podrían circular sin ser retenidas en los ganglios, alcanzando finalmente la circulación sanguínea.

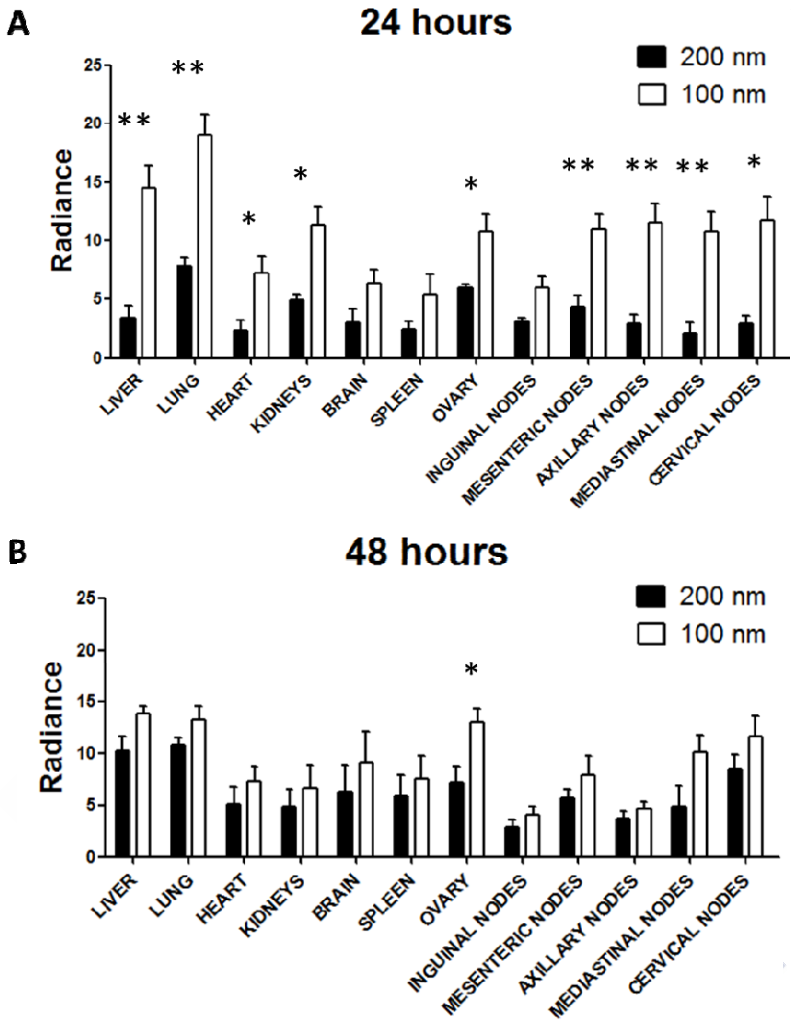

Figura 5. Biodistribución de nanocápsulas de PGA-PEG de 200 y 100 nm, marcadas con DiD, tras administración subcutánea. Se determinó la radianza (fotones/seg/cm^2/sr x 10^7) en los órganos y ganglios extraídos a las (A) 24 y (B) 48 horas post-inyección. (Media ± SEM; n=4). Test Mann Whitney ((*) $p < 0.05$, (**) $p < 0.01$).

ENSAYOS DE BIODISTRIBUCIÓN MEDIANTE RADIACTIVIDAD

Una vez confirmada la influencia del tamaño y, por tanto, el potencial interés de estos nanosistemas para la vectorización linfática de fármacos, se decidió evaluar su biodistribución marcando las nanocápsulas con In^{111} por presentar este radionúclido un tiempo de vida media adecuado para la realización de los ensayos (2.83 días). Para realizar un marcaje estable, se incorporó fosfoetanolamina conjugada con el agente quelante DTPA durante la preparación. El marcaje no modificó sustancialmente las características fisicoquímicas de las nanocápsulas y demostró ser estable para la realización de los ensayos *in vivo*.

Efecto del recubrimiento polimérico y vía de administración en la biodistribución

Como se comentó anteriormente la vía de administración e hidrofilia superficial de los nanosistemas también condiciona el mecanismo de acceso al sistema linfático. Para evaluar la influencia de estos factores, se administraron nanocápsulas de PGA y PGA-PEG marcadas con In^{111} o cloruro de In^{111} (como control) en la vena de la cola (para la administración intravenosa) o en las almohadillas plantares de ratas (para la administración subcutánea) y se sacrificaron a distintos tiempos para medir la radiactividad en órganos, ganglios, sangre y excretas con un contador gamma.

En el caso de la administración subcutánea se monitorizó la radiactividad remanente en las almohadillas plantares para valorar el drenaje desde el intersticio. A diferencia del control, que experimentó un drenaje muy rápido durante las primeras 24 horas, las nanocápsulas fueron drenadas de forma gradual durante una semana. Los estudios de biodistribución realizados por esta vía evidenciaron una gran acumulación de las nanocápsulas en los ganglios que drenan el lugar de inyección (poplíteos, ilíacos e inguinales), confirmando un drenaje fundamentalmente linfático (**Figura 6**). Aunque en niveles muy bajos y significativamente inferiores al control, también se detectó radiactividad asociada a las nanocápsulas en sangre y algunos órganos. Teniendo en cuenta que el acceso a los capilares sanguíneos desde el espacio intersticial está restringido por el elevado peso molecular de los nanosistemas, estos resultados podrían indicar que las nanocápsulas no retenidas en el sistema linfático alcanzan finalmente la circulación sanguínea.

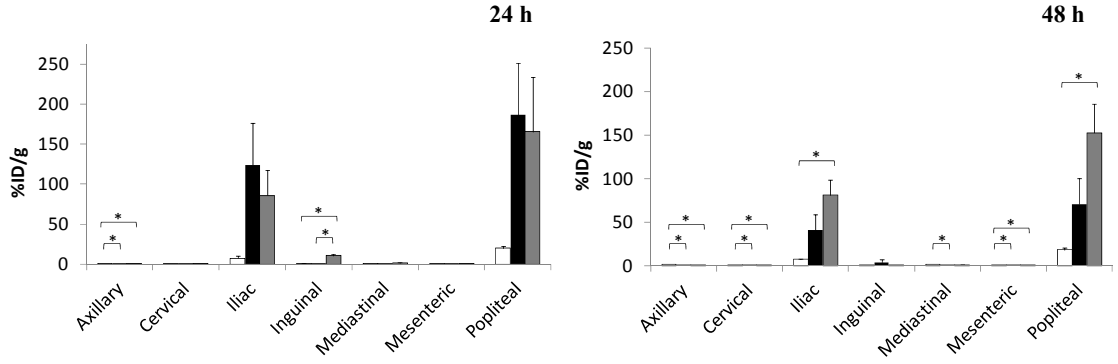

Figura 6. Distribución en los ganglios linfáticos a las 24 y 48 horas de la administración subcutánea de ^{111}InCl3 (□), ^{111}In-PGA-PEG-NCs (■) and ^{111}In-PGA-NCs (■). Los valores se expresaron como porcentaje de dosis inyectada por gramo de tejido (media ± SEM.; n=4). * Diferencias estadísticamente significativas ($p<0.05$).

Aunque no fue observado a tiempo cortos, las nanocápsulas administradas por vía intravenosa también alcanzaron los ganglios linfáticos. Así, a las 24 horas post-inyección se registraron niveles estadísticamente significativos en los ganglios axilares, cervicales, inguinales, mediastino y mesentéricos para las nanocápsulas de PGA-PEG y en inguinales, mediastino y mesentéricos para las nanocápsulas de PGA, aunque con valores muy inferiores a los registrados por vía subcutánea (**Figura 7**).

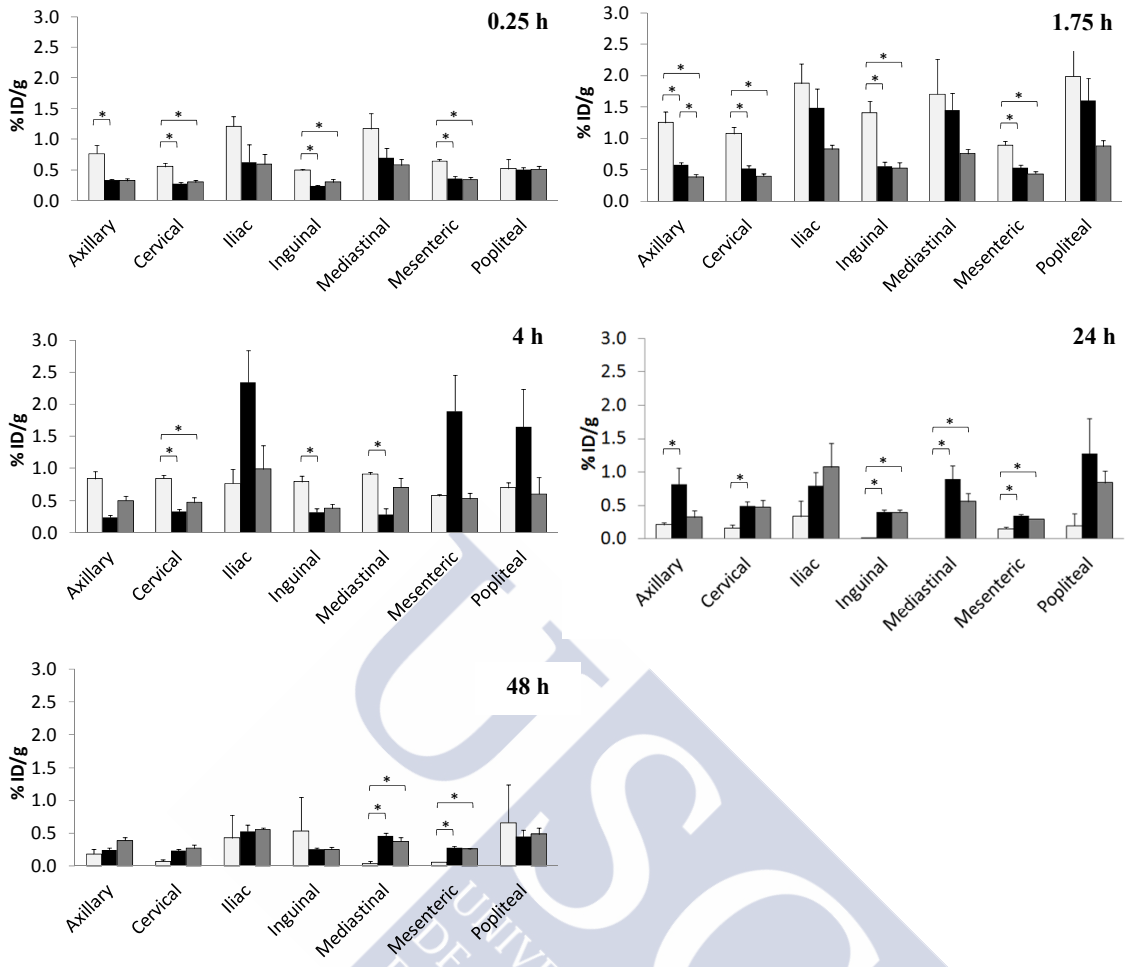

Figura 7. Distribución en los ganglios linfáticos tras la administración intravenosa de 111InCl3 (□), 111In-PGA-PEG-NCs (■) and 111In-PGA-NCs (▣). Los valores se expresaron como porcentaje de dosis inyectada por gramo de tejido (media ± SEM.; n=4). * Diferencias estadísticamente significativas ($p<0.05$).

Los mayores niveles de radiactividad para las nanocápsulas administradas por vía intravenosa se encontraron en el hígado y, en menor medida, en bazo (**Figura 8**). La actividad medida en las excretas también confirmó la excreción hepática y biliar como principal vía de eliminación de las nanocápsulas.

En general, el patrón de distribución observado para las nanocápsulas de PGA y PGA-PEG fue muy similar, aunque se encontraron algunas ligeras diferencias en hígado y pulmón a algunos tiempos. Concretamente, los niveles encontrados en estos órganos a las 4 y 24 horas post-administración para las nanocápsulas de PGA-PEG fueron menores que los encontrados para las nanocápsulas de PGA, lo que podría indicar un

menor reconocimiento por parte de los macrófagos de estos órganos. En lo que se refiere a la acumulación linfática, no se observaron diferencias destacables entre ambas formulaciones, sugiriendo que las pequeñas diferencias de hidrofilia superficial observadas en los ensayos de estabilidad coloidal apenas tienen repercusión cuando se administran *in vivo*.

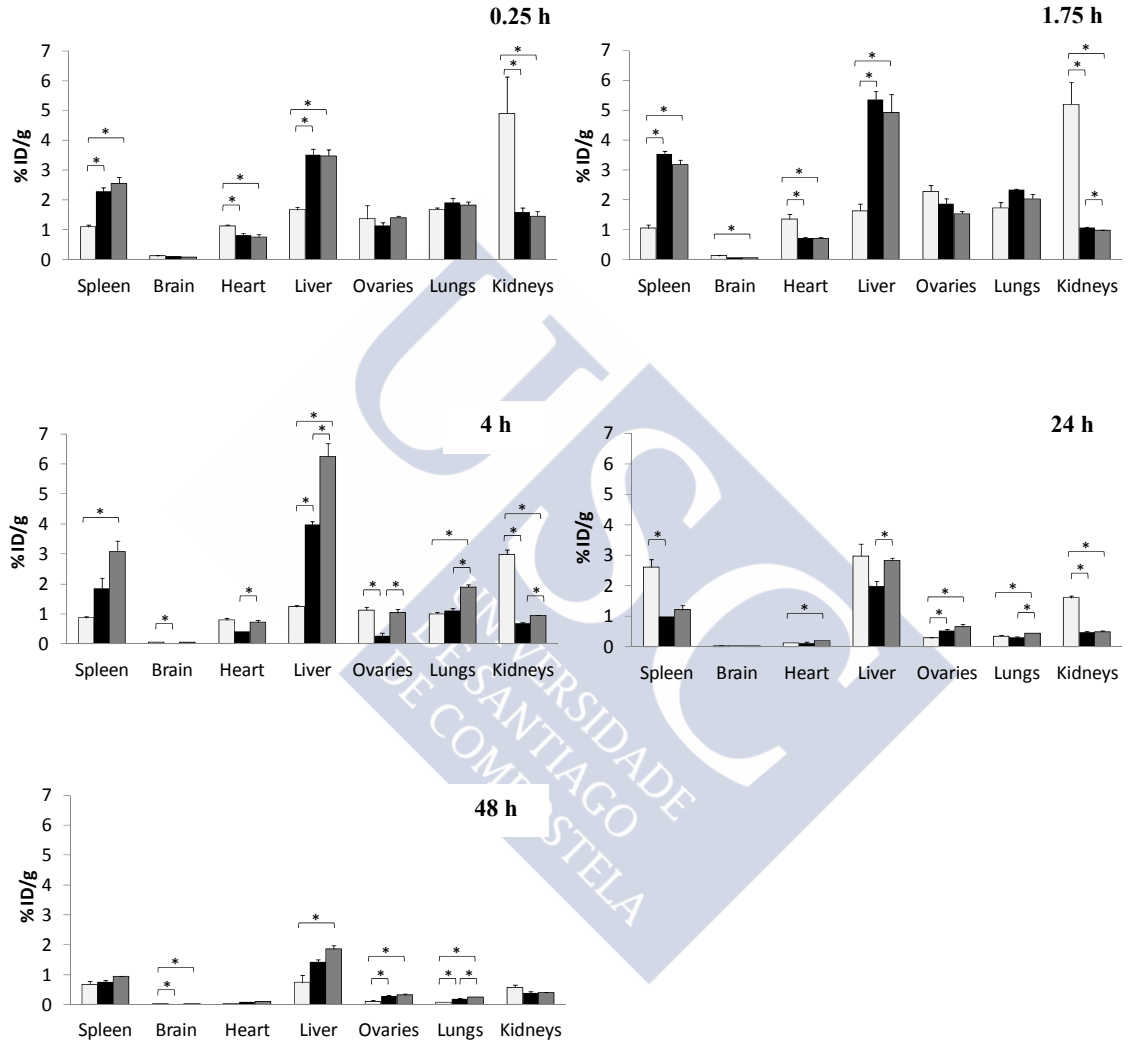

Figura 8. Distribución en los órganos tras la administración intravenosa de 111InCl3 (□), 111In-PGA-PEG-NCs (■) and 111In-PGA-NCs (▩). Los valores se expresaron como porcentaje de dosis inyectada por gramo de tejido (media ± SEM.; n=4). * Diferencias estadísticamente significativas ($p<0.05$).

El análisis comparativo de ambas vías de administración nos permitió concluir que la administración subcutánea propició una elevada acumulación de nanocápsulas en ganglios linfáticos específicos, mientras que la administración intravenosa condujo a una acumulación mucho más modesta en todos los ganglios examinados.

En este sentido, es importante tener en cuenta que determinadas patologías pueden alterar la biodistribución. En el caso del cáncer, se ha demostrado que la presencia de un tumor altera la biodistribución de los nanosistemas administrados por vía intravenosa, ya que la gran permeabilidad de los vasos sanguíneos tumorales favorece la extravasación al tumor [32,33]. El tamaño reducido de nuestras nanocápsulas podría favorecer el acceso al intersticio tumoral [34]. Asimismo, la alta presión intersticial en el interior del tumor podría favorecer su flujo hacia los vasos linfáticos peritumorales [8].

ENSAYOS *IN VIVO* DE LAS NANOCÁPSULAS CONTENIENDO DOCETAXEL

Una de las potenciales aplicaciones de los nanosistemas desarrollados es el tratamiento de tumores que metastatizan a través del sistema linfático como, por ejemplo, el cáncer de pulmón. Teniendo en cuenta que la administración por vía subcutánea para el tratamiento de un tumor en el pulmón debería realizarse en un lugar que permita el drenaje hacia los ganglios afectados, se decidió evaluar la posibilidad de administrar las nanocápsulas en la región interescapular. Para ello se realizó un ensayo de biodistribución mediante fluorescencia en ratones sanos, comparando la biodistribución de las nanocápsulas de PGA-PEG por vía intravenosa y vía subcutánea en este punto anatómico. Como cabía esperar, las nanocápsulas administradas por vía intravenosa mostraron una mayor acumulación en hígado y pulmón. Sorprendentemente, los niveles detectados en los ganglios linfáticos fueron comparables por ambas vías de administración, sugiriendo que la diferente organización estructural del tejido subcutáneo en este lugar no favorece un aumento de la presión intersticial que incremente el acceso de las nanocápsulas hacia los capilares linfáticos, como puede ocurrir, por ejemplo, si se inyecta en la pata [35]. Por otro lado, teniendo en cuenta que la vía subcutánea está desaconsejada para la administración del docetaxel porque por su naturaleza irritante podría producir un daños a nivel local durante el lento drenaje de las

nanocápsulas hacia el sistema linfático, se decidió seleccionar finalmente la vía intravenosa como vía de administración para la realización de los ensayos de eficacia antitumoral.

Toxicidad de las nanocápsulas de PGA-PEG conteniendo docetaxel

La evaluación toxicológica de las nanocápsulas de PGA-PEG cargadas con docetaxel se llevó a cabo en ratones sanos, administrando durante cinco días consecutivos nanocápsulas de PGA-PEG encapsulando docetaxel (a una dosis total de 30 y 60 mg/kg) por vía intravenosa, controlando el peso, aspecto y supervivencia de los animales. Para poder establecer la comparativa con la formulación comercial, otros animales fueron tratados con Taxotere® a las mismas dosis y con el mismo régimen de administración múltiple.

Los ratones tratados con la dosis más alta de Taxotere® (60 mg/kg) perdieron un 27% de su peso corporal y mostraron mala condición física, con signos de piloerección, temblor y debilidad **(Figura 9)**. Por el contrario, los ratones tratados con la misma dosis de docetaxel en las nanocápsulas no mostraron signos de toxicidad durante las administraciones ni en los diez días posteriores y su pérdida de peso fue inferior al 5%, evidenciando la menor toxicidad del tratamiento incluso a dosis superiores a las utilizadas con fines terapéuticos en este modelo animal.

La reducida toxicidad de las nanocápsulas frente al Taxotere® puede ser atribuida a la diferente distribución en el organismo y al uso de materiales con un mejor perfil de compatibilidad y toxicidad. De hecho, el ácido poliglutámico es un material particularmente atractivo por su biocompatibilidad, baja inmunicidad y su naturaleza biodegradable, lo que ha motivado su utilización, sólo o asociado con PEG, en diversos nanosistemas que se encuentran en fases avanzadas de evaluación clínica [14,36]. Por otro lado, las altas concentraciones de Tween® 80 que contiene el Taxotere® han demostrado ser responsables de parte de su toxicidad. Ciertos efectos secundarios conocidos de esta formulación como la retención de líquidos y reacciones de hipersensibilidad aguda son parcialmente causados por el Tween® [37].

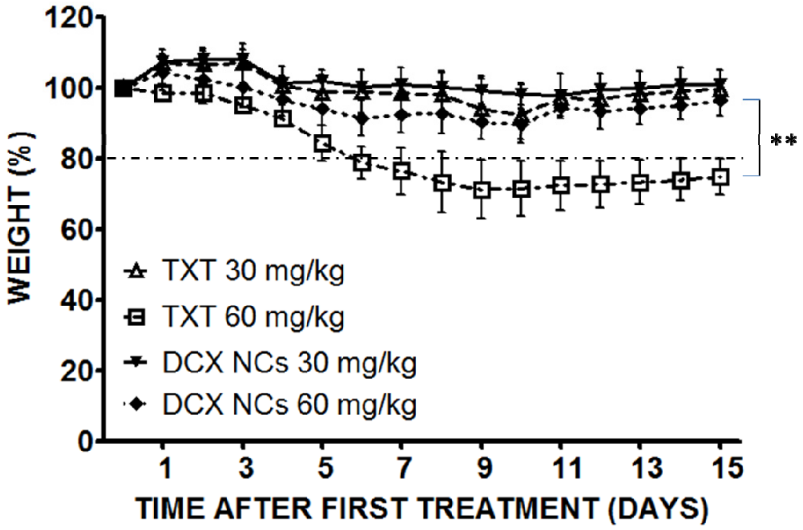

Figura 9. Evolución del peso de los ratones durante los 15 días siguientes a la administración del Taxotere® (TXT) o nanocápsulas de PGA-PEG cargadas con docetaxel (DCX NCs), con una dosis de 30 o 60 mg/kg. Datos expresados como media ± SEM.; n=3. Diferencias estadísticamente significativas se indican como ** ($p < 0.01$).

Eficacia antitumoral de las nanocápsulas de PGA-PEG en cáncer de pulmón metastásico

Para evaluar el potencial de las nanocápsulas para la vehiculización de fármacos antitumorales al sistema linfático se seleccionó un modelo ortotópico de cáncer de pulmón de células A459-Luc que metastatiza a los ganglios linfáticos del mediastino. Al ser un tumor de células de cáncer de pulmón implantado en su correspondiente órgano, este modelo consigue reproducir el microambiente tumoral y las rutas de diseminación del cáncer de forma más realista que los modelos tumorales heterotópicos clásicamente implantados a nivel subcutáneo [38]. Además, el carácter bioluminiscente de esta línea tumoral permite monitorizar la evolución del tumor en el IVIS® y cuantificar el número de células tumorales presentes en los órganos y ganglios linfáticos en el animal diseccionado.

Una vez identificado el momento en el que se produce la diseminación del tumor primario a los ganglios del mediastino (a los 13 días de la implantación tumoral), se

decidió estudiar la eficacia de las nanocápsulas de PGA-PEG sobre este tumor en dos estadíos diferentes.

En un primer ensayo se decidió evaluar la eficacia de las nanocápsulas de PGA-PEG en ratones con tumor en una fase inicial (sin metástasis en el ganglio del mediastino), realizando dos administraciones intravenosas de nanocápsulas cargadas con docetaxel (10 mg/kg por administración, dosis total 20 m/kg), Taxotere® a la misma dosis o nanocápsulas sin fármaco (blancas), los días 5 y 20 tras la implantación del tumor.

Los resultados mostraron que en el caso de los ratones sin tratamiento (control) o tratados con nanocápsulas blancas el tamaño del tumor aumentó exponencialmente hasta el tiempo final (día 37) **(Figura 10 A)**. Por su parte, el tratamiento con nanocápsulas encapsulando docetaxel demostró ser tan eficiente inhibiendo el crecimiento tumoral y la metástasis linfática como el Taxotere® **(Figura 10 B-D)**. La reducida carga tumoral encontrada en los ganglios tras el tratamiento con las formulaciones que contenían docetaxel (**Figura 10 D**) pudo ser atribuida al efecto directo del fármaco sobre las metástasis en los ganglios o secundaria a la inhibición del tumor primario, que pudo ver mermada su capacidad de propagación.

Para entender este resultado y evaluar el efecto sobre las metástasis se planteó otro ensayo de eficacia en el que los tratamientos comenzaron una vez consolidada la metástasis en los ganglios linfáticos.

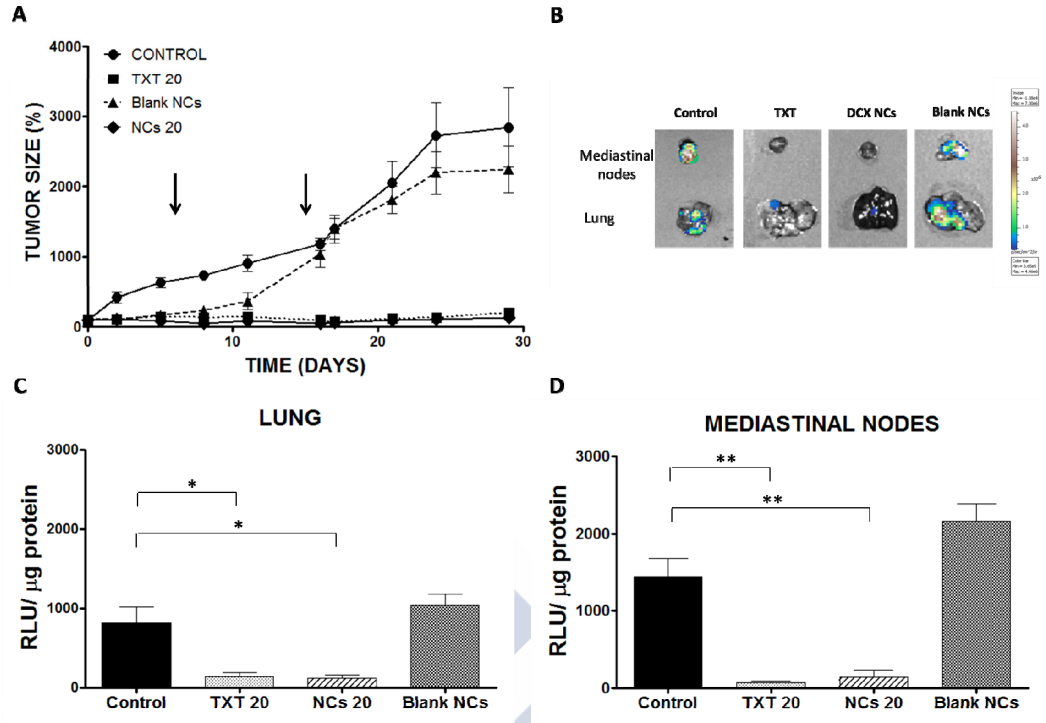

Figura 10. (A) Evolución del tamaño del tumor sin tratamiento (control) y tras la administración de nanocápsulas sin fármaco (Blank NCs), Taxotere® 20 mg/kg (TXT 20) y nanocápsulas con la misma dosis de docetaxel (NCs 20). Las flechas representan las dos administraciones realizadas. (B) Imagen que muestra la carga tumoral en pulmones y ganglios del mediastino. (C) Cuantificación de la actividad luciferasa (unidad relativa de luz por µg de proteína) en pulmones y (D) en los ganglios linfáticos del mediastino. Datos expresados como media ± SEM.; n=5. Las diferencias estadísticamente significativas se expresan como * ($p < 0.05$) y ** ($p < 0.01$).

En el segundo ensayo de eficacia los ratones fueron tratados con Taxotere® o nanocápsulas con docetaxel los días 20 y 27 posteriores a la inyección de las células tumorales. En este caso, se evaluaron dos dosis distintas de docetaxel, 10 y 20 mg/kg, y dos tiempos de finalización del estudio, los días 37 y 47, seleccionados en base a las condiciones físicas de los ratones. El día 37 los ratones control tuvieron que ser sacrificados por razones éticas debido a la elevada carga tumoral y el mal estado que presentaban. En este momento los tratamientos con nanocápsulas y Taxotere® mostraron una eficacia similar reduciendo el crecimiento tumoral (**Figura 11A**). Por el contrario, la monitorización del crecimiento tumoral hasta el día 47 reveló que las nanocápsulas a una dosis de 10 mg/kg fueron capaces de inhibir el crecimiento del

tumor con mayor eficacia que el Taxotere®. Los datos de supervivencia de los animales tratados con nanocápsulas a una dosis de 10 mg/kg de docetaxel también confirmaron la superioridad de los nanosistemas frente al Taxotere® administrado a la misma dosis (**Figura 11 B**).

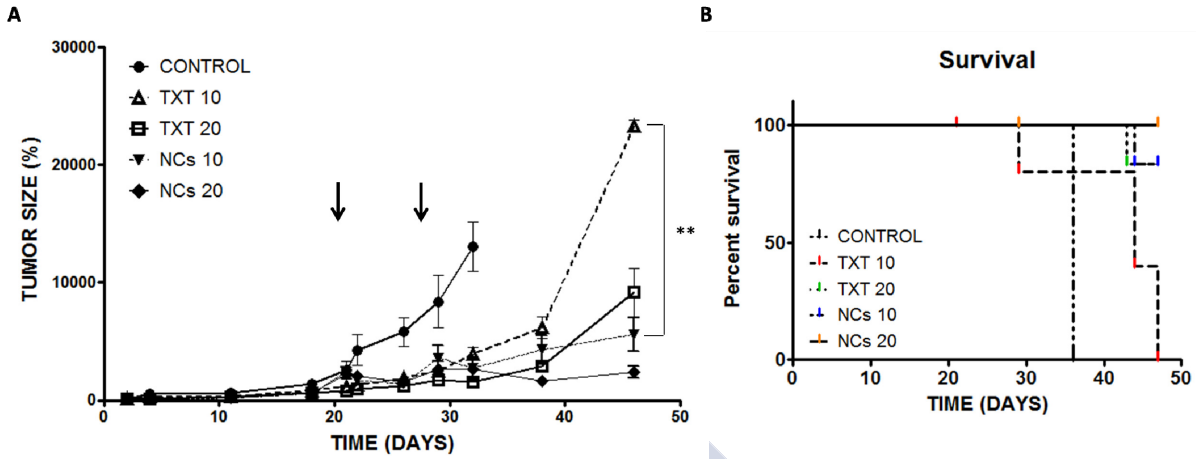

Figura 11. (A) Evolución del tamaño del tumor sin tratamiento (control) y tras la administración de nanocápsulas (NCs) con una dosis de docetaxel de 10 mg/k o 20 mg/kg o Taxotere® (TXT) a las mismas dosis (NCs 20). Las flechas representan las dos administraciones realizadas. Datos expresados como media ± SEM.; n=6. Las diferencias estadísticamente significativas se expresan como ** ($p < 0.01$). (B) Representación de supervivencia de Kaplan-Meier. El análisis estadístico Log-rank (Mantel Cox) indicó diferencias estadísticamente significativas entre Taxotere® 10 mg/kg (TXT 10) y nanocápsulas 10 mg/kg ($p= 0.0096$).

En este ensayo también se realizó la cuantificación de la actividad luciferasa en pulmones y ganglios **(Figura 12).** Los resultados obtenidos a día 37 no revelaron diferencias significativas entre las nanocápsulas y el Taxotere®. Sin embargo, la carga tumoral determinada tanto en pulmones como en los ganglios a día 47 fue muy inferior para el grupo tratado con las nanocápsulas, a cualquiera de las dosis **(Figura 12 A-B)**. Este aumento de la actividad antitumoral a tiempos tardíos, que ya ha sido previamente descrito para otras nanocápsulas podría indicar que estos nanosistemas necesitan más tiempo para ejercer su actividad antitumoral, pero una vez iniciado, proporcionan un efecto más duradero [39].

Además, al comparar los valores de actividad luciferasa de los ganglios antes (día 19 tras la inyección de las células) y después de los distintos tratamientos, se observó que las nanocápsulas administradas a una dosis de docetaxel de 20 mg/kg fue la única formulación capaz de disminuir específicamente la carga tumoral en los ganglios (**Figura 12C**). Por tanto, estos resultados indican que las nanocápsulas con docetaxel logran una mayor eficacia durante más tiempo sobre las metástasis linfáticas, confirmando su superioridad sobre la formulación comercial para el tratamiento del cáncer metastásico.

Globalmente, se puede concluir que el desarrollo y optimización de nanocápsulas con una cubierta basada en poliaminoácidos, como la obtenida con PGA-PEG, son sistemas eficaces para dirigir fármacos al sistema linfático. En el caso del cáncer metastásico esta estrategia permite actuar específicamente sobre las células tumorales presentes en los ganglios linfáticos, mejorando los resultados obtenidos con la formulación comercial convencional y disminuyendo su toxicidad. Este es uno de los puntos fuertes de este trabajo ya que, aunque en los últimos años se han desarrollado otros nanosistemas con el mismo propósito y con buenos resultados en términos de acumulación linfática y eficacia antimetastásica, en muchos casos no está claro si ésta se debe a un efecto directo sobre las células tumorales residentes en los ganglios o es secundaria a una reducción del tumor primario que limita su capacidad para diseminar.

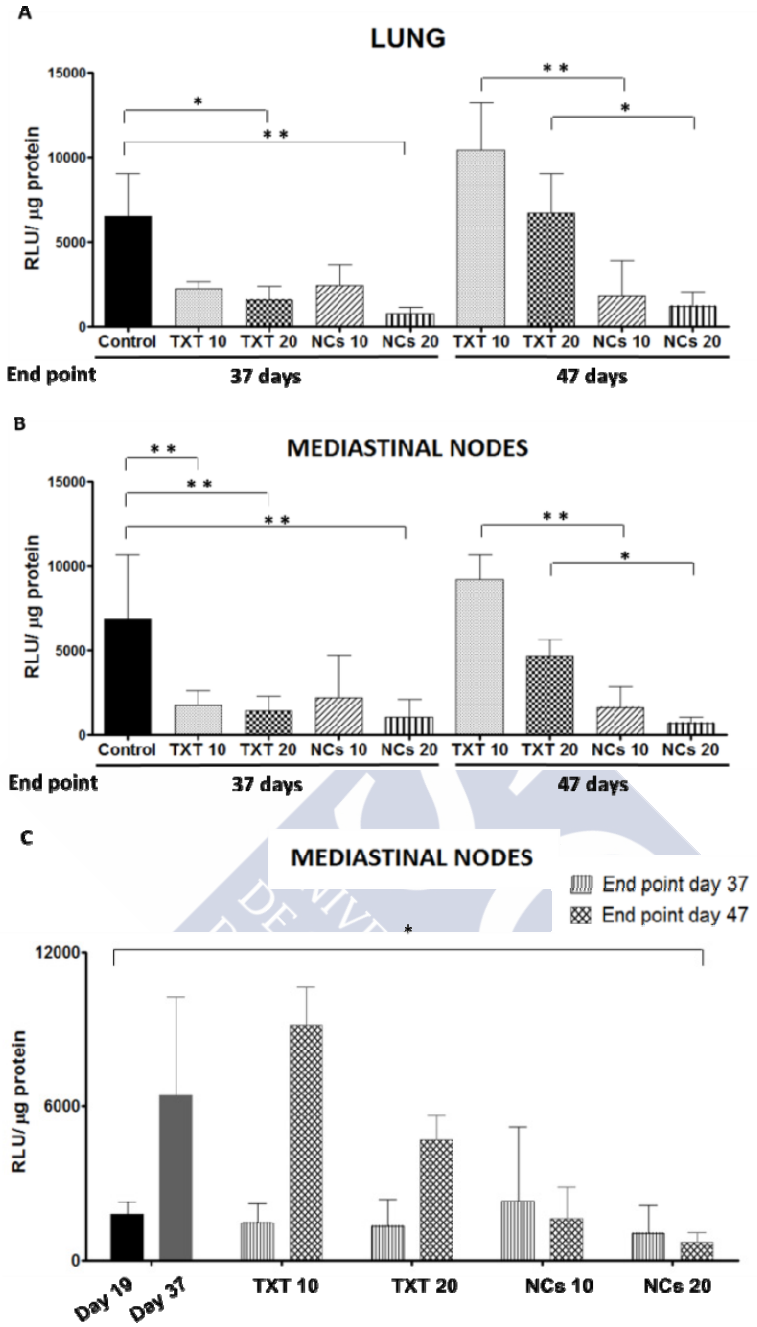

Figura 12. Cuantificación de la actividad luciferasa (unidad relativa de luz por µg de proteína) en pulmones (A) y (B-C) en los ganglios linfáticos del mediastino, a día 37 y 47 tras la inyección de las células tumorales. Los ratones fueron tratados con Taxotere® 10 y 20 mg/kg (TXT 10 and TXT 20, respectivamente) y nanocápsulas de PGA-PEG a 10 y 20 mg/kg (NCs 10 y NCs 20, respectively). Los animales no tratados fueron usados como control. C permite comparar la actividad luciferasa en los ganglios antes (día 19) y después de los tratamientos. Datos expresados como media ± SEM.; n=5. Las diferencias estadísticamente significativas se expresan como * ($p < 0.05$) y ** ($p < 0.01$).

CONCLUSIONES / CONCLUSIONS

USC
UNIVERSIDADE
DE SANTIAGO
DE COMPOSTELA

CONCLUSIONES

El trabajo experimental recogido en la presente memoria, se ha dirigido al diseño de nanocápsulas como nuevas plataformas para la vehiculización de fármacos antitumorales al sistema linfático. Los resultados han permitido extraer las siguientes conclusiones:

1. Se han elaborado nanocápsulas constituidas por un núcleo oleoso y una cubierta polimérica a base de PGA, PGA-PEG o PASN. La optimización del proceso de producción de las nanocápsulas mediante la técnica de desplazamiento de disolvente, estudiando los parámetros que pueden afectar al tamaño de partícula, ha permitido elaborar nanocápsulas de composición sencilla y tamaño reducido. Las nanocápsulas resultantes presentan un tamaño nanométrico (alrededor de 100 nm) y una carga superficial negativa comprendida entre -25 y -51 mV. Además, presentan una satisfactoria capacidad para encapsular y liberar de forma controlada fármacos hidrofóbicos como el docetaxel, así como una adecuada estabilidad en plasma humano.

2. La evaluación de la biodistribución de las nanocápsulas de PGA-PEG fluorescentes ha evidenciado su capacidad para acceder al sistema linfático con mayor rapidez que otras similares de mayor tamaño cuando se administran por vía subcutánea. Por otro lado, la evaluación de la biodistribución de las nanocápsulas de PGA y PGA-PEG marcadas con el radionúclido In^{111} ha confirmado la capacidad de ambas formulaciones para alcanzar los ganglios linfáticos tras una administración intravenosa y subcutánea. En concreto, la administración subcutánea ha demostrado conducir a una elevada acumulación de las formulaciones en los ganglios linfáticos drenantes, mientras que la administración intravenosa ha llevado a una acumulación más modesta de las formulaciones en los ganglios examinados y a una alta captación hepática.

3. La administración *in vivo* de nanocápsulas de PGA-PEG conteniendo docetaxel ha demostrado una menor toxicidad frente a la formulación comercial de referencia, Taxotere®. La evaluación de estas nanocápsulas en un modelo ortotópico de cáncer de pulmón A549 que metastatiza a los ganglios linfáticos del mediastino ha evidenciado su capacidad para inhibir el crecimiento tumoral y la metástasis linfática con mayor

eficacia que el Taxotere®. De hecho, a diferencia de la formulación comercial, las nanocápsulas han demostrado disminuir específicamente la carga tumoral en los ganglios del mediastino, confirmando la mayor eficacia in vivo de esta formulación.

CONCLUSIONS

The experimental work enclosed in this manuscript was aimed at the design of new nanocapsules as innovative platforms for the delivery of antitumor drugs to the lymphatic system. The results allowed us to withdraw the following conclusions:

1. Nanocapsules composed by an oily core and a polymeric PGA, PGA-PEG or PASN shell were successfully developed. The optimization of the production process of these formulations, using the previously described solvent displacement technique, through the evaluation of the parameters influencing particle size, has allowed the preparation of nanocapsules with simple composition and smaller size than those reported so far using this method. The resulting nanocapsules have a nanometric size (around 100 nm) and a negative surface charge of between -25 and -51 mV. Moreover, nanocapsules exhibit a satisfactory capacity to encapsulate and release hydrophobic drugs such as docetaxel in a controlled manner, as well as a suitable stability in human plasma during the studied time.

2. The biodistribution studies of DiD-loaded PGA-PEG nanocapsules demonstrated their ability to enter the lymphatic system faster than other similar nanosystems with bigger particle size, upon subcutaneous administration. On the other hand, the same study performed with PGA and PGA-PEG nanocapsules labeled with the radionuclide In^{111} confirmed the ability of both formulations to reach the lymph nodes upon intravenous and subcutaneous administration. In detail, the subcutaneous administration led to a high accumulation of the formulation in the draining lymph nodes while the intravenous one led to a much lower accumulation in all examined lymph nodes and to a high liver accumulation. In any case, the biodistribution pattern was similar for both formulations.

3. The *in vivo* administration of docetaxel-loaded PGA-PEG nanocapsules evidenced lower toxicity of this formulation in comparison with the corresponding commercially available drug, Taxotere®. This formulation has also shown its ability to inhibit tumor growth and lymphatic metastasis more efficiently than Taxotere®, in an orthotopic A549 lung cancer model which metastasizes to the mediastinal lymph nodes. In fact, contrary to the commercial drug, the nanocapsules specifically reduced the tumoral burden in the mediastinal nodes, confirming the higher *in vivo* efficacy of this formulation.

USC
UNIVERSIDADE
DE SANTIAGO
DE COMPOSTELA

ANEXO

USC
UNIVERSIDADE
DE SANTIAGO
DE COMPOSTELA

Internalization of PGA-PEG Nanocapsules in A549 Human Lung Adenocarcinoma Cells

Este trabajo ha sido realizado en colaboración con Alonso-Nocelo M[1], Vidal A[2], Abal M[1] y de la Fuente M[1].

[1]Translational Medical Oncology Group, Health Research Institute of Santiago de Compostela (IDIS) Clinical University Hospital/SERGAS, Santiago de Compostela, Spain.

[2]Cell Cycle and Oncology group CiClOn, IDIS, CIMUS. (USC). Santiago de Compostela, Spain.

USC
UNIVERSIDADE
DE SANTIAGO
DE COMPOSTELA

1 Introduction

The metastases are the most common reason of cancer death in patients with solid tumors, mainly because of the ineffectiveness of current therapies once tumor cells begin to spread [1,2]. The regional lymph nodes, once invaded by tumor cells, could act as reservoirs where cancer cells take root and seed into other parts of the body [3,4]. The lymphatic system is not easily accessible by conventional intravenous infusion of chemotherapeutics, thus limiting the amount of drug that reaches the lymph nodes [5]. Over the past decades, efforts have been made to improve drug delivery technologies that target anticancer drugs specifically to tumor cells. For this reason, the development of therapeutic strategies intended to target anticancer drugs to the tumor cells in lymph nodes has an enormous potential [6,7]. Bearing this in mind, we have recently developed PEGylated Polyglutamic Acid (PGA-PEG) nanocapsules, which exhibit features that make them attractive as lymphatic drug delivery carriers. To test the ability of these nanocapsules to penetrate into tumor-infiltrated lymph nodes we have performed *in vitro* internalization studies in A549 human lung adenocarcinoma cell line.

2 Materials and Methods

2.1 Cell lines and culture conditions

Lung adenocarcinoma A549, and Jurkat Jurkat E6.1 cell lines, were obtained from ATCC® (CCL-185™ and TIB-152™), and maintained in DMEM (Dulbecco's modified Eagle's Medium) (Sigma-Aldrich, Spain) and RPMI-1640 (GIBCO®, Barcelona, Spain) respectively, at 37ºC and 5% CO2. Both media were supplemented with 10% fetal bovine serum and 5% penicillin-streptomycin (GIBCO®). RPMI-1640 was also supplemented with 5% L-glutamine (Sigma-Aldrich).

2.2 Preparation of loaded nanocapsules

PGA-PEG nanocapsules were prepared by the solvent displacement technique. Size, polydispersity index, and zeta potential were determined by photon correlation spectroscopy (PCS) and laser Doppler anemometry (LDA) (Zetasizer Nano ZS

(Malvern Instruments, Malvern, UK). Morphology was evaluated by transmission electron microscopy (TEM) using a JEOL JEM-2010 microscope (Tokyo, Japan). The stability of nanocapsules was assessed in cell culture medium upon incubation at 37ºC under horizontal shaking. Particle size was measured over time by PCS for assessing the occurrence of cluster formation. Nanocapsules loaded with DiD were isolated by ultracentrifugation (84035xg for 1 hour at 15°C) and the concentration of DiD directly determined by UV spectrophotometry and high-performance liquid chromatography. Additionally, nanocapsules were loaded with docetaxel with similar encapsulation efficiency and characteristics.

2.3 Interaction of nanocapsules with lung cancer cells

For Laser Confocal Scanning Microscopy (LCSM) analysis, A549 monolayers were seeded on coverslips in a multiwell-24 plate (Thermo Fisher Scientific, Madrid, Spain) at $7.5x10^4$ cells/well in supplemented medium for 24 hours. Afterwards, the medium was removed and nanocapsules, diluted at a DiD concentration of 0.5 μg/ml and docetaxel concentration of 25 nM, were added to the wells. After 4 hours of incubation, cells were washed with cold phosphate saline buffer (PBS, Sigma) and fixed with 4% paraformaldehyde at room temperature for 10 minutes. Staining of the nuclei was performed using DAPI (Life Technologies) (1:1000). After staining, samples were washed with PBS and mounted with Mowiol 4-88 medium (Calbiochem). Samples were analyzed by LSCM at 63x magnification for the 2D. Images were captured with a scanning speed of 400 Hz and image resolution of 1024 x 1024 pixels.

Additionally, 2D co-cultures were prepared in order to perform Fluorescent Activated Cell Sorting (FACS). A549 and Jurkat E6.1 cells were seeded in a multiwell-6 plate (Thermo Fisher Scientific, Madrid Spain) for 24 hours at a concentration of $1x10^5$ cells per well of each cell type. Then, cells were treated with DiD loaded PGA-PEG nanocapsules in cell culture medium at a fluorescent probe concentration of 0.5 μg/ml. After 4 hours of incubation, cells were washed with phosphate saline buffer (PBS, Sigma, Spain) and harvested by trypsinization. Pellets were rinsed with PBS, counted and resuspended in 500 μl of PBS-FBS 2% for the analysis. Then, tubes were placed on ice and analyzed within 2 hours using a FACScan flow cytometer (BD Biosciences,

Madrid, Spain) at 488 nm excitation and a LP670 filter. The analysis of the results was performed using FlowJo Software (TreeStar Inc., Ashland, OR).

3 Results and Discussion

3.1 Characterization of PGA-PEG nanocapsules

Loaded nanocapsules had a mean size of 112 ± 12 nm, a low polydispersity (PI: 0.1), a negative surface charge (zeta potential: -38 ± 2 mV) and spherical shape morphology (**Table 1**). In order to analyze their interaction with the cells by confocal microscopy, fluorescent nanocapsules were obtained upon encapsulation of DiD and docetaxel into their oily core (encapsulation efficiency of 56%).

Table 1. Physicochemical characteristics of the PGA-PEG nanocapsules. Values are given as mean ± S.D; n=3.

Loading	Size (nm)	P.I.*	ζ Potential (mV)
DiD	112 ± 12	0.1	-38 ± 2
DiD + Docetaxel	109 ± 13	0.2	-39 ± 1

* P.I.: polydispersity index

3.2 Specific interaction of PGA- PEG nanocapsules with lung cancer cells

As observed in **Figure 1A**, DiD-loaded nanocapsules were efficiently internalized by the tumor cells after 4 hours of incubation; the green signal corresponding to the nanocapsules was evenly distributed into the cell cytoplasm and perinuclear area. In addition, cells presented a normal aspect, which suggest the absence of toxicity due to the formulations. On the other hand, when cells were incubated with DiD-Docetaxel loaded nanocapsules (**Figure 1B**) a cytotoxic effect was observed after internalization. Multinucleated cells as well as fragmented cell nuclei characterized this effect.

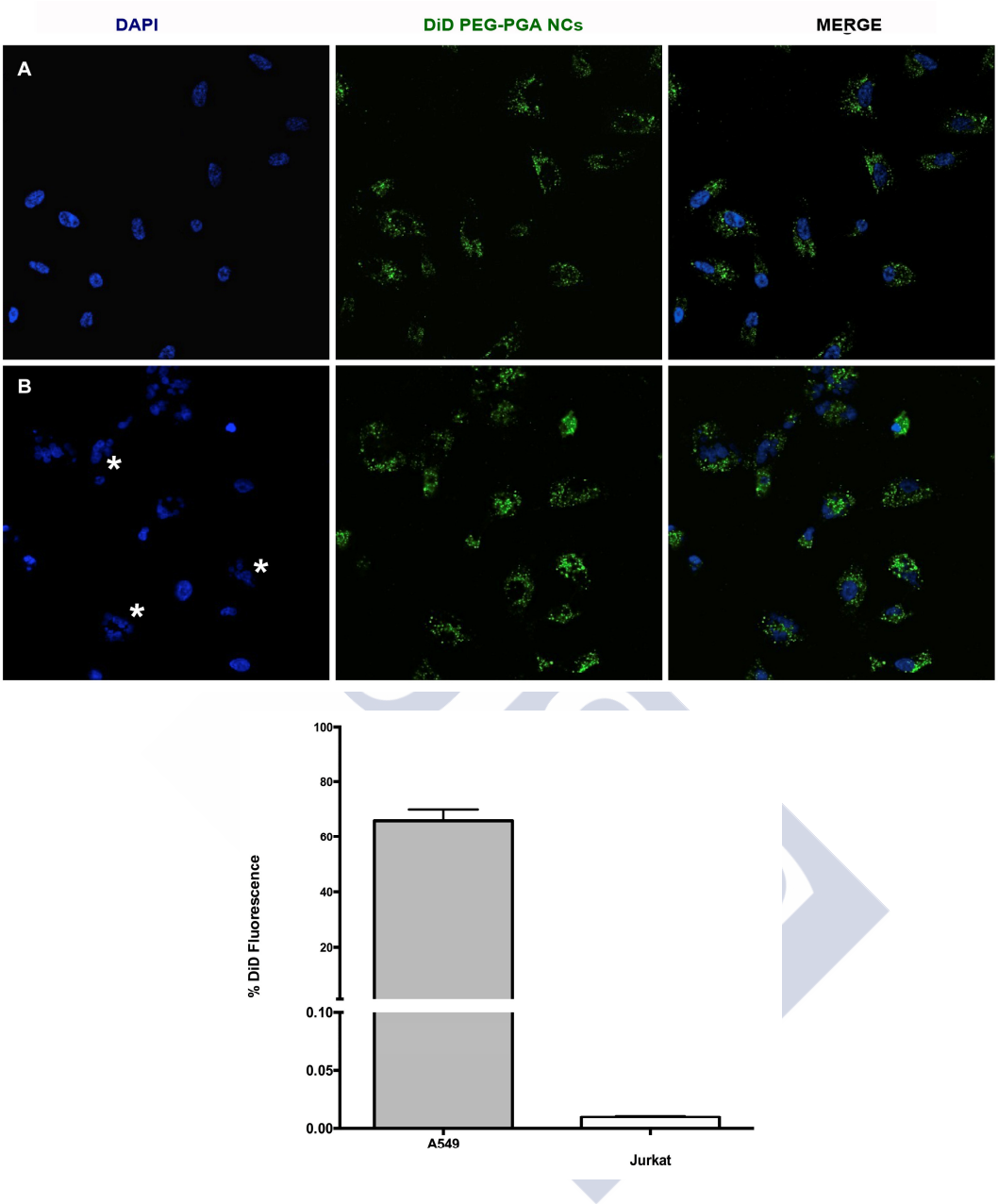

Figure 1. Cellular uptake studies. Cells were incubated for 4 hours with (A) DiD-loaded PGA-PEG nanocapsules (B) DiD-Docetaxel loaded PGA-PEG nanocapsules (green channel). Cell nuclei were stained with DAPI (blue channel). Accumulation of nanocapsules carrying DiD and docetaxel produced a cytotoxic effect characterized by nuclei fragmentation (asterisks). (C) Graphical representation of the DiD-loaded nanocapsules fluorescence uptake in co-cultures determined by Fluorescence Activated Cell Sorting (FACS). Bars represent the mean ± SD (n=3). Populations were gated separately in order to verify the specific uptake.

In addition, to confirm the specificity of the nanocapsules for the tumor cells, co-cultures of tumor cells and lymphocytes were established and incubated with DiD-loaded nanocapsules. Both cell populations, tumor cells and lymphocytes, were identified separately allowing an independent gating of each one. In the co-cultures 65.82% of the cells were positive for the DiD fluorescence. This percentage corresponded mostly to the tumor cells (65.81%) in comparison with Jurkat cells (0.01%). Therefore, these results clearly confirm that nanocapsules were preferentially internalized by the tumor cells.

4 Conclusions

We report here the capability of PGA-PEG nanocapsules to encapsulate fluorescent and therapeutic molecules, as wells as their ability to specifically interacted with the tumor cells, making the attractive as lymphatic drug delivery systems.

REFERENCES

[1] Gupta G P and Massague J 2006 Cancer metastasis: building a framework *Cell* **127** 679–95

[2] Sleeman J P 2000 The lymph node as a bridgehead in the metastatic dissemination of tumors. *Recent Results Cancer Res.* **157** 55–81

[3] Pantel K and Brakenhoff R H 2004 Dissecting the metastatic cascade *Nat Rev Cancer* **4** 448–56

[4] Sleeman J P and Thiele W 2009 Tumor metastasis and the lymphatic vasculature *Int J Cancer* **125** 2747–56

[5] Chandrasekaran S and King M R 2014 Microenvironment of tumor-draining lymph nodes: opportunities for liposome-based targeted therapy. *Int. J. Mol. Sci.* **15** 20209–39

[6] Oussoren C 2001 Liposomes to target the lymphatics by subcutaneous administration *Adv. Drug Deliv. Rev.* **50** 143–56

[7] Zhang X-Y and Lu W-Y 2014 Recent advances in lymphatic targeted drug delivery system for tumor metastasis. *Cancer Biol. Med.* **11** 247–54